DEPARTMENT OF CONSTRUCTION ENGINEERING AND ENGINEERING PROJECTS

Ph.D. Thesis

Inclusion of damage detection methods for the sustainable life cycle design of bridges in aggressive environments

Author:

Mehrdad Hadizadeh Bazaz

Supervisors:

Dr. Víctor Yepes Piqueras

Dr. Ignacio J. Navarro Martínez

Valencia, November 2024

Acknowledgements

Sincere appreciation is extended to everyone who has supported and encouraged me during the process that resulted in the completion of my doctoral dissertation. I would like to express my gratitude to the Universitat Politècnica de València for permitting me to conduct this research endeavor, which has been an invaluable experience that has contributed significantly to my professional and academic growth. I sincerely appreciate the support and guidance my thesis advisors, Víctor Yepes and Ignacio J. Navarro, provided, which has been indispensable during these years.

I must express my sincere gratitude to all my research group colleagues. Since then, every group member, including David, Zhou, Salvador, Iván, Andrés, Byron, Paola, Antonio, and Ximena, has my deepest gratitude. Upon arriving at ICITECH, Vicent and David greeted me with tremendous warmth. It has been a delight to share this experience with them, and I am grateful for their time and dedication in supporting me.

Furthermore, I want to thank my parents and other loving family members for their unwavering financial support and constant encouragement.

Additionally, I would like to express my gratitude to the Spanish Ministry of Science and Innovation. This study is supported by the project PID2020-117056RB-I00 and PID2023-150003OB-I00 which was supported by MCIN/AEI/10.13039/501100011033 and 'ERDF: A Way of Making Europe.

Thesis structure

This doctoral thesis is presented as a compilation of four published articles, and one article was submitted to the journal for review. The thesis is divided into ten chapters, including those articles.
The references of the articles, in order of appearance, are:

- 1st paper: Hadizadeh-Bazaz, M., Navarro, I. J., & Yepes, V. (2022). Performance comparison of structural damage detection methods b ased on Frequency Response Function and Power Spectral Density. DYNA Ingeniería e Industria (Online), 97(5), 493-500.

- 2nd paper: Hadizadeh-Bazaz, M., Navarro, I. J., & Yepes, V. (2023). Power Spectral Density method performance in detecting damages by chloride attack on coastal RC bridge. Structural Engineering and Mechanics, 85(2), 197-206.

- 3rd paper: Hadizadeh-Bazaz, M., Navarro, I. J., & Yepes, V. (2023). Life-Cycle Cost Assessment Using the Power Spectral Density Function in a Coastal Concrete Bridge. Journal of Marine Science and Engineering, 11(2), 433.

- 4th paper: Hadizadeh-Bazaz, M., Navarro, I.J., & Yepes, V. (2023). Durability assessment and re-design of coastal concrete bridge through a non-destructive damage detection method. 27th International Congress on Project Management and Engineering, AEIPRO, 10-13 de julio, Donostia/San Sebastián (Spain), pp. 386-401. DOI:10.61547/3371

- 5th paper: Hadizadeh-Bazaz, M., Navarro, I. J., & Yepes, V. (2023). Life Cycle Assessment of a Coastal Concrete Bridge Aided by Non-Destructive Damage Detection Methods. Journal of Marine Science and Engineering, 11(9), 1656.

- 6th paper: Hadizadeh-Bazaz, M., Navarro, I. J., & Yepes, V. (2024). Sustainability Life Cycle Assessment of Concrete Bridges in Coastal Regions Using Power Spectral Density Technique. (Submitted to the Jurnal Manuscript under review)

Awards and certificates received：

1. Award for the best work in the poster modality selected by jury at the VIII MEETING OF DOCTORAL STUDENTS OF THE UPV held at the Universitat Politecnoica de VAlencia on May 25, 2023.


UNIVERSITAT POLITÈCNICA DE VALÈNCIA

ESCUELA DE DOCTORADO

Premio al mejor trabajo en la modalidad de póster

seleccionado por el jurado

para

MEHRDAD HADIZADEH BAZAZ

En el VIII ENCUENTRO DE ESTUDIANTES DE DOCTORADO DE LA UPV celebrado en la Universitat Politècnica de València el 25 de mayo de 2023.

Lynne Paula Yenush
Directora de la Escuela de Doctorado

Francisco Juan Espinós Gutiérrez
Presidente del jurado

2. Second prize for the Jaume Blasco Innovation Award in the commission of the 27th International Congress of Project Management and Engineering.

AEIPRO IPMA SPAIN international project management association

Mondragon Unibertsitatea

27th International Congress on Project Management and Engineering

10-13 July 2023
Donostia-San Sebastián

CERTIFICATE OF AWARD
CERTIFICADO DE PREMIO

The Committee of Awards of the 27th International Congress on Project Management and Engineering,

La Comisión de Premios del XXVII Congreso Internacional de Dirección e Ingeniería de Proyectos

CERTIFIES / **CERTIFICA**

that the communication / que la comunicación

Durabilidad y rediseño de un puente de hormigón en ambiente costero mediante un método no destructivo de detección de daños

by the authors / de los autores

Mehrdad Hadizadeh-Bazaz; Ignacio J. Navarro; Víctor Yepes

has been awarded the / ha obtenido el

Accesit del Premio Jaume Blasco a la Innovación

VºBº de la Presidenta de AEIPRO
Dña. M. Socorro García Cascales

El Secretario de AEIPRO
D. José Luis Yagüe Blanco

3. Award for the best work in the poster modality selected by the jury At the IX MEETING OF DOCTORAL STUDENTS OF THE UPV held at the Universitat Politecnoica de VAlencia on May 23, 2024.

UNIVERSITAT POLITÈCNICA DE VALÈNCIA

ESCUELA DE DOCTORADO

Premio al mejor trabajo en la modalidad de póster
seleccionado por el jurado

para

MEHRDAD HADIZADEH BAZAZ

En el IX ENCUENTRO DE ESTUDIANTES DE DOCTORADO DE LA UPV celebrado en la Universitat Politècnica de València el 23 de mayo de 2024.

Lynne Paula Yenush
Directora de la Escuela de Doctorado

Presidente del jurado

Abstract

Recently, the health monitoring of every structure and infrastructure in different periods of its life, including construction, repair, and maintenance until the end of life to prevent sudden collapses before the end of the life of structure that calculated which causing significant financial and human losses, is essential for every person that uses them.

On the other hand, all these construction activities, repairs, and maintenance can harm the environment and society. So, using modern techniques for damage detection that consider the sustainability life cycle assessment and total maintenance costs to do on-time repair activities is valuable.

The concept of sustainability has evolved since the Brundtland Commission first defined it in 1987. Since then, scientific communities have developed sustainable design principles, methods, and criteria. However, many of these approaches lack

long-term feasibility. The United Nations has set the 2030 Sustainable Development Goals (SDGs).

In this context, it is vital to establish a sustainable life cycle strategy for concrete structures, minimizing costs and reducing environmental and social impacts throughout the entire lifespan, from construction to end-of-life stages. Advances in computer technology and sophisticated sensors have made it feasible to utilize non-destructive testing (NDT) methods to effectively monitor and maintain critical structures, such as bridges, reducing the risk of financial and human losses. This thesis explores the application of various non-destructive techniques for identifying structural damage and evaluates their implications for sustainability.

In this regard, it investigated the performance of non-destructive methods such as Frequency Response Function (FRF) and Power Spectral Density (PSD) in detecting the presence and absence of damage and the location of damage. The ability of the PSD to predict different types of damage in a structure, such as a coastal concrete bridge in aggressive environments exposed to damage and corrosion by chloride ions, was evaluated. Then, in the following, analyze the performance of using this damage prediction method on the sustainability life cycle assessment and environmental and social impacts, as well as the economic and cost aspects of using these methods at different stages during the life of an evaluated for a box-girder concrete bridge in Arosa in northwestern Spain.

In conclusion, this thesis demonstrates that integrating the PSD method for preventive maintenance into the life cycle design of concrete bridges significantly enhances sustainability performance. The findings show that the PSD method effectively detects, locates, and predicts damage, leading to better long-term management of coastal concrete bridges prone to corrosion. The comprehensive analysis, including life cycle assessment and multi-criteria decision-making, confirms that using the PSD method reduces environmental impact, minimizes costs, and improves the overall sustainability of bridge infrastructure, offering a robust framework adaptable to various infrastructure types for achieving broader sustainability goals.

Resumen

Recientemente, el monitoreo de la salud de cada estructura e infraestructura en diferentes periodos de su vida, incluyendo construcción, reparación y mantenimiento hasta el fin de su vida útil para prevenir colapsos repentinos antes del fin de vida calculado, los cuales causan pérdidas económicas y humanas significativas, es esencial para todas las personas que las utilizan.
Por otro lado, todas estas actividades de construcción, reparación y mantenimiento pueden dañar el medio ambiente y la sociedad. Por lo tanto, el uso de técnicas modernas para la detección de daños que consideren la evaluación del ciclo de vida

sostenible y los costos totales de mantenimiento para realizar reparaciones a tiempo es valioso.
El concepto de sostenibilidad ha evolucionado desde que la Comisión Brundtland lo definió por primera vez en 1987. Desde entonces, las comunidades científicas han desarrollado principios, métodos y criterios de diseño sostenible. Sin embargo, muchos de estos enfoques carecen de viabilidad a largo plazo. Las Naciones Unidas han establecido los Objetivos de Desarrollo Sostenible (ODS) para 2030.
En este contexto, es fundamental establecer una estrategia de ciclo de vida sostenible para las estructuras de hormigón, minimizando costos y reduciendo los impactos ambientales y sociales a lo largo de toda la vida útil, desde la construcción hasta las etapas de fin de vida. Los avances en tecnología informática y sensores sofisticados han hecho posible utilizar métodos de prueba no destructiva (NDT) para monitorear y mantener de manera efectiva estructuras críticas, como puentes, reduciendo el riesgo de pérdidas financieras y humanas. Esta tesis explora la aplicación de diversas técnicas no destructivas para identificar daños estructurales y evalúa sus implicaciones para la sostenibilidad.

En este sentido, se investigó el rendimiento de métodos no destructivos como la Función de Respuesta en Frecuencia (FRF) y la Densidad Espectral de Potencia (PSD) para detectar la presencia y ausencia de daños, así como la localización de los mismos. Se evaluó la capacidad de la PSD para predecir diferentes tipos de daños en una estructura, como un puente de hormigón costero en entornos agresivos expuestos a daños y corrosión por iones de cloruro. Luego, se analizó el rendimiento del uso de este método de predicción de daños en la evaluación del ciclo de vida sostenible y los impactos ambientales y sociales, así como los aspectos económicos y de costos del uso de estos métodos en diferentes etapas durante la vida útil de un puente de hormigón tipo cajón en Arosa, en el noroeste de España.

En conclusión, esta tesis demuestra que la integración del método PSD para el mantenimiento preventivo en el diseño del ciclo de vida de puentes de hormigón mejora significativamente el rendimiento de sostenibilidad. Los hallazgos muestran que el método PSD detecta, localiza y predice de manera efectiva los daños, lo que permite una mejor gestión a largo plazo de los puentes de hormigón costeros propensos a la corrosión. El análisis integral, que incluye la evaluación del ciclo de vida y la toma de decisiones multicriterio, confirma que el uso del método PSD reduce el impacto ambiental, minimiza costos y mejora la sostenibilidad general de la infraestructura del puente, ofreciendo un marco sólido adaptable a varios tipos de infraestructura para alcanzar objetivos de sostenibilidad más amplios.

Resum

Recentment, la monitorització de la salut de cada estructura i infraestructura en diferents períodes de la seua vida, incloent-hi la construcció, reparació i manteniment fins al final de la vida útil per evitar col·lapses sobtats abans del final calculat, els quals poden causar pèrdues econòmiques i humanes significatives, és essencial per a totes les persones que les utilitzen.
D’altra banda, totes aquestes activitats de construcció, reparacions i manteniment poden perjudicar el medi ambient i la societat. Per tant, és valuós utilitzar tècniques modernes per a la detecció de danys que consideren l’avaluació del cicle de vida sostenible i els costos totals de manteniment per a dur a terme activitats de reparació a temps.

El concepte de sostenibilitat ha evolucionat des que la Comissió Brundtland el va definir per primera vegada l’any 1987. Des de llavors, les comunitats científiques han desenvolupat principis, mètodes i criteris de disseny sostenible. No obstant això, molts d’aquests enfocaments manquen de viabilitat a llarg termini. Les Nacions Unides han establit els Objectius de Desenvolupament Sostenible (ODS) per a 2030.

En aquest context, és fonamental establir una estratègia de cicle de vida sostenible per a les estructures de formigó, minimitzant els costos i reduint els impactes ambientals i socials al llarg de tota la vida útil, des de la construcció fins a les etapes de final de vida. Els avenços en tecnologia informàtica i sensors sofisticats han fet possible utilitzar mètodes de proves no destructives (NDT) per a monitoritzar i mantenir de manera efectiva estructures crítiques, com ara ponts, reduint el risc de pèrdues financeres i humanes. Aquesta tesi explora l'aplicació de diverses tècniques no destructives per a identificar danys estructurals i avalua les seues implicacions per a la sostenibilitat.

En aquest sentit, es va investigar el rendiment de mètodes no destructius com la Funció de Resposta en Freqüència (FRF) i la Densitat Espectral de Potència (PSD) per a detectar la presència i absència de danys, així com la localització dels mateixos. Es va avaluar la capacitat de la PSD per a predir diferents tipus de danys en una estructura, com ara un pont de formigó costaner en entorns agressius exposat a danys i corrosió per ions de clorur. A continuació, es va analitzar el rendiment de l'ús d'aquest mètode de predicció de danys en l'avaluació del cicle de vida sostenible i els impactes ambientals i socials, així com els aspectes econòmics i de costos de l'ús d'aquests mètodes en diferents etapes durant la vida útil d'un pont de formigó de bigues caixó en Arosa, al nord-oest d'Espanya.

En conclusió, aquesta tesi demostra que la integració del mètode PSD per al manteniment preventiu en el disseny del cicle de vida de ponts de formigó millora significativament el rendiment de la sostenibilitat. Els resultats mostren que el mètode PSD detecta, localitza i prediu de manera efectiva els danys, cosa que permet una millor gestió a llarg termini dels ponts de formigó costaners propensos a la corrosió. L'anàlisi integral, que inclou l'avaluació del cicle de vida i la presa de decisions multicriteri, confirma que l'ús del mètode PSD redueix l'impacte ambiental, minimitza els costos i millora la sostenibilitat general de la infraestructura del pont, oferint un marc sòlid adaptable a diversos tipus d'infraestructures per a assolir objectius de sostenibilitat més amplis.

Table of Contents

1. Introduction 1
1.1. Background 2
1.2. Research objectives 5
1.3. Methodology 7
1.4. Dissertation structure 9
2. Performance comparison of structural damage detection based on frequency response function 11
2.1. Introduction 12
2.2. Damage detection methods 15
2.2.1. Frequency Response Function (FRF) 15
2.2.1. Power Spectral density (PSD) 20
2.3. Numerical example 21
2.3.1. Calebration of the numerical model 24
2.4. Results and Discussion 26
2.5. Conclusions 32
3. Power spectral density method performance in detecting damages 35
by chloride attack on coastal RC bridge 35
3.1. Introduction 36
3.2. Methods and materials 39
3.2.1. Model Description 39
3.2.2. Chloride damage prediction methods for the rebars of RC structure 41
3.2.3. Damage detection methods for the total of the RC bridge.............. 45
3.3. Results 49
3.4. Conclusions 53
4. Life-Cycle Cost Assessment Using the Power Spectral Density Function in a Coastal Concrete Bridge 55

4.1. Introduction 56
4.2. Materials and methods 59
4.2.1. Goal and Scope Definition 59
4.2.2. Service life prediction 62
4.2.3. Calculation Procedure for LCCA 67
4.3. Description of the Numerical Model 71
4.4. Results 75
4.5. Conclusions 84
Durability assessment and re-design of coastal concrete bridge through a non-destructive damage detection method 85
5.1. Introduction 86
5.2. Objectives 88
5.3. Methodology 88
5.3.1. Prediction strategies for corrosion deterioration in steel rebars 88
5.3.2. Damage detection through non-destructive damage detection methods 90
5.3.3. LCCA through the damage detection methods 93
5.4. Model description 95
5.4.1. Analysis in the numerical model description 96
5.5. Results 99
5.6. Conclusions 102
6. Life Cycle Assessment of a Coastal Concrete Bridge Aided by Non-Destructive Damage Detection Methods 103
6.1. Introduction 104
6.2. Materials and Methods 108
6.2.1. Service Life and Damage Prediction Methods 109
6.2.2. Life Cycle Assessment 113
6.3. Model Description 116
6.3.1. The Numerical Model Analyses 118
6.4. Results 121
6.5. Conclusions 126

7. Sustainability Life Cycle Assessment of Concrete Bridges in Coastal Regions Using Power Spectral Density Technique 127
7.1. Introduction 128
7.2. Methodology 131
7.2.1. Bridge model description 132
7.2.2. Service life prediction techniques 133
7.2.3. Sustainability life cycle assessment 138
7.2.4. MCDM model through the PSD method 144
7.2.5. Numerical model analysis 146
7.3. Repair activities description 148
7.4. Results and discussion 149
7.4.1. Service Life Prediction Methods Performance results 149
7.4.2. Life cycle impacts assessment results 151
7.4.3. Sustainability and MCDM Analysis Results 155
7.5. Conclusions 156
8Discussion of the results 159
9. 175
Conclusions and future work 175
9.1. General conclusions 176
9.1.1. Main conclusions 176
9.1.2. Methodological conclusions 177
9.2. Specific conclusions 178
9.3. Future lines of research 179
10.References 181

List of Figures

Figure 2.1. Transfer Function of FRF with Input Force to Displacement Response 15
Figure 2.2. The trust model information: (a) Geometry; (b) Active degree of freedom direction........22
Figure 2.3. Comparison of the FRFs according to the damaged and undamaged elements for the scenario 1........25
Figure 2.4. Comparison of The Predicted Damage with FRF and PSD methods and for different scenarios........29
Figure 2.5. Error Indices results for The Two methods of Damage Detection for the eight scenarios.........31

Figure 3.1 The process of chloride corrosion in steel rebar........37
Figure 3.2. The location map of the Arosa bridge in Spain........39
Figure 3.3. Arosa’s concrete bridge in cross-section........40
Figure 3.4. The geometry of a span of the bridge........40
Figure 3.5. The service life of rebars and chloride corrosion levels in RC structures........41
Figure 3.6. Numbering and dividing points in the three spans selected of the Arosa bridge........48
Figure 3.7. The deterioration of the reinforcements of the bridge according to chloride corrosion attacks every year for different locations.........50
Figure 3.8. Damage location and percentage due to chloride attack in the 5th year of the bridge life........51
Figure 3.9. Damage location and percentage due to chloride attack in the 10th year of the bridge life........51
Figure 3.10. Damage location and percentage due to chloride attack in the 15th year of the bridge life........51

Figure 3.11. Damage location and percentage due to chloride attack in the 33rd year of the bridge life 52

Figure 4. 1. The location map of the Arosa bridge in Spain. 60
Figure 4. 2. Dimensions of a span of the Arosa bridge........ 61
Figure 4. 3. The service life of rebars in an RC structure is according to Tuutti's model. 63
Figure 4. 4. The LCCA using the PSD for maintenance and repair of the concrete bridge. 69
Figure 4. 5. Numbering and division of sensor points in 1 of 40 spans of the Arosa bridge. 72
Figure 4. 6. The summary of analysis and calculation processes performed on the numerical model of the Arosa bridge 74
Figure 4. 7. The life-cycle cost assessment for the Arosa bridge until the end of the bridge life........ 83

Figure 5. 1. The cross-section dimension of the coastal and concrete Arosa bridge. 96
Figure 5. 2. Sensor point numbering and division in each section of a span of the Arosa bridg*e* 97
Figure 5. 3. Compare service life and repair time in the bridge by (a) PSD method and (b) Conventional method. 100
Figure 5. 4. Life cycle cost assessment in the bridge is done using (a) the PSD method and (b) the conventional method. 101

Figure 6. 1. Health monitoring and damage detection processes in a bridge structure. 107

Figure 6. 2. The general diagram stages of the damage detection method for the life cycle assessment that this research proposes..108
Figure 6. 3. Reinforcement concrete structure’s rebar service life according to Tuutti’s model (1982)..110
Figure 6. 4. The approaches to environmental life cycle assessment (Penadés-Plà et al., 2020)..114
Figure 6. 5. The indicators of E-LCIA through the ReCiPe method.....................115
Figure 6. 6. Methodologies, activities, and material used in this research............116
Figure 6. 7. The total view of the piers and deck of Spain’s reinforced concrete coastal Arosa bridge. 117
Figure 6. 8. Cross-section and dimensions of the Arosa coastal and concrete bridge. 117
Figure 6. 9. Counting and dividing points as sensors in an Arosa bridge span......119
Figure 6. 10. An overview of the study and computation procedures used for E-LCA for the bridge. 120
Figure 6. 11. The service lifetime for the repair of each element section ID of the concrete bridge. 121
Figure 6. 12. The percentage of the predicted damages for service life and repair period activities. 122
Figure 6. 13. The total quantification of environmental categories’ impacts on the Arosa Bridge 125

Figure 7. 1. Concise overview of the sustainability assessment stage of a concrete bridge structure using the PSD approach 131
Figure 7. 2. The geographical position and location of the Arosa Bridge..............132
Figure 7. 3. The measurements of the deck and columns of the central section of the Arosa bridge 133
Figure 7. 4. Service Life Prediction for Rebars in a Reinforced Concrete (RC) Structure using Tuutti's (1982) Model..134

Figure 7. 5. Environmental life cycle assessment indicators and method used 141
Figure 7. 6. The iterative phases, stakeholder categories, and subcategories of S-LCA according to the UNEP 2020 Guidelines 143
Figure 7. 7. MCDM flowchart for comprehensive design solution evaluation through the TOPSIS method 145
Figure 7. 8. Situation and numbering of sensor points on one span of the Arosa bridge 147
Figure 7. 9. Total repair activities to assess sustainability by PSD method........... 152
Figure 7. 10. Total LCC for the deck and columns of a span of the Arosa bridge through each method.. 152
Figure 7. 11. Total E-LCA for the deck and columns of a span of the Arosa bridge through each method.. 153
Figure 7. 12. Total S-LCA for the deck and columns of a span of the Arosa bridge through each method.. 154

Figure 8. 1. The process and functioning of the two damage detection methods based on FRF and PSD. 164
Figure 8. 2. The total LCCA differences through the PSD method compared to a conventional method.. 167
Figure 8. 3. The percentage of the benefit of using the PSD method in each category of E-LCA. 168
Figure 8. 4. The percentage of the benefit of using the PSD method in each category of S-LCA. 169
Figure 8. 5. The Sustainable Development Goals United Nations, (2015)............ 172

List of Tables

Table 2.1. Damage scenarios considered 23
Table 2.2. The measurements and stimulation DOFs set 24
Table 2.3. Summary of Average Errors and IQR 31

Table 3. 1. The Arosa structure's concrete mixtures and mechanical parameters....41
Table 3. 2. The chloride concentration at the concrete surface in the marine environment (Spanish Ministry of Public Works, 2008)..................................43
Table 3. 3. The coefficients D_0 (×10−12m^2/s) (Spanish Ministry of Public Works, 2008) 43
Table 3. 4. The Chloride corrosion rate depended on the Marine exposure class (Spanish Ministry of Public Works 2008)...44

Table 4. 1. The Arosa structure's concrete mixtures and mechanical parameters....61
Table 4. 2. Durability parameters for the Arosa bridge..65
Table 4. 3. Repair activity cost (EUR) according to Spain data code (2022) for the concrete and coastal Arosa bridge..70
Table 4. 4. Identified the location, time, amount of damage, and conventional service life of the Arosa bridge...75

Table 5. 1. Total repair activity cost (EUR) for the service life of the coastal Arosa bridge...98

Table 6. 1. Durability parameters in a coastal reinforced concrete bridge (Spanish Ministry of Public Works, 2008)..111
Table 6. 2. Environmental impact assessment results from two methods on the coastal bridge...123

Table 6. 3. Benefits of utilizing PSD in the environmental impacts category of a bridge span 124

Table 7. 1. Parameters of durability in a RC bridge located in a coastal area (Spanish Ministry of Public Works, 2008) 136
Table 7. 2. Simulation and measuring point numbers on a span of Arosa bridge.. 148
Table 7. 3. Arosa bridge location, time, damage, and service lifetime for repairing activities 150
Table 7. 4. Criteria and weights pairwise comparison matrix for the bridge by AHP 155
Table 7. 5. The score for each method of damage preparation is according to the TOPSIS approach. 156

Chapter 1
Introduction

1.1. Background

Today, sustainability and life cycle assessment are vital factors at every stage of a structure's life, including design, construction, use, repair, and maintenance, up to the end of its life. The main goal is to reduce environmental and social impacts while keeping costs low. This approach is fundamental during repair and maintenance, where sustainable practices are crucial. Evaluating the effectiveness of damage detection methods throughout a structure's life can help lower repair costs and reduce environmental impact.

The deterioration of the existing infrastructure has become a significant concern in developed countries. More than 30% of building endeavors are allocated towards preserving and refurbishing facilities that have incurred damage (Gil Benso et al., 2015). This emphasizes the significance of maintaining and improving infrastructure as a significant factor in long-term outcomes (Sierra et al., 2017).

Structural damage is identified through destructive or non-destructive techniques (Cui et al., 2023). Destructive methodologies rely on models that frequently involve extracting structural samples to evaluate the extent of harm. In contrast, non-destructive techniques refer to autonomous models that can detect structural damage using numerical software models without causing any harm to the structure (Rathod and Gupta, 2019). Non-destructive damage detection techniques can be monitored using signal-based technologies.

The utilization of contemporary, advanced computers and sensors has led to a rise in the prevalence of signal-based approaches in the field of structural health monitoring (Rizvi and Abbas, 2023). Various signal-based techniques encompass different domains, such as the time domain (Lan et al., 2023; Zuo and Guo, 2023), the frequency domain (Muñiz-Calvente et al., 2022; Marques et al., 2021), and the time-frequency domain (Skowronek et al., 2023; Karhade et al., 2022). These methodologies are employed to analyze the dynamic characteristics of structures (Chaupal and Rajendran, 2023).

Time-domain methodologies commonly use stochastic processes (Huang et al., 2023). Frequent-domain techniques can generate numerous responses and data points by configuring model-update equations. Some methods of dynamic frequency-domain approaches include modal curvatures (Pau and Eroglu, 2023; Jiang et al., 2023), modal strain energy (Nguyen and Livaoğlu, 2023; Omidi Soroor et al., 2023), mode shape (Nguyen and Wahab, 2023; Khanahmadi et al. 2023), natural frequency (Gillich et al., 2023; Zara et al., 2023), the frequency response function (FRF) (Zhu et al., 2022; Kurent et al., 2023), and the power spectral density function (PSD) (Tang et al., 2022; Shetty and Prabhu, 2023).

PSD is a method that analyzes the frequency response of a periodic or random signal to determine the distribution of mean power. In order to construct a second-order transfer function, this technique uses a sensitive nonlinear function of structural parameters (Fallah et al., 2023). Some studies have been done on damage detection using the PSD method. Fang et al. (2023a) evaluated a novel method for detecting bridge deterioration using complete ensemble empirical mode decomposition (CEEMD) and PSD sensitivity analysis of bridge signals under changing loads. Furthermore, Fang et al. (2023b) improved the efficiency of model updating and showed satisfactory identification results while investigating a method for substructural damage identification using response PSD sensitivity analysis. Bayati et al. (2019) experimented using a new method that combines the power spectral density function and the least-squares distance approach to detect signs of deterioration in concrete bridge piers. Gunawan (2019) evaluated the dependability of the PSD technique for seven 1 kg consolidated masses linked by eight identical linear elastic springs.

Concurrently, governments and people alike are increasingly interested in studying the environmental and social impacts of building lifespans and sustainability. The Brundtland Report's definition of sustainability, which integrates social, economic, and environmental considerations, posits sustainable development as meeting current needs without compromising the ability of future generations to fulfill their own needs (Keeble,1988).

Aligned with this principle, the judicious maintenance of infrastructure assumes critical importance in mitigating unnecessary costs and environmental impacts associated with constructing new assets. Nevertheless, the recent scholarly discourse has underscored the need to meticulously assess the consequences tied to infrastructure maintenance (Liljenström et al., 2022; Renne et al., 2022). This heightened attention stems from the acknowledgment that these ramifications may surpass those related to the initial infrastructure creation, particularly in cases of suboptimal design.

Life Cycle Assessment (LCA) has become a reliable tool for thoroughly assessing the effects of maintenance and making informed decisions. In recent years, extensive research has methodically examined the environmental consequences linked to various infrastructure projects throughout their entire lifespan, including structures such as buildings (Caruso et al., 2020), pavements (Kazemeini and Swei, 2023), railway tracks (Celauro et al., 2032), and urban infrastructure elements (Wang et al., 2020).

LCA is widely recognized as a highly effective method for evaluating the sustainability of concrete buildings. In addition, LCA is a methodical approach employed to assess the environmental and social impacts of a product, process, or activity throughout its entire life cycle, encompassing the extraction of materials to its ultimate disposal (as defined by ISO 14040:2006, ISO 14044:2006).

Creating infrastructures that effectively contribute to the sustainable future our society needs is a top priority and a significant challenge. Engineers and architects are responsible for managing these infrastructures' positive and negative effects on their life cycle. Some research has been done for sustainability and life cycle assessment. Barbhuiya and Das (2023) emphasize the significance of Land Cover Assessment in assessing the environmental effects of construction materials over their entire life cycle. They stress the necessity for standardized methodologies and future directions in LCA research, such as integrating LCA with Building Information Modeling, creating region-specific impact assessment methods, and incorporating social and economic factors. Backes et al. (2023) evaluate carbon-reinforced concrete (CRC) as an alternative to SRC and its environmental impact. They provide a detailed matrix of LCA scenarios, comparing CRC's environmental effect to SRC and innovative components. Also, Navarro et al. (2022) utilized analytic network process-based methods to build a coastal concrete bridge based on nine sustainability criteria. Their research compares five alternative designs' sustainability and life cycle performance to standard Analytical Hierarchy Process (AHP) methods.

Sustainable product design is essential in building. As a major environmental polluter, the construction sector accounts for 30% of world energy consumption, 30% of greenhouse gas emissions, and 40% of raw material exploitation (Choi, 2019). Cement output is expected to increase 1.4 times by 2030 (Imbabi et al., 2013). However, infrastructure is a critical economic and social growth driver since it ensures service delivery and territorial structure.

The International Monetary Fund believes spending 1% of GDP (Gross Domestic Product) on infrastructure would enhance global GDP by 1.5% after four years. In recent years, about 20% of World Bank loans have gone to transport infrastructure (Kyriacou et al., 2019). Construction accounts for 9% of Europe's GDP and 18 million direct employment (Favier et al., 2018). An in-depth analysis of a choice or action's long-term social, environmental, and economic effects is necessary for sustainability.

The construction industry is a prime example of a field that may greatly benefit from incorporating sustainability principles into business practices (Navarro et al., 2023). Designing for sustainability entails considering economic, environmental, and social factors. Thus, while environmental life cycle assessment (E-LCA) has become a standard methodologically and practically (ISO, 2006a, 2006b), social life cycle assessment (S-LCA) is a new field that needs continuous development. Assessing social life cycle implications for sustainability is complex and subjective. In 2009, the UNEP/SETAC (UNEP/SETAC, 2009) developed methodological guidelines for consistent SLCA of products to establish a future standard methodology for social assessments based on ISO 14040.

Given the wide variation in social criteria definitions and SLCA evaluation methods, standardized and conventional approaches are prioritized to align with the established LCA standards. For this reason, thorough product sustainability assessments do not yet have a standard, generally accepted methodology.

While there are standards and guidelines to assist with this process (ISO, 2006a, 2006b; UNEP/SETAC, 2020, 2021), there is still no consensus on how to incorporate life cycle assessment methods with various damage detection methods and how to account for performance with different damage courses in infrastructure sustainability assessments.

This doctorate thesis was carried out at the University Institute of Concrete Science and Technology (ICITECH) located at the Universitat Politècnica de València (UPV). The research group has a vast amount of expertise in this particular domain. The issue has generated many articles that have been a strong basis for this investigation.

1.2. Research objectives

The current doctoral dissertation suggests a comprehensive sustainability evaluation that focuses on the life cycle of constructions and aims to assist in their design by using damage detection techniques. The emphasis is placed on specific physical structures, namely bridges, that are exposed to aggressive environments.

This is due to the significant effects anticipated from the necessary upkeep to ensure these structures remain fully functional during their extended lifespans.

Considering the background provided and the highlighted gaps in knowledge, it is necessary to formulate numerous research questions about the evaluation of infrastructure sustainability and damage detection methods:

Research question 1: How do non-destructive damage identification methods perform in detecting different damages in materials like steel and concrete structures, considering damage factors like chloride corrosion and the structure's location and environment?

Research question 2: How much use of the PSD method as a non-destructive damage detection method can be useful in decreasing total maintenance and repair activity costs and affecting the LCCA for the whole life of the coastal concrete bridge?

Research question 3: How much can a non-destructive damage detection method such as the PSD method improve the impact on the environmental and social life cycle assessment at a structure's maintenance and repair activities?

Research question 4: How much does LCA benefit from non-destructive damage detection methods and deal with expert subjectivity during decision-making to enhance existing multi-criteria decision-making (MCDM) techniques applied in sustainable design?

Research question 5: How can a system for maintenance and repair structures be created to optimize design that aligns with sustainable life cycle assessment and supports the achievement of the Sustainable Development Goals according to non-distractive damage detection methods?

The current Ph.D. thesis introduces an advanced approach for the health monitoring of structures, based on the ISO 14040 standard and tailored explicitly for conducting complete sustainability assessments and designing and maintaining structures. This approach is used to assess alternative designs of particular coastal constructions, considering various aspects of sustainability.

The Ph.D. thesis was founded with the following objectives:

1. A review of existing literature related to structural health monitoring and damage detection methods in structures, as well as a review of existing literature on current trends in structural sustainability assessment techniques used to assess infrastructure, is conducted to find knowledge gaps in LCA, sustainability assessment, and technique decision-making using different approaches to non-destructive damage detection methods for maintenance and repair in bridge design.
2. To propose a methodology for the evaluation, the performance of some non-destructive damage detection methods compare in a bridge.

3. To propose a methodology for integrating a structure's economic, environmental, and social life cycle assessments using damage detection techniques into a single, ISO 14040-based approach.
4. To propose extending AHP techniques to MCDM evaluations to elucidate the relationships between decision criteria, mainly when non-destructive methods are utilized to identify potential damage related to decision-making processes.
5. Use the sustainability assessment approach to select a design and maintenance option for a structure in a coastal location, considering non-destructive damage detection methods through various approaches and their respective sustainability performances.
6. To obtain robust bridge designs, evaluate how economically, environmentally, and socially oriented structure maintenance strategies are impacted by modern methods compared to conventional approaches.

1.3. Methodology

The research methodology employed to accomplish the objectives outlined in this doctoral thesis is organized into distinct phases.

The initial phase involves a systematic review of the current state of infrastructure sustainability assessment and damage detection methods. The literature review examines various aspects. The first aspect of the literature review analyzes techniques for identifying damage and evaluating their effectiveness in determining the extent and location of damage in diverse environments and structures resulting from various factors that cause damage. The following aspect entails investigating and analyzing these approaches to the life cycle and long-term viability. Specifically, it involves exploring sustainability within the framework of infrastructures and employing MCDM techniques to assess them. Regarding the first aspect, the focus is on the particular criteria that are taken into account by the scientific community, as well as the specific techniques used for assessing impact. Regarding the final aspect, the emphasis lies on the implementation of weighting methods and the utilization of specific MCDM techniques. Research has also been conducted on handling linguistic variables in the decision-making process.

In the second phase, evaluate the performance and comparison of non-destructive methods of damage identification in detecting the location and amount of damage in a structure during the lifetime of a structure and examine the ability of each method to predict the time of these damages according to different failure factors in different types of structures. In this research, two non-destructive dynamic and signal-based damage detection methods, including FRF and PSD, have been evaluated and analyzed in a steel truss bridge structure according to different damage scenarios in the structural elements.

In the third phase, according to the comparison of the analyses of each method in predicting the location and amount of damage in a structure, the method with a better ability and less error in identifying the damage was selected as the base method for further detailed investigations in this research. In this regard, the performance of the PSD method has been investigated this time in a coastal concrete bridge structure, where most of its foundations are located and exposed to damage and corrosion during its lifetime. The performance of this method in identifying this type of damage by natural damage factors such as chloride ions and also the effect of this damage on the performance of this damage detection method has been evaluated.

In the fourth phase, there is a need to assess the economic aspects and life cycle cost (LCC) of using any damage methodology in the finished costs incurred in different stages of a structure from the beginning of the design to the end of the structure's life. According to this research, the performance and effect of the PSD method in reducing repair and maintenance costs during the lifetime of a coastal concrete bridge were analyzed. Then, the total costs and the economic aspect of this damage prediction method were compared to a conventional method of damage prediction and evaluated.

The fifth phase was to investigate the performance of the damage identification method in the structure during the assessment life cycle. For this reason, environmental and social effects were tested using the PSD method in the structure. The results of this evaluation determined how much of a positive effect this method has on reducing harmful effects on the environment and society.

In the final phase, the suggested infrastructure sustainability evaluation framework addresses coastal concrete bridge design through a damage detection method. Analyzing the life cycle's economic, environmental, and social aspects determines sustainability. Each design choice requires reliable upkeep. Generally, life cycle evaluations are used to demonstrate their flaws and knowledge gaps, and this thesis uses a complete ISO14040-based approach. A full methodology for damage detection and sustainability life cycle assessment includes functional units, system boundaries, and unit processes. The study uses economics to offer reliability-based optimal maintenance techniques for a life cycle approach in chloride-laden by PSD technique as a non-destructive damage detection for maintenance. MCDM integrates the three sustainability factors into one evaluation. A unique way to group AHP weights is presented to account for the non-probabilistic uncertainty in subjective weighing approaches like AHP. The research holistically evaluates environmental, economic, and social aspects affecting coastal bridge deck and piers sustainability.

1.4. Dissertation structure

The dissertation offers the study organized into several chapters as follows:

- **Chapter 1** presents the background, aims, and primary contributions of the study, along with the methods used to perform the research for the PhD thesis.
- **Chapter 2** evaluated two non-destructive damage detection methods: the Spectral Density Function-based and the Frequency Response Function-based. This case study compares the two approaches' ability to detect damage in a truss bridge under varying experimental conditions.
- **Chapter 3** investigates the ability of the PSD, as a non-destructive damage detection method, to diagnose damages caused by chloride ions in concrete structures. The method's accuracy in estimating the annual damage caused by chloride in various parts and positions exposed to seawater was analyzed. The Reinforced concrete (RC) bridge, which connects the island to the mainland via seawater, was numerically modeled and analyzed for this purpose.
- **Chapter 4** presents an approach to life cycle cost assessment (LCCA) for a span of a coastal concrete bridge according to the performance of the PSD method to predict and monitor the location and amount of damages caused by corrosion during a structure's life using different approaches.
- **Chapter 5** investigates the cost-effectiveness of two methods for predicting damage: the non-destructive dynamic damage detection approach and the conventional method through redesigning different concrete cover thicknesses for a coastal reinforced concrete bridge. The study evaluates the impact of chloride ions on the location and extent of decay throughout the bridge's lifespan while also examining the total costs associated with maintenance and repairs.
- **Chapter 6** proposes non-destructive damage detection methods' impact on the LCA and E-LCA compared to a conventional approach on a coastal concrete bridge.
- **Chapter 7** examines the sustainability and S-LCA according to maintenance and repair through a non-destructive dynamic damage detection method to introduce an innovative approach to evaluating the social aspect of sustainable infrastructure designs using the ISO 14040 standard. Eight multi-criteria parameters and TOPSIS are used for sustainability life cycle analysis. The AHP is used to determine the importance of criteria based on the judgments provided by a group of experts.

- **Chapter 8** provides an analysis of the findings derived from the preceding chapters.
- **Chapter 9** provides a concise overview of this doctoral dissertation's primary overarching and case-specific findings and proposes potential avenues for future investigation.

Chapter 2

Performance comparison of structural damage detection based on frequency response function

Authors:	Mehrdad Hadizadeh-Bazaz; Ignacio J. Navarro; Víctor Yepes		
Status:	Manuscript published		
Journal:	*DYNA*, 97(5). 493-500, 15 pages, 2022		
DOI:	10.6036/10504		
JCR IF (2023)	0.8		
	JCR Category	Ranking	Quartile
	General Engineering	121/179	Q3
Presentation:	Post-print (author version)		

Abstract

Recent catastrophic events have aroused great interest in the scientific community regarding the evaluation and prediction of the structural response along the life cycle of infrastructures. Efforts are put into developing adequate health monitoring systems to help prevent future human life and economic losses. Here, two non-destructive damage detection methods are presented: the Frequency Response Function-based and the Spectral Density Function-based methods. The damage detection performance of both methods is compared through a particular case study, where different damage scenarios are analyzed in a 2D truss bridge. The reliability of each method is studied in terms of different prediction errors. Numerical results show that the PSD method for damage detection on a steel truss bridge structure provides more accurate and robust results when compared to that based on FRF.

Keywords Structural Health Monitoring; Power Spectral Density Function; Frequency Response Function; Construction, Structures; Damage detection; Non-destructive

2.1. Introduction

The deterioration of the existing infrastructure has become a severe concern in developed countries. More than 30% of construction activity is currently related to the maintenance and refurbishment of damaged structures (Gil Benso et al., 2015), revealing infrastructure maintenance and improvement as a significant source of long-term impacts (Sierra et al., 2017). As a result, while there is much interest in optimal structure design to reduce construction costs (Paya-Zaforteza et al., 2010; García-Segura et al., 2017; Penadés-Plà et al., 2017), structural deterioration mitigation has become a focus of many researchers aiming to provide optimal maintenance strategies to reduce life cycle costs (Navarro et al., 2019; Sajedi et al., 2019; Navarro et al., 2018).In such a context, information regarding damage detection and location has been crucial to increasing the accuracy of damage prediction methods assumed in maintenance optimization.

Actual trends in health monitoring of structures rely on the dynamic response variations associated with structural systems when deteriorated. Dynamic properties such as mass, stiffness, and damping may assist in identifying the location and extent of damage to structures according to non-destructive damage detection for numerical model updating in a structure (Pedram et al., 2016; Li et al., 2015; Pehlivan, 2018). Recently, some investigations have used or assessed the reliability and performance of dynamic techniques, either numerical or experimental, for non-destructive damage detection in steel, concrete, or composite structures. Some dynamics and vibration-based damage detection methods were evaluated by some researchers, such as: frequency response functions (Garcia-Palencia et al., 2015; Sulaiman et al., 2017), power spectral density (Li et al., 2015; Esfandiari et al., 2018), natural frequencies (Sha et al., 2019; He & Zhu, 2011), measured modal flexibility (Wickramasinghe et al., 2020; Liu et al., 2018), modal strain energy (Yang et al., 2019; Teng et al., 2019), mode shapes (He et al., 2018). Some researchers have used these methods individually or combined two or more (Padil et al., 2020; Bagherahmadi & Seyedpoor, 2018; Barman et al., 2021). Also, to compare the performance of these methods of identifying damage, some of these methods have been compared (Altunışık et al., 2019; Rezvani & Sabour, 2018; Gomes & Silva, 2008; Kim & Eun, 2017). One of the most important ways to help engineers and experts choose and use the best method for the situation and type of structure is to compare the methods for diagnosing failure in different types and shapes of structures. Frequency response function (FRF) and power spectral density (PSD) methods are two common and popular methods based on the signal in damage detection. Comparing the performance and ability of these two methods in different conditions and structural shapes can be helpful information for researchers and engineers when selecting and using each of these methods in their studies.

In this regard, researchers on the FRF-based method followed some purposes. A structural model updating method based on FRF data and observed natural frequencies of the damaged structure was investigated according to the sensitivity equations to decrease model update nonlinearity. These sensitivity equations were also solved using Least Squares, non-linear (Esfandiari et al., 2010), and linear (Vahedi & Khoshnoudian, 2018). The capacity of the FRF approach was evaluated in a model by simulating the mass modeling errors, and the stiffness degradation of structural parts was explored simultaneously in the other case. The research showed that the FRF method for updating findings was resistant to incompleteness, noise, and modeling error (Shadan et al., 2016). Also, a study examined the benefits of substituting unmeasured FRFs with EDTF in an accurate sensitivity equation. Extensive numerical experiments were done comparing this technique's results with the dynamic expansion of observed mode shapes. Both techniques have advantages and disadvantages in mitigating the detrimental effects of incomplete measurement (Pedram & Esfandiari, 2019).

On the other hand, the PSD approach for damage detection was investigated in some publications. In a study, the pseudo excitation method (PEM) was used to get the dynamic response of structures and the power spectral density sensitivity to damage factors. This approach was used to repeatedly obtain damage parameters by the finite element model updating method in two numerical examples, including a flat-frame building and a 12-story shear building (Zheng et al., 2015). A unique algorithm and deterioration index for bridge concrete piers were developed. The power spectral density function was utilized to process structural responses. A damage index based on the least square distance was developed to diagnose the damage. The suggested algorithm and damage index may reliably identify and locate deterioration in bridge piers (Bayat1a et al., 2019). An industrial engineering researcher hypothesized that the method's accuracy highly depends on the degree of damage. They tested the dependability using a massive dataset of 3500 incidents in a spring model with five degrees of structural integrity. When the structural integrity declined by 5%, the reliability plummeted to 95% (Gunawan, 2019).

To date, the performance of FRF and PSD methods has been evaluated and compared for a variety of structural systems and follows different approaches. For instance, some researchers compared the quasi-linear sensitivity of FRF with the derivation-based sensitivity of PSD to develop a sensitivity-based damage detection approach in a numerical frame and an experimental beam model (Pedram et al., 2017). Moreover, in the numerical models of plate and shell structures, updating frequency domain models using PSD to overcome the shortcomings of incomplete measurement allowed the sensitivity equation according to measured natural frequencies of a few lower modes (Pedram et al., 2018). Because the performance of frequency-based methods can differ in different types of structures and under different conditions, and in addition, construction, maintenance, and repair costs are essential for structures such as bridges, in this study, the performance of these two methods was compared with different approaches for detecting the extent, amount and location of damages on a numerical model of a two-dimensional steel truss bridge. For this purpose, these methods were compared by numerical analysis of the different elements of the structural system by using sensitivity equations. These equations were solved through the linear least square algorithm and model updating approach by monitoring changes in dynamic characteristics such as stiffness and mass of undamaged and damaged structural elements. The Closeness Index (CI), the Mean Size Error (MSE), and the

Relative Error (RE) were used to evaluate the accuracy of predictions. Linearizing equations solve a non-linear relationship between structural parameters and observed response.

2.2. Damage detection methods

Generally, the FRF-based methods extract the structure data by exciting the degrees of freedom (DOF) and conducting measurements in the desired DOFs. The selection of these measurement locations significantly impacts obtaining adequate damage detection results. The number of measurement locations is limited practically and economically (Esfandiari et al., 2009; Farshadi et al., 2017). On the other hand, the PSD-based method is a second-order transfer function by a sensitive and utterly non-linear function of structural parameters (Zheng et al., 2015). The following paragraphs present the mathematical background of each technique.

2.2.1. Frequency Response Function (FRF)

FRF is a transfer function (H(ω)) in the frequency domain that relates the displacement response of a structural system with its forces, as shown in Figure 2.1. Therefore, such transfer function represents the structural behavior of the structure under analysis (Sulaiman et al., 2017). The transfer function (H(ω)) varies due to changes in mass, damping, and stiffness, making FRF an ideal method for detecting damage. Some research has mentioned equations related to the FRF (Padil et al., 2020; Esfandiari et al., 2010; Vahedi & Khoshnoudian, 2018; Shadan et al., 2016; Pedram & Esfandiari, 2019; Pedram et al., 2018).

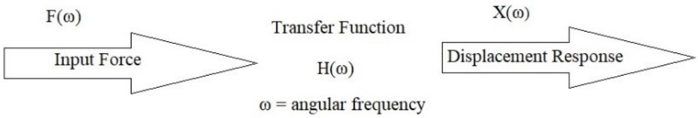

Figure 2.1. *Transfer Function of FRF with Input Force to Displacement Response*

The analytical equation defining the FRF can be derived from the equation of motion of a structural system with n degrees of freedom:

$$\boldsymbol{M}\ddot{\boldsymbol{x}}(\boldsymbol{t}) + \boldsymbol{C}\dot{\boldsymbol{x}}(\boldsymbol{t}) + \boldsymbol{K}\boldsymbol{x}(\boldsymbol{t}) = \boldsymbol{f}(\boldsymbol{t}) \qquad (2.1)$$

Where *M*, *C*, and *K* represent the structural system's mass, damping, and stiffness matrices, respectively, *f(t)* represents the input force vector applied to the system, and *x(t)* is the nodal displacement vector. Assuming that the force input is harmonic, exciting force *f(t)* and the resulting displacement *x(t)* can be expressed as:

$$\boldsymbol{f(t) = F(\omega)e^{i\omega t}} \qquad (2.2)$$

$$\boldsymbol{x(t) = X(\omega)e^{i\omega t}} \qquad (2.3)$$

Where *F(ω)* and *X(ω)* are the displacements and the applied force expressed in the frequency domain, respectively, and ω is the excitation frequency of the structure. Substituting Equations 2.2 and 2.3 in Equations 2.1:

$$[-\boldsymbol{M\omega^2} - \boldsymbol{i\omega C} + \boldsymbol{K}]\boldsymbol{X(\omega)} = \boldsymbol{F(\omega)} \qquad (2.4)$$

The equation can be rewritten to derive the analytical expression for the FRF transfer matrix *H(ω)*:

$$\boldsymbol{H(\omega)} = [-\boldsymbol{M\omega^2} + \boldsymbol{i\omega C} + \boldsymbol{K}]^{-1} \qquad (2.5)$$

A formula for changing the transfer matrix when the structural system is damaged from the above equations is given below. To do so, on the one hand, we shall consider that the structural response $X_i(\omega)$ of a particular degree of freedom i of the system, when a unitary harmonic load $F_l(\omega)$ is applied, can be expressed as:

$$\boldsymbol{X_i(\omega) = H_{il}(\omega)F_l(\omega) = H_{il}(\omega)} \qquad (2.6)$$

Where $F_l(\omega)$ is a vector with every component equal to zero except for the component *l*, which is equal to one, on the other hand, the structural response of a system can also be obtained as a linear superposition of modes:

$$\boldsymbol{X} = \sum_{r=1}^{n} \boldsymbol{\varphi_r q_r} \qquad (2.7)$$

Where φ is the mode shape matrix, and q represents the modal coordinate matrix. Thus, Equation. 2.1 can be rewritten as:

$$\boldsymbol{M\varphi_r \ddot{q}_r + C\varphi_r \dot{q}_r + K\varphi_r q_r = f(\omega)} \qquad (2.8)$$

Multiplying both sides of Equation 2.1 by the transposed mode shape matrix, we get:

$$(-\boldsymbol{\omega}^2\boldsymbol{\varphi}_r^T\boldsymbol{M}\boldsymbol{\Phi}_r + \boldsymbol{i\omega}\boldsymbol{\varphi}_r^T\boldsymbol{C}\boldsymbol{\Phi}_r + \boldsymbol{\varphi}_r^T\boldsymbol{K}\boldsymbol{\Phi}_r)\overline{\boldsymbol{q}}_r = \boldsymbol{\varphi}_r^T\boldsymbol{F}(\boldsymbol{\omega})\boldsymbol{e}^{\boldsymbol{i\omega t}} \quad (2.9)$$

This equation can be simplified into:

$$(-\boldsymbol{\omega}^2\boldsymbol{M}_r + \boldsymbol{i\omega}\boldsymbol{C}_r + \boldsymbol{K}_r)\overline{\boldsymbol{q}}_r = \boldsymbol{\varphi}_r^T\boldsymbol{F}(\boldsymbol{\omega}) \quad (2.10)$$

The relation between the mass, damping, and stiffness matrices can also be expressed in modal terms as:

$$\boldsymbol{C}_r = \boldsymbol{2\xi}_r\boldsymbol{\omega}_r\boldsymbol{M}_r \quad (2.11)$$

$$\boldsymbol{K}_r = \boldsymbol{M}_r\boldsymbol{\omega}_r^2 \quad (2.12)$$

Consequently, we can rewrite Equation 2.9 into:

$$(-\boldsymbol{\omega}^2 + \boldsymbol{i\omega}(\boldsymbol{2\xi}_r\boldsymbol{\omega}_r) + \boldsymbol{\omega}_r^2)\overline{\boldsymbol{q}}_r = \boldsymbol{\varphi}_r^T\boldsymbol{F}(\boldsymbol{\omega}) = \boldsymbol{\varphi}_{lr} \quad (2.13)$$

By placing Equation 2.12 into Equation 2.6, we get:

$$\boldsymbol{H}_{il} = \sum_{r=1}^{n} \frac{\boldsymbol{\varphi}_{ir}\boldsymbol{\varphi}_{lr}}{\boldsymbol{\omega}_r^2 - \boldsymbol{\omega}^2 + \boldsymbol{2i\omega\xi}_r\boldsymbol{\omega}_r} \quad (2.14)$$

Where φ_r represents the structural mode, ω_r is the natural frequency, and ξ_r is the modal damping. In fact, in the above equation, H_{il} is the displacement of the degree of freedom i when the unit load excites the degree of freedom l. When the structure has deteriorated, the modal response of the system changes as follows:

$$\boldsymbol{\varphi}_{rdi} = \boldsymbol{\varphi}_{ri} + \boldsymbol{\delta\varphi}_{ri} \quad (2.15)$$

Where φ_{rdi} represents the mode shape of the damaged structure for the degree of freedom i, and $\delta\varphi_{ri}$ stands for its deformation rate. Therefore, Equation 2.14 can be rewritten for a damaged structure as:

$$\boldsymbol{H_{ild}} \cong \sum_{r=1}^{nm} \frac{\boldsymbol{\varphi_{ird}\varphi_{lrd}}}{\boldsymbol{\omega_{rd}^2 - \omega^2 + 2i\omega\xi_{rd}\omega_{rd}}} + \sum_{r=nm+1}^{nm} \frac{\boldsymbol{\varphi_{ir}\varphi_{lr}}}{\boldsymbol{\omega_r^2 - \omega^2 + 2i\omega\xi_r\omega_r}} \tag{2.16}$$

Equation 2.16 approximation is not unrealistic because natural frequencies can be obtained with high accuracy. The second part of the Equation 2.16 deals with the unmeasured portion of natural frequencies and damping coefficients and reduces the effect of incomplete measurement. By inserting Equation 2.15 into the first part of Equation 2.16, it is derived that:

$$\boldsymbol{H_{ild}} \cong \boldsymbol{\widetilde{H}_{il} + \Delta H_{il}} = \sum_{r=1}^{nm} \frac{\boldsymbol{\varphi_{ir}\varphi_{lr}}}{\boldsymbol{\omega_{rd}^2 - \omega^2 + 2i\omega\xi_{rd}\omega_{rd}}} + \sum_{r=nm+1}^{n} \frac{\boldsymbol{\varphi_{ir}\varphi_{lr}}}{\boldsymbol{\omega_r^2 - \omega^2 + 2i\omega\xi_r\omega_r}} + \sum_{r=1}^{nm} \frac{\boldsymbol{\varphi_{ir}\delta\varphi_{lr}}}{\boldsymbol{\omega_{rd}^2 - \omega^2 + 2i\omega\xi_{rd}\omega_{rd}}} + \sum_{r=1}^{nm} \frac{\boldsymbol{\delta\varphi_{ir}\varphi_{lr}}}{\boldsymbol{\omega_{rd}^2 - \omega^2 + 2i\omega\xi_{rd}\omega_{rd}}} \tag{2.17}$$

The modal deformation rate $\delta\varphi_{lr}$ can be obtained by:

$$\boldsymbol{\delta\varphi_{lr}} \cong \sum_{q=1}^{n} \boldsymbol{\alpha_{rq}\varphi_{lq}} \tag{2.18}$$

Where α can be calculated as follows, by multiplying both sides of Equation 2.12 by the mode matrix φ_q and deriving it, we get:

$$\boldsymbol{\delta K\varphi_q + K\delta\varphi_q = \delta M\varphi_q\omega_q^2 + M\delta\varphi_q\omega_q^2 + 2M\varphi_q\omega_q\delta\omega} \tag{2.19}$$

Sorting Equation 2.19 appropriately, the value of α can be obtained as:

$$\begin{cases} \alpha_{rq} = \dfrac{\varphi_q^T(\delta K - \omega^2 \delta M)\varphi_r}{(\omega_r^2 - \omega_q^2)} & for \quad q \neq r \\ \alpha_{rq} = -\dfrac{\varphi_q^T(\delta M)\varphi_r}{2} & for \quad q = r \end{cases} \tag{2.20}$$

Since the mass changes due to deterioration are usually minor compared to the changes in stiffness, changes in mass are neglected when deriving the above equations. Taking this assumption into account (*δM= 0*), we can rewrite the second term of Equation 2.17, namely ΔH_{il} as:

$$\begin{aligned} \Delta H_{il} &= \sum_{r=1}^{nm} \frac{\varphi_{ir}\delta\varphi_{lr}}{\omega_{rd}^2 - \omega^2 + 2i\omega\xi_{rd}\omega_{rd}} + \sum_{r=1}^{nm} \frac{\delta\varphi_{ir}\varphi_{lr}}{\omega_{rd}^2 - \omega^2 + 2i\omega\xi_{rd}\omega_{rd}} \\ &= \sum_{r=1}^{nm}\sum_{q=1}^{n} \frac{\varphi_{ir}(\varphi_q^T\delta K\varphi_i)\varphi_{lq}}{(\omega_{rd}^2 - \omega^2 + 2i\omega\xi_{rd}\omega_{rd})(\omega_i^2 - \omega_q^2)} + \sum_{r=1}^{nm}\sum_{q=1}^{n} \frac{(\varphi_q^T\delta K\varphi_i)\varphi_{iq}\varphi_{lr}}{(\omega_{rd}^2 - \omega^2 + 2i\omega\xi_{rd}\omega_{rd})(\omega_i^2 - \omega_q^2)} \end{aligned} \tag{2.21}$$

Defined the stiffness matrix of healthy (K_h) and damaged (K_d) structures as follows:

$$K = APA^T \tag{2.22}$$

$$K_d = K + \delta K = A(P + \delta P)A^T \tag{2.23}$$

The matrix *A* is a function of the geometric properties of the elements, and the diagonal matrix *P* contains mechanical properties (like bending and axial stiffness). If we consider that the stiffness changes are reflected in changes in the *P* matrix, we will have the following:

$$\delta K = A\delta PA^T \tag{2.24}$$

Finally, if we place Equation 2.24 into Equation 2.21, we get an analytical expression for the variations in the transfer matrix due to the deterioration of the structural system:

$$\begin{aligned}\Delta H_{il} &= [\sum_{r=1}^{nm}\sum_{q=1}^{n}\frac{\varphi_{ir}(\varphi_q^T\,Adiag(A^T\varphi_r))\varphi_{lq}}{(\omega_{rd}^2-\omega^2+2i\omega\xi_{rd}\omega_{rd})(\omega_i^2-\omega_q^2)} \\ &+\sum_{r=1}^{nm}\sum_{q=1}^{n}\frac{\varphi_{iq}(\varphi_q^T\,Adiag(A^T\varphi_r))\varphi_{lr}}{(\omega_{rd}^2-\omega^2+2i\omega\xi_{rd}\omega_{rd})(\omega_i^2-\omega_q^2)}]\delta P \\ &= S_H\delta P\end{aligned} \quad (2.25)$$

2.2.1. Power Spectral density (PSD)

FRF methods rely on adequate monitoring of the structure to be analyzed. Given that it is neither practical nor economical to excite and monitor every degree of freedom of a structure, PSD-based methods are recognized as an alternative to overcome such limitations of FRF damage detection methods. Based on the equations in random vibrations, the spectral density function of a structural response can be expressed as following equations according to some research on the PSD method (Zheng et al., 2015; Pedram et al., 2017; Pedram et al., 2018).

$$S_{XX} = HS_{ff}H^T \quad (2.26)$$

S_{XX} is the output response PSD function, S_{ff} is the input response PSD function, and H is the transference function presented in the previous section. Taking into account Equation 2.17, S_{XX} can be obtained for a damaged structural system as:

$$\begin{aligned}S_{xxd} \cong \widetilde{H}S_{ff}\widetilde{H}^T + \Delta HS_{ff}\widetilde{H}^T + \widetilde{H}S_{ff}\Delta H^T \\ + \Delta H^T S_{ff}\Delta H^T\end{aligned} \quad (2.27)$$

From the above, it can be derived that the variation of the output response PSD function when the structural system under analysis is damaged can be expressed as follows:

$$\begin{aligned}\Delta S_{xx} &= S_{xxd} - \widetilde{H}S_{ff}\widetilde{H}^T \\ &= \Delta HS_{ff}\widetilde{H}^T + \widetilde{H}S_{ff}\Delta H^T\end{aligned} \quad (2.28)$$

Assuming the value of *ΔH* deduced in Equation 2.25, we can rewrite Equation 2.28 as:

$$\boldsymbol{\Delta S_{xx} \cong [S_H S_{ff} \widetilde{H}^T + \widetilde{H} S_{ff} S_H^T]\delta P} \qquad (2.29)$$

Taking into consideration the analytical expression of S_H presented in Equation 2.25, we can formulate the final sensitivity equation as follows:

$$\boldsymbol{S_s = S_H S_{ff} \widetilde{H}^T + \widetilde{H} S_{ff} S_H^T =} \qquad (2.30)$$

$$= [\sum_{r=1}^{nm}\sum_{q=1}^{n} \frac{\varphi_{ir}(\varphi_q^T\, Adiag(A^T\varphi_r))\varphi_{lq}}{(\omega_{rd}^2 - \omega^2 + 2i\omega\xi_{rd}\omega_{rd})(\omega_i^2 - \omega_q^2)}$$
$$+ \sum_{r=1}^{nm}\sum_{q=1}^{n} \frac{\varphi_{iq}(\varphi_q^T\, Adiag(A^T\varphi_r))\Phi_{lr}}{(\omega_{rd}^2 - \omega^2 + 2i\omega\xi_{rd}\omega_{rd})(\omega_i^2 - \omega_q^2)}]\, S_{ff}[\sum_{r=1}^{nm} \frac{\varphi_{ir}\varphi_{lr}}{\omega_{rd}^2 - \omega^2 + 2i\omega\xi_{rd}\omega_{rd}}$$
$$+ \sum_{r=nm+1}^{n} \frac{\varphi_{ir}\varphi_{lr}}{\omega_d^2 - \omega^2 + 2i\omega\xi_d\omega_d}]^T + [\sum_{r=1}^{nm} \frac{\varphi_{ir}\varphi_{lr}}{\omega_{rd}^2 - \omega^2 + 2i\omega\xi_{rd}\omega_{rd}}$$
$$+ \sum_{r=nm+1}^{n} \frac{\varphi_{ir}\varphi_{lr}}{\omega_d^2 - \omega^2 + 2i\omega\xi_d\omega_d}] S_{ff}[\sum_{r=1}^{nm}\sum_{q=1}^{n} \frac{\varphi_{ir}(\varphi_q^T\, Adiag(A^T\varphi_r))\varphi_{lq}}{(\omega_{rd}^2 - \omega^2 + 2i\omega\xi_{rd}\omega_{rd})(\omega_i^2 - \omega_q^2)}$$
$$+ \sum_{r=1}^{nm}\sum_{q=1}^{n} \frac{\varphi_{iq}(\varphi_q^T\, Adiag(A^T\varphi_r))\varphi_{lr}}{(\omega_{rd}^2 - \omega^2 + 2i\omega\xi_{rd}\omega_{rd})(\omega_i^2 - \omega_q^2)}]^T$$

Finally, the PSD function can be formulated as:

$$\boldsymbol{\Delta S_{xx} \cong S_s \delta P} \qquad (2.31)$$

Where *δP* represents the structural changes in the system's stiffness resulting from deterioration, by solving Equation 2.31, the changes in stiffness for damaged structures can be calculated by comparison with the response of the undamaged structure using the least square method. This equation is solved through iteration. The stiffness matrix of the undamaged structure is updated according to the calculated stiffness change, thus modifying the PSD in every iteration and model updating and causing more accurate damage prediction. The difference obtained between the damaged and the undamaged structure is as much as the damage aimed to evaluate.

2.3. Numerical example

The presented damage detection algorithm was applied to an eight-bay truss structure with the geometry, connectivity, and active DOFs shown in Figure 2.2. Each span is 1.5m for a total of 12m. The structure is modeled numerically using the finite element method, with structural elements stressed by axial loads. Truss elements are made from steel with Young's modulus of 200 Gpa and a mass density of 7300 kg/m3. The structure consists of 35 steel elements connected by 16 nodes. The cross-sectional areas for elements 1–8 (top chord), 9–16 (Bottom chord), 17–23 (vertical), and 24–

35 (Diagonal bracing) are respectively 1.8, 1.5, 1.0, and 1.2 (cm2). 29 active DOFs were considered, with 2 degrees of freedom per node (Figure 2.2(b)). Nodes can only move horizontally and vertically except for node 1, where no displacement is allowed, and node 9, where only horizontal motions are allowed. Every system element has steel material attributes.

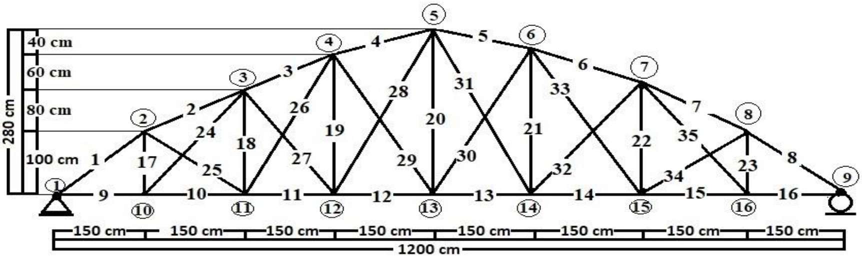

(a)

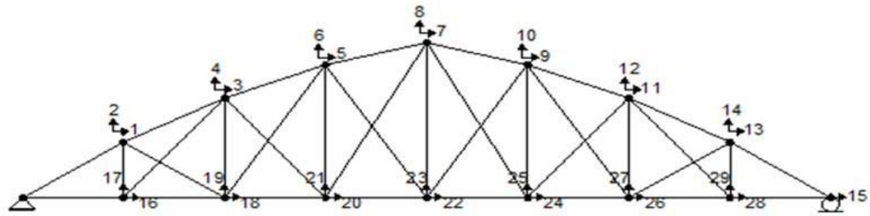

(b)

Figure 2.2. *The trust model information: (a) Geometry; (b) Active degree of freedom direction*

In this model, loads are applied at the structure's nodes so that only axial forces act on each element. Therefore, the structure's stiffness is given by the axial stiffness of the truss elements, defined by their cross-sectional area and the modulus of elasticity of the assumed material. A decrease in the steel modulus of elasticity shows how the steel will degrade since these values are assumed to remain constant.

The injury scenarios considered to determine the differences in the accuracy of the FRF and PSD damage detection methods are presented in Table 2.1 below. In order to identify more groups of possible damage to the structure, it is assumed that the damages can differ in each scenario.

Table 2.1. *Damage scenarios considered.*

Damage Mode	Element Number	Percentage of Damage
1	5	30
	14	50
2	14	40
	16	50
	23	60
3	3	30
	11	30
	32	30
	35	30
4	7	30
	19	40
	27	30
5	2	30
	9	40
	13	50
	29	40
	33	30
6	10	30
	17	30
	26	30
	34	30
7	6	40
	20	70
8	8	30
	24	40
	31	60

Damages in different structures can appear in different ways, which in concrete structures are usually on the surface and deep cracks on the structural elements. In steel structures, it appears as corrosion and rust in coastal environments. It shall be noted that there are not all the damage types that may appear on a structure. However, for simplicity and interpretation of the results, the actual comparative research is focused solely on deterioration caused naturally. The truss structure is modeled numerically using the finite element method by the Software.

2.3.1. Calebration of the numerical model

Excitation frequency ranges, selection, number and location of measurements, and simulation DOFs all play a role in the success of a model updating scheme using FRF and PSD data. For this purpose, selected a scenario of damage in Table 2.1 and used different DOFs set groups in Table 2.2 as base data for assessment by one of these methods. In this study, for selecting suitable DOFs set as the base data of the measurement locations and excitation loads data for analysis of the eight damage prediction scenarios, some groupsets were considered in Table 2.2 mentioned four of them as samples.

The rotating DOFs were not subjected to stimulation or measurement. Each set was analyzed using the FRF method to predict the damage percentage in the structure for the first scenario from Table 2.1.

Table 2.2. *The measurements and stimulation DOFs set*

Sets	Measurements DOFs	Stimulations DOFs	Test according to scenario 1		
			Predicted damage (%)		RMSE*
			Element 5	Element 14	
1	3-9-14-22-24	8-11-13-17-18-25	-5	25	30.4%
2	4-11-13-21-27	6-7-12-17-18-23	20	-5	39.5%
3	4-7-10-25-27	4-7-11-16-20-25	-8	-8	49.0%
4	9-13-15-17-19	7-9-11-14-17-18-27-28	40	48	7.2%

*RMSE: The Root Mean Square Error

Table 2.2 shows the RMSE for scenario 1 through the fourth set of the measurements and stimulations DOFs set are less than other sets. So, as base data to analyses in software for damage prediction by FRF and PSD methods for the eight damage scenarios of Table 2.1, the DOFs 9, 13, 15, 17, and 19 are selected as the measurement locations, and DOFs 7, 9, 11, 23, 25, and 29 as excitation loads were assumed.

Due to imperfections such as ambient noise, FE modeling mistakes, and measurement errors, inevitable errors, and variances in finite element model update results are inevitable. To test the suggested method's resilience against measurement error, 10% random error is considered for each FRF and PSD method.

For scenario 1, Figure 2.3 illustrates the comparison of the FRFs of damaged and undamaged buildings determined from vibration testing.

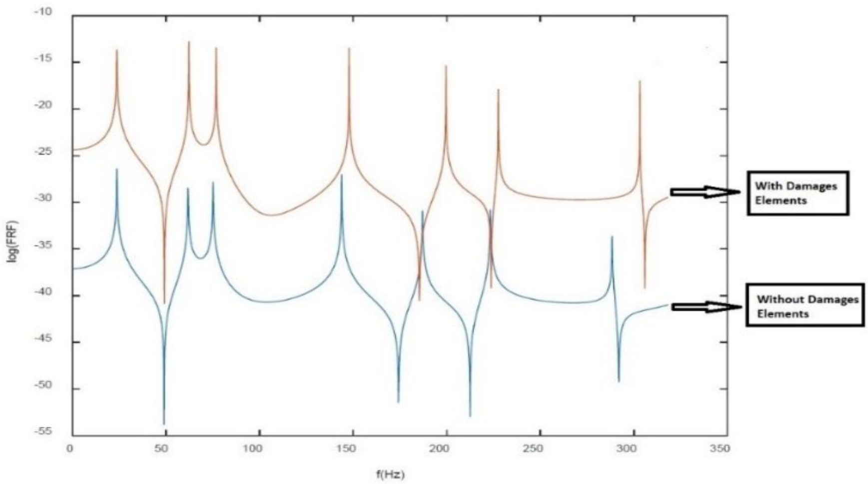

Figure 2.3. *Comparison of the FRFs according to the damaged and undamaged elements for the scenario 1*

As shown in Figure 2.3, response frequency by the FRF for undamaged and damaged structures was used to determine the structure damage situation. The diagram also shows that the first scenario using the FRF method at low frequencies is almost ineffective and gradually increases with increasing frequency at the selected excitation fourth set in Table 2.2, which indicates an increase in damage and a decrease in stiffness of some elements. The FRF data for the damaged structure was moved from the undamaged structure due to the structure's loss of stiffness due to the damage.

2.4. Results and Discussion

Each damage detection method, such as FRF and PSD Function, was compared with its anticipated damage rate on software and the actual damage rate in each damaged situation in Table 2.1 for comparison and assessment using MATLAB software and the formulae and equations.

As shown in Figure 2.4, the damage prediction results for each of the eight damaged situations in Table 2.1 are shown in a chart bar for each technique in Table 2.1.

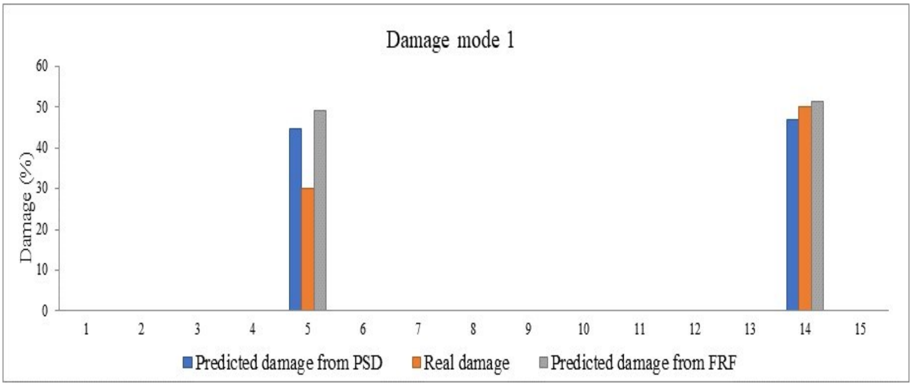

(a) Scenario 1

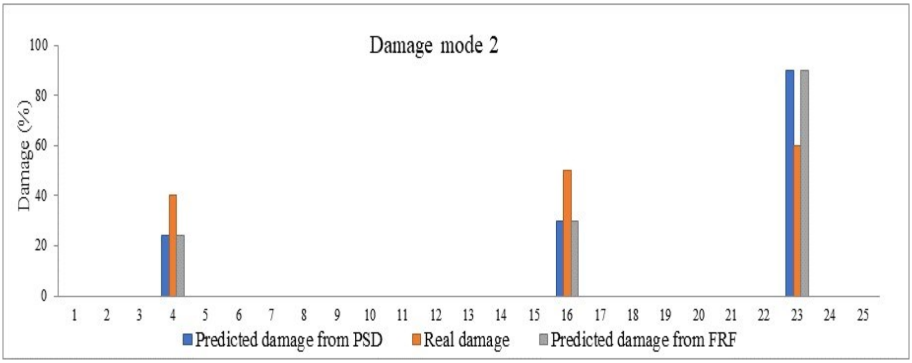

(b) Scenario 2

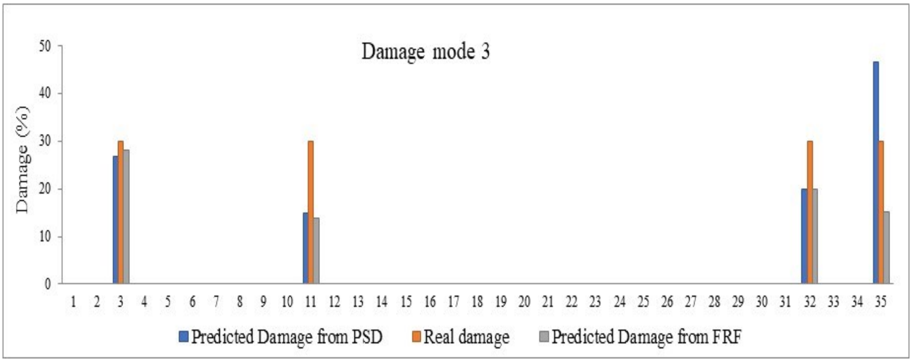

(c) Scenario 3

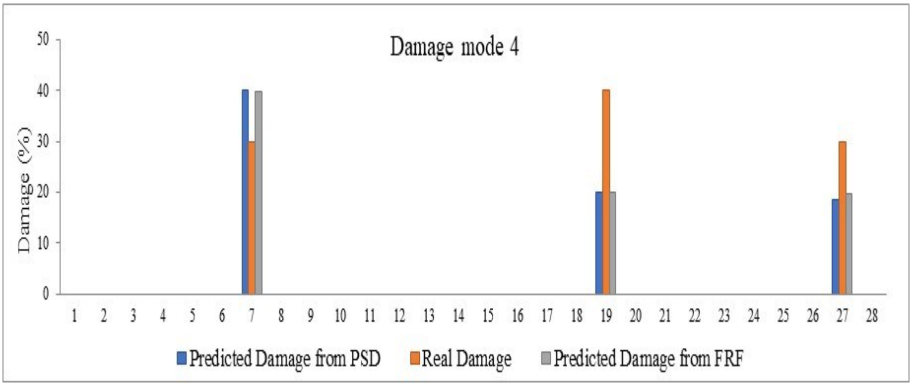

(d) Scenario 4

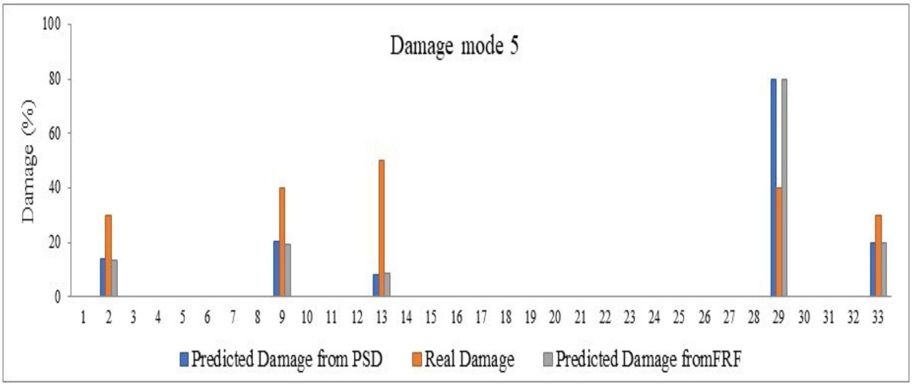

(e) Scenario 5

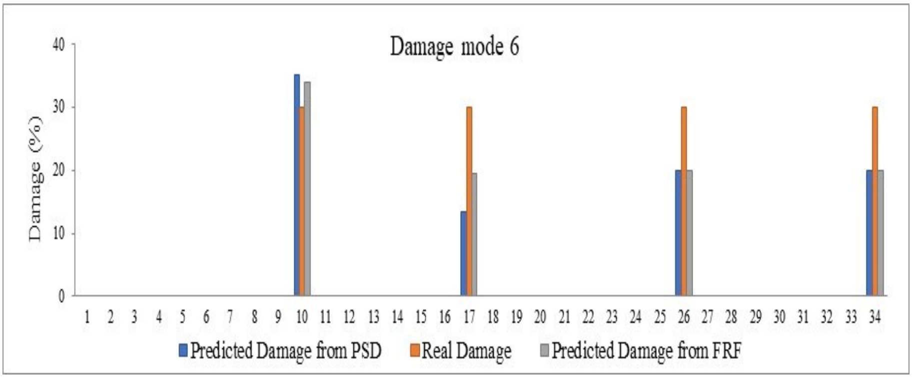

(f) Scenario 6

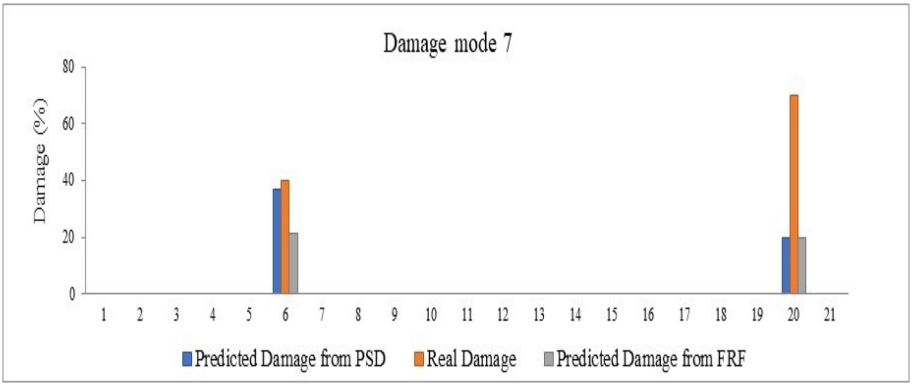

(g) Scenario 7

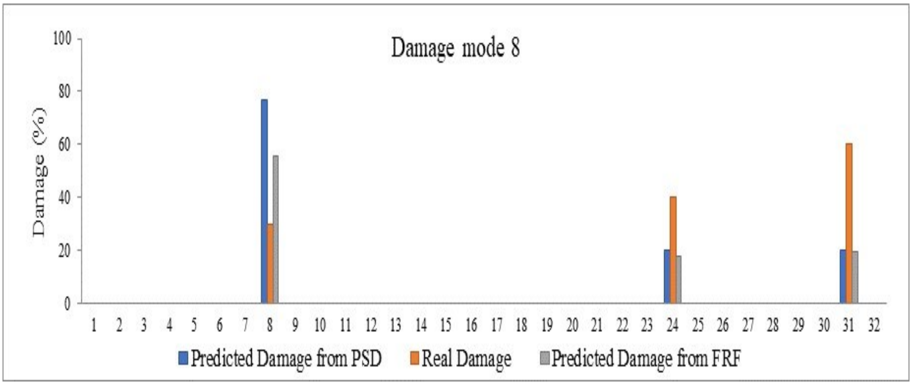

(h) Scenario 8

Figure 2.4. *Comparison of The Predicted Damage with FRF and PSD methods and for different scenarios*

In Figure 2.4, the teal damages are damaged elements from scenarios considered in Table 2.1 as actual damages. After analysis, the percentage of predicted damages by FRF and PSD methods for each scenario is compared according to the same conditions.

Three alternative error assessments are examined to quantify the quality of the predictions, namely the Closeness Index (CI), the Mean Size Error (MSE), and the Relative Error (RE) (Esfandiari et al., 2010).

The Closeness Index indicates how close the predicted amount of damage has relation to the actual damage to the structure:

$$CI = 1 - \frac{|\delta p_p - \delta p_a|}{|\delta p_a|} \tag{2.32}$$

Where δP_P is the predicted damage, and δP_a is the actual damage in each of the considered damage scenarios. A value of the closeness index equal to 1 means an exact fit of the prediction. The *MSE* is the average of the absolute differences between the actual and the predicted damage:

$$MSE = \frac{1}{n}\sum_{i=1}^{n}|\delta p_{ai} - \delta p_{pi}| \tag{2.33}$$

The n denotes the number of structural elements. The Relative Error Index of a prediction shall be calculated as:

$$\boldsymbol{RE} = \frac{\sum_{i=1}^{n}|\delta p_{ai}| - \sum_{i=1}^{ni}|\delta p_{ai}|}{\sum_{i=1}^{ni}|\delta p_{ai}|} \qquad (2.34)$$

Figure 2.5 shows the results of the abovementioned error indices for the two prediction methods. It can be observed that, in general, PSD shows better *CI* results, with prediction errors ranging from 0.36 to 0.73. As far as *MSE* is concerned, for the damage scenario 2, PSD presents slightly worse results than FRF. It shall be noticed that the error regarding damage scenario 5 is, as in the case of *CI* evaluation, the scenario with the highest error for both detection methods. This equation can be attributed to the model's numerical errors rather than the goodness of predictions. At last, the *RE* results do not show sensitivity to the damage scenario under study, presenting prediction errors that do not exceed 0.63 in the worst case. In general, PSD-based predictions result in lower *RE* values than those derived from the FRF method.

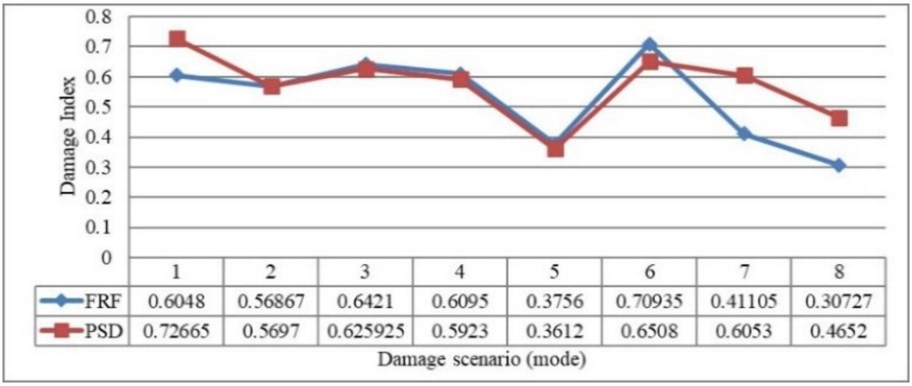

(a) Closeness Index

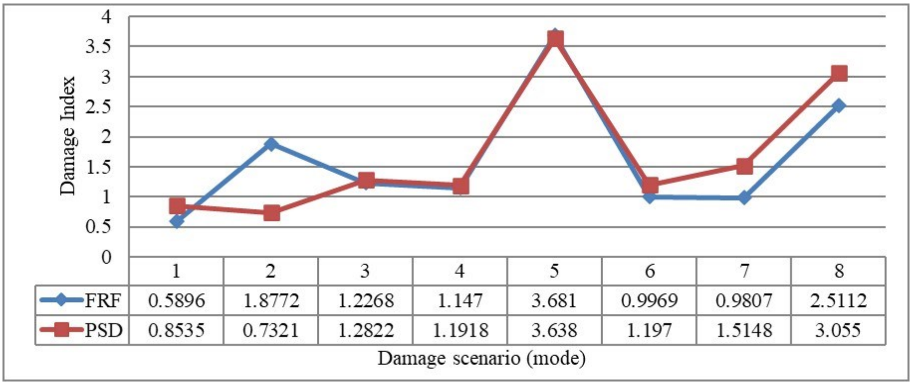

(b) Mean Size Error

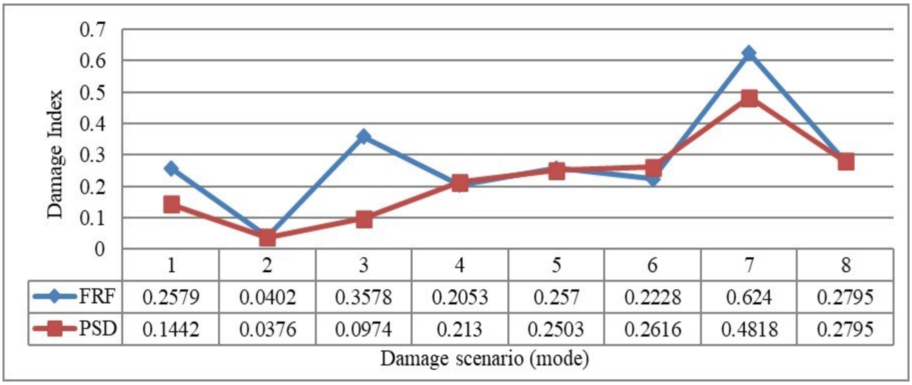

(c) Relative Error

Figure 2.5. *Error Indices results for The Two methods of Damage Detection for the eight scenarios.*

The average achieved for PSD and FRF in the three error metrics studied here is shown in Table 2.3. In addition, for each detection technique, the interquartile range (IQR) was determined to define the statistical dispersion of the data.

Table 2.3. *Summary of Average Errors and IQR*

Methods	CI		MSE		RE	
	Average	IQR*	Average	IQR*	Average	IQR*
FRF	0.529	0.355	1.351	2.644	0.281	0.433

PSD	0.575	0.303	1.246	2.30	0.221	0.352
*IQR: The interquartile range measurements						

Compared to FRF, PSD performs better in average results for each of the three error measures evaluated, with an average *CI* closer to one and average *MSE* and *RE* values closer to zero. In each of the three error measurements, PSD displays IQR values that are lower than those obtained using the FRF approach. According to the findings obtained for the case study under consideration, PSD outperformed FRF and provides more trustworthy damage prediction predictions.

As previously investigated based on numerical results, FRF and PSD methods have been compared on a numerical model of a 2D one-story by one-bay steel frame and a laboratory concrete beam vibration test (Pedram et al., 2017). The comparison result with the FRF was made only on two groups of damage scenarios based on sensitivity equations, which showed the PSD method's performance in detecting the location and extent of damages (Pedram et al., 2017).

However, the research analysis results on the steel truss bridge almost confirmed some of the other results on a steel one-bay frame and the concrete beam (Pedram et al., 2017), and also some comparison mentions on a plate, and a shall shape structure model without numerical analysis result through the FRF method (Pedram et al., 2018), show that the PSD method is more sensitive than FRF method in structural parameter changes, especially in the natural frequency range. While in other structural model shapes, for the low-frequency range and low or noise-free conditions, the FRF method was more accurate than PSD, this study on truss shape shows that the PSD method also has an almost more accurate and reliable performance in the low and medium-frequency ranges as calculated by software analyses. Thus, future studies are required to identify which method, PSD or FRF, performs best in detecting damages for different structural systems, materials, or structural variables.

2.5. Conclusions

Because damage detection in infrastructures such as bridges is critical, the current research examines the performance and accuracy of two dynamic and non-destructive approaches based on FRF and PSD in determining the amount of damage in the structural elements of a truss steel bridge. This comparison was made under the same conditions and with the DOFs' excitation and measurement properties. The quantified damages in this truss were predicted by analyzing these methods according to their solutions to sensitivity equations through the linear least-square algorithm and model updating approach. For analyzing each method, changes in dynamic characteristics such as stiffness and mass in undamaged and damaged structural elements were monitored. This issue is solved by linearizing equations, which is an inverse problem since the link between structural parameters and observed response is intrinsically non-linear. For a more accurate evaluation, The error Indices results were calculated. In particular, errors obtained with PSD-based prediction show average *CI* and *MSE* errors that were 8.5% lower than those obtained with FRF-based and 27% lower when considering *RE*. Regarding statistical dispersion, PSD results in IQR values between 14% and 23% lower than the dispersion observed when applying the FRF method.

In summary, it is best to compare their performance since comparing methods for detecting and predicting structural damage can show each method's superiority or lack of superiority depending on the conditions and structure. To improve the comparability of these methods, they should be tested on various structures, conditions, and materials. For the particular case study analyzed here, comparing the numerical results of the two methods revealed that the PSD is more accurate than FRF in predicting and diagnosing structural element damage in a metal truss structure with oblique elements.

Chapter 3

Power spectral density method performance in detecting damages by chloride attack on coastal RC bridge

Authors:	Mehrdad Hadizadeh-Bazaz; Ignacio J. Navarro; Víctor Yepes		
Status:	Manuscript published		
Journal:	*Structural Engineering and Mechanics, 85*(2), 197-206. 2023 Jan 25		
DOI:	10.12989/sem.2023.85.2.197		
JCR IF (2023)	2.2		
	JCR Category	Ranking	Quartile
	Civil and Structural Engineering	77/181	Q2
	Engineering, mechanical	75/180	Q2
Presentation:	Post-print (author version)		

Abstract

The deterioration caused by chloride penetration and carbonation plays a significant role in a concrete structure in a marine environment. The chloride corrosion in some marine concrete structures is invisible but can be dangerous in a sudden collapse. Therefore, as a novelty, this research investigates the ability of a non-destructive damage detection method named the Power Spectral Density (PSD) to diagnose damages caused only by chloride ions in concrete structures. Furthermore, the accuracy of this method in estimating the amount of annual damage caused by chloride in various parts and positions exposed to seawater was investigated. For this purpose, the RC Arosa bridge in Spain, which connects the island to the mainland via seawater, was numerically modeled and analyzed. As the first step, each element's bridge position and the chloride corrosion percentage in the reinforcements were calculated. The next step predicted the existence, location, and timing of damage to the entire concrete part of the bridge based on the amount of rebar corrosion each year. The PSD method was used to monitor the annual loss of reinforcement cross-section area, changes in dynamic characteristics such as stiffness and mass, and each year of the bridge structure's life using sensitivity equations and the linear least squares algorithm. This study showed that using different approaches to the PSD method based on rebar chloride corrosion and assuming 10% errors in software analysis can help predict the location and almost exact amount of damage zones over time.

Keywords Chloride attack; concrete bridge; damage identification; non-destructive technique; Power Spectral Density method (PSD); steel corrosion

3.1. Introduction

Since the formation of the Sustainable Development Goals in 2015, several scholars have focused on infrastructure upkeep and its implications on the economy, environment, and society (Navarro et al., 2018b; Garcia-Segura et al., 2018; Navarro et al., 2018c). Different deterioration mechanisms, such as chloride ion ingress (Navarro et al. 2018a, Zhang et al. 2021, Hou et al. 2021), carbonation (Sun et al. 2020, Ekolu 2020, Zheng et al.2021), or attack by other corrosive agents, such as sulfates, can cause damage to coastal and marine structures. The most dangerous hazard to concrete buildings is chloride-induced corrosion, resulting in excessive economic impacts from their maintenance because of the damage performed in RC structures (Shekhar et al., 2018; Goyal et al., 2018). The mechanism of chloride-induced corrosion has been assessed by some researchers in the past (Tang et al., 2016; Angst et al., 2019). In a coastal RC structure's rebars, chloride corrosion is done at two levels: initiation and propagation corrosion (Tuutti 1982). When chloride ions arrived at the reinforcement of the concrete structure, they corroded over time, like the process in Figure 3.1.

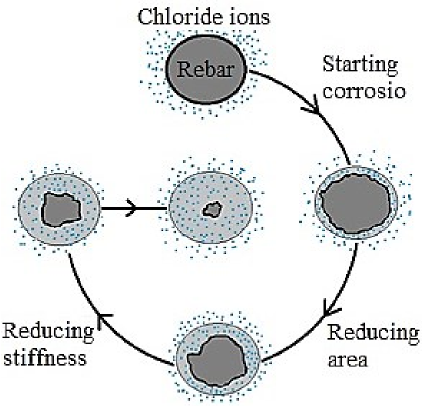

Figure 3.1 *The process of chloride corrosion in steel rebar*

The most challenging aspect of the chloride corrosion mechanism is no visible evidence of damage to the structure. Internal damage in reinforced concrete structures can be detected using destructive or non-destructive methods. Destructive methods depend on models that often involve removing structure samples to assess the damage. Nevertheless, non-destructive methods are independent models that can identify damage to a numerical model in software without affecting the structure (Rathod & Gupta, 2019). These non-destructive damage detection methods can be monitored according to signal-based techniques. Due to modern and intelligent computers and sensors, signal-based approaches for health monitoring have increased in structures (Yang et al., 2021). Some signal-based approaches include time-domain (Aloisio et al., 2020; Yu et al., 2021), frequency-domain (Pérez et al., 2021; Ronchei et al., 2021), and time-frequency domain (Wu et al., 2022; Tran et al., 2020). These methods reveal structural systems' dynamic characteristics (Najafabadi et al., 2017), and thus, when relevant damage has occurred due to different causes, such as chloride corrosion, In summary, time-domain methods are frequently used for stochastic processes (Seyedpoor et al., 2011). The frequency-domain methods can produce many responses and data from frequency points by specifying model updating equations (Arora, 2011). Some dynamic frequency-domain methods include: Natural Frequency (Wang, 2021; Khan et al., 2020), Power Spectral Density Function (Zheng et al., 2015; Pedram et al., 2017; Gao et al., 2021), Frequency Response Function (Rahmatalla et al., 2012; Niu, 2020), Mode Shape (Hou et al., 2018; Xu et al., 2020), Modal Strain Energy (Arefi & Gholizad, 2020; Khosravan et al., 2021), and Modal Curvatures (Dessi & Camerlengo, 2015; Ganguli, 2020, Pooya & Massumi, 2021). Finally, the data in the time-frequency domain is derived from the observed signal frequency over time (Aquino et al., 2021). Some time-frequency approaches for modal identification include Wavelet Transform (WT) (Silik et al., 2021), Blind Source Separation (BSS) (Li et al., 2020), and also Empirical Mode Decomposition (EMD) (Barbosh et al., 2020).

The Power Spectral Density (PSD) is a method based on frequency-domain techniques that uses a periodic or random signal's frequency response. The frequency response defines the mean power distribution. This method uses a sensitive nonlinear function of structural parameters to define a second-order transfer function (Nilsson & Liu 2015). In recent years, researchers in different fields have investigated the reliability of the PSD method for identifying various damage types. Bayat et al. (2019) tested a novel technique based on the PSD function and the Least Square Distance approach to identify deterioration in bridge concrete piers. Gunawan (2019) assessed the reliability of the PSD method on seven lumped masses (1 kg) that were connected by eight similar linear elastic springs. Hadizadeh-Bazaz et al. (2022) Compared the performance of Power Spectral Density (PSD) by Frequency Response Function in a steel bridge structure.

This study evaluated the PSD method's performance in identifying damages caused by a chloride attack on the RC Arosa bridge in Spain, where columns were located and contacted seawater. The damage on the bridge was analyzed according to changes in dynamic parameters and decreasing rebar cross-section areas during chloride corrosion time by new approaches using the PSD method as a frequency-domain technique by using sensitivity equations and the linear least square methodology. For years, some researchers have considered optimization and optimization methods with different methods and goals (Carbonell et al., 2011; Penadés-Plà et al., 2019). For this reason, this research result can help optimize maintenance costs and reduce life cycle costs (LCCA) and even other life cycle impacts (environmental and social) as a frequency-domain technique by using sensitivity equations and the linear least square methodology. For years, some researchers have considered optimization and optimization methods with different methods and goals (Carbonell et al., 2011; Penadés-Plà et al., 2019). For this reason, this research result can help optimize maintenance costs and reduce life cycle costs (LCCA) and even other life cycle impacts (environmental and social) as an accurate method. In order to avoid wasting time and money, it is essential to know the specific location of damage to buildings such as bridges.

3.2. Methods and materials

This study identifies the RC bridge damaged by chloride corrosion in steel reinforcements analyzed over the structure life by combining two-step methods. The initial step was determining the steel components' service life using Fick's second chloride diffusion equation. Then, in the second step, the existence, quantity, and location of chloride damage to the concrete caused by steel reinforcements' chloride corrosion were investigated according to the PSD method by measuring the frequency response function and monitoring changes in dynamic parameters. The bridge structural model description includes diameters and materials and is explained as follows.

3.2.1. Model Description

This concrete bridge is called the Arosa Bridge in Galicia, Spain (see Figure 3.2). This bridge is 1980 m long and has 40 spans (the first and end spans are 40 m, and the other 38 intermediate spans are 50 m). This construction's geometry and durability parameters were based on data from the literature (González et al., 2013; Pérez-Fadón, 1985; Pérez-Fadón, 1986).

Figure 3.2. *The location map of the Arosa bridge in Spain*

The concrete bridge deck is a single box girder. As indicated in Figure 3.3, the bridge deck is 13 m wide and 2.30 meters high. Two pedestrian walkways run along the deck's sides. Each walkway is 1.5 m wide.

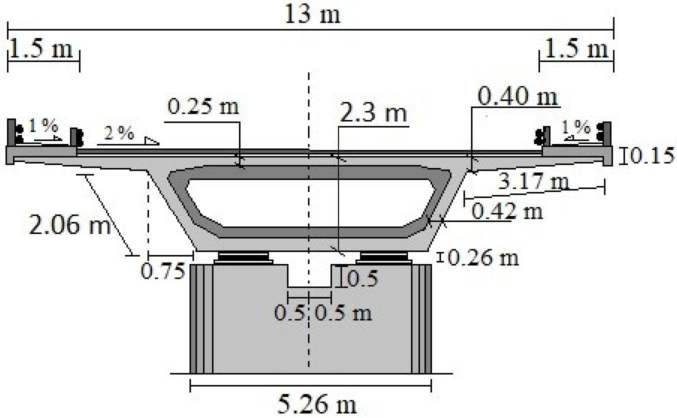

Figure 3.3. *Arosa's concrete bridge in cross-section*

The column dimensions are 5.26 m wide and 1.80 m thick. Under normal circumstances, the bridge deck is about 12 m above the sea and 9.6 m during high tide (see Figure 3.4).

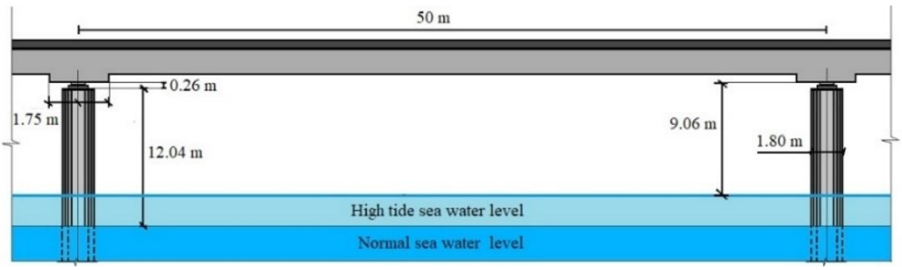

Figure 3.4. *The geometry of a span of the bridge*

The concrete cover on the reinforcements for the deck, 35 mm, and for the columns, 45 mm, was considered. The reinforcing steel quantity is 100 kg/m3 of concrete. Assumed concrete mixes and mechanical parameters for the bridge are in Table 3.1. (Pérez-Fadón, 1985).

Table 3. 1. *The Arosa structure's concrete mixtures and mechanical parameters.*

Properties (Units)	Water (l/m3)	Cement (kg/m3)	Gravel (kg/m3)	Sand (kg/m3)	f_{cm} (MPa)	E_c (GPa)	w/c (%)
Amount	218.5	485.6	926.7	827.9	40	29	0.45

According to Table 3.1, the concrete mix for the bridge has a water-to-cement ratio (w/c) of 0.45 and contains 485 kg/m3 of cement.

3.2.2. Chloride damage prediction methods for the rebars of RC structure

Most metals are vulnerable and susceptible to natural and manufactured influences, particularly in coastal areas where chloride ions cause corrosion. Corrosion is common in reinforced concrete structures like bridges and concrete marine structures. According to the deterioration model proposed by Tuutti (1982), these commissions and damages by chloride in rebars of a concrete structure have some service life levels, such as the initiation and propagation phases depicted in Figure 3.5. (Tuutti, 1982; Hájková & Šmilauer, 2018).

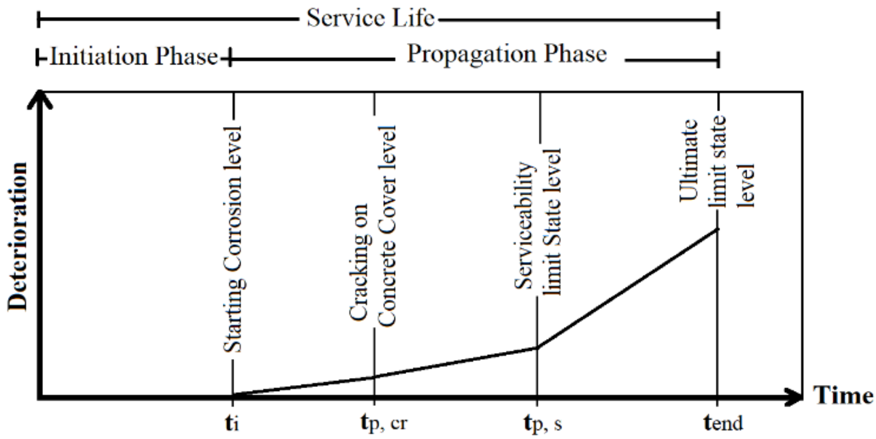

Figure 3.5. *The service life of rebars and chloride corrosion levels in RC structures*

As illustrated in Figure 3.5, chloride corrosion begins in the Initiation corrosion Phase. At the initiation phase, there are chlorides, but at an amount that is less than the chloride threshold (that means it is not enough to start the corrosion process). The propagation phase of chloride ion activity includes some levels such as commencing corrosion, cracking on the concrete cover, the serviceability limit state and the last level is, and the ultimate limit state (Zhang et al., 2019).

According to the fellow equation, the total time to chloride corrosion (t_l) is estimated as the service life of reinforcements of the bridge structure by summing the initiation and propagation phases together (Spanish Ministry of Public Works, 2008).

$$t_l = t_i + t_p \qquad (3.1)$$

Where t_i is the corrosion initiation period, defined as the time, it is the time for the chlorides to reach the rebars and a high enough concentration to start corrosion (chloride threshold, dependent on the steel properties and to some extent on the concrete properties). Also, t_p is the corrosion propagation period of time that spreads through a structural member until it deteriorates significantly (Spanish Ministry of Public Works, 2008).

3.2.2.1 *Initiation chloride corrosion Phase (t_i)*

According to Fick's second law of chloride diffusion mathematical model and the Spanish concrete design code, the initiation of chloride corrosion is the time to reach a particular concentration to befall from the surface of concrete covers through the following (Spanish Ministry of Public Works 2008; Khan et al., 2017).

$$C(x,t) = C_s . \left(1 - erf\left(\frac{x}{2\sqrt{D_{0.x} . (\frac{t_0}{t})^{\alpha} . t}} \right) \right) \qquad (3.2)$$

Where *C(x,t)* is the chloride concentration (*wt%/binder*) at the concrete cover depth x (mm) and during time t (years). C_s is the surface chloride concentration (*wt%/binder*) at the concrete cover surface. The approximate value of C_s can be extracted according to Table 3.2. The *erf(.)* is the Gauss error function. α is the age factor considered 0.5, as the Spanish concrete design code. t_0, as the reference time is considered 28 days, change the unit to year (t_0=0.0767), and also D_0, is the non-steady-state chloride diffusion coefficient (mm^2/years) at the age t_0 can be obtained from Table 3.3. (Spanish Ministry of Public Works, 2008; Crank, 2004).

Table 3. 2. *The chloride concentration at the concrete surface in the marine environment (Spanish Ministry of Public Works, 2008).*

Marine exposure class	**Aerial (IIIa)**		**Submerged (IIIb)**	**In Tidal Zone (IIIc)**
Distance from the coast	Up to 500m	500–5000m	Any	-
C_s (% of concrete weight)	0.14	0.07	0.72	0.50

Table 3. 3. *The coefficients D_0 (×10−12m²/s) (Spanish Ministry of Public Works, 2008).*

Type of cement	**w/c= 0.40**	**w/c= 0.45**	**w/c= 0.50**	**w/c= 0.55**	**w/c= 0.60**
CEM I	8.9	10.0	15.8	19.7	25.0
CEM II/A-V	5.6	6.9	9.0	10.9	14.9
CEM III	1.4	1.9	2.8	3.0	3.4

In this investigation, according to the Arosa bridge situation and distance from the salt water, the amount of the *Cs* was considered 0.14 for the deck and upside of the bridge columns and 0.72 and 0.50 for the submerged and in tidal zone sections of the columns, respectively. Furthermore, the coefficients D_0 according to the type of cement and w/c were assumed to be 10. However, the chloride transport time (*t*) can be calculated using the inverse of Equation 3.2 as Equation 3.3.

$$t = \frac{x^2}{4D}\left[erf^{-1}\left(\frac{C_s - C(x,t)}{C(x,t)}\right)\right]^{-2} \qquad (3.3)$$

Where the *D* is the chloride diffusion coefficient, which varies with the age of the concrete ($D=D(t_0)(t_0/t)^n$). Additionally, when $C(x,t)$ reached threshold concentration C_t and also, if $C(x,t)=C_t$, then the Initiation Period of chloride diffusion (t_i) determined as follows in Equation 3.4 (Spanish Ministry of Public Works, 2008; Khan et al., 2017; Sobhani & Ramezanianpour, 2007; Bendat et al., 1980).

$$t_i = \frac{x^2}{4D}\left[erf^{-1}\left(\frac{C_s - C_t}{C_s}\right)\right]^{-2} \qquad (3.4)$$

Moreover, the critical chloride concentration value under normal conditions as the mean value can be considered 0.6% of the cement weight. When the chloride concentration (*C*) is greater than or equal to the value of the critical chloride concentration (C_{th}), the initial corrosion time of the steel bar equals the transport time (t), indicating that corrosion and damage to the rebars begin at this time. In contrast, less than this value means that damage in the reinforcements has not started (Spanish Ministry of Public Works, 2008; Navarro et al., 2019).

3.2.2.2 *Propagation chloride corrosion Phase (t_p)*

This stage begins after the Initiation stage of chloride diffusion when chloride ions on the surface of the inner rebars start to corrode steel reinforcements. Chloride corrosion cause reduces the cross-sectional area and stiffness of the steel bars over the years. The Spanish concrete design code (Spanish Ministry of Public Works, 2008) gives the following equation for calculating this time:

$$\boldsymbol{t_p = \frac{80}{\phi}\frac{d}{V_{corr}}} \qquad (3.5)$$

Where t_p is the propagation time in years. Also, d is concrete cover thickness, the ϕ is the reinforcement diameter, and V_{corr} is the corrosion rate. The approximate value can be obtained from Table 3.4.

Table 3. 4. *The Chloride corrosion rate depended on the Marine exposure class (Spanish Ministry of Public Works 2008).*

Marine exposure class	Aerial (IIIa)	Submerged (IIIb)	In Tidal Zone (IIIc)
V_{corr} (µm/year)	20	4	50

To calculate the propagation time, the approximate speed of chloride corrosion on rebars, V_{corr}, depends on the situation of the structure elements considered in Table 3.4. In addition, the deck's concrete cover (d) was considered 35 mm and 45 mm for columns with a rebar diameter of 32 mm in the concrete Arosa bridge.

Overall, according to the initiation and the propagation levels for chloride corrosion of reinforcements of an RC marine or coastal structure, the damage induced by corrosion to the reinforcement can be calculated as a percentage using the equation below:

$$\boldsymbol{Dam_{steel}(t) = \frac{t - t_i}{t_p} \times 100} \qquad (3.6)$$

In Equation 3.6, Dam_{steel} is the percentage of reinforcement damage by chloride corrosion for every year (t) during propagation t_p.

The damage percentage was analyzed for the RC bridge's deck and columns according to the different situations and marine exposure classes, such as the aerial, submerged, and Tide zones. Moreover, the changes in stiffness and loss of cross-section area of reinforcement for identifying damages on the concrete of the RC structure were obtained according to this chloride corrosion damaged percentage during structure life.

3.2.3. Damage detection methods for the total of the RC bridge

In this analysis, the PSD method, which is non-destructive and dynamic, was used to identify these damages in the concrete part according to the percentage of damages of corroded rebars by chloride. For this purpose, changes in the dynamic characteristics of each year and situation due to decreasing cross-sectional areas and rebar stiffness were considered in this investigation.

3.2.3.1 *Power Spectral Density Method*

The PSD is a vibration and signal-based method; therefore, this method was obtained according to the frequency response function (FRF) method as following equations (Hadizadeh-Bazaz et al., 2022; Zheng et al., 2015; Pedram et al., 2017). The transfer function is defined as Equation 3.7.

$$\boldsymbol{H}(\boldsymbol{\omega}) = (\boldsymbol{K} - \boldsymbol{\omega}^2\boldsymbol{M} + \boldsymbol{i\omega C})^{-1} \qquad (3.7)$$

K, *M*, and *C* are the matrices of stiffness, mass, and damping, respectively; ω is the frequency, and $i=\sqrt{-1}$. The PSD equation of structural response simplifies as Equation 3.8.

$$\boldsymbol{S}_{\boldsymbol{XX}}(\boldsymbol{\omega}) = \boldsymbol{H}^*(\boldsymbol{\omega})\boldsymbol{S}_{\boldsymbol{FF}}(\boldsymbol{\omega})\boldsymbol{H}^{\boldsymbol{T}}(\boldsymbol{\omega}) \qquad (3.8)$$

Where S_{FF} is the PSD inputs matrix at all of the active Degree Of Freedom (DOF); $H^*(\omega)$ is the complex conjugate of a transfer function. As shown in Equation 3.8, the power spectral density is a second-order function of the FRF, which can be a highly nonlinear response to structural elements.

To model updating based on the sensitivity equation, Equation 3.8 is to expand as the following format by considering ($K-\omega^2M+i\omega C=Z(\omega)$) in the below equation.

$$\boldsymbol{Z}^*(\boldsymbol{\omega})\boldsymbol{S}_{\boldsymbol{XX}}(\boldsymbol{\omega}) = \boldsymbol{S}_{\boldsymbol{FF}}(\boldsymbol{\omega})\boldsymbol{H}(\boldsymbol{\omega}) \qquad (3.9)$$

Where $Z(\omega)$ is the impedance matrix and the transfer function inverse, Equation 3.9 for the damaged structure due to chloride corrosion to the structure's reinforcement is as follows.

$$[\boldsymbol{Z}^*(\boldsymbol{\omega}) + \boldsymbol{\Delta Z} * (\boldsymbol{\omega})][\boldsymbol{S_{XX}}(\boldsymbol{\omega}) + \boldsymbol{\Delta S_{XX}}] = \boldsymbol{S_{FF}}(\boldsymbol{\omega})[\boldsymbol{H}(\boldsymbol{\omega}) + \boldsymbol{\Delta H}(\boldsymbol{W})] \quad (3.10)$$

According to Equations 3.10 and 3.9, the power spectral density function equation is changed by considering ($\Delta Z(\omega)=\Delta K-\omega 2\Delta M+i\omega\Delta C$) and ($H_D(\omega)=[Z(\omega)+\Delta Z(\omega)]^{-1}$) where $H_D(w)$ is the FRF of damaged RC structure during rebars damaged by chloride corrosion every year by Equation 3.6, therefore, Equation 3.10 can be rewritten as Equation 3.11.

$$\boldsymbol{\Delta S_{XX}}(\boldsymbol{\omega}) = \boldsymbol{H_D^*}(\boldsymbol{\omega})\boldsymbol{S_{FF}}(\boldsymbol{\omega})\boldsymbol{\Delta H}(\boldsymbol{\omega}) - \boldsymbol{H_D^*}(\boldsymbol{\omega})\boldsymbol{\Delta Z^*}(\boldsymbol{\omega})\boldsymbol{S_{XX}}(\boldsymbol{\omega}) \quad (3.11)$$

H^*_D is the complex conjugate of the damaged RC structure transfer function during reinforcement chloride corrosion, according to Equation 3.6.

As the expression of the exact ΔH presented by Esfandiari et al., 2009 in Equation 3.12)

$$\boldsymbol{\Delta H}(\boldsymbol{\omega}) = -\boldsymbol{H_D}(\boldsymbol{\omega})(\boldsymbol{\Delta K} - \boldsymbol{\omega^2 \Delta M} + \boldsymbol{i\omega C})\boldsymbol{H}(\boldsymbol{\omega}) \quad (3.12)$$

Equation 3.11 can be rewritten by using Equations 3.8 to Equations 3.12 as follows.

$$\boldsymbol{\Delta S_{XX}}(\boldsymbol{\omega}) = -\boldsymbol{H_D^*}(\boldsymbol{\omega})\boldsymbol{S_{FF}}(\boldsymbol{\omega})\boldsymbol{H_D}(\boldsymbol{\omega})(\boldsymbol{\Delta Z}(\boldsymbol{\omega}))\boldsymbol{H}(\boldsymbol{\omega}) - \boldsymbol{H_D^*}(\boldsymbol{\omega})(\boldsymbol{\Delta Z^*}(\boldsymbol{\omega}))\boldsymbol{H^*}(\boldsymbol{\omega})\boldsymbol{S_{FF}}(\boldsymbol{\omega})\boldsymbol{H}(\boldsymbol{\omega}) \quad (3.13)$$

To identify the damages caused by corrosion on the reinforcement bars and its effect on the structural behavior of the system, the stiffness of each reinforced concrete element is modified in proportion to the corrosion damage calculated for each time for the rebars. The following is a list of the modifications made to the stiffness, mass, and damping matrices due to changes in dimensionless structural parameters.

$$\begin{cases} \boldsymbol{\Delta K} = \sum_{n=1}^{ne} \boldsymbol{K_n \Delta P_n^K} \\ \boldsymbol{\Delta M} = \sum_{n=1}^{ne} \boldsymbol{M_n \Delta P_n^M} \\ \boldsymbol{\Delta C} = \sum_{n=1}^{ne} \boldsymbol{C_n \Delta P_n^C} \end{cases} \quad (3.14)$$

Where K_n, M_n, and C_n are the stage of stiffness, mass, and damping matrices of the structural elements of a structure, ΔP_n^K, ΔP_n^M, and ΔP_n^C indicate that structural parameter changes are between -1 and 1. The monitoring of changes in stiffness and mass and damping of the structure due to possible damage to a structure through the

PSD damage identification method during the lifetime of this structure has been calculated using Equation 3.14, then according to Equation 3.13 and considering ($\Delta Z(\omega)=\Delta K-\omega^2\Delta M+i\omega\Delta C$). So, depending on changes in dynamic characters because of damage causes such as chloride corrosion damages, the sensitivity matrices assigned to the n^{th} structure parameter for obtaining the unknown stiffness, mass, and damping ratios are as follows.

$$\begin{cases} \boldsymbol{S^K = -H_D^*(\omega)S_{FF}(\omega)H_D(\omega)K_nH^T(\omega)} \\ \quad \boldsymbol{-H_D^*(\omega)K_nH(w)S_{FF}(\omega)H^T(\omega)} \\ \boldsymbol{S^M = \omega^2(H_D^*(\omega)S_{FF}(\omega)H_D(\omega)M_nH^T(\omega)} \\ \quad \boldsymbol{+H_D^*(\omega)M_nH(w)S_{FF}(\omega)H^T(\omega)} \\ \boldsymbol{S^C = i\omega(-H_D^*(\omega)S_{FF}(\omega)H_D(\omega)C_nH^T(\omega)} \\ \quad \boldsymbol{+H_D^*(\omega)C_nH(w)S_{FF}(\omega)H^T(\omega)} \end{cases} \qquad (3.15)$$

The final equation of PSD for calculating changes in dynamic properties parameter during damage repeat for every year can be predicted from Equation 3.16.

$$\boldsymbol{\Delta S_{xx} = S^K\Delta p_K + S^M\Delta p_M + S^C\Delta p_C} \qquad (3.16)$$

The sensitivity Equation 3.16, according to the changes in the structural parameters, is linear. To obtain analyses according to the nonlinear optimization, changes in dynamic characters depend on the initial damage analysis in each structure element during the time monitoring and obtained. In addition, a balanced focus on these elements reduces estimate errors in finite element method model updating with the appropriate solution using standard least squares. In this study, the identification of damages for different parts using the PSD method and through the sensitivity equation with consideration for the time for each year of the structure's life is presented in the form of an updated model according to the scenarios of predicting the corrosion damage of rebars by chloride ions evaluated and investigated the reinforced concrete structure.

3.2.3.2 *Numerical model evaluation*

With the development of computers and the increasing speed and performance, using non-destructive and independent models according to numerical models of structures to identify damage is attractive to many engineers and researchers. In this study, the performance of the PSD method, which is a vibration and signal-based method, was used to look for damage caused by chloride ions on a numerical model of a concrete bridge in a coastal area.

For the health monitoring of the bridge structure each year from the beginning corrosion time to the end corrosion time of the reinforced concrete bridge reinforcement, some points and sensors were considered for the numerical model of the bridge at specific distances from each other. Then, as in Figure 3.6, they were renumbered from 1 to 183 on the deck and columns of these selected spans. These three spans in the middle of the bridge were selected from forty spans because these parts could be the most chloride attack. However, the bridge was analyzed in software with almost the same signal information and conditions all over the bridge.

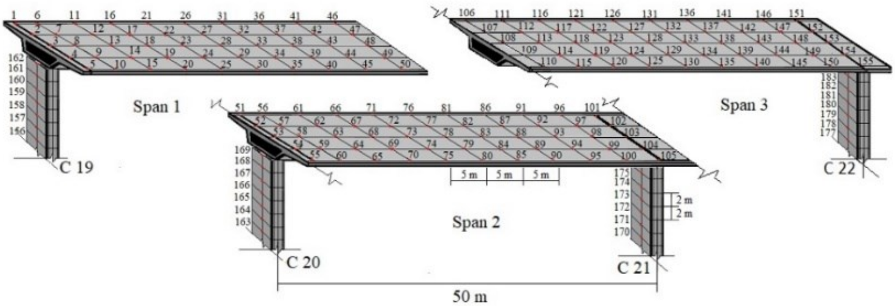

Figure 3.6. *Numbering and dividing points in the three spans selected of the Arosa bridge*

Figure 3.6 shows the three spans from the middle of the total numerical model of the Arosa bridge. Numbering starts from 1 to 155 for the bridge deck and from 156 to 183 for columns C19 to C22.

To monitor the amount of damage at each location of the bridge sections for each year, consider some points as simulation points and some other points as measurement points. The position and situation of these excitations and measurement points for annual test monitoring and analysis were assumed to be fixed every year. For this analysis assessment, some points at the center of each span over the supports and points at the middle of the columns were selected as the simulation points, and the rest were selected as the measurement points.

Therefore, in these three spans of the bridge for the deck, points 3, 28, 53, 78, 103, 128, and 153 were selected as stimulation points, and also, for the columns points 159, 166, 173, and 180 were considered as stimulation points. Moreover, in this numerical investigation, the performance of chloride ions in destroying any part of this coastal concrete bridge assumed 10% noise and errors. Identifying the location and extent of damage to the bridge due to corrosion of the internal rebars of the reinforced concrete bridge was done as a new approach.

Overall, in this study, the damage caused to the rebars of each element of the concrete coastal bridge was identified according to the location and the distance of each part to the seawater, which can affect the rate of corrosion and damage to the rebars and metal parts of the structure, and with using the equations related to the service life and the corrosion rate of the reinforcements by chloride, which was mentioned in the previous sections, predicted the amount of damage to the rebars of each part and area of the bridge, then according to these damages that the corrosion by chloride causes a reduction the diameter and stiffness of reinforcements and rebars can be calculated and model updating for every year. By taking into consideration the changes in dynamic characteristics, the percentage of the damages was determined for different parts of the bridge structure depending on the situation of each element (including submerged, in tide zone, and dry parts such as deck and the upper parts of columns bridge) in each year compared to the previous year amount of damages by considering a constant location and frequency interval from the excitation points for each year in software. These changes in the characteristics of the structure are caused by the damage caused by chloride ions, which cause changes in the quantity of FRF data in each year from the failure of the structure to the undamaged structure (after 28 days from the construction of the structure) is different. Finally, according to the difference, the frequency response has been monitored and analyzed through the PSD equation via software in the numerical model of the bridge. The PSD method's performance in detecting damage caused by the presence and activity of chloride ions was analyzed according to MATLAB software and finite element-based by Open Sees software.

3.3. Results

The damage identified to the bridge structure caused by the chloride attack was analyzed as the first step of damage in the reinforcements according to each section's position to the seawater. So, damage prediction for reinforcements in every year of bridge life from beginning to end chloride corrosion of rebars is shown in Figure 3.7.

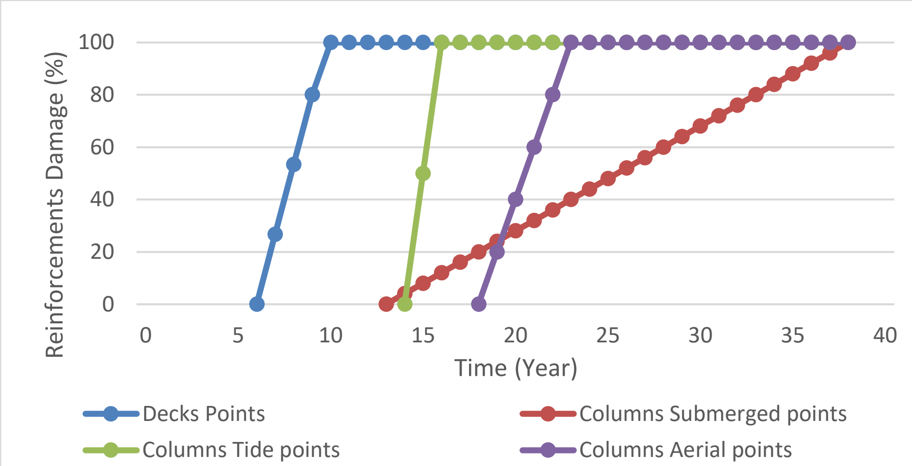

Figure 3.7. *The deterioration of the reinforcements of the bridge according to chloride corrosion attacks every year for different locations.*

The results in Figure 3.7 show the monitoring of the damage prediction of rebars that cause a loss in the area section of the damage prediction of rebars that cause a loss in the area section of reinforcement at each measurement and simulation point of the numerical Arosa bridge model (see Figure 3.6). The damages in reinforcements of the decks' points, including points 1 to 155, started only six years after the bridge was built. 26.67, 53.33, and 80 percent were corroded and damaged in the seventh, eighth, and ninth years. On the other hand, the chloride corrosion damages rebars for every part, and the elements of the columns are different. This kind of damage percentage for the submerged point zone (area sections between points 156-157, 163-164, 170-171, 177-178) began from the thirteenth year, and damages regularly increased by about 4 percent every year until the thirty-eighth years. In addition, the damage amount for reinforcements in the tide points zone (area sections between points 157-158, 164-165, 171-172, 178-179) started from the fourteenth year of the bridge's life. After one year in the fifteenth year damaged, these reinforcements increased dramatically by about 50 percent, and in the sixteenth year, they completely corroded. Finally, the columns' rebars in the aerial point zone (the area sections between points 158-162, 165-169, 172-176, 179-183) began in the eighteenth year until the twenty-three year with increasing damages of about 20 percent in every year after beginning corrosion.

However, the amount and location of corrosion along one RC bridge's structural element can differ according to various reasons caused during or after construction. The amount of damage to each element of the reinforced concrete bridge has been obtained using the PSD technique presented above. Moreover, quantified damages in the bridge are obtained by average damage percentages for every area between four measurement points in different parts of the concrete bridge structure spans during the chloride corrosion in reinforcements. The damage results for each obtained element are presented below for different time horizons (Figure 3.8 to Figure 3.11).

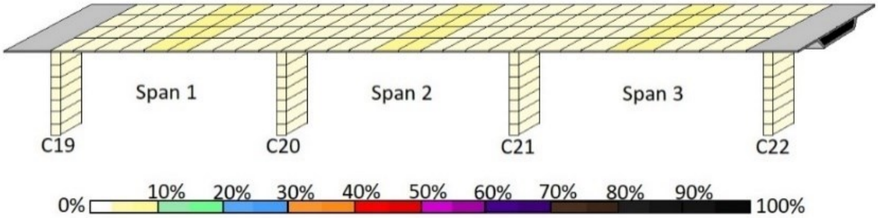

Figure 3.8. *Damage location and percentage due to chloride attack in the 5th year of the bridge life*

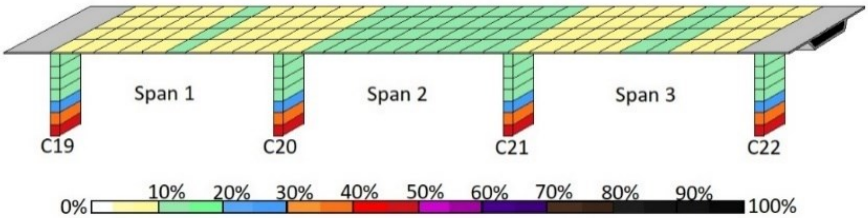

Figure 3.9. *Damage location and percentage due to chloride attack in the 10th year of the bridge life*

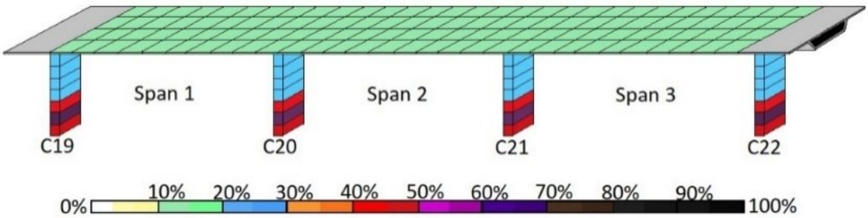

Figure 3.10. *Damage location and percentage due to chloride attack in the 15th year of the bridge life*

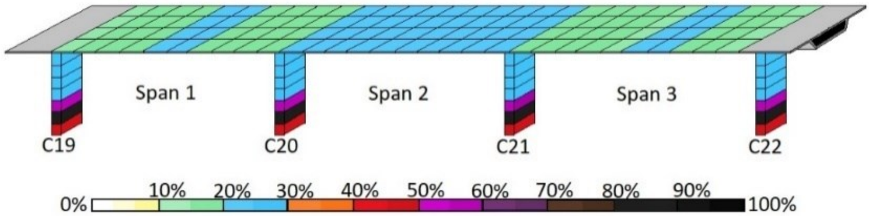

Figure 3.11. *Damage location and percentage due to chloride attack in the 33rd year of the bridge life*

The above figures show the damage percentage in different concrete parts according to the beginning corrosion time in the reinforcements of each zone of the RC Arosa bridge in terms of distance from seawater and chloride ions. According to Figures 3.8 to 3.11, the amount and location of concrete structural damages predicted by the PSD-based method from the fifth year by starting rebars corrosion at the deck and until end reinforcements corrosion in 33th years of the bridge life at the submerged zone of columns of the bridge. The damage in the deck points (1–155) was less than ten percent in the 5th year and between ten and thirty percent in the 33rd year. Nevertheless, damage situations in all parts of the columns are different. The damages percentage for areas between measurement points in the submerged zone (points 156, 157, 163, 164, 170, 171, 177and 178) that sections are sink in seawater in the 5th year (Figure 3.8) are less than five percent. After five years, in the 10th year, about fifty percent of the reinforcement was corroded (Figure 3.7), and the concrete of these areas was damaged by about forty percent. In the 33rd year, the bridge life damage percentage increased by about fifty percent.

On the other hand, the quantified damages in the points located in the tide zone (points 157, 156, 164, 165, 171, 172, 178, and 179) between the 5th year to the 33rd year (Figure 3.8 to Figure 3.11) are less than five percent in 5th year and about forty percent in 10th year and about sixty percent in the 15th year and finally in the 33rd year these parts damaged more than seventy percent. Furthermore, the damage percentage for the aerial columns points zone in the 10th year of the bridge life (Figure 3.9) is less than twenty percent. However, by starting rebars, corrosion in upside columns areas in the 15th year increased the concrete damage to about thirty percent in the 15th and 33rd years when the chloride corrosion was almost done, as shown in Figure 3.7.

3.4. Conclusions

Because the performance and accuracy of various non-destructive and dynamic methods on the numerical model for various factors are increasing over time thanks to modern computers and sensors for the maintenance of important structures such as bridges, and furthermore because all methods for damage detection for different damage causes in different kinds of structures and environments have not been assessed. So research into these methods for various structures, the environment, and the factors that cause damage is critical. Considering these issues, this study has specifically evaluated the feasibility of the PSD method as a damage detection approach with a different approach to detect damage caused only by chloride ions in concrete buildings. On the other hand, the accuracy and effectiveness of this method in detecting this type of damage by chloride ions in every part of these coastal structures during their lifetime have been discussed.

The result of this research helps reduce the costs of repairing and maintaining the bridge structure, prevent sudden damage and collapse of this structure, and thus maintain the safety of human lives. The results of the analysis of the numerical model on software by PSD methods showed that naturally, corrosion by chloride was different for every situation and the bridge element's distance from the seawater. Also, the speed and acceleration of the corrosion of bars in every part were not the same, causing damage to other parts. Over time, the damage increased slowly in the deck and upper columns that were not in contact with seawater and chloride ions. Also, parts of the pillar bases submerged in seawater have seen less speed over time than other parts of the bridge, which can be due to a lack of oxygen and air, which indicates the presence of too much oxygen in increasing the rate of failure. The chloride device is effective. However, the damage to the points and parts of the columns in the tidal range is severe, dangerous, and worrying because, only after a few years and in a short time, this area of the columns was severely damaged by chloride attack.

As Summarize the results of used PSD method to identify chloride damages on the concrete part of the RC bridge and reinforcement chloride corrosion, the below conclusions can be obtained:

- The PSD method's analysis showed that this method has high accuracy in detecting the location of internal and external concrete damages caused by reinforcement chloride corrosion in a coastal RC structure.
- One of the significant issues with testing on an experimental model is the inability to determine the internal condition and amount of damage to each part of a concrete structure, especially inside a coastal concrete bridge. While using the numerical model and by PSD method, determining and identifying the location and quantified damage during the structure's life was easier, cheap, and any destructive to structure to make information from the inner part of the structure.
- The PSD method for identifying damages due to chloride corrosion was efficient and reliable in lower frequency ranges between the stimulation points and the measurement points at software, which could be an advantage for small structures.
- In general, bearings and dampers control nonlinear behavior between columns and decks, affecting the PSD method's detection of concrete damages due to chloride corrosion on the entire bridge.

- One of the drawbacks of frequency-domain methods like the PSD is locating the measuring and excitation points, which requires trial and error to locate these points, especially for large and critical structures like bridges. Because improper stimulation and measuring points can affect the final results, this field requires skilled experts.
- Numbers of the excitation points and measuring points could help bridges and structures detect damage more accurately, but increasing these sensors requires powerful and fast computers, which is a significant disadvantage of the PSD method for analysis in the numerical model of the bridge.

Although chloride-induced damage to coastal RC structures is particularly harmful, it generally starts on the inside of the structure, which causes significant inner and

Chapter 4

Life-Cycle Cost Assessment Using the Power Spectral Density Function in a Coastal Concrete Bridge

Authors:	Mehrdad Hadizadeh-Bazaz; Ignacio J. Navarro; Víctor Yepes		
Status:	Manuscript published		
Journal:	*Journal of Marine Science and Engineering, 11(2), 433. 2023 Feb 16.*		
DOI:	10.3390/jmse11020433		
JCR IF (2023)	2.7		
	JCR Category	Ranking	Quartile
	Engineering, marine	6/25	Q1
Presentation:	Post-print (author version)		

Abstract

Recently, the repair and maintenance of structures has been necessary to prevent these structures' sudden collapse and to prevent human and financial damage. A natural factor in marine environments that destroys structures and reduces their life is the presence of chloride ions. So, regular health monitoring of concrete coastal buildings for on-time repair is essential. This study investigates the performance of the power spectral density (PSD) method as a non-destructive damage-detection method to monitor the location and amount of damage caused by chloride ions during a structure's life using different approaches according to life-cycle assessment (LCA) and life-cycle cost assessment (LCCA). In this regard, chloride corrosion damage dependent on zone distance from seawater was first calculated to obtain the service life of each part of a coastal concrete bridge according to the conventional method. Based on rebar corrosion each year, the next stage forecasted the bridge's concrete deterioration. The PSD method monitored the annual loss of reinforcement cross-sectional area, changes in dynamic characteristics such as stiffness and mass, and the bridge structure's life using sensitivity equations and the linear-least-squares algorithm. Finally, according to the location and quality of damage in each year of bridge life until the end of life, LCC and maintenance and repair costs of the PSD method were compared with the conventional method. The results showed that this strategy was very effective at lowering and optimizing the maintenance and repair costs caused by chloride corrosion.

Keywords life-cycle cost assessment (LCCA); non-destructive damage-detection technique; chloride ion attack; steel corrosion; power spectral density method (PSD); concrete coastal bridge

4.1. Introduction

For many years, discussions about costs during the lifetime of structures have been one of the most important topics among researchers and engineers. In general, the costs of any civil structure activity include the costs of design and construction, repair and maintenance, and finally, the destruction of the structure at the end of its life. In particular, for bridges, the costs associated with maintenance and repair are an important portion of the costs resulting from their life cycle. Many factors are effective in reducing the maintenance costs of structures over time. A factor that can reduce repair and maintenance costs in structures such as bridges is accurate health monitoring and damage detection methods to predict the time and location of damage to structural elements during the structure's life cycle.

Damage-identification methods in structures are carried out using destructive or nondestructive techniques. Destructive approaches depend on models, which often include the removal of structural samples to assess damage. On the other hand, non-destructive techniques are independent models that may identify damage with a numerical software model without causing harm to the structure (Rathod & Gupta, 2019). Non-destructive damage-detection techniques may be monitored utilizing technologies based on signals. The employment of modern, high-tech computers and sensors has increased the popularity of signal-based methodologies in structural health monitoring (Yang et al., 2021). There are many different signal-based techniques, some of which include the time domain (Aloisio et al., 2020; Yu et al., 2021), the frequency domain (Pérez & Font-Moré, 2021; Ronchei et al., 2021), and the time–frequency domain (Wu et al., 2022; Tran et al., 2020). These methodologies are used to examine structures' dynamic properties (Najafabadi et al., 2017). Stochastic processes are standard in time-domain methodologies (Seyedpoor et al., 2019). Frequency-domain techniques may create many responses and data points by configuring model-update equations (Arora, 2011). Mode shape (Hou et al., 2017; Xu et al., 2020), modal curvatures (Dessi & Camerlengo, 2015; Ganguli, 2020; Pooya & Massumi, 2021), natural frequency (Wang, 2021; Khan et al., 2020), modal strain energy (Arefi & Gholizad, 2020; Khosravan et al., 2021), the frequency response function (Rahmatalla et al., 2012; Niu, 2020), and the power spectral density function (Zheng et al., 2015; Pedram et al., 2017; Gao et al., 2021) are some methods of dynamic frequency-domain approaches. Lastly, required data and information in the time–frequency domain are obtained by changing the recorded signal frequency over time (Aquino et al., 2021). Empirical mode decomposition (EMD) (Barbosh et al., 2020), the wavelet transform (WT) (Silik et al., 2021), and blind source separation (BSS) (Li et al., 2020) are some examples of time–frequency approaches that may be utilized for modal identification.

As a frequency-domain approach, power spectral density (PSD) employs the frequency response of a periodic or random signal, which defines the mean power distribution. In order to construct a second-order transfer function, this technique uses a sensitive nonlinear function of structural parameters (Nilsson & Liu, 2015). In recent years, researchers in different fields have investigated the reliability of the PSD method for identifying various damage types. Bayat1a et al. (2019) tested a novel technique based on the PSD function and the least-squares distance approach to identify deterioration in concrete bridge piers. Gunawan, (2019) assessed the reliability of the PSD method for seven 1 kg lumped masses connected by eight similar linear elastic springs. Hadizadeh-Bazaz et al. (2022) compared the performance of power spectral density (PSD) with the frequency response function for a steel bridge structure.

On the other hand, investigating the performance of non-destructive damage-detection methods for life-cycle assessment (LCA) and life-cycle cost analysis (LCCA) is necessary for finding suitable and affordable repair and maintenance methods for essential and costly structures. Life-cycle cost analysis (LCCA) can obtain costs during a structure's life. This approach can reduce and optimize total costs at each level of the structure's life cycle, including initial cost, maintenance cost, repair and replacement, personnel casualties or loss of goods during operation, road-use cost, and indirect loss of socioeconomic benefits (Molina-Moreno et al., 2017; Penadés-Plà et al., 2018; Navarro et al., 2020). Studies have carried out LCCA for structures during their life cycles. Frangopol et al. (2017), using analysis, prediction, optimization, and decisionmaking, investigated a bridge's life-cycle performance and cost assessment. Goh et al. (2019) developed an integration model to leverage the fuzzy analytical hierarchy process (fuzzy AHP) and life-cycle cost analysis (LCCA) in evaluating highway infrastructure investments using their proposed model, which assessed the quantitative factors of cost components. Heidari et al. (2020) developed a probabilistic and uncertain model to evaluate pavements' life-cycle costs and environmental effects by considering managerial flexibilities.

Researchers have previously studied and assessed LCCA using non-destructive damage-detection methods for health monitoring in different structures (Kleingesinds et al., 2021; Kamariotis et al., 2022; Mitseas et al., 2015). Some studies have investigated LCC through the PSD method as a non-destructive damage-detection technique. Micheli et al. (2019) evaluated a performance-based design with life-cycle costs for damping systems built into a 39-story structure in a time-domain frequency technique for wind load and a multivariate stochastic process to optimize a damping system design under different wind conditions using the PSD method. In addition, Chu et al. (2022) looked at the life-cycle wind-resistant performance of a long-span suspension bridge built in the coastal region of China. They used the Bayesian spectral density approach to quantify multisource time-varying effects and uncertainties and to provide a reference for future designs of long-span bridges. Root-mean-square (RMS) tests were used to investigate responses to buffeting and were thought to be time-independent.

This research evaluated the performance of the non-destructive damage-prediction PSD method for a coastal concrete structure and, as well, the importance of using this method in LCCA to reduce overall costs of the maintenance and repair phase of the structure due to chloride ions in marine and coastal environments by a different approach during the lifetime of this structure. In this regard, the LCCA of repairing and maintaining a coastal concrete bridge in northwest Spain exposed to damage by chloride ion attack was investigated with PSD as a frequency-domain technique using sensitivity equations, and the linear least-squares methodology was monitored during its lifetime. Health monitoring of this structure was analyzed annually using a variety of approaches and also according to changes in dynamic components, including stiffness and mass of the rebars and other elements of the bridge's structure.

4.2. Materials and methods

Life-cycle analysis (LCA) is a widely used approach that has recently established a strong foothold in the international environment and has been standardized (ISO 14040, 2006; ISO 14044, 2006). The LCA approach involves modeling a process, product, or service and evaluating the impact of each activity on several factors, including cost, the environment, and society as a whole, amongst other considerations (Navarro et al., 2018; Navarro et al., 2018b). Regarding durability, a life-cycle cost analysis (LCCA) can be used to determine the most cost-effective and sustainable solution (Penadés-Plà et al., 2017). LCCA of the repair and maintenance techniques for different structures based on a variety of structural-element damage-diagnosis and prediction methods have differing costs and performances. So, consideration of the various factors that cause damage, such as corrosion by the attack of chloride ions on the metal parts of a structure in coastal environments, can help to determine the relative cost-effectiveness of non-destructive and frequency-based methods and more traditional approaches to damage identification.

4.2.1. Goal and Scope Definition

This research pursues several essential goals. The first goal is to investigate the performance of a non-destructive damage-detection method in detecting the quantity, location, and amount of damage caused by chloride ion corrosion of the steel sections and the whole parts and elements of a coastal structure during its lifetime. The second goal is economic comparison of the PSD method for repair and maintenance costs and a general check of the performance of this method in LCA and LCCA along with other conventional methods in service-life predictions and identifying damage. This study aims to improve the early phases of design by providing additional information about the effects of corrosion-prevention designs on concrete buildings and structures. For this purpose, these comparisons and tests have been carried out on a coastal concrete bridge with pillars in seawater undergoing corrosion and erosion.

4.2.1.1 *Model description*

The concrete bridge is called the Arosa bridge in Galicia, Spain (see Figure 4.1). This bridge is 1980 m long and has 40 spans (the first and end spans are 40 m, and the other 38 intermediate spans are 50 m). This construction's geometry and durability parameters were based on data from the literature (León et al., 2013; Pérez-Fadón Martínez, 1985; Pérez-Fadón Martínez, 1986).

Figure 4. 1. *The location map of the Arosa bridge in Spain.*

The concrete bridge deck is a single box girder. As indicated in Figure 4.2, the bridge deck is 13 m wide and 2.30 m high. There are two walkways on the sides of the deck with widths of 1.5 m. The columns are 5.26 m wide and 1.80 m thick. Under normal circumstances, the bridge deck is about 12 m above sea level and 9.6 m during high tide.

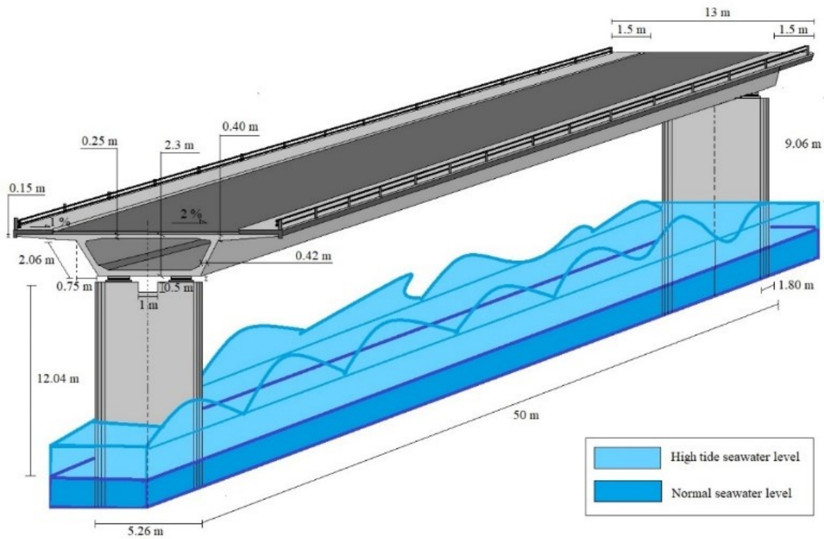

Figure 4. 2. *Dimensions of a span of the Arosa bridge*

The concrete cover on the deck reinforcements was considered to be 35 mm, and for the columns, 45 mm. The reinforcing steel quantity is 100 kg/m3 of concrete (Pérez-Fadón Martínez, 1985).

4.2.1.2 *Functional Unit*

Both the conventional and the PSD-based methods for LCCA were performed on the same functional unit consisting of construction, maintenance, and repair activities for the service life of the bridge. The dimensions of the span of the bridge include a concrete deck measuring 50 m in length and 13 m wide, with two piers standing in seawater. The material's manufacturing techniques may vary. Table 4.1 shows the assumed mechanical characteristics and concrete mixtures of the bridge.

Table 4. 1. *The Arosa structure's concrete mixtures and mechanical parameters.*

Properties (units)	Water (l/m^3)	Cement (kg/m^3)	Gravel (kg/m^3)	Sand (kg/m^3)	f_{cm} (MPa)	E_c (GPa)	w/c (%)
Amount	218.5	485.6	926.7	827.9	40	29	0.45

According to Table 4.1, the reference design has a characteristic compressive strength fcm equal to 40 MPa, and a modulus of elasticity Ec equal to 29 GPa. The concrete mix for the bridge has a water-to-cement ratio (w/c) of 0.45 and contains 485.6 kg/m3 of cement.

4.2.2. Service life prediction

The service life of the RC bridge, which is damaged by chloride corrosion to its steel reinforcements, was analyzed over the structure's lifetime using damage detection and prediction techniques. The initial step was to determine the steel components' service life using Fick's second chloride-diffusion equation. Then, in the second step, the existence, quantity, and location of chloride damage to the concrete caused by corrosion of the steel reinforcements were investigated using the PSD method, by measuring the frequency response function and monitoring changes in the dynamic parameters. The service life prediction description for the bridge using different methods and materials of the reinforced concrete bridge is as follows:

4.2.2.1 *Prediction Techniques for Chloride Degradation in RC Rebars*

Most steel is fragile and easily damaged by natural and manufactured factors, especially in coastal regions where chloride ions, which cause corrosion, are in high concentrations. Reinforced concrete structures, such as bridges and concrete coastal constructions, are regularly susceptible to corrosion. According to the deterioration model proposed by Tuutti, 1982, corrosion and damage caused by chloride in the rebars of a concrete structure have certain service-life levels (Hájková et al., 2018).

As demonstrated in Figure 4.3, chloride corrosion commences in an initiation phase. There are chlorides present in the initiation phase, but they are fewer than the chloride threshold (which means there are not enough to start the corrosion process). The propagation phase of chloride ion activity comprises stages such as starting corrosion, cracking in the concrete cover, the serviceability limit state, and the final limit state (Zhang et al., 2019).

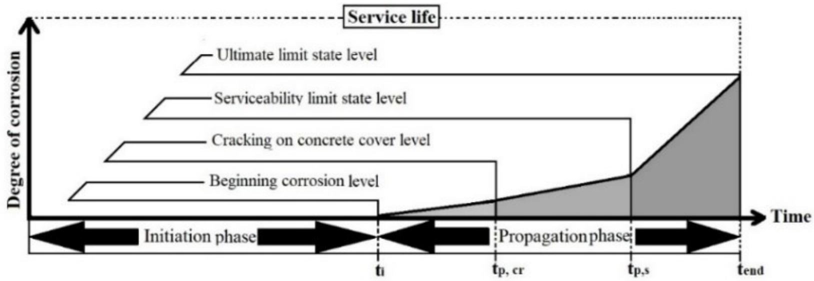

Figure 4. 3. *The service life of rebars in an RC structure is according to Tuutti's model.*

According to the following Equation, the total time of chloride corrosion (t_l) is the service life of the bridge structure's reinforcements, obtained by summing the initiation and propagation phases together.

$$t_l = t_i + t_p \tag{4.1}$$

The corrosion initiation period (t_i) is the time it takes for chlorides to build up to a concentration that causes corrosion to begin on the rebars (the chloride threshold, dependent on the steel properties and, to some extent, on the concrete properties). Additionally, tp is the time it takes for corrosion to permeate throughout a structural part before it starts to fail substantially (Spanish Ministry of Public Works, 2008).

In order to calculate the initiation time, a physical model must obtain the movement of chloride ions within the concrete cover. Existing models for predicting the time required to commence corrosion are based mainly on the assumption of a Fickian process. This assumes that the porous concrete cover is a homogeneous material with ions moving via a diffusion process in sufficient humidity. This diffusive mechanism depends on chloride between the surface and the cover of the concrete structure. According to Fick's equation for chloride diffusion in concrete cover, this analysis will use a deterministic solution. This analysis will use the Fib Bulletin 34, 2006 equation, which assumes a constant, time-independent surface chloride concentration. So, the expected level of chloride in the concrete cover with depth *x* and at a particular time *t* can be written as:

$$C(x.t) = C_s.\left(1 - erf\left(\frac{x}{2\sqrt{D_{0.x}.(\frac{t_0}{t})^{\alpha}.t}}\right)\right) \tag{4.2}$$

Where *C(x.t)* denotes the chloride content (weight percent/binder) at concrete cover depth *x* (mm) and time *t* (years). At the concrete cover surface, C_s represents the surface chloride concentration (wt%/binder). The Gauss error function is denoted by *erf(.)*. According to the Spanish concrete design code, the age factor (*a*) equals 0.5.

When using t_0 as a reference point, 28 days are converted to years (t_0 = 0.0767), and D_0 is the non-steady-state chloride diffusion coefficient at time t_0 (mm^2/years). However, the chloride transport time (t) can be calculated using the inverse of Equation 4.2, as given in Equation 4.3 (Spanish Ministry of Public Works, 2008; Khan et al., 2017).

$$\boldsymbol{t = \frac{x^2}{4D}\left[erf^{-1}\left(\frac{C_s - C(x.t)}{C(x.t)}\right)\right]^{-2}} \qquad (4.3)$$

In this case, D is the chloride-diffusion coefficient, which changes with the age of the concrete *($D = D(t_0)(t_0/t)^n$)*. Additionally, if $C(x.t) = C_t$ and when $C(x.t)$ reaches its threshold concentration C_t, the initiation period of chloride diffusion (t_i) is calculated using Equation 4.4 as follows (Spanish Ministry of Public Works, 2008; Crank, 2004).

$$\boldsymbol{t_i = \frac{x^2}{4D}\left[erf^{-1}\left(\frac{C_s - C_t}{C_s}\right)\right]^{-2}} \qquad (4.4)$$

According to Alonso & Sanchea, 2009 The chloride threshold values obtained from natural experiments include a broad range, from more than 0.4 to even 4 percent. Where in this study and also some research (Navarro et al., 2019; Bru et al., 2018; Frontera & Cladera, 2022), according to the Spanish concrete design code [56], the critical chloride concentration (C_{th}) must be determined by the designer in line with the structure's unique concerns that under normal conditions, a value of 0.6% of the cement weight can be used to assess the limit state in relation to passive reinforcement corrosion. Therefore, the critical chloride concentration value under normal conditions as the mean value can be considered 0.6% of the cement weight. The initiation time ti is said to be reached when the chloride concentration at the rebars reaches the critical chloride threshold Cth. This means that corrosion and damage to the rebars start at this time. On the other hand, less than this value means that damage to the reinforcements has not begun (Spanish Ministry of Public Works, 2008).

The propagation chloride corrosion phase (t_p), which starts when chloride ions on the surface of the inner rebars start to erode steel reinforcements, starts after the initiation stage of chloride diffusion. Over time, chloride corrosion reduces the steel bars' stiffness and cross-sectional area. The following calculation is provided for determining this time by the Spanish concrete design code (Spanish Ministry of Public Works, 2008):

$$\boldsymbol{t_p = \frac{80}{\phi}\frac{d}{V_{corr}}} \qquad (4.5)$$

As Equation 4.5, tp is the propagation time in years. Additionally, d is the thickness of the concrete cover, ϕ is the diameter of the reinforcement, and V_{corr} is the corrosion rate.

According to the Spanish Ministry of Public Works, 2008 tables and elements situation of the Arosa bridge from the seawater, some data for analysis of this assessment can be obtained as follows in Table 4.2.

Table 4. 2. *Durability parameters for the Arosa bridge.*

Marine exposure class	C_s (% of concrete weight)	V_{corr} (µm/year)	D_0 ($\times10^{-12}$m²/s)	C_{crit} (%)	d (m)	
					Deck	Piers
Aerial (IIIa)	0.14	20	10.0	0.6	0.035	0.045
Submerge(IIIb)	0.72	4				
In Tidal Zone (IIIc)	0.50	50				

Damage over time caused by corrosion can be predicted as a percentage using the following formula, which considers the initiation and propagation levels for chloride corrosion of the reinforcements of an RC marine or coastal construction.

$$\boldsymbol{Dam_{steel}(t) = \frac{t - t_i}{t_p} \times 100} \qquad (4.6)$$

In Equation 4.6, Damsteel represents the percentage of reinforcement damaged due to chloride corrosion for each year (t) that has passed from the beginning of the propagation t_p.

Different scenarios and marine exposure classifications, including Aerial, Submerged, and in Tide zone, were considered to determine the percentage of damage to the RC bridge's deck and columns. In addition, the percentage of chloride corrosion damage to the concrete of the RC structure was acquired, along with the results of the changes in stiffness and loss of cross-section reinforcement area for damage identification.

4.2.2.2 *Damage detection using the PSD method*

The PSD technique was applied in this research to evaluate damage to the concrete components. The percentage damage of chloride-corroded rebars was utilized to determine which strategy to apply. This study accounted for differences in dynamic characteristics across years and situations due to changes in cross-sectional area and rebar stiffness. Given that PSD relies on vibration and signals, this was derived from the frequency response (FRF) using the following equations (Zheng et al., 2015; Pedram et al., 2017; Hadizadeh-Bazaz et al., 2022; Hadizadeh-Bazaz et al., 2023a).

The transfer function is defined in Equation 4.7:

$$\boldsymbol{H(\omega) = (K - \omega^2 M + i\omega C)^{-1}} \quad (4.7)$$

K, *M*, and *C* denote the stiffness, mass, and damping matrices; they denote the frequency, and *i* = -1 is the identity matrix. The equation of structural response using power spectral density is written in Equation 4.8.

$$\boldsymbol{S_{XX}(\omega) = H^*(\omega) S_{FF}(\omega) H^T(\omega)} \quad (4.8)$$

The complex conjugate of a transfer function is denoted as $H^*(\omega)$, and SFF is the PSD input matrix at all of the active Degrees Of Freedom (DOF). Equation 4.8 demonstrates that the power spectral density is a second-order function of the FRF, which may be a highly nonlinear response to structural features.

The model updating based on the sensitivity equation and by considering ($K\text{-}\omega^2\Delta M + i\omega\Delta C = \Delta Z(\omega)$) and ($H_D(\omega) = [Z(\omega) + \Delta Z(\omega)]^{-1}$), where $H_D(w)$ is the frequency response function from the structure damaged by chloride corrosion, *Z(ω)* is the impedance matrix, and the transfer function is inverse. Therefore, the damaged elements' power spectral density function equation can be written as Equation 4.9.

$$\boldsymbol{\Delta S_{XX}(\omega) = H_D^*(\omega) S_{FF}(\omega) \Delta H(\omega) - H_D^*(\omega) \Delta Z^*(\omega) S_{XX}(\omega)} \quad (4.9)$$

According to the conventional chloride damage prediction method, H^*_D is the complex conjugate of the damaged RC structure transfer function during reinforcement chloride corrosion.

As the expression of the exact *ΔH* presented by Esfandiari et al. (2009) in Equation 4.10:

$$\boldsymbol{\Delta H(\omega) = -H_D(\omega)(\Delta K - \omega^2 \Delta M + i\omega C) H(\omega)} \quad (4.10)$$

Equation 4.9 can be rewritten using Equations 4.8 and Equations 4.10 as follows:

$$\boldsymbol{\Delta S_{XX}(\omega) = -H_D^*(\omega) S_{FF}(\omega) H_D(\omega) \big(\Delta Z(\omega)\big) H(\omega) - H_D^*(\omega) \big(\Delta Z^*(\omega)\big) H^*(\omega) S_{FF}(\omega) H(\omega)} \quad (4.11)$$

To determine the corrosion damage of the reinforcing bars and its influence on the system's structural behavior, the stiffness of each RC element is varied in proportion to the corrosion damage of the rebars over time. The structural stiffness equation is:

$$\boldsymbol{\Delta k = \sum_{n=1}^{ne} K_n \Delta P_n^K} \quad (4.12)$$

In Equation 4.12, K_n is the level of stiffness matrices of the structural elements of a structure. $\Delta P^K{}_n$ indicates that structural parameter changes are between -1 and 1.

The sensitivity matrices allocated to the *n* th parameter of the structure for determining the passive stiffness ratios and for RC bridges damaged by chloride corrosion through to Equation 4.11 are as follows:

$$\boldsymbol{S^s = -H_D^*(\omega)S_{FF}(\omega)H_D(\omega)K_nH(\omega) - H_D^*(\omega)K_nH(w)S_{FF}(\omega)H(\omega)} \qquad (4.13)$$

The ultimate Equation of PSD for estimating changes in dynamic characteristics parameter during damage for every year may be predicted using Equation 4.14:

$$\boldsymbol{\Delta S_{xx} = S^S \Delta p_S} \qquad (4.14)$$

Δp_S illustrates the changes in structural stiffness due to chloride corrosion and deterioration over time according to the equations for chloride corrosion deterioration of reinforcements, using the power spectral density method to monitor the health of the changes in the stiffness and loss of cross-sectional areas in the RC marine bridge elements during their lifetime by the frequency response function of the bridge elements and using the least-squares technique.

4.2.3. Calculation Procedure for LCCA

Life-cycle cost assessment is an essential criteria to consider when assessing the performance of a bridge. The LCCA for the bridge in this study was assessed according to location and percentage of yearly damage predicted using damage-detection methods. The life-cycle and life-cycle cost in each structure stage usually includes manufacturing, construction, use and maintenance, and, finally, the end of the structure's life. Therefore, the following formulae can be used to represent the expected total cost throughout the bridge's life cycle (Frangopol et al., 2017; Frangopol et al., 2016).

$$\boldsymbol{C_T = C_I + C_M + C_{INS} + C_R + C_{Dam}} \qquad (4.15)$$

In Equation 4.15, the initial cost is shown as C_I ; C_M is the maintenance cost; C_{INS} is the cost of inspections; C_R is the total repair cost; C_{Dam} is the expected damage cost. The total cost for the repair activity of the concrete bridge can be calculated according to the following items:

$$\boldsymbol{C_R(t_V) = C_{DNRC}(t_V) + C_{DRC}(t_V) + C_{SM}(t_V) + C_{PE}(t_V) + C_S(t_V) + C_C(t_V)} \qquad (4.16)$$

Where t_V, is the interval time investigated; C_{DNRC} is the cost of demolition of non-reinforced concrete parts such as the structure's cover, C_{DRC} is the cost of demolition of reinforced concrete parts of the structural parts of the bridge, C_{SM} is the cost of separation and classification of materials resulting from demolition, C_{PE} is the cost of preparing equipment for repairing the concrete and rebars of the columns and deck of the bridge, C_S is the overall cost of buying and replacing damaged steel reinforcements, C_C is the total cost of the concrete parts of the bridge damaged over the time period. Due to various damage factors, such as corrosion and damage caused by the presence of chloride ions in coastal structures, as well as other factors, such as floods and earthquakes following a Poisson process, the total life-cycle damages in each structural part and elements of a bridge can be computed within the time interval (Frangopol et al., 2017; Dong & Frangopol, 2016):

$$\boldsymbol{C_D(t_v) = \sum_K^{N(t_v)} D(t_k).e^{-rt_k}} \qquad (4.17)$$

In Equation 4.17, $N(t_v)$ is the number and amount of damage factors on a structure during the time interval. D is the percentage of the annual damages at the time t_v, which in this study referred to yearly damages caused by chloride corrosion and predicted by the PSD method. r is the discount rate in this study (r =5%). According to the Poisson model, by a mean rate λ_f, the time t_k follows throughout uniform interval distribution $[0, t_v]$. The estimated annual damage percentage in elements under hazard effects can be written as ($N(t_v) = \lambda_f \times t_v$) (Frangopol et al., 2017; Yeo, 2005).

$$\boldsymbol{E[C_D(t_v)] = \frac{\lambda_f \, . \, E(D)}{r} \, . (1 - e^{-rt_k})} \qquad (4.18)$$

In Equation 4.18, $E[C_D(t_v)]$ is the value of damaged and corroded bridge elements.

This study analyzed the LCCA related to the repair and maintenance stage of a chloride-corroded concrete bridge using the power spectral density method at different stages of the bridge's life for each section and span location (see Figure 4.4).

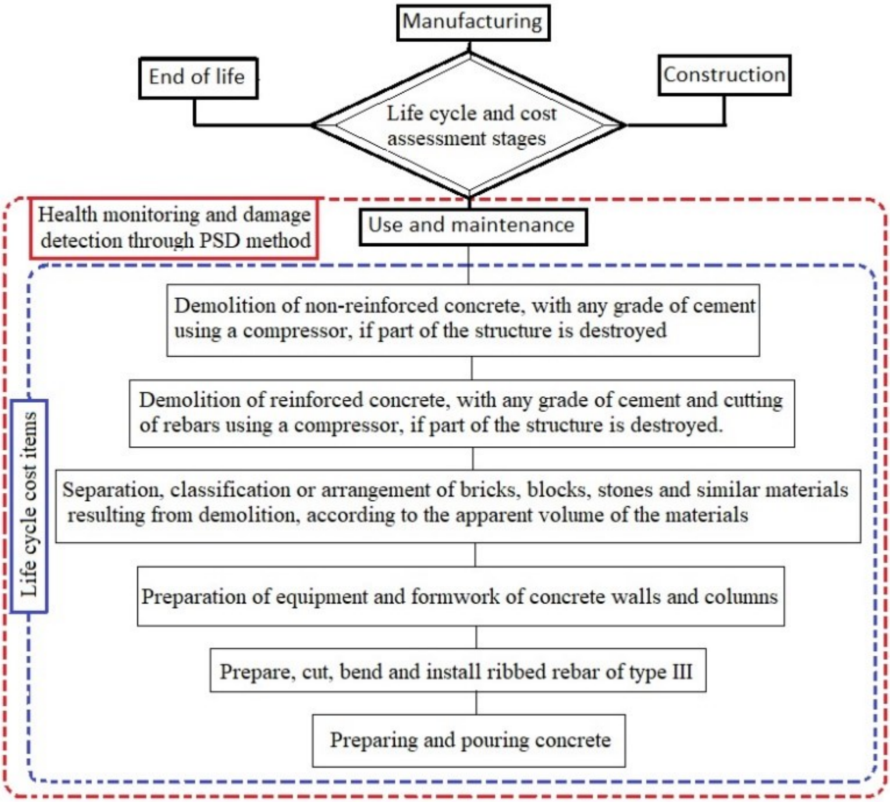

Figure 4. 4. *The LCCA using the PSD for maintenance and repair of the concrete bridge.*

According to the above figure, this study analyzes the monitoring of the repair and maintenance costs of the Arosa bridge, demolition of damaged parts, separation and classification of damaged material, preparation and installation of new reinforcements, and concrete activity costs and materials during the bridge life evaluated. In this study, the damage that chloride ions can cause to the foundations and deck of the bridge has been specifically addressed. In this regard, we investigated the accuracy and performance of the PSD to reduce the bridge's repair and maintenance costs. Table 4.3 shows the costs of repairing the concrete and coastal Arosa bridge according to national construction-related databases of Spain (MITMA, 2022).

Table 4. 3. Repair activity cost (EUR) according to Spain data code (2022) for the concrete and coastal Arosa bridge.

No	Maintenance and repair activities	Description / Includes	Price per unit (€)	Unit
1	Demolition of the unreinforced concrete parts	Debris clearing, loading, and transport of demolished material to authorized manager up to a distance of 60 Km	30.20	m^3
2	The reinforced concrete parts demolition	Debris clearing, loading, and transport of demolished material to authorized manager up to a distance of 60 Km	33.07	m3
3	Management, separation, and categorization of debris resulting from destruction	Loading and transport of non-hazardous construction (except earth and stones) consisting of bricks, tiles, and ceramic materials or a mixture of these	7.78	ton
4	Install and subsequently remove formwork for Repair concrete activity	Executed with double-folded, wood cleaning, wetting, application of release agent, and use of complementary elements for its stability and adequate execution	33.91	m^2
5	Repair and replace damaged bar steel with corrugated bar steel with improved ductility characteristics	Including cutting and bending, placement of overlaps, breakout, and binding annealed wire and separators	1.81	kg
6	Prepare and pour concrete.	Concrete activities in the elevation of piles, stirrups, headboards, beams, deck boards, slabs, walls, and frames	121.35	m^3

Finally, for LCCA, the total bridge repair and maintenance costs according to the percentage of damage predicted for the whole bridge is obtained from the following Equation (Lee, 2006).

$$\boldsymbol{E[C_T\,(\bar{x}.t_v)] = C_I + C_M + \sum_{t=1}^{t_v} \left[\frac{\left(\sum_{t=1}^{N(t_v)} E[C_{DNRC}\,(\bar{x}.t)] + \sum_{t=1}^{N(t_v)} E[C_{DRC}\,(\bar{x}.t)] + \sum_{t=1}^{N(t_v)} E[C_{SM}\,(\bar{x}.t)] + \sum_{t=1}^{N(t_v)} E[C_{PE}\,(\bar{x}.t)] + \sum_{t=1}^{N(t_v)} E[C_S\,(\bar{x}.t)] + \sum_{t=1}^{N(t_v)} E[C_C\,(\bar{x}.t)]\right)}{(1+r)^t} \right] + C_D} \tag{4.19}$$

The LCCA cost for overall maintenance and repair properties demonstrated by $E[C_{Total}\,(\bar{x}.t_{int})]$ during the lifetime of the bridge structure; $\sum_{t=1}^{N(t_v)} E[C_{DNRC}\,(\bar{x}.t)]$, $\sum_{t=1}^{N(t_v)} E[C_{DRC}\,(\bar{x}.t)]$, $\sum_{t=1}^{N(t_v)} E[C_{SM}\,(\bar{x}.t)]$, $\sum_{t=1}^{N(t_v)} E[C_{PE}\,(\bar{x}.t)]$, $\sum_{t=1}^{N(t_v)} E[C_S\,(\bar{x}.t)]$, and $\sum_{t=1}^{N(t_v)} E[C_C\,(\bar{x}.t)]$ are the total costs of demolishing the unreinforced concrete parts; the demolition, management, and separation of the reinforced concrete parts; and categorization of debris resulting from the destruction, installation, and subsequent removal of each concrete repair activity; repair and replacement of damaged bar steel with corrugated bar steel with improved ductility characteristics; and costs of preparing and pouring concrete during and until the end of bridge life, respectively.

Overall, in the calculation and analysis for this research, the life cycle of coastal concrete bridge elements was investigated according to the location of structural elements to seawater. Then, using the PSD method, the extent and location of the damage caused during the bridge's life in different years were predicted and calculated. Finally, the costs of maintenance and repair of this concrete bridge were investigated according to the type of damage that can be caused by chloride corrosion. In addition, the performance and accuracy of this method were evaluated in detecting the location, extent, and time of failure and how much use of this method can reduce the maintenance and repair costs of a structure.

4.3. Description of the Numerical Model

The use of non-destructive and independent models based on numerical models of structures to detect damage is appealing to engineers and researchers as computers and sensors develop in speed and capability. The PSD approach, a vibration and signal-based method, investigated damage induced by chloride ions on a numerical model of a coastal concrete bridge. The numerical model of the bridge considered certain locations and sensors at specific distances from each other for health monitoring of the bridge structure each year from the start to the end of the concrete bridge reinforcement's corrosion period. The deck and column numbers of these particular spans were renumbered from 1 to 167, as seen in Figure 4.5. One of the bridge's forty spans was selected as the most vulnerable to chloride attack because it is located in the deepest part of the seawater. In addition, its columns are at the highest point above sea level, and the bridge is more exposed to tides and seawater here than at the beginning or end spans, which are shorter, and some are out of the seawater.

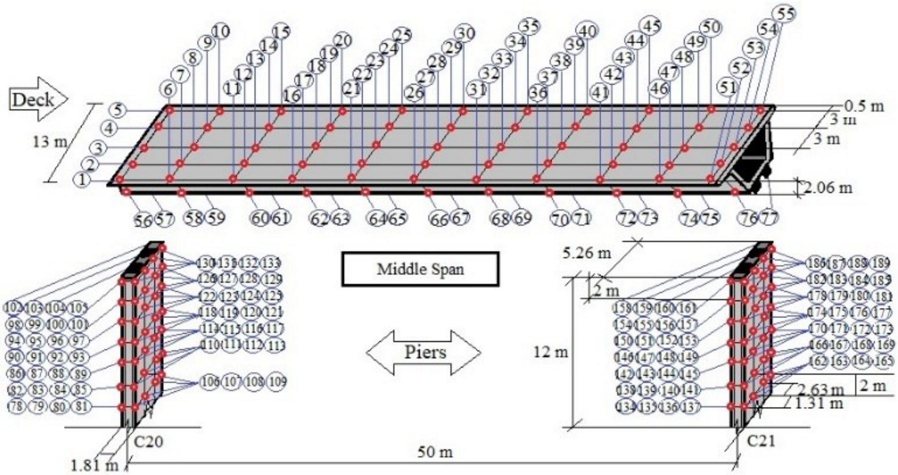

Figure 4. 5. *Numbering and division of sensor points in 1 of 40 spans of the Arosa bridge.*

Figure 4.5 demonstrates the numbering of the sensor points for analysis. Numbers 1 to 77 correspond to bridge deck points, which are spaced 5 m from each other in length and 3 m apart in the width of the bridge. The point numbers in one pier start at 78 and continue to 189 in the other. The points on the lengths of the piers are 2.63 m in width and 2 m in height from each other. The points on the widths of the piers are approximately 1.80 m apart.

To monitor the amount of damage at each bridge location during each year of chloride attack, we considered some points as simulation points and others as measurement points. The position and situation of these simulation and measurement points for annual test monitoring and analysis were assumed to be fixed for each year analyzed.

In this respect, some sites within a variety of sections and components were chosen to serve as simulation points, and others were chosen as measurement points. The distance between the simulation points and the measurement points varied widely. Thus, on the bridge deck span, points 3, 18, 33, 48, 58, 59, 64, 65, 70, 71, 76, and 77 were selected as simulation points; and between piers, points 86, 89, 98, 101, 115, 116, 127, 128, 135, 136, 147, 148, 159, 160, 162, 165, 174, 177, 186, and 189 were considered. These points were analyzed for each year of bridge life with constant location. The locations of these simulation and measurement points were assumed to be fixed until the end of the analysis as well as until the end of the structure's life for each year of its life. This assumption was critical to the investigation because it allowed the researchers to determine how the locations of these points changed over time. In this analysis, the number and locations of sensors on the bridge span were determined by trial and error, as most techniques using software comparing sensor distances and frequency responses to calculate the distances between these sensors point to each other. On the other hand, the number and location of these sensors determine the distance between them. So, reducing the number of sensors causes an increase in the distance between the sensors, which can cause a decrease in the received signals from simulation points; even if considering a long distance, this creates a problem for receiving frequencies at measurement points, which can affect the results.

Moreover, the effect of the chloride ions in destroying any component of the concrete coastal bridge was estimated to be subject to 10% noise and error within the scope of this numerical analysis. The PSD method's ability to detect damage caused by the presence and activity of chloride ions was analyzed using MATLAB software, and the finite-element-based software Open Sees was utilized. Figure 4.6 depicts a summary of the studies conducted to assess the PSD and a conventional methods approach, its efficacy in predicting the location and quantification of structure failure, and its influence on decreasing the maintenance and repair expenses of concrete and coastal structures.

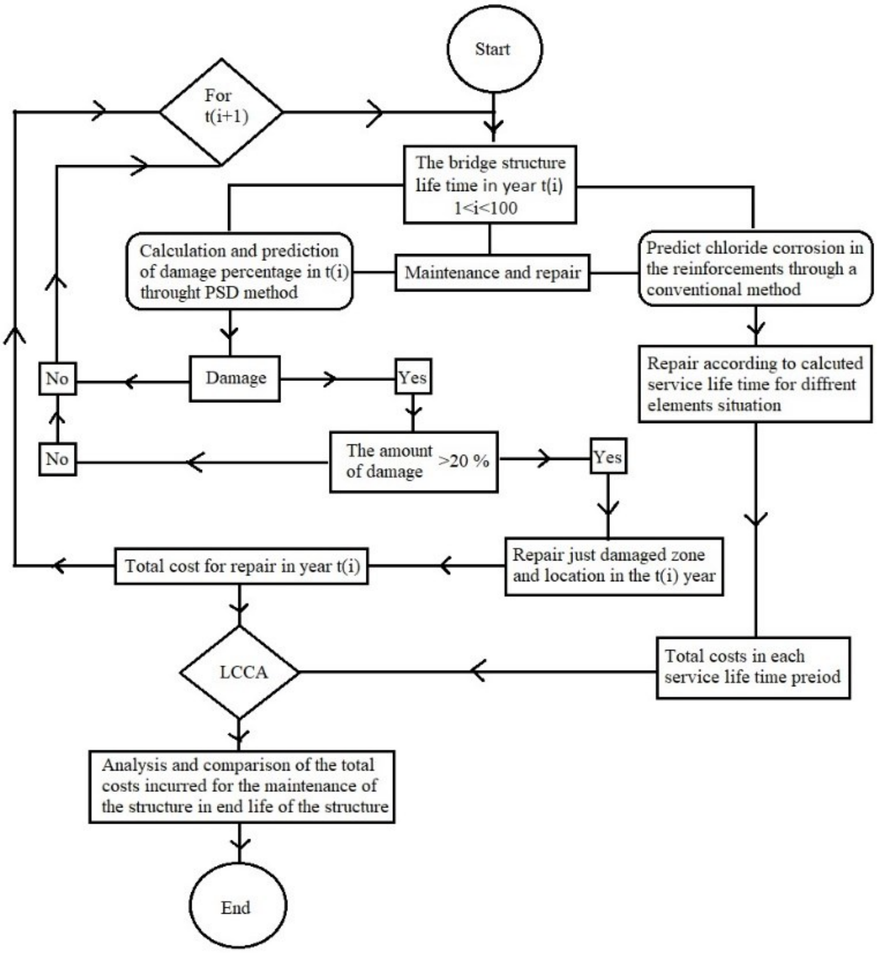

Figure 4. 6. *The summary of analysis and calculation processes performed on the numerical model of the Arosa bridge*

As shown in the flowchart in Figure 4.6, the cost of repair and maintenance of a bridge structure is considered while assuming 100 years to be end of life. The amount and location of predicted damage to the bridge for each year of the structure's life was analyzed. Then, the repair operation in the event of damage to the structure and more than 20% damage to the elements and regions was considered. Selection of the percentage damage to represent the start of damage could vary according to the importance for monitoring the time to repair and carry out maintenance to the structure. In this study bridge model, 20% damage was considered to be noticeable, and this was viewed as the beginning of damage for the software analysis. Then, we added up the annual expenses of repairing and maintaining the bridge, as well as the cost of the techniques that calculated the service-life interval and repair costs based on 20% damage to components (obtained using the PSD method and another technique). These approaches have been used to compare and contrast the bridge's various parts every few years.

4.4. Results

The results of examining the ability of a non-destructive method to detect damage and analyze the state of repair and maintenance costs of a span of the Arosa bridge located in the marine environment and the lower part of the bridge piers immersed in seawater exposed to corrosion and damage by ions of chloride ions were evaluated. Table 4.4 shows the repair time for each area between the measurement and stimulation points in the Arosa bridge span. These times were obtained according to damages equal to or greater than 20% as the percentage of base damage for bridge repair using the PSD method and according to the service lifetime of the conventional method in calculating the appropriate period and interval for the repair and maintenance of reinforced concrete structures exposed to corrosion and proximity to chloride ions.

Table 4. 4. *Identified the location, time, amount of damage, and conventional service life of the Arosa bridge.*

Section No	Location		Service life and repair period (for Damage more than 20%)			
			Damage prediction methods			
			PSD		Conventional	
	Area No	The zone between points	Damage (%)	Repair time (year)	Damage (%)	Repair time (year)
S1 (Deck)	A1	p1, p2, p6, p7	-	100	26.67	6
	A2	p2, p3, p7, p8	20.04	65		
	A3	p3, p4, p8, p9	20.04	65		
	A4	p4, p5, p9, p10	-	100		
	A5	p1, p6, p56, p58	20.05	32		
	A6	p56, p57, p58, p59	20.16	27		

	A7	p5, p10, p57, p59	20.05	32		
S2 (Deck)	A8	p6, p7, p11, p12	20.04	65	26.67	6
	A9	p7, p8, p12, p13	20.07	51		
	A10	p8, p9, p13, p14	20.07	51		
	A11	p9, p10, p14, p15	20.04	65		
	A12	p6, p11, p58, p60	20.15	42		
	A13	p58, p59, p60, p61	20.06	36		
	A14	p10, p15, p59, p61	20.15	42		
S3 (Deck)	A15	p11, p12, p16, p17	20.05	32	26.67	6
	A16	p12, p13, p17, p18	20.22	30		
	A17	p13, p14, p18, p19	20.22	30		
	A18	p14, p15, p19, p20	20.05	32		
	A19	p11, p16, p60, p62	20.16	27		
	A20	p60, p61, p62, p63	20.20	22		
	A21	p15, p20, p61, p63	20.16	27		
S4 (Deck)	A22	p16, p17, p21, p22	20.22	19	26.67	6
	A23	p17, p18, p22, p23	20.95	19		
	A24	p18, p19, p23, p24	20.95	19		
	A25	p19, p20, p24, p25	20.22	19		
	A26	p16, p21, p62, p64	20.50	18		

	A27	p62, p63, p64, p65	21.14	18		
	A28	p20, p25, p63, p65	20.50	18		
S5 (Deck)	A29	p21, p22, p26, p27	21.77	18	26.67	6
	A30	p22, p23, p27, p28	22.41	18		
	A31	p23, p24, p28, p29	22.41	18		
	A32	p24, p25, p29, p30	21.77	18		
	A33	p21, p26, p64, p66	21.77	18		
	A34	p64, p65, p66, p67	22.41	18		
	A35	p25, p30, p65, p67	21.77	18		
S6 (Deck)	A36	p26, p27, p31, p32	21.77	18	26.67	6
	A37	p27, p28, p32, p33	22.41	18		
	A38	p28, p29, p33, p34	22.41	18		
	A39	p29, p30, p34, p35	21.77	18		
	A40	p26, p31, p66, p68	20.50	18		
	A41	p66, p67, p68, p69	21.14	18		
	A42	p30, p35, p67, p69	20.50	18		
S7 (Deck)	A43	p31, p32, p36, p37	20.16	27	26.67	6
	A44	p32, p33, p37, p38	20.20	22		
	A45	p33, p34, p38, p39	20.20	22		
	A46	p34, p35, p39, p40	20.16	27		

	A47	p31, p36, p68, p70	20.05	32		
	A48	p68, p69, p70, p71	20.22	30		
	A49	p35, p40, p69, p71	20.05	32		
S8 (Deck)	A50	p36, p37, p41, p42	20.15	42	26.67	6
	A51	p37, p38, p42, p43	20.06	36		
	A52	p38, p39, p43, p44	20.06	36		
	A53	p39, p40, p44, p45	20.15	42		
	A54	p36, p41, p70, p72	20.05	84		
	A55	p70, p71, p72, p73	20.07	51		
	A56	p40, p45, p71, p73	20.05	84		
S9 (Deck)	A57	p41, p42, p46, p47	20.06	36	26.67	6
	A58	p42, p43, p47, p48	20.22	30		
	A59	p43, p44, p48, p49	20.22	30		
	A60	p44, p45, p49, p50	20.06	36		
	A61	p41, p46, p72, p74	-	100		
	A62	p72, p73, p74, p75	20.99	24		
	A63	p45, p50, p73, p75	-	100		
S10 (Deck)	A64	p46, p47, p51, p52	-	100	26.67	6
	A65	p47, p48, p52, p53	20.07	51		

	A66	p48, p49, p53, p54	20.07	51		
	A67	p49, p50, p54, p55	-	100		
	A68	p46, p81, p74, p76	20.50	32		
	A69	p74, p75, p76, p77	20.16	27		
	A70	p50, p55, p75, p77	20.50	32		
S11 (Column20)	A71	p78, p79, p82, p83, p106, p107, p110, p111	21.1	14	20	17
	A72	p79, p80, p83, p84, p107, p108, p111, p112	21.1	14		
	A73	p80, p81, p84, p85, p108, p109, p112, p113	21.1	14		
S12 (Column20)	A74	p82, p83, p86, p87, p110, p111, p114, p115	24.23	15	50	14
	A75	p83, p84, p87, p88, p111, p112, p115, p116	24.23	15		
	A76	p84, p85, p88, p89, p112, p113, p116, p117	24.23	15		
S13 (Column20)	A77	p86, p87, p90, p91, p114, p115, p118, p119	26.63	16	20	18
	A78	p87, p88, p91, p92, p115, p116, p119, p120	26.63	16		
	A79	p88, p89, p92, p93, p116,	26.63	16		

		p117, p120, p121				
S14 (Column20)	A80	p90, p91, p94, p95, p118, p119, p122, p123	21.48	17	20	18
	A81	p91, p92, p95, p96, p119, p120, p123, p124	21.48	17		
	A82	p92, p93, p96, p97, p120, p121, p124, p125	21.48	17		
S15 (Column20)	A83	p94, p95, p98, p99, p122, p123, p126, p127	26.45	19	20	18
	A84	p95, p96, p99, p100, p123, p124, p127, p128	26.45	19		
	A85	p96, p97, p100, p101, p124, p125, p128, p129	26.45	19		
S16 (Column20)	A86	p98, p99, p102, p103, p126, p127, p130, p131	22.11	19	20	18
	A87	p99, p100, p103, p104, p127, p128, p131, p132	22.11	19		
	A88	p100, p101, p104, p105, p128, p129, p132, p133	22.11	19		
S17 (Column21)	A89	p134, p135, p138, p139, p162, p163, p166, p167	21.1	14	20	17
	A90	p135, p136, p139, p140,	21.1	14		

		p163, p164, p167, p168				
	A91	p136, p137, p140, p141, p164, p165, p168, p169	21.1	14		
S18 (Column21)	A92	p138, p139, p142, p143, p166, p167, p170, p171	24.23	15	50	14
	A93	p139, p140, p143, p144, p167, p168, p171, p172	24.23	15		
	A94	p140, p141, p144, p145, p168, p169, p172, p173	24.23	15		
S19 (Column21)	A95	p142, p143, p146, p147, p170, p171, p174, p175	26.63	16	20	18
	A96	p143, p144, p147, p148, p171, p172, p175, p176	26.63	16		
	A97	p144, p145, p148, p149, p172, p173, p176, p177	26.63	16		
S20 (Column21)	A98	p146, p147, p150, p151, p174, p175, p178, p179	21.48	17	20	18
	A99	p147, p148, p151, p152, p175, p176, p179, p180	21.48	17		
	A100	p148, p149, p152, p153, p176, p177, p180, p181	21.48	17		
S21 (Column21)	A101	p150, p151, p154, p155, p178, p179, p182, p183	26.45	19	20	18

	A10 2	p151, p152, p155, p156, p179, p180, p183, p184	26.45	19		
	A10 3	p152, p153, p156, p157, p180, p181, p184, p185	26.45	19		
	A10 4	p154, p155, p158, p159, p182, p183, p186, p187	22.11	19		
S22 (Column21)	A10 5	p155, p156, p159, p160, p183, p184, p187, p188	22.11	19	20	18
	A10 6	p156, p157, p160, p161, p184, p185, p188, p189	22.11	19		

As mentioned in Table 4.4, for a more effective evaluation of the deck of the bridge span, it was divided into ten sections with distances of 5 m. In addition, each bridge column was divided into six sections with a distance of 2 m. Each deck section was divided into seven area ranges between the measurement points. In this division, the first four ranges of each section in Table 4.4 represent the upper part of the bridge deck box, and the following three peaks are related to the area of the sides and bottom of the deck in one section of the bridge. Each section of the piers is divided into three adjacent parts of equal volume.

The results of the PSD approach to damage detection and the performance of this method in reducing repair and maintenance costs are compared to the conventional method using the Spanish concrete code EHE-08 (Spanish Ministry of Public Works, 2008) to determine service life according to chloride corrosion deterioration to decrease the total cost of maintenance and repair. Analysis is carried out in the same conditions until the end lifetime of this structure. Conventional methods predicted regular service life and repair periods for damage by corrosion caused by chloride ions. The total estimated costs for repairs for the life (100 years) of the Arosa bridge, which is subject to damage by chloride ions, using PSD and conventional methods, are shown in Figure 4.7.

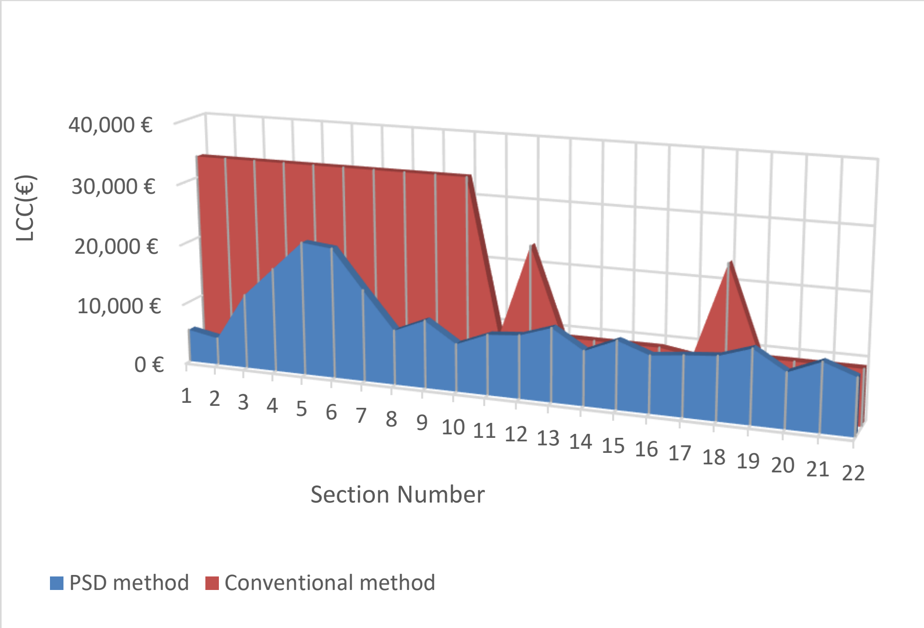

Figure 4. 7. *The life-cycle cost assessment for the Arosa bridge until the end of the bridge life*

The total LCC for one span of the Arosa bridge through PSD and conventional methods was calculated at about EUR 248,001.19 and EUR 470,113.12, respectively. The LCC for the columns using the PSD method was approximately EUR 122,688.59, and the cost using the conventional method was EUR 135,707.47. Furthermore, for a 50 m length of one span of the bridge, the costs using the PSD method and the conventional method in diagnosing and predicting the location and amount of damage were EUR 125,312.60 and EUR 334,405.64, respectively. Overall, using the PSD method for maintenance and repair of the bridge could save approximately EUR 222,111.92. These costs relate to all costs incurred for regular and continuous repair and maintenance of the Arosa coastal bridge for 100 years. Therefore, to more accurately examine the accuracy of the PSD method in reducing costs compared with the conventional methods of predicting structural damage, the LCC of total expenses for bridge repair and maintenance was investigated and analyzed according to a discount rate of 5 percent.

4.5. Conclusions

The results show that the use of the PSD method, as a non-destructive and dynamic damage detection method, has acceptable performance in detecting the presence, location, and amount of damage due to chloride ion attacks on a coastal structure such as the Arosa concrete bridge. In addition, according to the LCC results during the life of the bridge structure, which is assumed to be 100 years as the end of life, the use of this method with a different approach significantly reduces the costs of repair and maintenance, especially in the deck section.

In conclusion, the PSD method, as a non-destructive method of identifying struc-tural damage, have acceptable performance in identifying damages caused by chloride corrosion in different places, including concrete and internal rebars of RC bridge that were damaged and were not visible with the eyes. In addition, this research on the PSD method as a non-destructive method has shown that chloride corrosion damages had a minor influence on the analysis through the PSD method performance. Furthermore, this method was used in various analyses to determine the time and quantify damages in each location of the coastal bridge structure based on the distance of each element to the seawater. These areas include submerged and tide zone columns and dry parts such as the top of the columns and the deck. Moreover, using this method for LCCA of this bridge will play an essential role in reducing approximately 40% of the total LCC and maintenance and repair during the bridge life because of accurate prediction of location and amount and time of damages caused by corrosion. So, the PSD method can significantly optimize costs through on-time maintenance and repair of structures. In general, what is clear is that non-destructive methods of damage detection have more advantages compared to destructive methods in the LCA discussion, especially in the maintenance and repair phase. However, the ability and accuracy of each non-destructive damage detection method to detect the presence, location, and amount of damage in each part of the structures, considering that each is suitable for different conditions and types of construction and environment, make them more advantageous than others.

However, after ruling out other causes of damage, such as during bridge inspection, this study uses the PSD method to identify only structural deterioration caused by reinforcement corrosion and that chloride ions are the cause. On the other hand, the electrochemical methods, e.g., linear polarization resistance (LPR), galvanostatic pulse (GP), or electrochemical Impedance spectroscopy (EIS), were not used to determine the corrosion rate due to the technical nature of the tests and the undesirable extension of the entire testing process. For this reason, the approach to identifying the corrosion process has been simplified, being aware of a certain probability of damage.

Chapter 5

Durability assessment and re-design of coastal concrete bridge through a non-destructive damage detection method

Authors:	Mehrdad Hadizadeh-Bazaz; Ignacio J. Navarro; Víctor Yepes
Status:	Manuscript published
Journal:	*27th International Congress on Project Management and Engineering Donostia-San Sebastián,* 10th -13th July 2023
DOI:	10.61547/3371
Presentation:	Post-print (author version)

***This paper achieved second place in the Jaume Blasco Innovation Award at the 27th International Congress, 2023.**

Abstract

Experts and governments have long focused on reducing the costs of repairing and maintaining crucial structures such as bridges through continuous maintenance and repair. In the meantime, using appropriate methods for identifying possible damage and researching how much a partial re-design will lower the costs of repairing and maintaining a structure over its lifetime, considering the structure's environment and damage causes. This study explores the cost-effectiveness of two damage prediction methods using the power spectral density (PSD) method compared to the conventional method of detecting damage by re-designing different concrete cover thicknesses for a coastal reinforced concrete bridge. The study evaluates the impact of chloride ions on the location and extent of damage over the bridge's lifetime and compares the total maintenance and repair costs. The results show that while the PSD method is effective for concrete structures with low concrete covers, increasing the concrete cover thickness may result in higher repair costs.

Keywords Life cycle cost assessment; non-destructive damage detection methods; coastal concrete bridge; steel corrosion; chloride corrosion; maintenance and repair techniques

5.1. Introduction

Engineers and scholars have debated structural lifetime costs for decades. Design, building, repair, maintenance, and demolition are necessary expenses of civil structure activities. Bridges' life cycle costs include maintenance and repair expenditures. Many variables lower building maintenance expenses over time. Accurate health monitoring and damage detection technologies to forecast structural element deterioration throughout a structure's life cycle may save repair and maintenance expenses. Destructive and non-destructive technologies are employed to identify structural deterioration (Su, Dong, & Pei, 2022). Tests sometimes include removing structural samples to measure damage in destructive techniques. However, non-destructive methods may detect cracks or damages without harming the structure (Momeni & Ebrahimkhanlou, 2022). Several signal-based approaches as non-destructive methods include the time, frequency, and time-frequency domains (Liu et al., 2023). Some usable frequency domain techniques as variations in dynamic features, including natural frequency (Khodadadi & Mirjalili, 2022; Loya, Aranda-

Ruiz & Zaera, 2022), modal Curvatures (Yang et al., 2022; Nguyen et al., 2020), mode shape (Hassani, Mousavi, & Gandomi 2022; Zhang et al., 2022), modal strain energy (MSE) (Shirazi et al., 2023; Daneshvar, 2022; Nguyen, & Livaoğlu 2022), frequency response functions (FRF), and power spectral density (PSD) (Fang et al. 2023; Hadizadeh-Bazaz, Navarro, & Yepes 2022) are employed in vibration-based damage detection, some popular non-destructive testing methods.

On the other hand, it is necessary to investigate the performance of some non-destructive damage detection methods in different situations and conditions in order to the life cycle assessment (LCA) that includes environmental impact (Navarro, Yepes, Martí & González-vidosa, 2018) and social impact (Navarro, Yepes, & Martí, 2018) and in addition, life-cycle cost analysis (LCCA) of these techniques to decrease total costs in different stages of a structure from design and construction to end the life of the civil structure. Various research looked at the LCCA in some buildings and with other methods and conditions in the lifetime of some civil structures. Mirzaeefard, Mirtaheri, & Hariri-Ardebili, (2023) assessed the damage cost in several limit states of a pile-supported wharf damaged by corrosion. Then the LCC analysis considers crane damage and inspection and maintenance expenses. Vasishta, Mehany, & Killingsworth, (2023) compared the environmental and life-cycle costs of precast and cast-in-place (CIP) construction technologies. Thus, using Open LCA software and the NIST guidelines for LCCA, a cradle-to-grave methodology was applied to examine these consequences for precast and cast-in-place building systems. Heidari, Heravi, & Esmaeeli, (2020) developed a probabilistic and uncertain approach to estimate the life-cycle costs and environmental impacts of pavements.

The performance of each non-destructive damage identification method and the life cycle and life cycle cost assessment of each technique in any type of structure and according to different conditions and situations requires a detailed investigation. Although in this regard, Hadizadeh-Bazaz, Navarro, & Yepes (2023) examined the efficacy of the non-destructive damage-prediction PSD technique for a coastal concrete structure and its relevance in LCCA to decrease maintenance and repair costs due to chloride ions in marine and coastal environment.

This study employs the PSD method to identify damages for a coastal concrete bridge designed by changing the concrete cover for various parts and elements exposed to chloride ion corrosion in order to evaluate the performance of this damage detection method on LCC by changing the thickness of the cover as one of the influential factors in chloride corrosion damage. For this purpose, the effect of increasing the concrete cover of the structure on the performance of the PSD method was analyzed and compared with the conventional method in predicting the chloride corrosion damage prediction method during the lifetime of this marine concrete bridge. Then LCCA and total costs related to differentiation and maintenance were compared and analyzed using these methods for different concrete covers. During this bridge's lifetime (100 years), PSD, as a frequency-domain approach, was tracked utilizing sensitivity equations and the linear least squares method. This structure's health was monitored yearly using these techniques and under changes in dynamic components, such as the stiffness and mass of rebars and bridge construction parts. The result of this study can help engineers and specialists in this field for more information about the performance and drawbacks of this dynamic and non-destructive damage detection method in coastal and marine environments.

5.2. Objectives

The following are some of the main goals of this research:

• Analyze the ability of the PSD method to detect damage and corrosion in the case of changes in the thickness of the concrete cover of the structure.

• Determining the amount of effects of damage detection through a non-destructive method effectively reduces the total costs of repairing and maintaining the structure.

5.3. Methodology

To analyze the effect of increasing the concrete cover of the structure and to evaluate non-destructive damage detection methods for detecting corrosion damage in the case of minor changes in the design and implementation of a coastal concrete bridge was done in stages. The first stage utilized Fick's second chloride diffusion equation to estimate steel component service life for different concrete cover thicknesses. Then, using the PSD approach, the presence, amount, and location of chloride damage were determined for the various concrete cover scenarios for the RC bridge. Finally, according to damages predicted for each area and element of the structure, determine the total life cycle cost for each section of the structure for repair activities in the lifetime of a structure by considering the discount rate for LCCA.

5.3.1. Prediction strategies for corrosion deterioration in steel rebars

Most steel is fragile and easily broken by both natural and manufactured things. These corrosions are common in coastal areas, where large amounts of corrosion-causing chloride ions are present. In marine and coastal regions, structures like bridges and buildings made of reinforced concrete often cause corrosion in steel rebars.

The total time until chloride corrosion (t_l) according to the damages and chloride corrosion by Tuutti (1982) is the service life of the reinforcements of the bridge structure when the initiation and propagation phases are assumed together, as shown in the following equations (Spanish Ministry of Public Works, 2008).

$$\boldsymbol{t_l = t_i + t_p} \tag{5.1}$$

The corrosion initiation period (t_i) is the time it takes chlorides to reach a concentration that starts rebar corrosion (chloride threshold, dependent on the steel properties and, to some extent, on the concrete properties). The t_p is also the time it takes corrosion to spread across a structural section before it fails (Spanish Ministry of Public Works, 2008).

A physical model tracks chloride ions in concrete cover to determine initiation time using Fickian models, assuming a uniform porous cover that diffuses ions in suitable humidity. Chloride drives diffusive action between the surface and cover, and Fick's equation is used to determine chloride diffusion in the cover. The equation from Fib Bulletin 34 (2006) assumes a constant, time-independent surface chloride concentration. The predicted chloride level in the concrete cover at depth x and time t is:

$$\boldsymbol{C(x.t) = C_s.\left(1 - erf\left(\frac{x}{2\sqrt{D_{0.x}.(\frac{t_0}{t})^{\alpha}.t}}\right)\right)} \tag{5.2}$$

Where $C(x,t)$ is the chloride concentration at depth x and time t, and C_s is the concentration of chloride ions at the concrete's outside surface. The chloride transport time t into the concrete element is given by the inverse action on Equation 5.2, which in this equation is considered $C(x,t)=C_t$.

$$\boldsymbol{t_i = \frac{x^2}{4D}\left[erf^{-1}\left(\frac{C_s - C_t}{C_s}\right)\right]^{-2}} \tag{5.3}$$

In this instance, D refers to the chloride diffusion coefficient, which shifts over time as the concrete ages according to the formula $D = D_0(t_0)(t_0/t)^n$. After the initiation stage of chloride diffusion, the propagation chloride corrosion phase (t_p) begins when chloride ions on the surface of the inner rebars begin to corrode steel reinforcements. The stiffness and cross-sectional area of the steel bars are gradually decreased by chloride corrosion. The Spanish Concrete Design Code (2008) offers the formula below to determine the propagation time:

$$\boldsymbol{t_p = \frac{80}{\phi}\frac{d}{V_{corr}}} \tag{5.4}$$

Where d is the concrete cover's thickness, ϕ is the diameter of the rebar, and V_{corr} is the corrosion rate.

In this study, according to the Spanish concrete design code (2008), the durability parameters for the Arosa bridge were considered as follows for calculating conventional chloride corrosion in steel rebars. The C_s (% of concrete weight) for the aerial, submerged, and tidal zones are equal to 0.14, 0.72, and 0.5, respectively. And also, V_{corr} values for the aerial, submerged, and tidal areas are equal to 20, 4, and 50 (μm/year), respectively. In addition, D_0 is equal to 10 ($\times 10^{-12}$m^2/s).

According to the Spanish concrete design code (2008), as shown in this study and other research (Navarro, Martí, & Yepes, 2019; Bruet et al., 2018; Frontera, & Cladera, 2022), the critical chloride concentration (C_{th}) must be determined by the designer in accordance with the specific concerns related to the structure, whereas under normal conditions, a value of 0.6% of the cement weight can be used to evaluate the limit state in terms of passive reinforcement corrosion. In addition to this analysis, in this study, the thickness of the concrete cover of the structure in the deck part was performed for the thicknesses of 3 (Refrense), 3.5, 4, 5, and 6 cm and for the columns with the thickness of the concrete cover of 4 (Refrense), 4.5, 5, 6, and 7 cm.

The following formula, which considers the initiation and propagation levels for chloride corrosion of reinforcements of an RC maritime or coastal structure, may be used to forecast, as a percentage, the damages throughout the period produced by chloride corrosion.

$$\boldsymbol{Dam_{steel}(t) = \frac{t - t_i}{t_p} \times 100} \qquad (5.5)$$

Where the *Damsteel* is the percentage of reinforcement damaged by chloride corrosion for each year (*t*) since the start of the propagation *tp*.

The damage to the RC bridge's deck and columns were based on scenarios and marine exposure classifications, such as Aerial, Sub-merged, and Tide zone. Also, the percentage of chloride corrosion damage to the concrete of the RC structure was found, along with the results of changes in stiffness and loss of cross-section rebar area for damage identification.

5.3.2. Damage detection through non-destructive damage detection methods

A structure's integrity can be assessed using non-destructive damage detection methods. Preserving structures requires these methods. They can spot damage before it worsens. The power spectral density methods(PSD) are used in modal analysis, a non-destructive damage detection method. A structure's natural frequencies, vibration modes, and damping ratios are measured using modal analysis. PSD can detect modal parameter changes that indicate damage. The PSD of vibration signals determines the response's spectral content, which can mean damage if the modal parameters change. Due to its reliance on vibration and signals, the PSD was calculated using the frequency response function with the help of the following equations (Zheng et al., 2015; Pedram, Esfandiari & Khedmati, 2017; Hadizadeh-Bazaz, Navarro, & Yepes, 2023). The structural response PSD equation is simplified as follows:

$$\boldsymbol{S_{XX}(\omega) = H^{*}(\omega)S_{FF}(\omega)H^{T}(\omega)} \quad (5.6)$$

Where S_{FF} is the PSD inputs matrix for every active degree of freedom (DOF) and $H^{*}(\omega)$ is the complex conjugate of a transfer function according to the following equation:

$$\boldsymbol{H(\omega) = (K - \omega^{2}M + i\omega C)^{-1}} \quad (5.7)$$

K, M, and *C* represent the matrices of stiffness, mass, and damping, respectively; denotes the frequency, and I equals -1 times the frequency. Model updating based on the sensitivity equation for the power spectral density equation can be expanded as follows by considering (*K-ω2M+iωC=Z(ω*) in the below equation:

$$\boldsymbol{Z^{*}(\omega)S_{XX}(\omega) = S_{FF}(\omega)H^{T}(\omega)} \quad (5.8)$$

Where in this equation, *Z(ω)* is the impedance matrix, and the transfer function inverse that this equation for corrosion damages caused by structure is as follows:

$$\boldsymbol{[Z^{*}(\omega) + \Delta Z^{*}(\omega)][S_{XX}(\omega) + \Delta S_{XX}] = S_{FF}(\omega)[H^{T}(\omega) + \Delta H^{T}(\omega)]} \quad (5.9)$$

The power spectral density function equation is modified by taking into account ($\Delta Z(\omega)=\Delta K-\omega^{2}\Delta M+i\omega\Delta C$) *and* ($H_{D}(\omega)=[Z(\omega)+\Delta Z(\omega)]^{-1}$) was modified. Where $H_{D}(w)$ was the frequency response function of damaged structural elements in each year of structure life. Therefore, the up equation can be simplified as follows:

$$\boldsymbol{\Delta S_{XX}(\omega) = H_{D}^{*}(\omega)S_{FF}(\omega)\Delta H^{T}(\omega) - H_{D}^{*}(\omega)\Delta Z^{*}(\omega)S_{XX}(\omega)} \quad (5.10)$$

H^{*}_{D} is the complex conjugate of the damaged structure elements transfer function during reinforcement chloride corrosion from conventional chloride corrosion deterioration proses in coastal structures. As the expression of the exact *ΔH* presented by Hadizadeh-Bazaz, Navarro, & Yepes (2022); Esfandiari et al. (2009) in the following equation:

$$\boldsymbol{H(\omega) = -H_{D}(\omega)(\Delta K - \omega^{2}\Delta M + i\omega C)H^{T}(\omega)} \quad (5.11)$$

Therefore PSD, according to the mentioned equations, can rewrite as follows:

$$\boldsymbol{\Delta S_{XX}(\omega) = -H_{D}^{*}(\omega)S_{FF}(\omega)H_{D}(\omega)(\Delta Z(\omega))H^{T}(\omega) - H_{D}^{*}(\omega)(\Delta Z^{*}(\omega))H^{*}(\omega)S_{FF}(\omega)H^{T}(\omega)} \quad (5.12)$$

To determine the effects of corrosion on reinforcement bars and the system's structural behavior, each reinforced concrete element's stiffness and other dynamic properties in proportion to the corrosion damage computed for the rebars at each time. The stiffness, mass, and damping matrices modify due to dimensionless structural parameter changes:

$$\begin{cases} \Delta K = \sum_{n=1}^{ne} K_n \Delta P_n^K \\ \Delta M = \sum_{n=1}^{ne} M_n \Delta P_n^M \\ \Delta C = \sum_{n=1}^{ne} C_n \Delta P_n^C \end{cases} \quad (5.13)$$

The stage of stiffness, mass, and damping matrices of a structure's structural components are *Kn*, *Mn*, and *Cn*. where structural parameter variations are between -1 and 1.

The monitoring of changes in stiffness, mass, and damping of a structure owing to probable damage to a structure using the PSD damage detection technique has been estimated by considering *(ΔZ(ω)=ΔK-ω2ΔM+iωΔC)*. The sensitivity matrices allocated to the *nth* parameter of structure for getting the unknown stiffness, mass, and damping ratios are as follows, based on changes in dynamic characteristics caused by damage causes such as chloride corrosion damages.

$$\begin{cases} S^K = -H_D^*(\omega)S_{FF}(\omega)H_D(\omega)K_n H^T(\omega) \\ \quad -H_D^*(\omega)K_n H(w)S_{FF}(\omega)H^T(\omega) \\ S^M = \omega^2(H_D^*(\omega)S_{FF}(\omega)H_D(\omega)M_n H^T(\omega) \\ \quad +H_D^*(\omega)M_n H(w)S_{FF}(\omega)H^T(\omega) \\ S^C = i\omega(-H_D^*(\omega)S_{FF}(\omega)H_D(\omega)C_n H^T(\omega) \\ \quad +H_D^*(\omega)C_n H(w)S_{FF}(\omega)H^T(\omega) \end{cases} \quad (5.14)$$

The final equation of PSD for estimating changes in dynamic characteristics parameter during damage repetition for each year is given by the following equation**:**

$$\Delta S_{xx} = S^K \Delta p_K + S^M \Delta p_M + S^C \Delta p_C \quad (5.15)$$

Where ΔpK, ΔpM, and ΔpC use chloride corrosion deterioration of reinforcement equations and the power spectral density method to monitor the changes in stiffness and reinforcement loss cross-section areas in the RC marine bridge elements over time.

5.3.3. LCCA through the damage detection methods

One of the essential things to consider when evaluating a bridge's performance is its life-cycle cost. The LCCA for the bridge was calculated using the location and percentage of damages expected annually by damage-detecting methods. Each stage of a structure's life cycle and life cycle cost typically includes production, construction, usage and maintenance, and eventually, the end of the structure's existence. As a result, the following formulas may be used to estimate the bridge's projected cost during its life cycle (Hadizadeh-Bazaz, Navarro, & Yepes, 2023; Frangopol, Dong, Sabatino, 2017).

$$\boldsymbol{C_T = C_I + C_M + C_{INS} + C_R + C_{Dam}} \qquad (5.16)$$

Where the C_I represents the initiation cost, C_M represents the maintenance cost, C_{INS} represents the inspection cost, C_R represents the total repair cost, and C_{Dam} represents the anticipated damage cost in the calculation. The entire cost of the concrete bridge repair operation may be determined using the following items:

$$\boldsymbol{C_R(t_V) = C_{DNRC}(t_V) + C_{DRC}(t_V) + C_{SM}(t_V) + C_{PE}(t_V) + C_S(t_V) + C_C(t_V)} \qquad (5.17)$$

Where t_v is the interval time period studied; C_{DNRC}, is the cost of demolishing non-reinforced concrete parts like the structure's cover; C_{DRC}, is the cost of demolishing reinforced concrete parts like the bridge's structural parts; C_{SM}, is the cost of sorting and recycling demolition debris; C_{PE}, the cost of preparing equipment for repairing the bridge's concrete and rebars; and C_S, is the overall cost of buying and replacing damaged steel reinforcements, and also C_C is the total cost of the concrete parts include material and activities of the bridge damaged over the time. Corrosion and damages caused by the presence of chloride ions in coastal structures, as well as other factors, such as floods and earthquakes following a Poisson process, can all be factored into the total life-cycle damages in each structural part and element of a bridge within the time interval (Hadizadeh-Bazaz, Navarro, & Yepes, 2023; Frangopol, Dong, Sabatino, 2017; Dong, & Frangopol, 2016).

$$\boldsymbol{C_D(t_v) = \sum_{K}^{N(t_v)} D(t_k).\, e^{-rt_k}} \qquad (5.18)$$

$N(t_v)$ is the number and amount of damage factors on a structure during the interval. As anticipated by the PSD approach, annual damages due to chloride corrosion are denoted by D, where D is expressed as a percentage of the yearly damages at time t_v. The discount rate used here is represented by (r = 5%). According to the Poisson model, tk follows the uniform interval distribution $[0,\ t_v]$ with a mean rate λ_f. The projected yearly proportion of bridge element damage owing to hazard effects may be stated as ($N(t_v) = \lambda_f \times t_v$). Therefore, the corrosion damages bridge element's value can be obtained from the following equation (Hadizadeh-Bazaz, Navarro, & Yepes, 2023; Frangopol, Dong, Sabatino, 2017; Yeo, 2005).

$$\boldsymbol{E[C_D(t_v)] = \frac{\lambda_f \,.\, E(D)}{r} \,.\, (1 - e^{-rt_k})} \quad (5.19)$$

At the last step of the LCCA process, the equation calculates the overall expenses of bridge repair and maintenance in proportion to the percentage of damage projected for the whole bridge by the following equation (Lee, Cho, & Cha, 2006):

$$\boldsymbol{E[C_T\,(\bar{x}.t_v)] = C_I + C_M + \sum_{t=1}^{t_v} \left[\frac{\left(\sum_{t=1}^{N(t_v)} E[C_{DNRC}\,(\bar{x}.t)] + \sum_{t=1}^{N(t_v)} E[C_{DRC}\,(\bar{x}.t)] + \sum_{t=1}^{N(t_v)} E[C_{SM}\,(\bar{x}.t)] + \sum_{t=1}^{N(t_v)} E[C_{PE}\,(\bar{x}.t)] + \sum_{t=1}^{N(t_v)} E[C_S\,(\bar{x}.t)] + \sum_{t=1}^{N(t_v)} E[C_C\,(\bar{x}.t)]\right)}{(1+r)^t} \right] + C_D} \quad (5.20)$$

Where in this equation, $\sum_{t=1}^{N(t_v)} E[C_{DNRC}\,(\bar{x}.t)]$, $\sum_{t=1}^{N(t_v)} E[C_{DRC}\,(\bar{x}.t)]$, $\sum_{t=1}^{N(t_v)} E[C_{SM}\,(\bar{x}.t)]$, $\sum_{t=1}^{N(t_v)} E[C_{PE}\,(\bar{x}.t)]$, $\sum_{t=1}^{N(t_v)} E[C_S\,(\bar{x}.t)]$, and also $\sum_{t=1}^{N(t_v)} E[C_C\,(\bar{x}.t)]$ are respectively the total costs of demolishing the unreinforced concrete parts, the reinforced concrete parts demolition, management, separation, and categorization of debris resulting from destruction, installation, and subsequent removal formwork for repair concrete activity, repair and replacement damaged bar steel with corrugated bar steel with improved ductility characteristics and also prepare and pour concrete costs during and until end of coastal structure life. In this analysis, the LCC of the whole structure is determined and assessed based on the damage sustained by the structure each year, the quantity of corrosion of metal components during the structure's life, and the structure's service life.

Overall the methodology of this study this investigation encompasses a comprehensive analysis and calculation methodology, which includes the following steps:

First, according to the Spanish Ministry of Public Works (2008), the service life and damages caused by chloride corrosion on the inner rebars of reinforced concrete structures in marine or coastal environments involved chloride corrosion predicted through a conventional technique. Then, according to the change in diameter and changes in dynamic properties such as stiffness and mass of reinforcement for every element for every year of the bridge life (100 years), the amount of corrosion damage depending on the situation of each element of the bridge structure to seawater calculated as Dam_{steel} in Equation 5.5. In the second step, according to the rebars, damages for every bridge section through the PSD method as a non-destructive and dynamic damage detection method monitored damage percentage in every concrete bridge section of the deck and columns yearly. For this purpose, sensitive equations and considering different dynamics that characterize the structures every year after building the bridge were analyzed and calculated as Equations 5.15. Finally, the total cost and LCC for maintenance and also whole repairs activities and materials (concrete, rebars) needed according to damages predicted *D(t)* in the first and second step for every element were obtained and then calculated by using Equation 5.20, updating for every year and every element and section of the bridge by considering discount rate 5% calculated and then annalizes compared.

5.4. Model description

The Arosa Bridge is a coastal concrete bridge in Galicia, Spain. Its name comes from its location. This bridge measures a total of 1980 meters in length and consists of 40 spans (the first and end spans are 40 m, and the other 38 intermediate spans are 50 m). The geometry and durability characteristics of this design were derived from research that was published in the past (González, Aguilera, & García, 2013; Pérez-Fadón, 1985; and Pérez-Fadón, 1986). As seen in Figure 5.1, a single box girder supports the concrete bridge deck by 13 meters wide (including two 1.5-meter-wide walkways) and 2.30 meters high. The column is 5.26 m broad and 1.80 m thick. During high tide, the bridge deck is 9.6 m above the seawater.

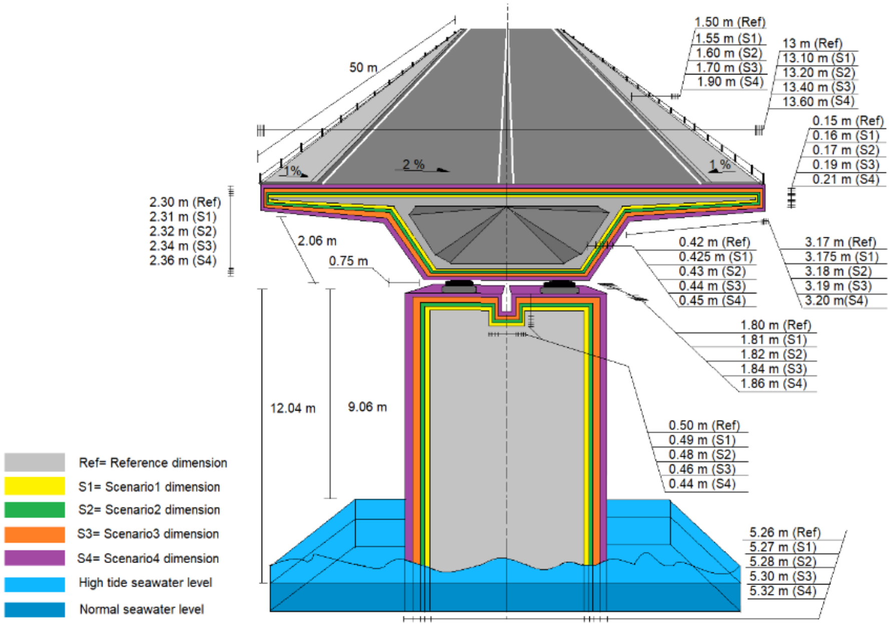

Figure 5. 1. *The cross-section dimension of the coastal and concrete Arosa bridge.*

According to Figure 5.1, the dimensions and sizes for the actual and original dimensions of the bridge (reference dimensions), as well as the different design scenarios of different thicknesses of the bridge in the case of increasing the thickness of the concrete cover in the deck and columns of the bridge in order to the performance of a damage detection method in the thickness of the concrete cover scenarios for each thickness increase, including 0.5 cm, then 1 cm, then 2 cm, and finally 3 cm.

5.4.1. Analysis in the numerical model description

As computers and sensors become faster and more capable, the use of non-destructive, independent models based on numerical models of buildings to identify damage is tempting to engineers and academics. Using the PSD vibration and signal-based technique, chloride ions damaged a coastal concrete bridge numerical model. The bridge's numerical model evaluated specified places and sensors at certain distances for health monitoring each year from the start to the conclusion of the concrete bridge reinforcement's corrosion period. Figure 5.2 shows a span with a deck and two piers numbered 1 to 167. The bridge's deepest stretch is the most susceptible to chloride assault.

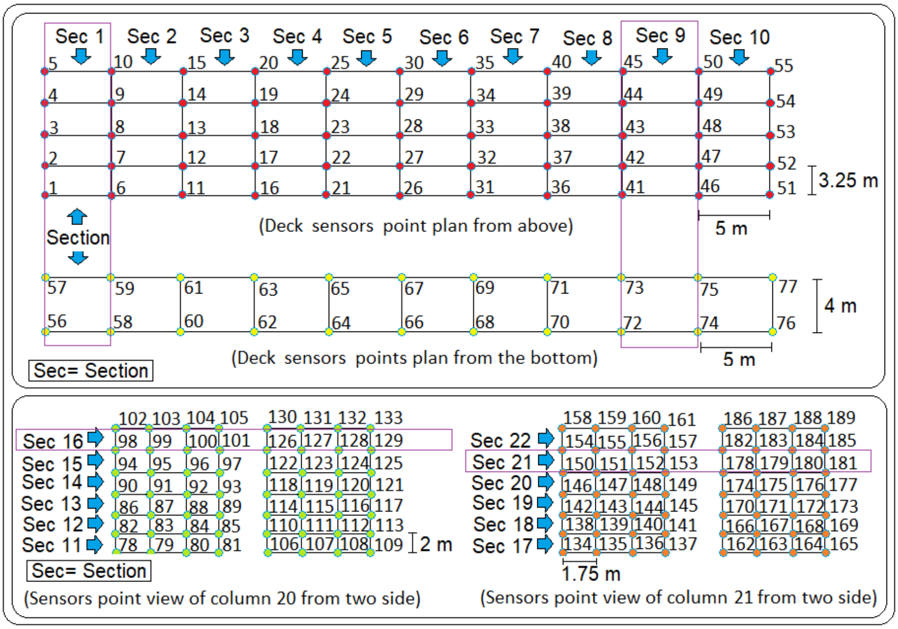

Figure 5. 2. *Sensor point numbering and division in each section of a span of the Arosa bridge*

In Figure 5.2, sensor points numbered from 1 to 77 for the bridge deck are 5 m apart in length and 3 m apart in breadth. One pier numbered 78 to 189, is 1.75 m wide and 2 m high, with 1.80 m separating the pier width locations. Some points were determined as simulation points, and others were measuring points to track chloride attack damage at each bridge position. These simulation and measurement points were believed to be fixed for yearly test monitoring and analysis. In addition, depending on each scenario of concrete cover, the situation and distance were a little bit changed according to increasing concrete cover in different analyses for each scenario of the deck and column of the bridge. So, on the bridge deck span, simulation points 3, 18, 33, 48, 58, 59, 64, 65, 70, 71, 76, and 77 were chosen, and between piers, points 86, 89, 98, 101, 115, 116, 127, 128, 135, 136, 147, 148, 159, 160, 162, 165, 174, 177, 186, 189, and 189 were evaluated. These points were assessed for each year of the bridge's existence in the same position.

In general, numerical analysis of LCC using a non-destructive method to find damage in concrete and coastal bridge structures in order to repair and maintain damage caused by corrosion by chloride ions for different scenarios of cover thickness design has some stages. In the first stage, damage detection in reinforced concrete was analyzed using various methods, including the PSD and conventional methods. Following that, the operation and repair activities were considered to determine the repair and maintenance costs during the structure's lifetime for the damages to each area and part of the bridge that was greater than 20%. In the last stage, according to the determination of the repair time of each element and the percentage of base damage, the total costs for repairing the structure during its life are calculated using 10% noise and error. These analyses and monitoring were done for every concrete cover scenario to compare the performance of increasing thickness of concrete cover in the same structure in performance to damage detection methods and LCCA through corrosion. Analyses were done via MATLAB and Open Sees software to examine the PSD and conventional methods.

According to the Spain Ministry of Transport, Mobility and Urban Agenda cod and costs (2022), the repair activity cost (EUR) for the concrete and coastal Arosa bridge includes in Table 5.1.

Table 5. 1. *Total repair activity cost (EUR) for the service life of the coastal Arosa bridge.*

No	Maintenance and repair activities	Description / Includes	Price per unit (€)	Unit
1	Unreinforced concrete demolition	Debris removal, loading, and transfer to approved management within 60 km	30.20	m^3
2	Reinforced concrete demolition	Debris removal, loading, and transfer to approved management within 60 km	33.07	m3
3	Dismantling, sorting, and categorizing waste	Loading and transporting bricks, tiles, ceramics, or a combination of these non-hazardous building materials (excluding dirt and stones)	7.78	Ton
4	Repair concrete formwork and remove them	Double-folded, wood cleaning, wetting, release agent, and complimentary materials for stability and proper execution	33.91	m^2
5	Replace and replace damaged bar steel with corrugated bar steel with enhanced ductility	Including cutting and bending, placement of overlaps, breakout, and binding annealed wire and separators	1.81	Kg
6	Total new concrete activities	Prepare and pour concrete piles, stirrups, headboards, beams, deck boards, slabs, walls, and frames	147.01	m^3

The total costs of repairing this bridge using the materials and activities mentioned in Table 5.1 can be estimated using the number of breakdowns and damage incidents each year as the basis for the cost estimate. It was compared to both the PSD and the conventional approaches.

5.5. Results

The results of examining the PSD method with a different approach in detecting the location and extent of damage to a coastal reinforced concrete bridge exposed to corrosion and damage by chloride ions for each year of the life of this bridge for different design scenarios increased the thickness of the concrete cover of the structure was compared with the results of the conventional method in diagnosing service life and predicting damage caused by chloride for different scenarios. Figure 5.3 depicts the average time and period of repair and maintenance for each section of the bridge using two methods and for different scenarios, based on the bridge's life span of 100 years and 20% damage as a percentage of the base damage in each element and part of the bridge.

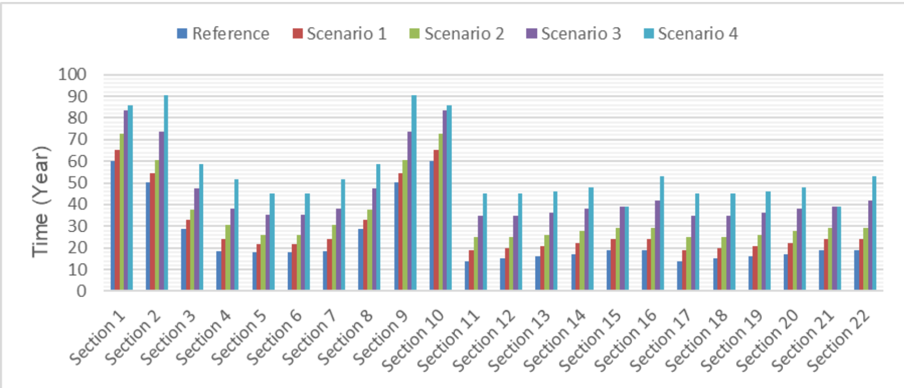

(a)

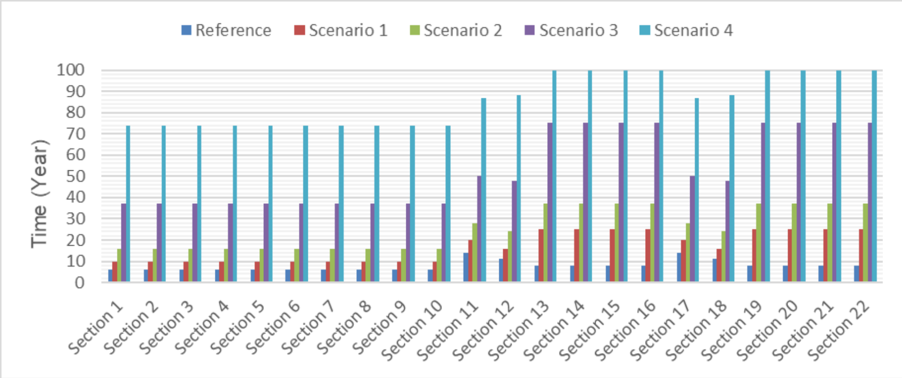

(b)

Figure 5. 3. *Compare service life and repair time in the bridge by (a) PSD method and (b) Conventional method.*

Figure 5.3 shows different scenarios of concrete cover thickness, including reference dimensions: 3 cm thick cover for the deck and 4 cm thick concrete cover for columns in the span of the bridge. As reference dimensions, according to the different concrete covers of the bridge in scenarios 1 to 4, they increase respectively by 0.5, 1, 2, and 3 cm. The service life period for repairing the bridge in the bridge lifetime (100 years) by considering damage elements 20% and more than through to the PSD method for scenarios 1 to 4 for the deck sections are respectively average about 3, 12, 17 and 27 years for the period repair time. And, for the columns, this time for service life, the columns for scenarios 1 to 4 are respectively about 3, 10, 20, and 28 years. On the other hand, this analysis using the conventional method according to four different scenarios increases for the deck, for scenarios 1, 2, 3, and 4, about 2, 10, 30, and 70 years, respectively, and also, by this method, average service life period for the columns sections for scenarios 1 to 4, respectively 10, 20, 60 and 80 years.

The results of the final LCD according to the different scenarios in the design of the concrete cover thickness of the structure in order to repair the structure according to the method of detecting and predicting PSD damage in comparison with the conventional method for different sections of the deck and columns of a span of the bridge are shown in Figure 5.4.

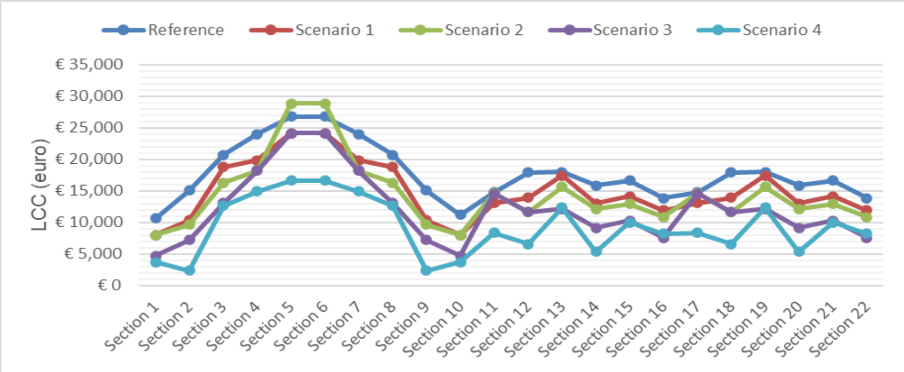

(a)

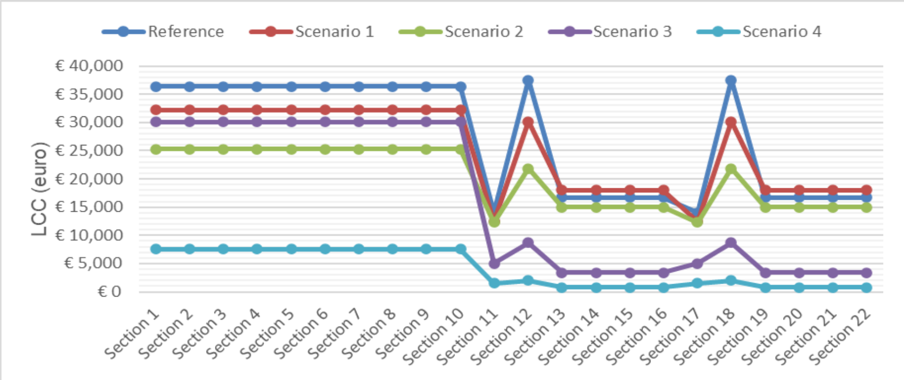

(b)

Figure 5. 4. *Life cycle cost assessment in the bridge is done using (a) the PSD method and (b) the conventional method.*

According to the results of Figure 5.4, it is shown that the difference in the total price for the repair and maintenance of a bridge span for the reference dimensions of the bridge using the PSD method is about 261445 euros, according to the discount rate of 5% during the life of the structure. Meanwhile, according to the different scenarios of the thickness of the concrete cover of the structure, for the first to third scenarios, the difference in the cost of using the PSD method compared to the conventional method is about 246,675 euros, 128,253 euros, and 90,902 euros for a bridge span. But, the fourth scenario shows that the conventional method has a lower cost difference of 112,570 euros.

5.6. Conclusions

In conclusion, the performance of the PSD method in the case of a change in the thickness of the concrete cover of the bridge and the performance and accuracy of this method in detecting the location and the amount of damage caused by corrosion in each year of the structure's life showed that the PSD method has a more suitable performance. It is better than the conventional method of detecting damage caused by corrosion. Also, the PSD method detected the amount and location of damage in each year of the structure's life in each part and element of the bridge separately. In contrast, the conventional method predicts damages in an integrated manner in the deck part, which shows its superiority. The PSD method effectively detects the damage's location in different bridge elements.

Moreover, the total LCC for total repair and maintenance activities costs can be saved by the PSD methods for damage detection by about 59.7%, 57.7%, 71.2%, and 74.45% through the reference and scenarios 1–3. On the other hand, through the concrete cover design dimensions of scenario number 4, the conventional method can save about 44.1% of the total cost of repair and maintenance activities.

Overall, this research showed that the PSD method could determine where and how badly chloride ions have damaged a reinforced concrete structure near the coast. It was also found that increasing the thickness of the concrete cover and the distance of the rebars from the surface and sensor points can negatively affect the performance of this method. To minimize the effects of concrete cover on PSD damage detection, choosing appropriate sensor locations and using high-sensitivity sensors to detect signal changes is vital. In addition, using advanced signal processing techniques, such as wavelet analysis or Fourier transform, can help extract damage-related features from the signals even in the presence of a thick concrete cover.

Chapter 6

Life Cycle Assessment of a Coastal Concrete Bridge Aided by Non-Destructive Damage Detection Methods

Authors:	Mehrdad Hadizadeh-Bazaz; Ignacio J. Navarro; Víctor Yepes		
Status:	Manuscript published		
Journal:	*Journal of Marine Science and Engineering, 11(9), 1656.*		
DOI:	10.3390/jmse11091656		
JCR IF (2023)	2.7		
	JCR Category	Ranking	Quartile
	Engineering, marine	6/25	Q1
Presentation:	Post-print (author version)		

Abstract

Recently, using economic damage identification techniques to ensure the safety of bridges has become essential. But, investigating the performance of those techniques for various conditions and environments and, in addition, a life cycle assessment (LCA) through these methods depending on the situation and during the life of a structure could help specialists and engineers in this field. In these regards, analyzing the implementation of a technique for the restoration and maintenance stages of costly structures such as bridges can illustrate the effect of each damage detection method on the LCA. This research assessed non-destructive abilities and a dynamic approach to predict the amount and location of damages in the LCA. For this purpose, the power spectral density (PSD) technique's performance by different approaches in identifying corrosion damages for a coastal bridge and the effectiveness of using this technique on reducing the environmental impact compared with a conventional method were evaluated. The results demonstrate a reduction of the environmental impacts by approximately 23% when using the PSD during the bridge's service life. In conclusion, the PSD approach does well in anticipating the damage quantity and location on a coastal bridge, which reduces the environmental impacts during the repair and maintenance.

Keywords sustainability; non-destructive damage identification technique; life cycle assessment (LCA); environmental impacts assessment; concrete coastal bridge; corrosion; power spectral densitymethod (PSD)

6.1. Introduction

The Brundtland Report's definition of sustainability, which integrates social, economic, and environmental requirements, is defined as the "development that satisfies the needs of the present without compromising the capacity of future generations to satisfy their own needs" (Keeble, 1988). In line with this idea, the adequate maintenance of infrastructures is essential to avoid unnecessary expenses and environmental impacts associated with the construction of new assets. Nevertheless, in recent years, there has been a notable emphasis among academics on evaluating the consequences linked to infrastructure maintenance (Liljenström & Björklund, 2022; Renne et al., 2022). This is due to the recognition that these effects might surpass those related to infrastructure creation if the design is inadequate. In this context, LCA has arisen as a powerful decision tool to evaluate maintenance impacts. In recent years, comprehensive research has assessed the environmental ramifications associated with diverse infrastructural developments across their entire life cycle, such as buildings (Caruso et al., 2020), pavements (Kazemeini et al., 2023), railway tracks (Celauro et al., 2023), or urban infrastructure elements (Wang et al., 2020).

In light of the societal and economic significance of transportation networks and the substantial economic and environmental consequences linked to the establishment and upkeep of transportation infrastructure, there has been a notable focus in recent years on conducting life cycle assessments for bridges (Balogun et al., 2020). Pons et al. (Pons et al., 2018) evaluated and contrasted the environmental impacts generated by building several kinds of earth-retaining walls to guide designers in picking the most appropriate solution for each height to decrease emissions. Navarro et al. (Navarro et al., 2020) examined the long-term performance designs of structure from the LCA impacts standpoint by using simple additive weighting (SAW) and the analytic hierarchy process (AHP) to assess the consequences of bridges' end-of-life cycle stages. Penadés-Plà et al. (2019) conducted an environmental evaluation utilizing a single criterion that reliably indicates the environmental effect as a first approximation of the environmental aim for the assessment performance of an optimization method. Navarro et al. (2019a) used a weighted criterion decision-making strategy to review the use of such methodologies in infrastructure sustainability evaluation implications and criteria by employing the analytic hierarchy process. Niu and Fink (2019) assess the sustainability of modern timber fridges by using an LCA-based approach. Navarro et al. (2019b) analyzed the financial and environmental consequences of 18 potential designs for a pre-existing concrete bridge deck subject to chloride exposure based on the maintenance interval. Reliability-based maintenance optimization for life cycle costs and environmental implications in concrete by 10% silica fume is the most cost-effective way to avoid reinforcing steel corrosion and decrease deck design life cycle costs by 76%. In addition to silica fume, other studies have also reported a similar outstanding performance of fly ash to increase concrete's durability and reduce maintenance needs (Longarini et al ., 2014; Orozco et al., 2023). Cheng et al. (2021) contributed to the field of sustainable structure by developing a BIM-LCA strategy for completely evaluating the life cycle embodied environmental impact (LCEEI) of buildings during the design stage. Khorgade et al. (2022) compare the bridge life cycle performance with carbon fiber polymer and steel reinforcements. Navarro et al. (2018a) assessed the LCA impacts of 15 prevention options on the deck of bridge exposed to a chloride environment through the Eco-Indicator 99 method used to assess the effects. They also assessed the social impacts of bridge decks in aggressive environments (Navarro et al., 2018b). Peng et al. (2022) focus their work on the maintenance optimization of bridges, considering a variety of economic, environmental, and social criteria.

Almost all research on economic and environmental impact assessment along the use and maintenance stages of infrastructure for repair activities uses conventional damage estimation methods or non-destructive and destructive damage prediction methods. However, other approaches could potentially be used to determine damages in an infrastructure of any kind and increase the accuracy of the prediction. These methods to predict damage could be either destructive or non-destructive. The destructive tactics use models, which typically include removing structural samples to assess damages. However, non-destructive approaches are independent models that may determine whether or not there is damage to a numerical model without actually inflicting any damage to the structural elements (Rathod et al., 2019). Non-destructive damage detection methods can use technologies based on signals. The application of different non-destructive methods to detect damage quantification and location to maintain and repair structures is of great interest in the sustainability assessment of structures.

In structural health monitoring, using modern and innovative high-tech computers and sensors has contributed to a growth in the adoption of signal-based techniques (Yang et al., 2021). Among the various signal-based methods are those that operate in either the time domain technique (Baybordi & Esfandiari, 2023; Yao et al., 2023), the frequency domain technique (Li et al., 2032; Chen, 2022), or the time-frequency domain technique (Liu et al., 2023; Yang, 2023). Some dynamic frequency-domain approaches used as non-destructive damage detection methods include natural frequencies (Khan et al., 2020; Wang, 2021), modal curvatures (Ciambella et al., 2019; Ganguli, 2020), modal strain energies (Alavinezhad et al., 2022; Le & Ho, 2022), frequency response functions (FRF) (Zhang et al., 2023; Kurent et al., 2023), and power spectral density (PSD) (Fang et al., 2023; Hadizadeh-Bazaz et al., 2022). Of these methods, the PSD is one of the frequency-domain techniques that use the responses of a periodic or randomized stimulus in frequencies to describe the mean power repartition. This approach employs a sensitive nonlinear function of structural factors to generate a transfer function of the second order (Nilsson & Liu, 2015). Recently, researchers from various disciplines have examined the performance of the PSD technique in detecting distinct forms of damage to structures. Hadizadeh-Bazaz et al. (2023a) investigated the performance of PSD to determine the amount and location of damages on a coastal bridge caused by corrosion. Bayat et al. (2019) evaluated a method according to the PSD and the least square to detect failures in a concrete bridge. Gunawan et al. (2019) evaluated the PSD approach’s dependability using seven masses in eight linear elastic repartition springs. Meanwhile, the PSD technique performed in life cycle cost assessment (LCCA) has recently been evaluated by Hadizadeh-Bazaz et al. (2023b). However, the PSD method's performance in other life cycle assessment cases, such as environmental and social impacts, has not been evaluated in the past. Figure 6.1 illustrates a flowchart of the methodology and level processes used to detect damage by the PSD approach to maintain and repair concrete bridge structures.

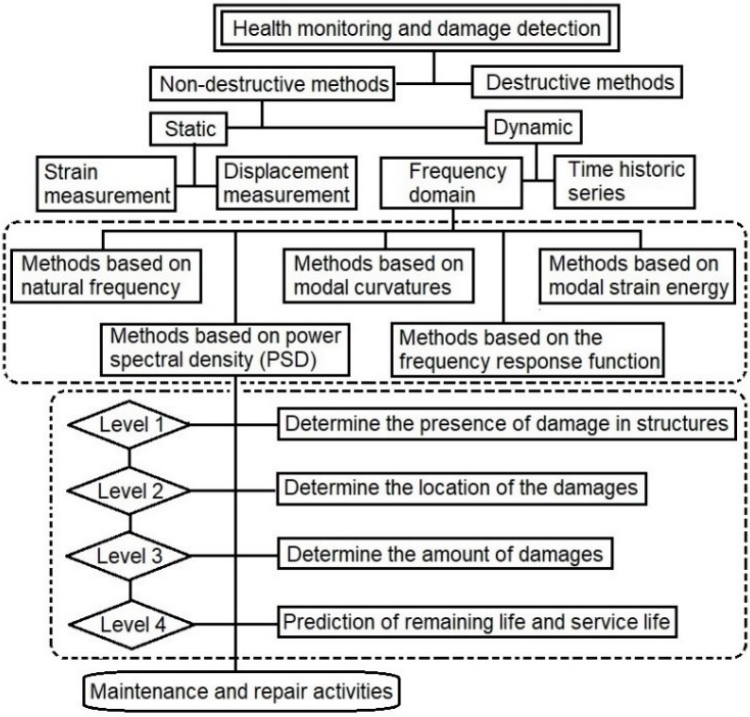

Figure 6. 1. *Health monitoring and damage detection processes in a bridge structure.*

This research evaluated the LCA of a bridge in an exposed coastal environment. In this work, a non-destructive technique was used to aid the analysis of the environmental impacts during maintenance activities. These results were then compared with those that resulted from applying conventional damage prediction methods. The estimation of the damage of each element over time was performed by using various methods according to dynamic component changes of the structure, such as the stiffness and mass of the bridge structural elements.

Following that, the LCA was carried out under the principles of ISO standards 14040 (2006) and 14044 (2006). In this study, a variety of preventative strategies were taken into consideration. The necessary upkeep procedures for each scenario were included in these options throughout the period of time under consideration. During the evaluation, their individual contributions to the anticipated length of a structure's service life were calculated. The derived estimates of service life were utilized as inputs for the LCA to quantify the environmental effects caused by each assessed measure as part of the life cycle.

6.2. Materials and Methods

In recent years, the life cycle has gained widespread acceptance and has been standardized in a variety of countries throughout the world (ISO 14040, 2006; ISO 14044, 2006). Economic, environmental, and societal impact considerations are just some elements that may be considered when modeling a process, product, or service using the LCA technique (Soust-Verdaguer et al., 2021). Since the evaluation of other aspects of life cycle assessment, including the environmental and social impacts, can be used in the analysis of the performance of non-destructive dynamic methods of the structure in environmental conditions and different kinds of structures, in this investigation, the environmental impacts of the repair activities on a concrete and coastal bridge exposed to corrosion by chloride ions were evaluated using the PSD as a non-destructive signal-based method. However, Figure 6.2 demonstrates the general diagram of the methodology stages of the damage detection method for the LCA in this research.

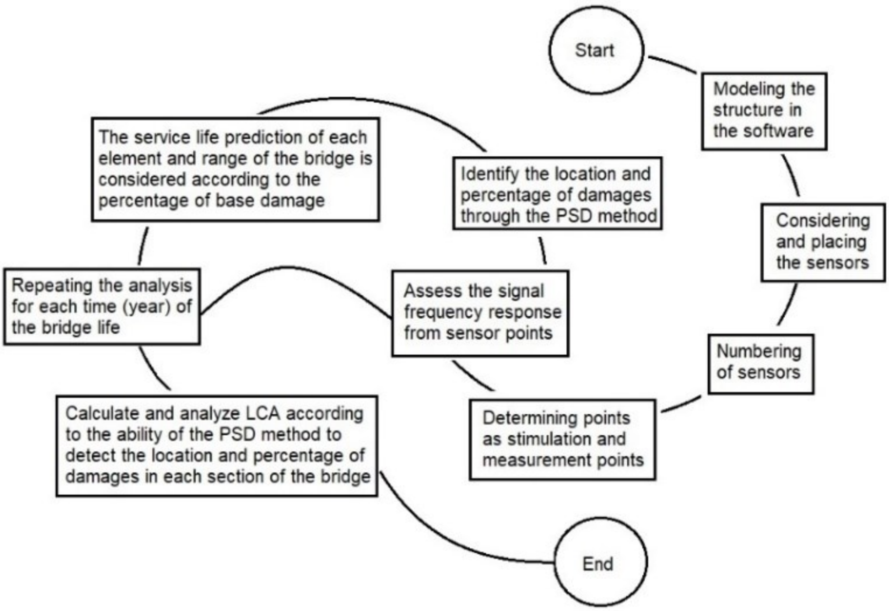

Figure 6. 2. *The general diagram stages of the damage detection method for the life cycle assessment that this research proposes.*

As the diagram in Figure 6.2 shows, this research investigated the performance aspect of the LCA that was used. In addition, it evaluated the PSD method's performance as a signal-based method with a different approach to diagnosing the damage caused by chloride ions to repair and maintain a bridge.

The evaluation results of this research can show the effectiveness of using this method compared with conventional methods in reducing the environmental effects during the repair and maintenance of a bridge.

6.2.1. Service Life and Damage Prediction Methods

Repairing and maintaining structures during their lifetime involves different methods for identifying and predicting possible damage. One of these methods is the PSD method. This research took into account the amount of corrosion and damage to rebars in different parts of a reinforced concrete bridge that was corroded by chloride ions. The impacts of using this method on the environmental impact of the considered structure have been discussed. So, the PSD equation can be obtained according to the transfer function as the following equations (Hadizadeh-Bazaz et al., 2022; Hadizadeh-Bazaz et al., 2023a; Zheng et al., 2015; Pedram et al., 2017):

$$\boldsymbol{H(\omega) = (K - \omega^2 M + i\omega C)^{-1}} \qquad (6.1)$$

Where K is the stiffness, M is the mass, and C is the damping matrices. i is the identity matrix equal to -1. Equation 6.2 is the form that may be used to write the structural response equation in accordance with the power spectral density.

$$\boldsymbol{S_{XX}(\omega) = H^{*}(\omega) S_{FF}(\omega) H^{T}(\omega)} \qquad (6.2)$$

S_{FF} is the PSD inputs matrix at degrees of freedom (DOF). In addition, $H^*(\omega)$ is expressed as the complex conjugate of a transfer function. The PSD was shown to be a second-order function of the frequency response function in Equation 6.2, suggesting that it was a highly nonlinear response in structural characteristics.

Structures made of concrete, like bridges and coastal concrete structures, are often prone to corrosion. The damage produced by chloride corrosion in reinforced concrete buildings is said to have certain service life levels in the degradation model established in Figure 6.3 by Tuutti (Tuutti, 1982).

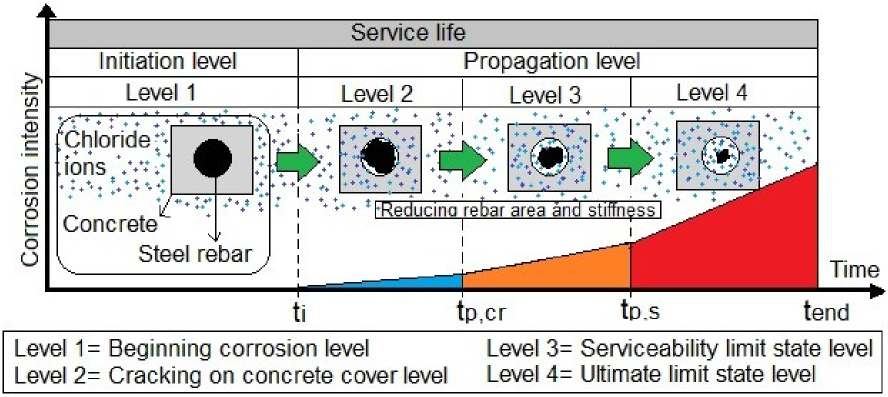

Figure 6. 3. *Reinforcement concrete structure's rebar service life according to Tuutti's model (1982).*

As seen in Figure 6.3, corrosion by chloride began at the first corrosion level. In the initial phase, the chlorides were below the chloride threshold. The propagation phase of chloride ion activity included commencing corrosion, structure cover cracking, the serviceability state, and the ultimate limit state (Zhang et al., 2019). The overall time of the service life of the bridge's reinforcements by chloride corrosion is shown in the equations below (Spanish Ministry of Public Works, 2008).

$$t_l = t_i + t_p \tag{6.3}$$

The corrosion initiation period (t_i) refers to the time required for chloride concentrations to rise to the point where corrosion might occur on the rebars. The chloride threshold is determined by the steel qualities and, to some degree, the concrete parameters. In addition, the period t_p refers to the amount of time required for corrosion to spread across an entire structural element before the part begins to fail significantly. This research used a deterministic solution based on Fick's law according to the chlorine diffusion in the RC structure. The equation used in this study was derived from Fib Bulletin 34 (2006), whereby it is assumed that the surface chloride concentration remains constant and does not vary with time. The calculation of the initiation stage of chloride diffusion (t_i) may be determined using the equation provided in reference (Spanish Ministry of Public Works, 2008).

$$t_i = \frac{x^2}{4D}\left[erf^{-1}\left(\frac{C_s - C(x.t)}{C(x.t)}\right)\right]^{-2} \tag{6.4}$$

Where in the equation, *D* refers to the diffusion coefficient of the chloride for every age of the concrete obtained as

$$\boldsymbol{D = D(t_0).(\frac{t_0}{t})} \qquad (6.5)$$

Regarding the durability parameters, it was assumed here that the conditioning deterioration mechanism was caused by airborne chlorides. According to Fick's second law of diffusion, the advance of chlorides through the concrete cover over time depends mainly on two parameters, namely, a diffusion coefficient and a critical chloride threshold, which depend on the concrete mixture (Fib Bulletin 34, 2006):

$$\boldsymbol{C(x,t) = C_s \cdot \left(1 - erf\frac{x}{2\sqrt{D_0 \cdot t \cdot \left(\frac{t_0}{t}\right)^{\alpha}}}\right)} \qquad (6.6)$$

Where $C(x,t)$ refers to the chloride concentration in time t (measured in years) and at a depth x from the surface, D_0 is the chloride diffusion coefficient, C_s is the surface chloride content, t_0 is the primary time, expressed in years, and usually considered as $t_0 = 0.0767$ (equal to 28 days), and $\alpha = 0.5$ is an age factor.

Conversely, the level of chloride corrosion propagation (t_p) commenced subsequent to the starting stage of chloride diffusion, whereby chloride ions present on the surface of the inner rebars initiated the erosion of steel reinforcements. Over a prolonged period, the process of chloride corrosion gradually diminished the stiffness and area of the cross-section of the reinforcements. The Spanish concrete design code offers the following computation for estimating this time:

$$\boldsymbol{t_p = \frac{80}{\phi}\frac{d}{V_{corr}}} \qquad (6.7)$$

Where d is the concrete cover thickness. V_{corr} shows the chloride corrosion rate, and ϕ is the diameter of the rebar.

Based on the Spanish Ministry of Public Works (2008) findings, pertinent information on the condition of the marine bridge in the seawater may be derived for analytical purposes, as shown in Table 6.1.

Table 6. 1. *Durability parameters in a coastal reinforced concrete bridge (Spanish Ministry of Public Works, 2008)***.**

Marine Exposure Classification	C_s (% of Concrete Weight)	V_{corr} (μm/Year)	D_0 ($\times 10^{-12} m^2/s$)
Aerial (IIIa)	0.14	20	10.0
Submerged (IIIb)	0.72	4	
In tide zone (IIIc)	0.50	50	

The following formula for the chloride corrosion of reinforcements in coastal bridges may be used to predict the amount of damage produced by corrosion as a percentage (Hadizadeh-Bazaz et al., 2023b).

$$\boldsymbol{Dam_{st\,rebar}(t) = \frac{t - t_i}{t_p} \times 100} \tag{6.8}$$

$Dam_{st\,rebar}$ is the percentage of reinforcement affected by chloride ions in every time (t) since propagation t_p.

Using the sensitivity equation, we can model the updating process by considering the following equations:

$$\Delta \boldsymbol{Z(\omega) = \Delta K - \omega^2 \Delta M + i\omega \Delta C} \tag{6.9}$$

$$\boldsymbol{H_D(\omega) = [Z(\omega) + \Delta Z(\omega)]^{-1}} \tag{6.10}$$

$H_D(\omega)$ is the frequency response of the corroded bridge according to Equation 6.8, and $Z(\omega)$ refers to the impedance matrix and is the inverse transfer function. So, the damaged elements through the PSD equation can be as follows.

$$\boldsymbol{S_{XX}(\omega) = H_D^*(\omega) S_{FF}(\omega) \Delta H(\omega) - H_D^*(\omega) \Delta Z^*(\omega) S_{XX}(\omega)} \tag{6.11}$$

The complex conjugate bridge failure transfer function for reinforced chloride corrosion is H^*_D, depending on the failure prediction approach.

The following equation is an expression of the precise ΔH that was provided by Esfandiari et al. (2009):

$$\boldsymbol{\Delta H(\omega) = -H_D(\omega)(\Delta K - \omega^2 \Delta M + i\omega C) H(\omega)} \tag{6.12}$$

It is possible to rewrite Equation 6.10 by making use of Equation 6.11 and Equation 6.13 in the following manner:

$$\boldsymbol{\Delta S_{XX}(\omega) = -H_D^*(\omega) S_{FF}(\omega) H_D(\omega) \big(\Delta Z(\omega)\big) H(\omega) - H_D^*(\omega) \big(\Delta Z^*(\omega)\big) H^*(\omega) S_{FF}(\omega) H(\omega)} \tag{6.13}$$

The dynamic characteristics of each element were changed in the reinforcement's corrosion damage over time to assess the effect that corrosion had on the structural behavior of the system. This was done so that corrosion damage may be attributed to the system. The equations for the structural stiffness, mass, and damping matrices can be obtained as follows:

$$\begin{cases} \Delta K = \sum_{n=1}^{ne} K_n \Delta P_n^K \\ \Delta M = \sum_{n=1}^{ne} M_n \Delta P_n^M \\ \Delta C = \sum_{n=1}^{ne} C_n \Delta P_n^C \end{cases} \quad (6.14)$$

The structural components' stiffness, mass, and damping matrix levels are K_n, M_n, and C_n. The observed changes in structural parameters $\Delta P_n{}^K$, $\Delta P_n{}^M$, and $\Delta P_n{}^C$ fall within the range of −1 to 1. According to Equation 6.13 and a chloride-corroded RC bridge, the sensitivity matrices for the structure's nth parameter determine passive stiffness ratios:

$$\begin{cases} S^K = -H_D^*(\omega)S_{FF}(\omega)H_D(\omega)K_nH^T(\omega) \\ \qquad -H_D^*(\omega)K_nH(w)S_{FF}(\omega)H^T(\omega) \\ S^M = \omega^2(H_D^*(\omega)S_{FF}(\omega)H_D(\omega)M_nH^T(\omega) \\ \qquad +H_D^*(\omega)M_nH(w)S_{FF}(\omega)H^T(\omega) \\ S^C = i\omega(-H_D^*(\omega)S_{FF}(\omega)H_D(\omega)C_nH^T(\omega) \\ \qquad +H_D^*(\omega)C_nH(w)S_{FF}(\omega)H^T(\omega) \end{cases} \quad (6.15)$$

Finally, the PSD equation for calculating the dynamic characteristic parameter changes for the anticipated damages is as follows:

$$\Delta S_{xx} = S^K \Delta p_K + S^M \Delta p_M + S^C \Delta p_C \quad (6.16)$$

In order to monitor the changes in dynamics, such as stiffness and reinforcement loss in cross-section areas over time in the concrete marine bridge elements, Δp_k, Δp_M, and Δp_C illustrate the differences in the structural stiffness caused by deterioration over time using the PSD method and equations for the corrosion of the reinforcement.

The construction phase of bridges or tunnels is often associated with several environmental implications and dangers. These include diminished water exchange, habitat destruction, biodiversity loss, heightened levels of suspended solids, and water quality degradation.

6.2.2. Life Cycle Assessment

6.2.2.1 *Environmental Impact Assessment*

In general, the environmental consequences and dangers that are present throughout the building phase for bridges and tunnels include a reduction in the amount of water exchange, loss of habitat, a decrease in the amount of biological diversity, an increase in suspended particles, and contamination of water quality.

The midpoint and endpoint approaches are two methodologies used in the environment life cycle assessment, an inventory of the life cycle to intelligible indications. The impact on the environment is the focus of the endpoint method, whereas environmental effects are the focus of the midpoint approach. An alternative view is that the midpoint approach is the direct cause, and the endpoint approach is the long-term result. The midpoint and the endpoint are expressed in Figure 6.4.

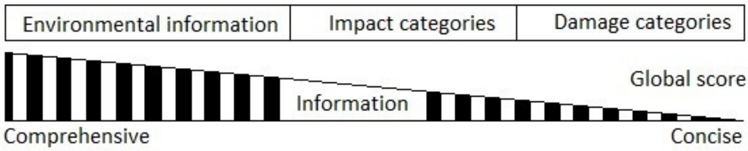

Figure 6. 4. *The approaches to environmental life cycle assessment (Penadés-Plà et al., 2020).*

The midpoint technique yields more comprehensive information, whereas the endpoint approach yields more compact information. Climate change processes, products, and services release gases into the atmosphere that cause environmental issues like ozone loss and global warming, which is a midpoint approach. In the long term, these gas releases will hurt the environment, people's health, and finances. In this case, ozone loss can cause more skin cancer cases, which can be an endpoint method. The four main LCA approaches were CML (Institute of Environmental Sciences, institute of the Faculty of Science of Leiden University, Leiden, Netherland), ReCiPe 2016 (National Institute for Public Health and the Environment, Bilthoven, Netherland), IMPACT 2002+ (Industrial Ecology & Life Cycle Systems Group, GECOS, Swiss Federal Institute of Technology Lausanne (EPFL), Lausanne, Switzerland), and TRACI (Sustainable Technology Division National Risk Management Research Laboratory Office of Research and Development U.S. Environmental Protection Agency Cincinnati, OH). SimaPro® (Data quality guideline for the Ecoinvent database version 3. St. Gallen, Switzerland) and Ecoinvent® (The ecoinvent Database is a Life Cycle Inventory (LCI) database that supports various types of sustainability assessments. Zurich, Switzerland) are the most popular databases (Barahmand & Eikeland, 2022). ISO 14040 and ISO 14044 have standardized specifications for different systemic analysis approaches. Figure 6.5 demonstrates the ReCiPe (Goedkoop et al., 2009; Huijbregts et al., 2016) method for the midpoint and endpoint indicators.

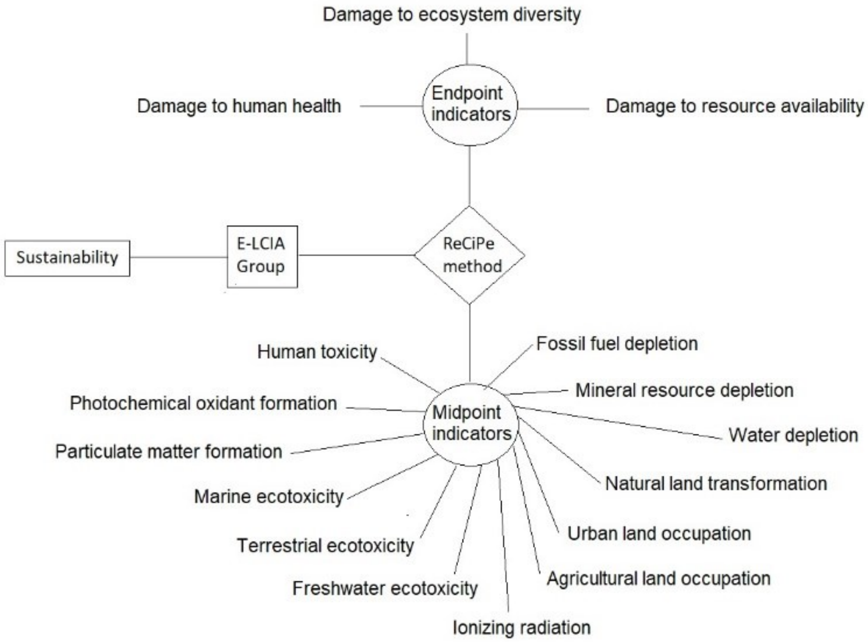

Figure 6. 5. *The indicators of E-LCIA through the ReCiPe method.*

As shown in Figure 6.5, the environment assessment according to the ReCiPe method for midpoint includes human toxicity, photochemical oxidant formation, particulate matter formation, marine ecotoxicity, terrestrial ecotoxicity, freshwater ecotoxicity, and ionizing radiation, which are among the various environmental factors that can have adverse effects on ecosystems and human health. The topics of interest include agricultural land occupation, urban land occupation, natural land transformation, water depletion, mineral resource depletion, and fossil fuel depletion. Conversely, the terminal point encompasses various classifications of harm, including ecosystems, human health, and resources.

The LCA in a structure like a bridge is specified in four phases. These phases may consider all the actions required from the initial design through the end structure's service life: manufacturing, construction, maintenance, repair, and destruction at the end of the structure's lifetime (see Figure 6.6).

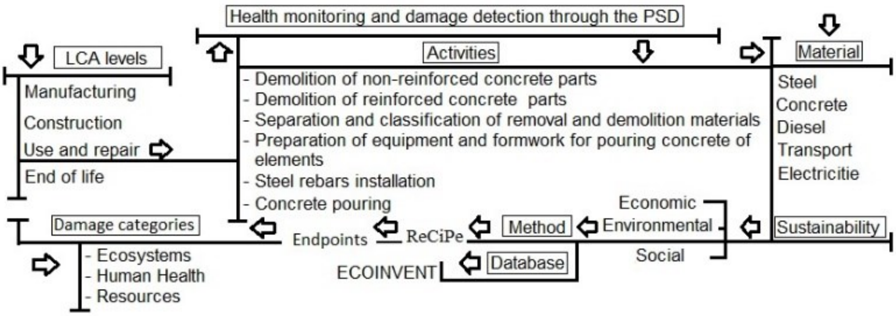

Figure 6. 6. *Methodologies, activities, and material used in this research.*

This study analyzed the maintenance level that included some activities for maintaining and repairing a coastal RC bridge using the PSD approach as a non-destructive method to determine the location and quantify the damages caused by corrosion during the bridge's lifetime. E-LCIA was assessed using the ECOINVENT (Association, 2023) database via the ReCiPe method. For this purpose, the endpoint included damage categories such as ecosystems, human health, and resources.

The maintenance and repair stage during the use of a structure includes all of the procedures required during the bridge's life.

6.3. Model Description

The methodology presented above was applied to an existing concrete bridge located near the shore. The bridge used as a model for the present investigation was the reinforced concrete bridge in Arosa, in the Spanish region of Galicia (Figure 6.7). The data required to define the geometry of this bridge were gathered from the scientific literature (León et al., 2013; Pérez-Fadón Martínez, 1985; Pérez-Fadón Martínez, 1986). In particular, the bridge measured 1980 m in length. The initial and final spans each had a span length of 40 m, while the intermediate spans had a length of 50 m.

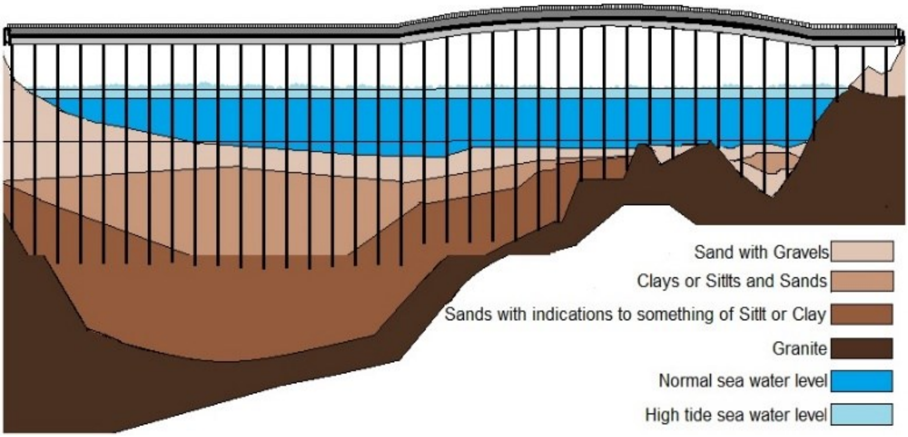

Figure 6. 7. *The total view of the piers and deck of Spain's reinforced concrete coastal Arosa bridge.*

The deck of this bridge was of a box-girder type and lay approximately 9.6 m above the mean high water level, being thus exposed to a high concentration of airborne seawater chlorides. Figure 6.8 presents the dimensions of the bridge deck (Pérez-Fadón Martínez, 1985; Pérez-Fadón Martínez, 1986), which were as follows: 13 m in width and 2.30 m in height. There were two walkways on each side of the deck. The width of each of them on the sides of the deck was 1.5 m. The bridge's transverse and longitudinal piers were 5.26 m and 1.80 m, respectively.

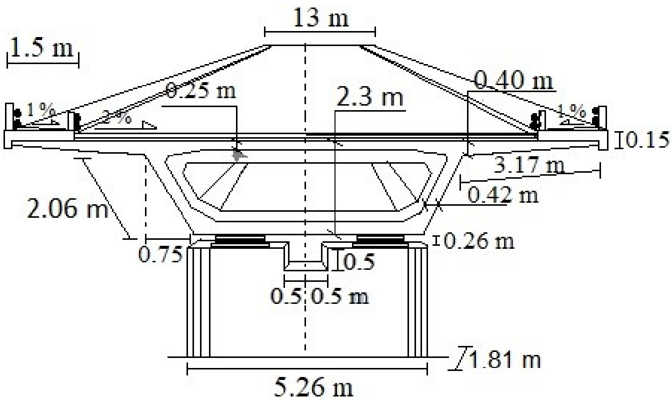

Figure 6. 8. *Cross-section and dimensions of the Arosa coastal and concrete bridge.*

It was estimated that the steel amount for this bridge was 100 kg per cubic meter of concrete (Pérez-Fadón Martínez, 1985). The steel reinforcement concrete cover was 35 mm for the deck and was increased to 45 mm for the piers, which were located in the so-called splash, tidal, and spray exposure zones (XS3 exposure zone according to UNE EN 1992-1-1).

The concrete mix of the structure included a water-to-cement ratio w/c = 0.45 and contained 218.5 l/m^3 of water, 485.6 kg/m^3 of cement, 926.7 kg/m^3 of gravel, and 827.9 kg/m^3 of sand, where every value was referred to a m^3 of the resulting concrete. In addition, the characteristic compressive strength f_{cm} equaled 40 MPa, and the modulus of elasticity Ec equaled 29 GPa.

Furthermore, according to the concrete mix considered in this study and following the provisions from, the diffusion coefficient to be considered for the present case study was $D_0 = 10 \times 10^{-12}$ m^2/s, and the critical chloride threshold C_{crit} = 0.6%. The third parameter that determined the chloride advance through concrete over time was the so-called surface chloride concentration, which depended on the chloride content in contact with the concrete element. Based on the distance between the structure and the seawater, a surface chloride content of 3.34% ($C_{s,0}$) was used to assess the bridge deck.

6.3.1. The Numerical Model Analyses

As computers and sensors improve in capacity and speed, non-destructive numerical models of structures are used to identify damages. Based on vibration and signals, the PSD technique studied damage caused by chloride ions on a computational model of a coastal bridge. The numerical model of the reinforced concrete bridge reinforcement used defined regions and sensors at certain distances for health monitoring every year from the start of the corrosion period to the end. As seen in Figure 6.9, these spans' deck and column numbers were renumbered from 1 to 167.

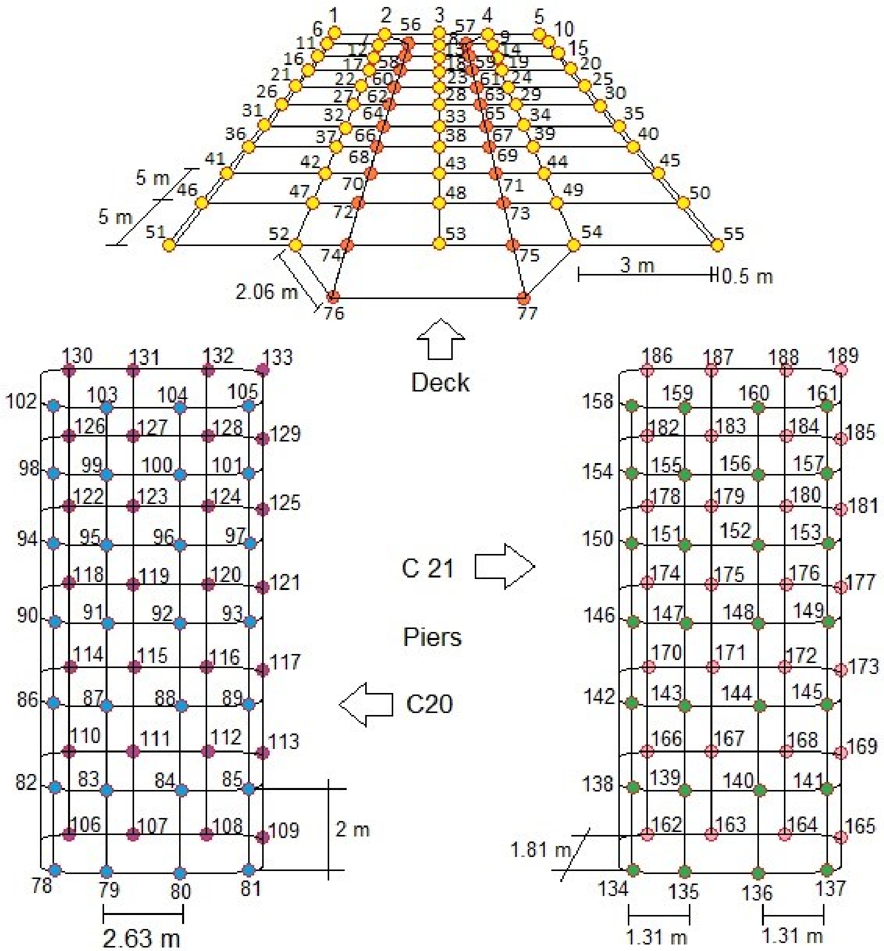

Figure 6. 9. *Counting and dividing points as sensors in an Arosa bridge span.*

The numbering of the sensor locations for assessment is shown in Figure 6.9. The numbers 1 through 77 correspond to deck bridge locations 5 m apart in length and 3 m apart in breadth. The point totals on one column began at 78 and went to 189 on the other. The sensors on the columns' lengths were 2.63 m apart in breadth and 2 m apart in height. The column widths were roughly 1.80 m apart.

Some sites were points of simulation, and some were measuring points to track chloride attack damage at each bridge position. These points were believed to be fixed for yearly test monitoring and analysis. In this regard, certain portions and components were selected as simulation points, and others were selected as locations for measurement points. The simulated and measured points were far apart. Thus, the simulated points on the deck were 3, 18, 33, 48, 58, 59, 64, 65, 70, 71, 76, and 77, and between piers, the points were 86, 89, 98, 101, 115, 116, 127, 128, 135, 136, 147, 148, 159, 160, 162, 165, 174, 177, 186, and 189. The locations of the measurement and stimulation points were assumed to be fixed and under the same conditions throughout the experiment. Because of this assumption, the researchers could track how these sites moved over time. This experiment employed trial and error to determine the number and location of sensors on the bridge span as software often computes sensor distances and frequency responses. The number and location of sensors determined their distance. Reducing the number of sensors increased their distance, which reduced the simulation point signals. This affected the frequency of reception at the measuring stations, even at large distances, influencing the findings.

Additionally, chloride ions damage concrete components. This numerical study estimated 10% noise and error for the coastal bridge. PSD could detect damage via MATLAB, and Open Sees was used to examine the chloride ions. Figure 6.10 summarizes the research on PSD and the ability of traditional techniques to anticipate structural failure and reduce repair costs for coastal bridges.

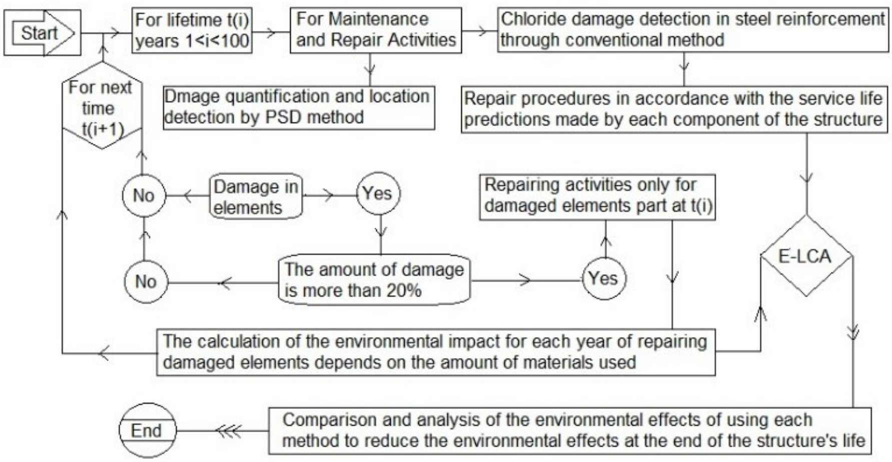

Figure 6. 10. *An overview of the study and computation procedures used for E-LCA for the bridge.*

The environmental impact assessment through a non-destructive damage detection method for repairing and maintaining a bridge over its expected lifetime of one hundred years is depicted in flowchart form in Figure 6.10. The annual wear and tear on the bridge was analyzed in detail. After that, the repair operation was examined for structural, elemental, and area damage exceeding twenty percent. The percentage of damage that represented the commencement of damage depended on how important it was to monitor building repair and maintenance times. The annual impact on the environment of repairing and maintaining the facility was subsequently calculated.

6.4. Results

A non-destructive approach to assess the quantity and location of damages on a corroded and eroded coastal bridge was tested in the first stage. In order to identify the damages brought on by chloride corrosion in the RC bridge structure, the performance of the PSD approach in comparison with the conventional method was evaluated, and the results were compared and contrasted. The service life period time in Arosa Bridge, according to the quantity of damages based on the beginning repair, is shown in Figure 6.11.

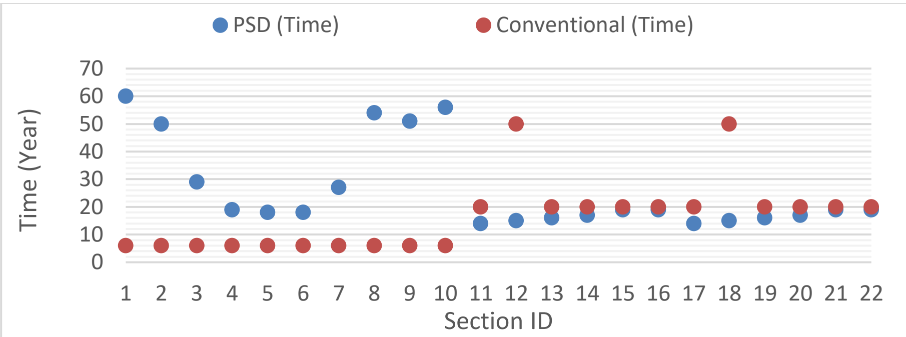

Figure 6. 11. *The service lifetime for the repair of each element section ID of the concrete bridge.*

As shown in Figure 6.11, the desired time (years) to carry out the repair activities of each section of this bridge span was calculated during the life of this structure (100 years). The amount of damage to the base was assumed to be 20% for the purpose of carrying out repair activities (Hadizadeh-Bazaz et al ., 2023b). Therefore, when the percentage of damage in one bridge element was more than 20%, this time (year) was the service life period for repair activities. The amount for each bridge section number of this case study is shown in Figure 6.12. And this amount could be different according to the importance and conditions of the structure.

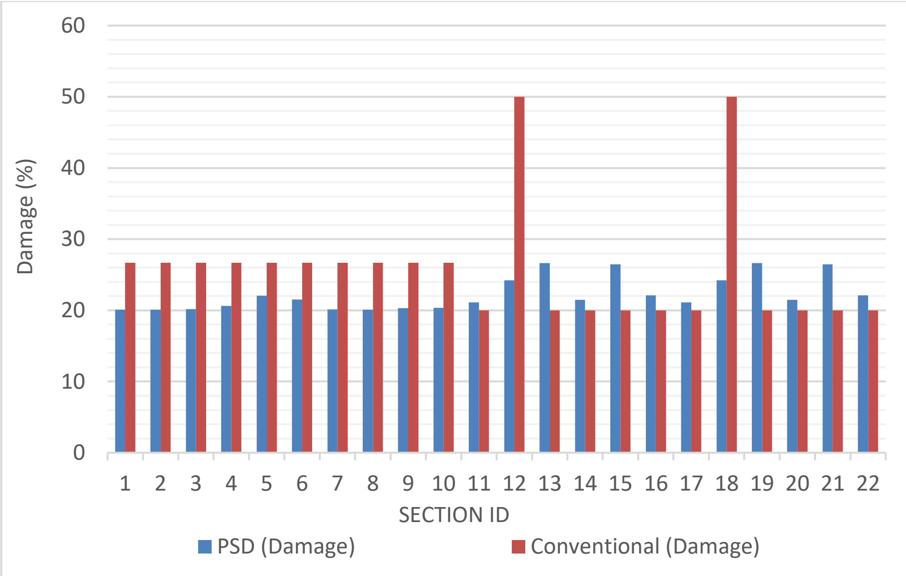

Figure 6. 12. *The percentage of the predicted damages for service life and repair period activities.*

As shown in Figure 6.12, the percentage of damage obtained to calculate the service lifetime and repair period in every part of the bridge in Figure 6.11 showed that the PSD method could be more accurate for each section ID considered, on average, if the damage reached 20% to 22%, predicting that it would reduce more damage to the structure, perform life service earlier and on time, and prevent more damage and more cost for repair.

Furthermore, as a defect of the conventional method of determining the service lifetime for most parts and sections of the bridge, it was determined that the amount of damage was about 27% or more. According to the obtained results, this problem would involve the most significant risk and financial loss, especially for the sections of the bridge foundations that were in the tide zone (12 and 18), and would cause more corrosion by chloride ions because the damage in these parts for the conventional method of timed first-life service, repair, and maintenance was predicted, which was around 50%. But the PSD method predicted the time when the amount of damage was around 24% as the first time (year) to carry out repair and service life activities, which could reduce the repair and maintenance costs and life risks as well as decrease the environmental effects in the repair and maintenance phase of this bridge.

As follows, according to the predicted times for each section of the bridge using the PSD and the conventional techniques for repairing the damaged parts of the bridge, the performance of PSD as a method of identifying damage in the structure in the changing environmental impact was evaluated and compared in the stage of bridge repair and maintenance. Generally, the results of the assessment of the environmental impact by ReCiPe for endpoint using ECOINVENT for the deck and columns of the bridge through these methods are presented in Table 6.2.

Table 6. 2. Environmental impact assessment results from two methods on the coastal bridge

	Environmental Impact (Points)			
	Desk		Columns	
	Conventional	PSD	Conventional	PSD
Ecosystem quality				
Agricultural land occupation	1872.4	268.3	2313.8	685.4
Climate change, ecosystems	46,192.7	6620.7	57,082.6	16,909.2
Freshwater ecotoxicity	5.9	0.8	7.3	2.1
Freshwater eutrophication	23.4	3.3	29.0	8.5
Marine ecotoxicity	129.2	18.5	159.6	47.2
Natural land transformation	22,668.7	3249.0	28,012.8	8298.0
Terrestrial acidification	151.4	21.7	187.1	55.4
Terrestrial ecotoxicity	512.9	73.5	633.8	187.7
Urban land occupation	444.1	63.6	548.8	162.5
Human health				
Climate change, human health	58,117.0	8329.8	71,818.1	21,274.2
Human toxicity	72,315.3	10,364.8	89,363.6	26,471.6
Ionizing radiation	60.7	8.7	75.0	22.2
Ozone depletion	3.7	0.5	4.6	1.3
Particulate matter formation	7975.7	1143.1	9855.9	2919.5
Photochemical oxidant formation	206.7	29.6	255.5	75.6
Resources				
Fossil depletion	49,089.4	7035.9	60,662.3	17,969.6
Metal depletion	8142.3	1167.0	10,061.9	2980.5

Table 6.2 demonstrates the environmental impact results of the Open LCA 2.0 software for three categories, including the ecosystem quality, human health, and resources.

The difference in E-LCA impacts when maintenance by the PSD method was compared with the conventional method in the Arosa bridge is shown in Table 6.3.

Table 6. 3. *Benefits of utilizing PSD in the environmental impacts category of a bridge span*

Impact Category	Difference	Impact Category	Difference
Ecosystem Quality		**Human Health**	
Agricultural land occupation	3232.5	Climate change, human health	100,331
Climate change, ecosystems	79,745.4	Human toxicity	124,842.5
Freshwater ecotoxicity	10.3	Ionizing radiation	104.7
Freshwater eutrophication	40.5	Ozone depletion	6.54
Marine ecotoxicity	223	Particulate matter formation	13,768.9
Natural land transformation	39,134.4	Photochemical oxidant formation	356.9
Terrestrial acidification	261.4	**Resources**	
Terrestrial ecotoxicity	885.5	Fossil depletion	84,746.2
Urban land occupation	766.71	Metal depletion	14,056.6

Table 6.3 shows the differences in values for the subcategories of the ecosystem quality category, including agricultural land occupation, climate change for ecosystems, freshwater ecotoxicity, freshwater eutrophication, marine ecotoxicity, natural land transformation, terrestrial acidification, terrestrial ecotoxicity, and urban land occupation, which were equal to 3232.54, 79,745.45, 10.32, 40.55, 223.05, 39,134.41, 261.40, 885.54, and 766.71, respectively, using the conventional method and PSD for a bridge span including two columns and a 50 m long deck. Also, this value difference between the two methods for the subsets of the human health category included climate change (human health), human toxicity, ionizing radiation, ozone depletion, particulate matter formation, and photochemical oxidant formation, respectively, with values of 100,331.05, 124,842.53, 104.79, 6.54, 13,768.97, and 356.95. And finally, the value differences for the subset of the resources category, including fossil depletion and metal depletion, were 84,746.24 and 14,056.66, respectively.

Furthermore, the E-LCA for the deck and columns of a span of the bridge through two methods to damage detection methods for maintenance and repair activities are shown in Figure 6.13.

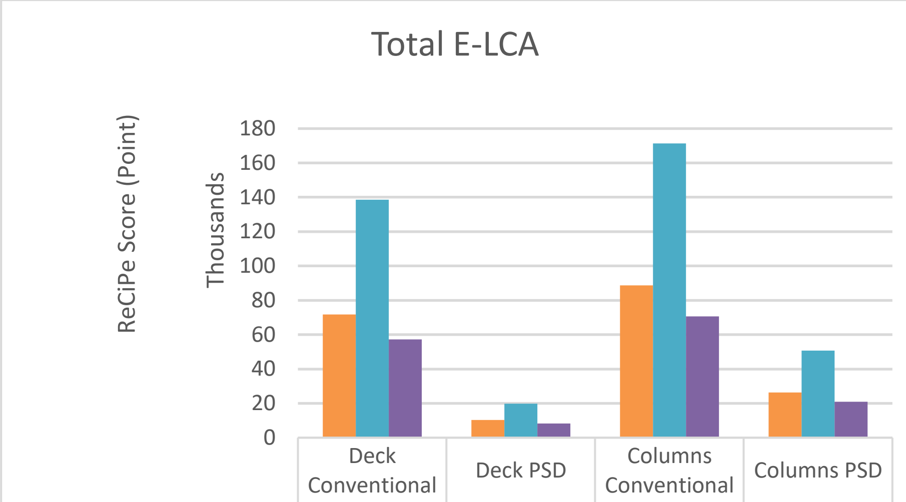

	Deck Conventional	Deck PSD	Columns Conventional	Columns PSD
Total Ecosystem quality	71,730.73	10,281.04	88,641.22	26,257.67
Total Human health	138,679.37	19,876.67	171,372.98	50,764.82
Total Resources	57,231.84	8202.94	70,724.23	20,950.23

Figure 6. 13. *The total quantification of environmental categories' impacts on the Arosa Bridge*

The analysis results showed the PSD method's significant effect on reducing this bridge's environmental impact. The PSD method reduced the amount of total ecosystem impact, compared with a conventional approach in maintenance and repair of the deck of a span of the bridge, with a decrease of about 61,449.68 points; for total human health as one of the vital impacts, it helped to reduce the impact by about 118,802.69 points. And also, the total resources in the deck of the bridge through the PSD method could save about 49,028.9 points. Finally, in the columns of the coastal bridge, for total ecosystem quality, human health, and resources, the use of the PSD method could result in less harm to the environment, by about 62,363.55, 120,608.15, and 49,774 points, respectively.

Overall, the final results showed that the total difference in the effect of using PSD compared with the conventional method on the whole ecosystem quality, human health, and resources in the bridge deck and two columns of a span was less than during the bridge's life.

6.5. Conclusions

The results of the LCA and the performance of a non-destructive method of detecting damage in a structure to repair and maintain a structure, and therefore, the design and construction of the bridge, showed the use of these methods in reducing inappropriate and harmful environmental effects. The life cycle assessment analysis and the performance of the non-destructive and dynamic method of detecting damage in a structure showed here that the PSD method, which is a dynamic and non-destructive method, outperformed conventional techniques in terms of its ability to predict damage in a coastal reinforced concrete bridge in an environmental impact assessment.

The application of PSD for predicting maintenance needs along the use and maintenance life cycle stages of a structure, in comparison with conventional methods, allows the designer to estimate not only the occurrence of damages over time but also their approximate location. This provides a more realistic prediction of the impacts of maintenance of any kind throughout the infrastructure lifecycle, leading to more valuable decision-oriented results. In this research, and for the case study analyzed, it was shown that the use of the PSD method, in comparison with the conventional method in terms of environmental impact, could reduce the predicted harmful effects on the environment by 14.33% in the deck and 29.62% in the columns of the bridge in the stage of bridge repair and maintenance.

Future studies will look at using PSD-based maintenance prediction algorithms in structures to analyze societal consequences throughout the infrastructure's life cycle. It would also be interesting to include PSD-based methodologies in sustainable decision-making tools to obtain more realistic scenarios from the usage stage of an infrastructure life cycle and make more practical judgments during the design phase.

Chapter 7

Sustainability Life Cycle Assessment of Concrete Bridges in Coastal Regions Using Power Spectral Density Technique

Type of paper	Journal article
Authors:	Mehrdad Hadizadeh-bazaz; Ignacio J. Navarro; Víctor Yepes;
Status:	Submitted and under review in a journal

Abstract

Abstract. In light of the recent introduction of the Sustainable Development Goals, there has been a heightened emphasis on mitigating the adverse effects of construction activities. To fully understand the environmental and economic impacts of various aspects such as products, processes, and projects, life cycle assessment (LCA) is critical. This study examines the sustainability life cycle assessment of the Power Spectral Density (PSD) method, including Environmental Life Cycle Assessment (E-LCA), Social Life Cycle Assessment (S-LCA), and Life Cycle Cost Assessment (LCCA). The primary focus is on the method's capability to identify and quantify corrosion-induced damage to structures over time, particularly from chloride ions. For the sustainability life cycle analysis, the study employs eight multicriteria parameters and the Technique for Order Preference by Similarity to an Ideal Solution (TOPSIS) method. The results indicate that the PSD method, a non-destructive damage detection technique, effectively predicts corrosion-induced damage. This predictive ability, compared to other methods for estimating the service life of reinforced concrete structures, supports the maintenance and repair of coastal concrete bridges throughout their lifespan. The research confirms the PSD method's effectiveness, yielding sustainability benefits such as reduced costs and lower environmental and societal impacts over its lifetime.

Keywords Multi-criteria decision-making; Sustainability; Topsis; Power Spectral Density (PSD); Life cycle assessment (LCA); Non-destructive damage detection techniques

7.1. Introduction

In today's scontext, assessing the longevity and stability of structures has become increasingly crucial due to the imperative of maintaining and repairing them. Sustainable development, as outlined in the Brundtland Report, refers to the process of fulfilling current demands without jeopardizing the capacity of future generations to fulfill their own needs. This definition suggests a harmonious equilibrium among economic expansion, social progress, and environmental preservation. (Brundtland & Comun, 1987).

Sustainable activities and decisions should be predicated on the comprehensive evaluation of their economic, environmental, and social ramifications throughout a given period. Implementing the idea of sustainability in the industry is particularly relevant in the building sector, where the sustainable design of goods plays a crucial role (Navarro et al., 2023; Navarro et al., 2019). The construction sector has emerged as a prominent contributor to environmental strain within our society. This is primarily due to its significant role in accounting for 30% of worldwide energy consumption, 40% of raw material extraction, and 30% of greenhouse gas emissions (Choi, 2019).

Life cycle assessments (LCA) are generally acknowledged as a very efficient approach for assessing the sustainability of concrete buildings. LCA is a systematic approach used to evaluate the environmental and social ramifications of a product, process, or activity across its whole life cycle, including the extraction of materials through its final disposal (ISO 14040:2006 /AMD 1:2020; ISO 14044:2006 /AMD 2:2020). Engineers and architects are responsible for balancing the positive and negative life cycle-related effects generated by the infrastructures they design, making the design of infrastructures that effectively contribute to the sustainable future demanded by our society a priority and a significant challenge.

Consequently, a recent study has been conducted on the evaluation of infrastructures, concentrating on their effects on the economy, the environment, and society. Although considerable attention has been given to the sustainable design of bridges, interest has grown in the sustainability assessment of a wide variety of infrastructure types, including pavements (Kazemeini and Swei, 2023; Kothari et al., 2022), buildings (Sánchez-Garrido et al., 2022; Caruso et al., 2020), railway tracks (Celauro et al., 2023; PONS et al., 2020), and others. Bridges are vital transportation infrastructure for land accessibility but are costly for road expansion. Recent research has aimed at reducing bridge construction and maintenance costs (Hadizadeh-Bazaz et al., 2023b; Zhao and Li, 2022; Carbonell et al., 2011).

The application of multicriteria decision-making (MCDM) techniques has proven to be the most suitable approach for assessing conflicting sustainability dimensions in a multistakeholder and long-term context like infrastructure design. Using MCDM methodologies, the decision-maker can evaluate complicated issues containing many inconsistent criteria based on the opinions of a panel of experts or decision-relevant stakeholders (Navarro et al., 2022).

In this regard, selecting and applying methods for detecting non-destructive damage in structures play a pivotal role in ensuring sustainability and assessing a structure's life cycle. Determining the extent of damage in a building can involve both destructive and non-destructive approaches. Destructive strategies rely on models that typically require the removal of structural samples to assess damages (Bjørheim et al., 2022). In contrast, non-destructive techniques are model-independent, enabling structural integrity evaluation through numerical modeling without physically harming the building components (Jodhani et al., 2023). These non-destructive methods often involve signal-based technologies and have witnessed increased adoption due to advancements in high-tech computers and sensors in structural health monitoring (Chaupal and Rajendran, 2023).

Signal-based methods for non-destructive damage detection operate in either the time domain (Malekghaini et al., 2023), the frequency domain (Cai and Zhu, 2023; Cai et al., 2023), or a combination of both (the time and frequency domain) (Liu et al., 2023; Yang et al., 2023). Among these methods, dynamic frequency-domain approaches, such as the power spectral density (PSD) (Hadizadeh-Bazaz et al., 2023a; Fang et al., 2023), frequency response functions (FRF) (Hassani et al., 2023; Jalali and Rideout, 2022), modal curvatures (Ganguli, 2020; Ciambella et al., 2019), modal strain energies (Nguyen and Livaoğlu, 2023; Pooya and Massumi, 2022), and natural frequencies (Wang, 2021; Khan et al., 2020), have gained prominence. The PSD technique, operating in the frequency domain, leverages the frequency response of both periodic and random signals to characterize power distribution precisely. This method utilizes a highly responsive nonlinear function based on structural elements, effectively generating a second-order transfer function (Nilsson and Liu, 2015).

Some studies have been conducted to assess life cycle impacts, such as environmental impact and life cycle cost assessment, through the non-destructive damage detection method (Hadizadeh-Bazaz et al., 2023b; Navarro et al., 2023). However, the performance of non-destructive damage detection methods on social impact assessment and the sustainability of a structure has not been explored yet.

Furthermore, society generally addresses sustainability concerns via ecological reductionism, which oversimplifies the complex character of these challenges. However, assessing sustainability issues requires integrating several scientific disciplines, a process called "orchestration of sciences" (Munda, 2016). One effective method for using a multidisciplinary approach to sustainability assessment is by utilizing MCDM methodologies (Sousa et al., 2021). Recent research has focused on developing tools and techniques to evaluate infrastructure sustainability and provide valuable insights for future design decisions in different structures. Various strategies have been used to achieve this goal. Applying a broad range of MCDM methodologies, researchers have spent the last several years developing tools and methods to analyze the sustainability of infrastructure and generate meaningful findings to guide future design activities in a wide range of buildings. However, the MCDM approach to sustainable infrastructure evaluation has not yet been agreed upon. However, other researchers argue that using several MCDM methods should lead to valid findings for sustainability assessments (Hwang et al., 1981). Therefore, this study analyzed the performance evaluation S-LCA and sustainability life cycle assessment by the TOPSIS method as a novelty through the PSD technique as a non-destructive and dynamic method, as well as the performance of this damage detection method to spatially assess the social life cycle. Annual structural health monitoring by the PSD method was performed, taking into account changes in dynamic components such as rebar stiffness and mass and numerous bridge parts, which were compared by conventional method results.

7.2. Methodology

In recent times, exploring a structure's sustainability life cycle assessment has become imperative to analyze its environmental and social impacts and life cycle costs. The life cycle assessment can yield diverse perspectives at various stages of a structure's existence, including manufacturing, construction, utilization and maintenance, and eventual decommissioning (Martínez-Muñoz et al., 2022). Researchers and engineers are keen on understanding the efficacy of non-destructive methods in detecting structural damage throughout all stages, from the initial planning and construction phases to the end of a structure's life. This pursuit aims to mitigate adverse environmental, social, and economic impacts. Figure 7.1 provides a concise overview of the levels involved in this study, which evaluates the sustainability of a bridge during maintenance and repair activities by implementing a non-destructive damage detection method, thereby reducing impacts on a coastal concrete bridge afflicted by damage throughout its lifespan.

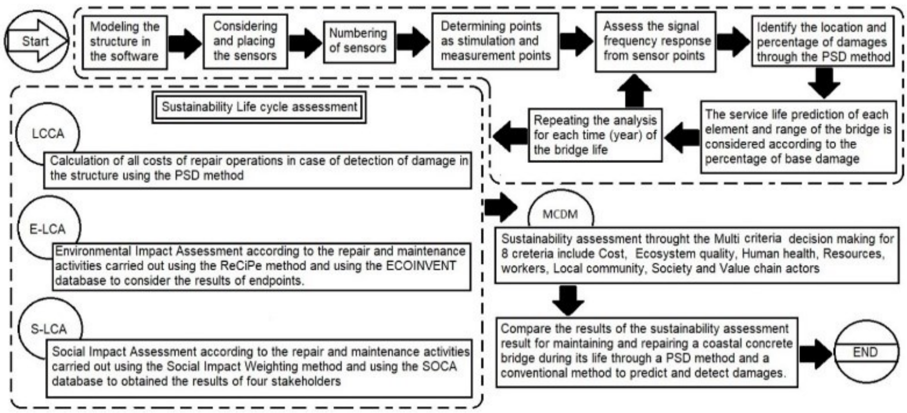

Figure 7. 1. *Concise overview of the sustainability assessment stage of a concrete bridge structure using the PSD approach.*

This study used The PSD technique as a non-destructive dynamic method to predict damage during the maintenance and repair of a concrete bridge structure throughout its long-term durability. Subsequently, the following sections delineate the analyzed model and elaborate on the materials and methods employed in this comprehensive assessment.

7.2.1. Bridge model description

The analysis was conducted on a bridge span featuring a single box deck, known as the Arosa Bridge, in Galicia, Spain (refer to Figure 7.2). This concrete structure spans a total length of 1980 m and is comprised of 40 spans. The initial and concluding spans measure 40 m each, while the 38 intermediate spans are each 50 m long. This structure's geometric attributes and durability factors were deduced using data extracted from pertinent literature (León et al., 2013; Pérez-Fadón Martínez, 1985; Pérez-Fadón Martínez, 1986).

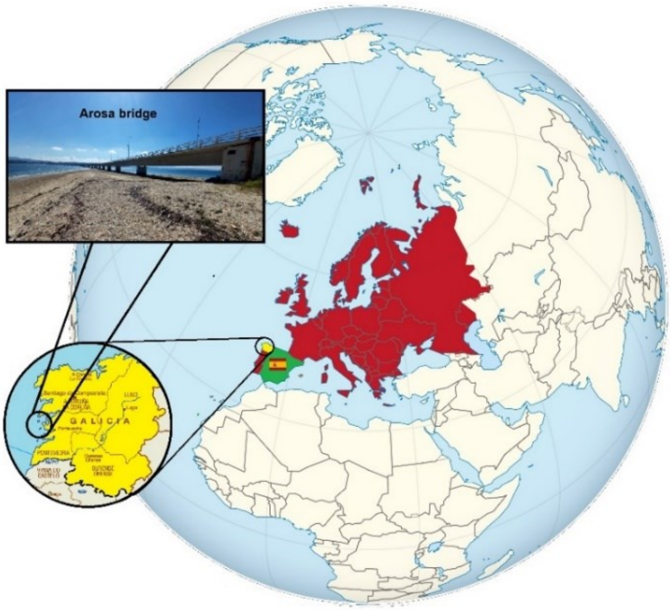

Figure 7. 2. *The geographical position and location of the Arosa Bridge*

The box-girder bridge deck stands 9.6 m above the tide zone level, facing exposure to elevated levels of airborne saltwater chlorides. The dimensions of the bridge deck, as illustrated in Figure 7.3, are 13 m in width and 2.30 m in height. Accompanied by two walkways on either side, each measuring 1.5 m wide, this deck presents a comprehensive structure. The transverse and longitudinal dimensions of the bridge piers are 5.26 m and 1.80 m, respectively (Pérez-Fadón Martínez, 1985; Pérez-Fadón Martínez, 1986).

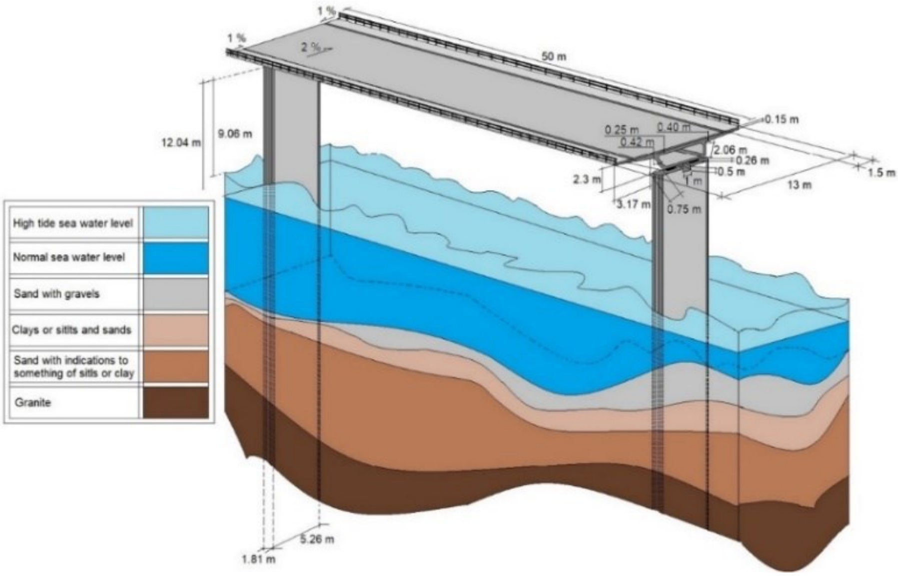

Figure 7. 3. *The measurements of the deck and columns of the central section of the Arosa bridge.*

The steel content of the bridge was evaluated at 100 kg/m3 of concrete (Pérez-Fadón Martínez, 1985). In the splash, tidal, and spray exposure zones (XS3 exposure zone per UNE EN 1992-1-1), the deck reinforcement measured 35mm, while the pier reinforcement was 45mm. The concrete mix for this bridge features a water-to-cement (*w/c*) ratio of 0.45. The composition includes 218.5 liters per cubic meter of water, 485.6 kg/m3 of cement, 926.7 kg/m^3 of gravel, and 827.9 kg/m^3 of sand. Additionally, the modulus of elasticity (E_c) is 29 GPa, and the compressive strength (f_{cm}) is 40 MPa. Construction of this bridge used Type II Portland cement. This particular cement variant offers a moderate level of resistance against chlorides and sulfate salts, which have the potential to weaken both concrete and reinforced steel.

7.2.2. Service life prediction techniques

The research investigates the application of the PSD method to predict potential damage to rebars in a coastal reinforced concrete structure exposed to chloride ions. The study assesses the precision of this method in predicting injuries, its influence on life cycle assessment, and the structure's environmental impact. The PSD equation, derived through the transfer function, is presented as follows (Hadizadeh-Bazaz et al., 2022; Hadizadeh-Bazaz et al., 2023a; Zheng et al., 2015; Pedram et al., 2017):

$$\boldsymbol{H(\omega) = (K - \omega^2 M + i\omega C)^{-1}} \qquad (7.1)$$

The matrices *K*, *M*, and *C* denote stiffness, mass, and damping, respectively. The matrix '*i*' is the identity matrix with a value of -1. Equation 7.2 represents the structural response equation that can be formulated based on the power spectral density.

$$\boldsymbol{S_{XX}(\omega) = H^*(\omega) S_{FF}(\omega) H^T(\omega)} \qquad (7.2)$$

S_{FF} represents the matrix of PSD inputs across all active Degrees of Freedom (DOF), while $H^*(\omega)$ is the complex conjugate of a transfer function. Equation 7.2 illustrates that the power spectral density is a second-order function of the Frequency Response Function (FRF), signifying its highly nonlinear response to structural parameters.

Corrosion is a prevalent issue in reinforced concrete bridges and coastal constructions. The degradation model depicted in Figure 7.4 by Tuutti associates service life with chloride-induced corrosion and damage in concrete rebars (Tuutti, 1982).

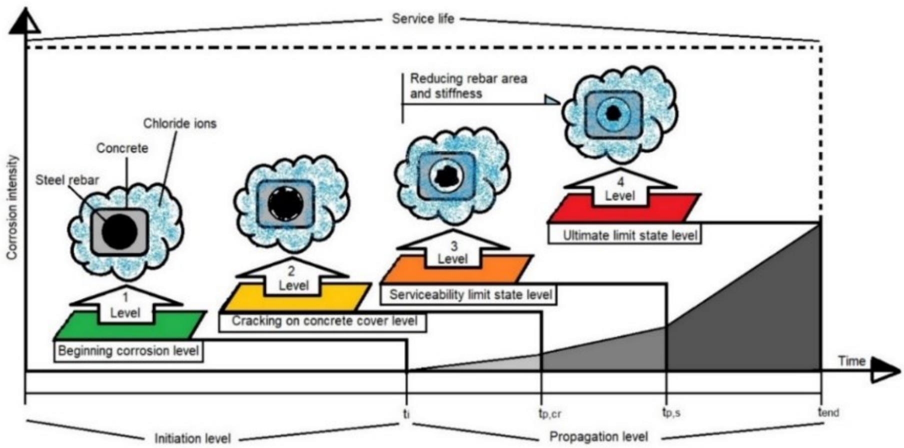

Figure 7. 4. *Service Life Prediction for Rebars in a Reinforced Concrete (RC) Structure using Tuutti's (1982) Model.*

Figure 7.4 illustrates the onset of chloride corrosion, with initial chloride levels below the threshold. The activity of chloride ions moves through stages that include corrosion, concrete cover cracking, limits on how long it can be used, and its final limit state (Zhang et al., 2019). The following equation estimates the total time needed for chloride corrosion to happen (t_i), which is the service life of the bridge's reinforcements (Spanish Ministry of Public Works, 2008). It does this by combining the initiation and propagation phases.

$$t_l = t_i + t_p \tag{7.3}$$

The corrosion initiation period (t_i) is the duration required for chlorides to accumulate sufficiently to induce rebar corrosion. The chloride threshold is dependent on the properties of both steel and concrete. The period (t_p) is when corrosion propagates throughout a structural member before leading to severe failure. In this study, Fick's equation will be employed to analyze chlorine diffusion in concrete deterministically. As per Fib Bulletin 34 (2006), the calculation assumes a constant, time-independent surface chloride concentration. The initiation of chloride diffusion can be calculated using the following equations (Spanish Ministry of Public Works, 2008).

$$t_i = \frac{x^2}{4D}\left[erf^{-1}\left(\frac{C_s - C(x.t)}{C(x.t)}\right)\right]^{-2} \tag{7.4}$$

D is the chloride diffusion coefficient for each concrete age, calculated as:

$$D = D(t_0).\left(\frac{t_0}{t}\right) \tag{7.5}$$

According to Fick's second law of diffusion, a diffusion coefficient and a critical chloride threshold are the main factors affecting how chlorides progress through the concrete cover. These parameters are contingent upon the composition of the concrete mixture (Fib Bulletin 34, 2006).

$$C(x,t) = C_s \cdot \left(1 - erf\frac{x}{2\sqrt{D_0 \cdot t \cdot \left(\frac{t_0}{t}\right)^{\alpha}}}\right) \tag{7.6}$$

Where $C(x,t)$ represents the chloride concentration in the water at a specific depth x below the surface at a given time t (measured in years). D_0 is the coefficient of chloride diffusion, C_s is the concentration of chloride on the surface, t_0 is the initial time, typically assumed to be t_0 = 0.0767 (equivalent to 28 days), and α = 0.5 is the aging factor.

According to Fick's second law of diffusion, a diffusion coefficient and a critical chloride threshold are the main factors affecting how chlorides progress through the concrete cover. These parameters are contingent upon the composition of the concrete mixture (Fib Bulletin 34, 2006).

Alonso et al. (2009) found that natural chloride thresholds varied from more than 0.4 to 4 percent. The Spanish concrete design code (Spanish Ministry of Public Works, 2008) requires the designer to determine the critical chloride concentration (C_{th}) based on the structure's unique concerns. Under normal conditions, 0.6% of the cement weight is considered to assess the limit state for passive reinforcement corrosion.

Thus, the mean critical chloride concentration is 0.6% of cement weight under typical circumstances. The initiation time t_i begins when the rebars' chloride concentration hits C_{th}. This starts rebar corrosion and destruction. However, reinforcing harm does not occur if it is less (Spanish Ministry of Public Works, 2008).

On the other hand, the process of chloride corrosion spreading (t_p) begins after the first phase of chloride diffusion, when chloride ions are found on the surface of the inner rebars, beginning the deterioration of steel reinforcements. Over time, chloride corrosion reduces rebar stiffness and cross-sectional area. The Spanish concrete design code estimates this time as follows (Spanish Ministry of Public Works, 2008):

$$t_p = \frac{80}{\phi}\frac{d}{V_{corr}} \tag{7.7}$$

The variable d represents the thickness of the concrete cover. V_{corr} represents the rate at which chloride causes corrosion, whereas ϕ denotes the diameter of the rebar. According to the findings of the Spanish Ministry of Public Works (Spanish Ministry of Public Works, 2008), Table 7.1 provides valuable information for analyzing the state of the marine bridge in the sea.

Table 7. 1. *Parameters of durability in a RC bridge located in a coastal area (Spanish Ministry of Public Works, 2008)*

Marine exposure classification	C_s (% of concrete weight)	V_{corr} (μm/year)	D_0 ($\times 10^{-12} m^2/s$)
Aerial	0.14	20	10.0
Submerged	0.72	4	
In tide zone	0.50	50	

The subsequent equation, which pertains to the corrosion of reinforcements due to chloride in coastal bridges, can be employed to forecast the extent of damage caused by corrosion, expressed as a percentage (Hadizadeh-Bazaz et al., 2023a).

$$Dam_{st\,rebar}(t) = \frac{t-t_i}{t_p} \times 100 \tag{7.8}$$

D_{amst} rebar refers to the proportion of reinforcement influenced by chloride ions over a given period (t) starting from the initiation of propagation (t_p).

The updating process can be modeled by considering the equations derived from the sensitivity equation.

$$\Delta Z(\omega) = \Delta K - \omega^2 \Delta M + i\omega \Delta C \tag{7.9}$$

$$\boldsymbol{H_D(\omega) = [Z(\omega) + \Delta Z(\omega)]^{-1}} \tag{7.10}$$

The frequency response of the corroded bridge, denoted as $H_D(\omega)$, is determined by Equation 7.8. The impedance matrix is represented by $Z(\omega)$, corresponding to the inverse transfer function. The potential sources of harm in the PSD equation can include the following:

$$\boldsymbol{S_{XX}(\omega) = H_D^*(\omega)S_{FF}(\omega)\Delta H(\omega) - H_D^*(\omega)\Delta Z^*(\omega)S_{XX}(\omega)} \tag{7.11}$$

The transfer function for the failure of a complicated conjugate bridge due to reinforced chloride corrosion is denoted as H^*_D, and its value depends on the chosen approach for predicting the failure.

The subsequent statement represents the exact ΔH value as reported by Esfandiari et al. (2009) using the following equation:

$$\boldsymbol{\Delta H(\omega) = -H_D(\omega)(\Delta K - \omega^2 \Delta M + i\omega C)H(\omega)} \tag{7.12}$$

Equation 7.10 can be reformulated by utilizing Equation 7.11 and Equation 7.13 as follows:

$$\boldsymbol{\Delta S_{XX}(\omega) = -H_D^*(\omega)S_{FF}(\omega)H_D(\omega)\big(\Delta Z(\omega)\big)H(\omega) - H_D^*(\omega)\big(\Delta Z^*(\omega)\big)H^*(\omega)S_{FF}(\omega)H(\omega)} \tag{7.13}$$

To measure how corrosion affected the system's structural behavior, each element's dynamic characteristics altered in the reinforcement's corrosion damage over time. This allows system corrosion to be attributed. Structural stiffness, mass, and damping matrix equations are:

$$\begin{cases} \boldsymbol{\Delta K = \sum_{n=1}^{ne} K_n \Delta P_n^K} \\ \boldsymbol{\Delta M = \sum_{n=1}^{ne} M_n \Delta P_n^M} \\ \boldsymbol{\Delta C = \sum_{n=1}^{ne} C_n \Delta P_n^C} \end{cases} \tag{7.14}$$

The structural components' stiffness, mass, and damping matrix levels are denoted as K_n, M_n, and C_n, respectively. The measured alterations in structural parameters ΔP_n^K, ΔP_n^M, and ΔP_n^C are within the range of -1 to 1. The sensitivity matrices for the nth parameter of a chloride-corroded RC bridge, as determined by Equation 7.13, are responsible for determining the passive stiffness ratios of the structure.

$$\begin{cases} \boldsymbol{S^K = -H_D^*(\omega)S_{FF}(\omega)H_D(\omega)K_nH^T(\omega)} \\ \quad \boldsymbol{-H_D^*(\omega)K_nH(w)S_{FF}(\omega)H^T(\omega)} \\ \boldsymbol{S^M = \omega^2(H_D^*(\omega)S_{FF}(\omega)H_D(\omega)M_nH^T(\omega)} \\ \quad \boldsymbol{+H_D^*(\omega)M_nH(w)S_{FF}(\omega)H^T(\omega)} \\ \boldsymbol{S^C = i\omega(-H_D^*(\omega)S_{FF}(\omega)H_D(\omega)C_nH^T(\omega)} \\ \quad \boldsymbol{+H_D^*(\omega)C_nH(w)S_{FF}(\omega)H^T(\omega)} \end{cases} \tag{7.15}$$

The PSD equation calculates changes in dynamic characteristic parameters for expected damages.

$$\Delta S_{xx} = S^K \Delta p_K + S^M \Delta p_M + S^C \Delta p_C \qquad (7.16)$$

Using the PSD method and reinforcement corrosion equations, Δp_k, Δp_M, and Δp_C show changes in structural stiffness resulting from degradation over time in concrete marine bridge elements.

Environmental risks are commonly involved with bridge and tunnel construction. These include decreased water exchange, habitat loss, biodiversity loss, suspended particulates, and water quality degradation.

7.2.3. Sustainability life cycle assessment

The life cycle concept has achieved widespread acceptance and standardization across numerous nations worldwide (ISO 14040, 2006, ISO 14044, 2006). When using the LCA method to model it, it is essential to look at all of the economic, environmental, and social effects of a process, product, or service (Soust-Verdaguer et al., 2021). A non-destructive identification method determined how badly a coastal concrete bridge was damaged. Corrosion from various stages of the cement's life cycle has been causing the bridge to fall apart.

The goal was to determine if the PSD method could be used as a moving, non-destructive way to find problems in this reinforced concrete bridge. Following this investigation, we applied sustainability life cycle impact methodologies, focusing on social impact assessments. These assessments form an integral part of the multi-criteria evaluation employed to determine the projected lifespan of the bridge.

7.2.3.1 *LCCA through the PSD method*

The LCC procedure, outlined in ISO 15686-5:2017, covers the building's life cycle cost analysis. LCC covers the building's life span, analysis period, future inflation rate, discount rate of future prices to present price, engineering and construction expenses, repair and maintenance costs, and environmental disposal costs. ISO 15686-5:2017 defines maintenance costs as the total cash flows spent for this purpose, enabling a complete knowledge of the LCC process and its intricacies. The failure structure in ISO 15686-5:2017 is universal; however, the LCC process is complicated due to numerous circumstances.

Life-cycle cost assessment is crucial when evaluating bridge performance. Using damage detection technologies, the bridge's LCCA was based on location and annual damage prediction. Manufacturing, building, usage and maintenance, and disposal are typical stages of a structure's life cycle and cost. The following calculations can indicate the projected total cost during the bridge life cycle (Hadizadeh-Bazaz et al., 2023b; Frangopol et al., 2017; Dong and Frangopol, 2016).

$$C_T = C_I + C_M + C_{INS} + C_R + C_{Dam} \qquad (7.17)$$

Equation 7.17 represents the various costs associated with a system. C_I denotes the starting cost, C_M represents the maintenance cost, C_{INS} signifies the cost of inspections, C_R denotes the total repairing cost, and C_{Dam} represents the expected damage cost. The entire cost for the repair activity of the concrete bridge can be determined based on the following components:

$$C_R(t_V) = C_{DNRC}(t_V) + C_{DRC}(t_V) + C_{SM}(t_V) + C_{PE}(t_V) + C_S(t_V) + C_C(t_V) \qquad (7.18)$$

Where the t_v represents the time period under study; C_{DNRC} the cost of demolishing non-reinforced concrete components such as the structure's cover; C_{DRC} the cost of demolishing reinforced concrete components such as the bridge's structural parts; C_{SM} the cost of sorting and recycling demolition debris; C_{PE} the cost of preparing equipment for repairing the bridge's concrete and rebars; and C_S the total cost including all these components; The C_C refers to the overall cost associated with repairing the concrete section of the bridge that has deteriorated over time. Damages that result from chloride ions in constructions, along with other damage factors such as earthquakes and floods following a Poisson process, can all be factored into the total amount of life-cycle impacts in each structural part and element of a bridge within the time. Applying the Poisson process to structural damage allows for the modeling of the probability of various damage-causing events, such as earthquakes, floods, or chloride ion penetration, occurring during the lifespan of a structure. The occurrence of each of these occurrences may be random and independent; however, they can nonetheless be forecasted based on their average frequency (Chiu et al., 2014). For instance in this study, a Poisson process is used to approximate the frequency at which a bridge will be subjected to damage caused by chloride ions throughout 100 years. By comprehending the mean frequency at which these occurrences occur, engineers may enhance their ability to forecast the overall life-cycle effects on the bridge and strategize appropriately for maintenance and reconstruction.

$$C_D(t_v) = \sum_{K}^{N(t_v)} D_{dam}(t_k) . e^{-rt_k} \qquad (7.19)$$

In Equation 7.19, $N(t_v)$ represents the quantity and magnitude of detrimental variables affecting a structure within a specific time period. D_{dam} is the proportion of the yearly damages created by chloride ions and predicted by the PSD method at the time t_v. This study's discount rate, denoted as r, is 5%. According to the Poisson model, the time tk follows a uniform interval distribution $[0, t_v]$ with a mean rate of λ_f. The annual damage percentage in items exposed to hazard effects can be expressed as ($N(t_v) = \lambda_f \times t_v$).

$$\boldsymbol{E}[\boldsymbol{C_D}(\boldsymbol{t_v})] = \frac{\boldsymbol{\lambda_f} \cdot \boldsymbol{E}(\boldsymbol{D})}{\boldsymbol{r}} \cdot (\boldsymbol{1} - \boldsymbol{e}^{-\boldsymbol{r}\boldsymbol{t_k}}) \quad (7.20)$$

In Equation 7.20, $E[C_D(t_v)]$ represents the monetary worth of bridge components that have been affected by both damage and corrosion.

Ultimately, as the LCCA, the total expenses for bridge repair and maintenance are determined based on the projected proportion of damages for the entire bridge section, as per the following equation.

$$\boldsymbol{E}[\boldsymbol{C_T}\,(\bar{\boldsymbol{x}}.\boldsymbol{t_v})] = \boldsymbol{C_I} + \boldsymbol{C_M} + \sum_{t=1}^{t_v} \left[\frac{\left(\begin{array}{c} \sum_{t=1}^{N(t_v)} \boldsymbol{E}[\boldsymbol{C_{DNRC}}\,(\bar{\boldsymbol{x}}.\boldsymbol{t})] \\ + \sum_{t=1}^{N(t_v)} \boldsymbol{E}[\boldsymbol{C_{DRC}}\,(\bar{\boldsymbol{x}}.\boldsymbol{t})] \\ + \sum_{t=1}^{N(t_v)} \boldsymbol{E}[\boldsymbol{C_{SM}}\,(\bar{\boldsymbol{x}}.\boldsymbol{t})] \\ + \sum_{t=1}^{N(t_v)} \boldsymbol{E}[\boldsymbol{C_{PE}}\,(\bar{\boldsymbol{x}}.\boldsymbol{t})] \\ + \sum_{t=1}^{N(t_v)} \boldsymbol{E}[\boldsymbol{C_S}\,(\bar{\boldsymbol{x}}.\boldsymbol{t})] \\ + \sum_{t=1}^{N(t_v)} \boldsymbol{E}[\boldsymbol{C_C}\,(\bar{\boldsymbol{x}}.\boldsymbol{t})] \end{array} \right)}{(\boldsymbol{1}+\boldsymbol{r})^{\boldsymbol{t}}} \right] + \boldsymbol{C_D} \quad (7.21)$$

The life cycle cost analysis evaluates the total cost of maintenance and repair for characteristics over the lifetime of the bridge structure, as evidenced by the expected value of the cumulative total cost ($E[C_{Total}\,(\bar{x}.t_{int})]$). $\sum_{t=1}^{N(t_v)} E[C_{DNRC}\,(\bar{x}.t)]$, $\sum_{t=1}^{N(t_v)} E[C_{DRC}\,(\bar{x}.t)]$, $\sum_{t=1}^{N(t_v)} E[C_{SM}\,(\bar{x}.t)]$,$\sum_{t=1}^{N(t_v)} E[C_{PE}\,(\bar{x}.t)]$, $\sum_{t=1}^{N(t_v)} E[C_S\,(\bar{x}.t)]$, and $\sum_{t=1}^{N(t_v)} E[C_C\,(\bar{x}.t)]$ are respectively the total costs of demolishing the unreinforced concrete parts, the reinforced concrete parts demolition, management, separation, and categorization of debris resulting from destruction, installation, and subsequent removal of formwork for repair concrete activity, repair, and replacement of damaged bar steel with corrugated bar steel with improved ductility characteristics, and also preparing and pouring concrete costs during and until the end of bridge life.

This research looked at the whole life cycles of coastal concrete bridge parts, considering their locations in saltwater and the activities that go along with them. The assessment incorporated the costs of repairing the concrete and coastal Arosa bridges, utilizing national construction-related databases from Spain (MITMA, 2022). The PSD approach was employed for forecasting and estimating the bridge's degradation over time. Furthermore, the study examined the expenses of maintaining and repairing the concrete bridge, specifically focusing on corrosion-induced damage. The effectiveness and precision of this method in identifying the location, extent, and timing of failures were thoroughly evaluated. Its capability to minimize structural maintenance and repair costs was also assessed.

7.2.3.2 *E-LCA through the PSD method*

The infrastructure of bridges exerts adverse environmental impacts, contributing to diminished river flow, habitat destruction, decreased biological diversity, heightened levels of suspended particles, and water pollution. E-LCA utilizes two main strategies, midpoint and endpoint techniques, to furnish comprehensive life cycle indicators. The endpoint technique primarily emphasizes the overall environmental influence, while the midpoint approach focuses on specific environmental implications. A contrasting perspective posits the midpoint method as the immediate catalyst, whereas the endpoint approach represents the ultimate consequence (Penades-Pla et al., 2020). The approaches were analyzed according to some methods, including CML, ReCiPe 2016, IMPACT 2002+, and TRACI, and through some databases such as SimaPro and Ecoinvent® (Barahmand and Eikeland, 2022). The categories and subcategories of these approaches in general and the method processes used in this study are shown in Figure 7.5.

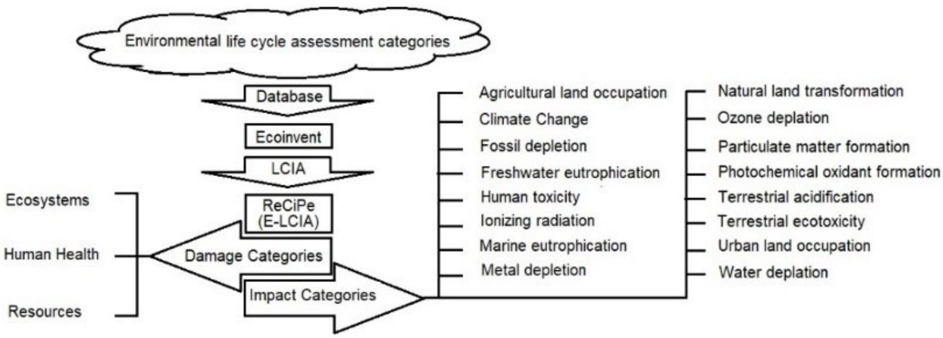

Figure 7. 5. *Environmental life cycle assessment indicators and method used*

Figure 7.5 shows that the ReCiPe method for midpoint environmental assessment takes into account many things, such as ionizing radiation, photochemical oxidant formation, particulate matter formation, marine ecotoxicity, terrestrial ecotoxicity, freshwater ecotoxicity, and human toxicity. These factors can potentially have detrimental effects on ecosystems and human health. The focal points include agricultural land encroachment, urban land encroachment, natural land conversion, water depletion, mineral resource depletion, and fossil fuel depletion. In contrast, the terminal point involves diverse damage categories such as ecosystems, human health, and resources.

This research utilized the PSD methodology to identify and quantify corrosion damage on a coastal RC bridge over its lifespan according to endpoint approaches because the endpoint approach gives us final damage categories that give us the opportunity to assess the PSD method results as a non-destructive damage detection method. The ECOINVENT (Association, 2023) database and the ReCiPe approach were employed for the E-LCIA. The endpoint encompasses the environment, human health, and resource loss. The maintenance and repair stage of bridge usage encompasses all necessary processes.

7.2.3.3 *S-LCA through the PSD method*

UNEP's Life Cycle Initiative released the first Social Life Cycle Assessment Guidelines in 2009 (Benoît and Mazijn, 2009). Since then, researchers and practitioners have utilized these Guidelines to evaluate products' social and socio-economic implications across their lifespan. S-LCA has grown from a small group of academics to encompass industry, policymakers, and business partners (Benoît et al., 2020).

Consequently, S-LCA involves four key stages: aim and scope definition, inventory analysis, impact assessment, and interpretation (refer to Figure 7.6). S-LCA provides valuable social and socio-economic decision-making insights to enhance organizational social performance and stakeholder well-being (Navarro et al., 2022). By amalgamating E-LCA modeling and systematic evaluation with the social sciences, S-LCA offers a comprehensive perspective.

Figure 7.6 shows how the impact categories and subcategories looked at in S-LCA can affect stakeholders in a good or bad way throughout the life cycle of a product (UNEP, 2020; UNEP, 2021).

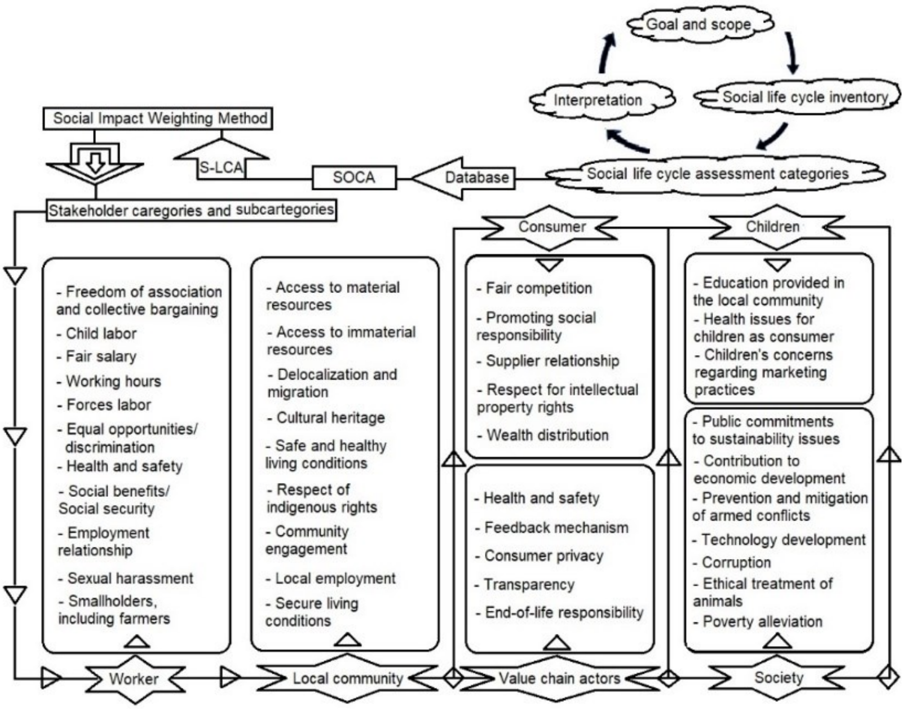

Figure 7. 6. *The iterative phases, stakeholder categories, and subcategories of S-LCA according to the UNEP 2020 Guidelines*

In summary, conducting a social impact assessment within a life cycle assessment is a thorough and intricate procedure. It involves a comprehensive evaluation of the social consequences associated with a project or product throughout its life cycle. The primary objective is to ensure that social sustainability is considered alongside environmental and economic factors, thereby contributing to more responsible and ethical decision-making practices.

The SOCA database extends the Ecoinvent v.3.3 databases, offering clear and extensive data for conducting S-LCA (Eisfeldt, 2017). The SOCA database supplied data for the social impact assessment utilizing an ordinal risk scale comprising six distinct risk levels. This was necessary as specific indicators are measured in various units (such as percentages, absolute values, etc.) and require conversion to a standardized unit of measurement. Each risk level is linked to moderate risks, where medium risk is represented by a factor of 1, and the other risk levels are assigned specific factors (Kovačič Lukman et al., 2021). The OpenLCA software was utilized to conduct the social assessment using the SOCA database (Eisfeldt, 2017).

Furthermore, the weighing method of the criteria is a crucial step in decision-making, as it will determine the outcome of an evaluation (Navarro et al., 2023). Due to the lack of a widely accepted method for social impact assessment, the "Social Impacts Weighting Method" is rather basic, with impact categories corresponding to one indicator.

Therefore, The social component was assessed using the Social Impact Weighting Method and the SOCA database, with stakeholders actively participating. According to SOCA, social stakeholders include workers, local communities, society, and value chain actors. These stakeholder groups follow the Guidelines and demonstrate how the studied structures fit into Spanish society.

7.2.4. MCDM model through the PSD method

Multi-criteria decision-making approaches leverage aggregated data to make optimal economic, environmental, and social decisions. Decision-making often involves identifying and selecting various alternatives while considering their conflicting attributes (Penades-Pla et al., 2020). Some widely used classical MCDM methods in civil engineering and construction include SAW, COPRAS (a scoring approach), TOPSIS, VIKOR (utility/value methods), and MIVES (a utility-based tool). The absence of consensus on the most accurate MCDM approach is evident in literature surveys, which typically showcase a variety of methods. For instance, to supplement the explanation of the findings, an overall index, the Global Structural Sustainability Index (GSSI) method was introduced to assess the sustainability performance of each option throughout its life cycle (Zavadskas et al., 2015).

The Analytic Hierarchy Process (AHP) divides complex decision problems into a hierarchical framework. This lets people decide by comparing criteria and options pairwise and ranking them. Using pairwise comparison techniques, AHP figures out how critical and subjective different criteria are by comparing and contrasting other options. Unlike producing an index, these approaches rank suggested solutions in order of dominance.

This research looks at the TOPSIS method for MCDM to see how long a concrete coastal bridge can last for maintenance and repair work. It does this by looking at eight criteria of life cycle impact and using non-destructive damage detection methods. The process flowchart for calculations through the TOPSIS technique is depicted in Figure 7.7.

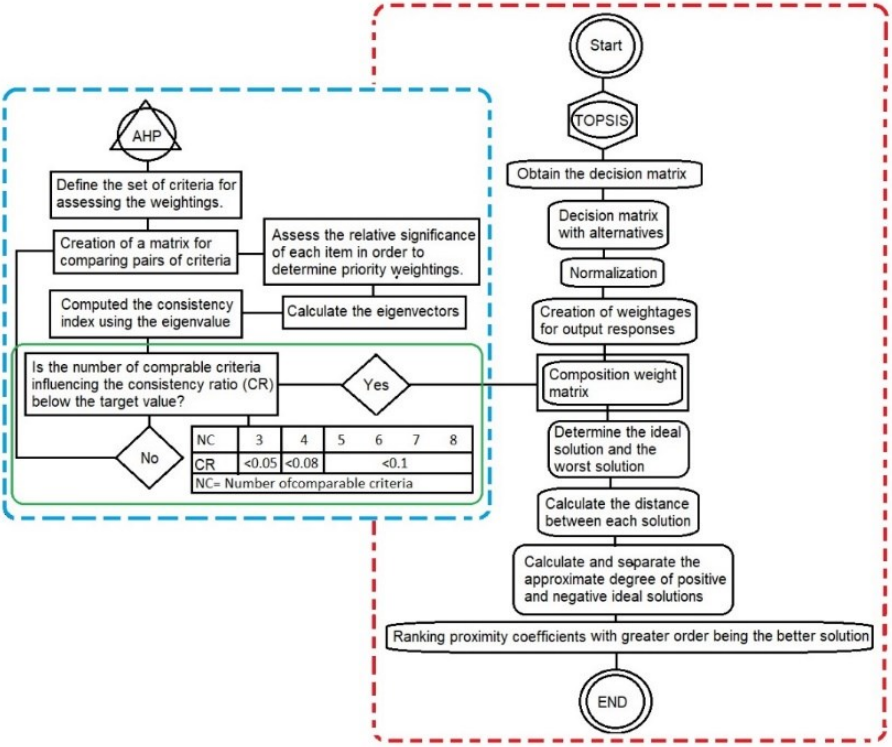

Figure 7. 7. *MCDM flowchart for comprehensive design solution evaluation through the TOPSIS method*

TOPSIS (Technique for Order Preference by Similarity to Ideal Solution) ranks solutions based on their proximity to the optimal and worst possible choices. The best alternatives are intermediate between the perfect option and the worst one. The TOPSIS method is characterized by its proximity to the positive ideal solution (PIS) and its distance from the negative ideal solution (NIS). The first stage involves standardizing the scores (r_{ij}) for each alternative i and criteria j in the following manner (Sánchez-Garrido et al., 2022; Navarro et al., 2023):

$$\acute{r}_{ij} = \frac{r_{ij}}{\sqrt{\sum_{j=1}^{m} r_{ij}^2}} \quad (7.22)$$

In Equation 7.22, the number of criteria included in the decision problem is shown as m. The standardized scores $\acute{r}_{ij}$ are multiplied by the appropriate criterion weights wi to get the standardized, weighted score v_{ij}.

The distances to the positive ideal solution (D_i^+) and negative ideal solution (D_i^-) are calculated as follows:

$$D_i^+ = \sqrt{\sum_{j=1}^{n} (v_{ij} - v_j^+)^2} \tag{7.23}$$

$$D_i^- = \sqrt{\sum_{j=1}^{n} (v_{ij} - v_j^-)^2} \tag{7.24}$$

The variables v_j^+ and v_j^- represent the highest and lowest scores, respectively, for criteria *j*, taking into account all possible alternatives *i*.

Ultimately, an index C_i^* is established to quantify the ultimate performance of each option *i*, considering its relative position to the positive and negative ideal solutions.

$$C_i^* = \frac{D_i^-}{(D_i^+ + D_i^-)} \tag{7.25}$$

According to the TOPSIS approach, the optimal solution will have the highest proximity index C_i^*.

7.2.5. Numerical model analysis

The numerical model analysis for structural damage detection has garnered significant attention among engineers and researchers. According to this study, the PSD method was used to investigate the damage that chloride ions do to a computer model of a coastal concrete bridge. The technique focused on vibration and signal analysis.

Stimulation and measurement points were placed on the bridge model to monitor its structural health annually and assess the corrosion damage situation. Figure 7.8 shows how deck and column numbers on specific spans were renumbered from 1 to 189 to simplify tracking.

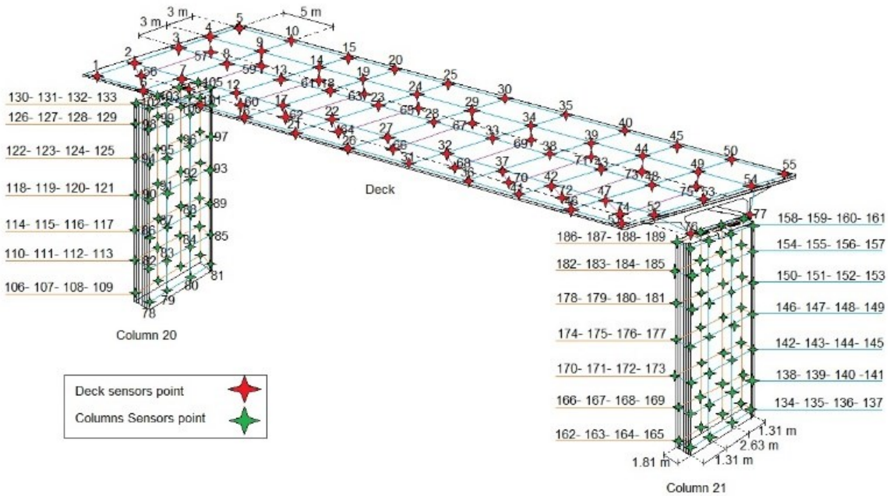

Figure 7. 8. *Situation and numbering of sensor points on one span of the Arosa bridge.*

Figure 7.8 shows the numbers that have been assigned to different points that are used as sensors for analysis. The numbering system, ranging from 1 to 77, corresponds to points on the bridge deck, each spaced at 5 m meter intervals lengthwise and 3 m intervals widthwise across the bridge. In addition, the numerical sequence within each pier initiates at 78 and extends up to 189 in the adjacent column. The distance between points on the longer and broader sides of the columns measures 2.63 m, with a height between them of 2 m. Furthermore, the width of the pier, or the shorter side, is approximately 1.80m between each other. Specific points were designated as simulation points, while others served as measurement points, allowing for the annual assessment of damage severity resulting from chloride attacks at various bridge sections.

For consistent annual test monitoring and analysis, the locations and conditions of these excitation and measurement points were maintained unchanged from one analysis year to the next. Specific locations across different sections and components were assigned as simulation points, while others served as measurement points, as shown in Table 7.2.

Table 7. 2. *Simulation and measuring point numbers on a span of Arosa bridge.*

Location	Stimulation points	Measuring points
Deck	3, 18, 33, 48, 58, 59, 64, 65, 70, 71, 76, 77.	remaining points (Between 1 to 77) in the deck
Pier 20	86, 89, 98, 101, 115, 116, 127, 128.	remaining points (Between 78 to 133) in the Column 20
Pier 21	135, 136, 147, 148, 159, 160, 162, 165, 174, 177.	remaining points (Between 134 to 189) in the Column 21

These locations in Table 7.2 were consistently evaluated yearly throughout the bridge's lifespan, maintaining a fixed placement.

This study assumed that the positions of these stimulation and measurement sites remained constant over the structure's lifespan. This assumption served as the foundation for evaluating the changes in these points over time. Also, the expected effect of chloride ions on any part of this coastal concrete bridge was changed by 10% to account for errors and noise in the numbers used in the study. The effectiveness of the PSD approach in detecting chloride-induced damage was evaluated using MATLAB software and the Open Sees program.

7.3. Repair activities description

In order to extend the longevity of structures like bridges, several repair methods and approaches adhere to the European standard EN 1504-9. These include patch repair, regular repair, repair using sacrificial anode, galvanic cathodic protection (GCP), impressed current cathodic protection (ICCP), and complete replacement of the damaged component of the existing structure (Wittocx et al., 2022).

The principles (7 to 11) that can be employed to address damage caused by reinforcement corrosion are as follows: (7) Preservation or Restoration of Passivity, (8) Enhancement of Resistivity, (9) Cathodic Control, (10) Cathodic Protection, and (11) Control of Anodic Areas. Additionally, the concrete is sequentially restored following principles 1 to 6 to repair concrete damage after the rebars. The six principal purposes of this product are: (1) preventing the entry of unwanted substances, (2) managing moisture levels, (3) repairing concrete, (4) reinforcing structures, (5) enhancing physical durability, and (6) providing resistance against chemicals (NBN EN 1504-9; Renne et al., 2022).

In this regard, some activities were done to repair damaged parts detected by the PSD method as a non-destructive damage detection method, as shown in Figure 7.9.

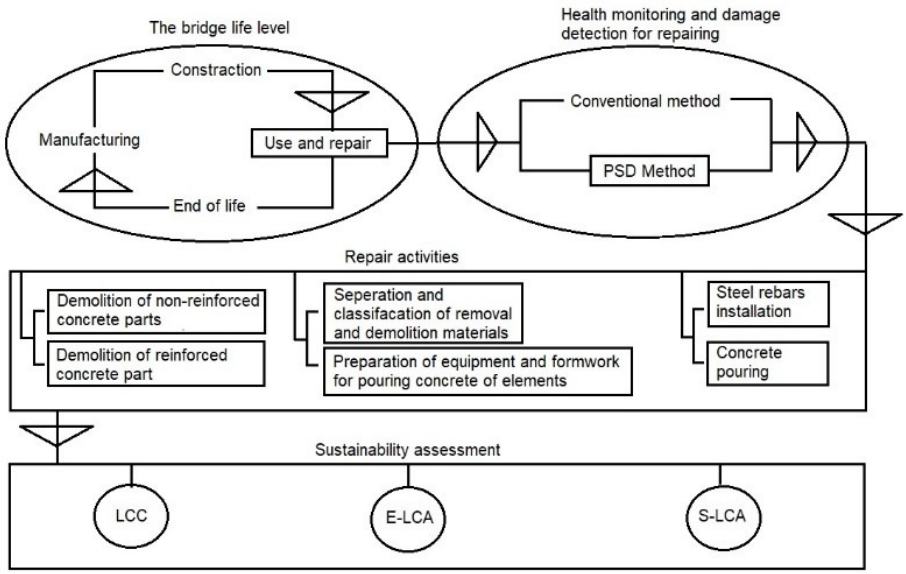

Figure 7. 9. *Total repair activities to assess sustainability by PSD method.*

As shown in Figure 7.9, in this study, the PSD method of monitoring as a damage detection method was used for the level of use and maintenance for repair activities. These repairing activities include the demolition of non-reinforced and forced concrete parts, the separation and classification of removal and demolition materials, and then the preparation of equipment and formwork for pouring concrete of the structure elements, as following steel rebars installation and finally, concrete pouring that they are main activities that use for this analysis.

7.4. Results and discussion

7.4.1. Service Life Prediction Methods Performance results

In the first step, a non-destructive and dynamic damage detection method was used to check how long the cement used in a bridge would last during the repair and maintenance period. It is imperative to obtain insights into the efficacy of this method in pinpointing the location and extent of damage throughout the projected lifespan of the bridge, spanning a century.

A comparison of the PSD method with a conventional method for predicting corrosion caused by chloride ion attacks in a coastal setting, specifically for reinforced concrete bridges (Hadizadeh-Bazaz et al., 2023a), was done to see how well the PSD method worked. Table 7.3 shows the repair times for different parts of the Arosa bridge span, based on where they were measured and where they were simulated.

The PSD methodology facilitated the computation of bridge repair durations for damages surpassing the 20% threshold of the base damage. These times were worked out based on the estimated service life of the conventional method. The goal was to find the best time to fix and maintain reinforced concrete structures exposed to chloride ions and corrosion.

Table 7. 3. *Arosa bridge location, time, damage, and service lifetime for repairing activities.*

Section No.	Location and situation of each section	Damage prediction techniques			
		PSD		Conventional	
		Damage (%)	Repair time (year)	Damage (%)	Repair time (year)
Section 1	Deck	20.06	60	26.67	6
Section 2		20.08	50	26.67	6
Section 3		20.15	29	26.67	6
Section 4		20.64	19	26.67	6
Section 5		22.04	18	26.67	6
Section 6		21.5	18	26.67	6
Section 7		20.14	27	26.67	6
Section 8		20.08	54	26.67	6
Section 9		20.31	51	26.67	6
Section 10		20.34	56	26.67	6
Section 11	Column 20	21.1	14	20	17
Section 12		24.23	15	50	14
Section 13		26.63	16	20	18
Section 14		21.48	17	20	18
Section 15		26.45	19	20	18
Section 16		22.11	19	20	18

Section 17	Column 21	21.1	14	20	17
Section 18		24.23	15	50	14
Section 19		26.63	16	20	18
Section 20		21.48	17	20	18
Section 21		26.45	19	20	18
Section 22		22.11	19	20	18

As delineated in Table 7.3, the Arosa bridge deck span was systematically divided into ten segments, each spanning 5 meters. This meticulous division was undertaken to enhance the precision and effectiveness of the assessment process. Furthermore, the individual bridge columns were subdivided into six segments with a uniform spacing of 2 meters. Notably, the data indicates that the conventional method predicts identical repair times for entire spans of bridge decks. In contrast, the PSD method yields varying predictions for initiating maintenance and repair activities, thereby offering a nuanced and differentiated perspective on the projected service lifetime of these bridge components.

7.4.2. Life cycle impacts assessment results

Exploring various dimensions of LCA results, encompassing economic, environmental, and social considerations, is crucial. This investigation, particularly in the context of the Arosa bridge, aims to elucidate the disparities in repair activity assessments facilitated by the PSD method as opposed to a conventional approach to service life prediction. The objective is to empower engineers and experts to mitigate both the adverse environmental impact and the financial costs associated with the maintenance of such structures. To this end, a comprehensive analysis focuses on the economic aspects and expenditures of repairing and maintaining the Arosa Bridge (Hadizadeh-Bazaz et al., 2023b).

A comparative LCCA examination of the conventional method for predicting damage to this concrete bridge and its environs is presented in Figure 7.9. This detailed breakdown encompasses the columns and deck of a single bridge span, offering valuable insights into the economic implications of employing different predictive methodologies.

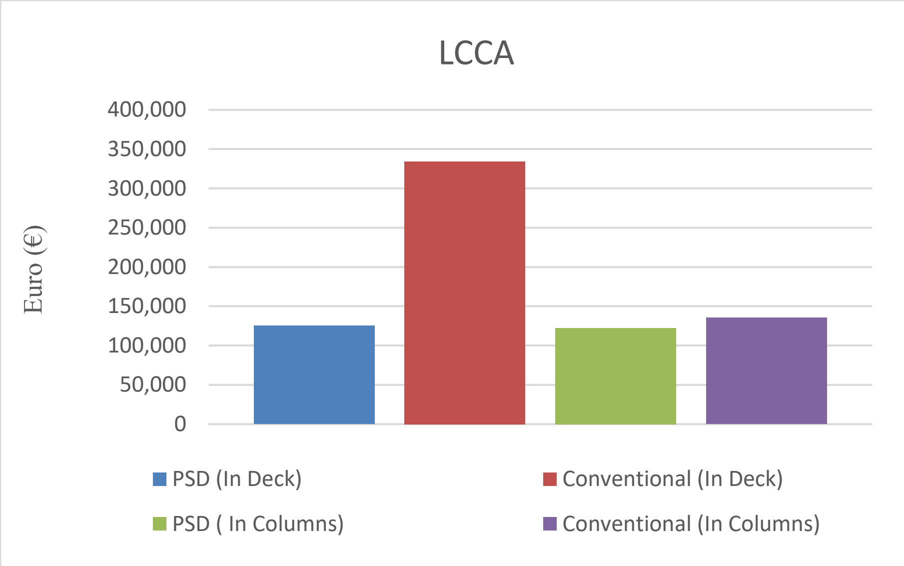

Figure 7. 10. *Total LCC for the deck and columns of a span of the Arosa bridge through each method.*

As depicted in Figure 10, the life cycle cost for a single span of the Arosa bridge was determined to be approximately 248,001.19 euros through the implementation of the PSD approach, contrasting with 470,113.12 euros when conventional methods were employed. Employing the PSD approach for the bridge's maintenance and repair could yield an estimated cost savings of approximately 222,111.92 euros. These expenses encapsulate all costs incurred over 100 years for the routine and continuous repair and upkeep of the Arosa coastline bridge. The LCC of all bridge repair and maintenance costs underwent scrutiny to evaluate the efficacy of the PSD technique in reducing costs compared to alternative methods of predicting structural deterioration. To provide a more precise understanding of the cost savings enabled by the PSD approach, this analysis incorporated a 5% discount rate.

Subsequent to this economic assessment, Figure 10 illustrates the impact of the PSD method on the environmental aspects of the Arosa Bridge in a corrosive environment, specifically focusing on the deck and columns of the bridge. This depiction compares against a conventional approach, shedding light on the environmental implications of utilizing different predictive methodologies.

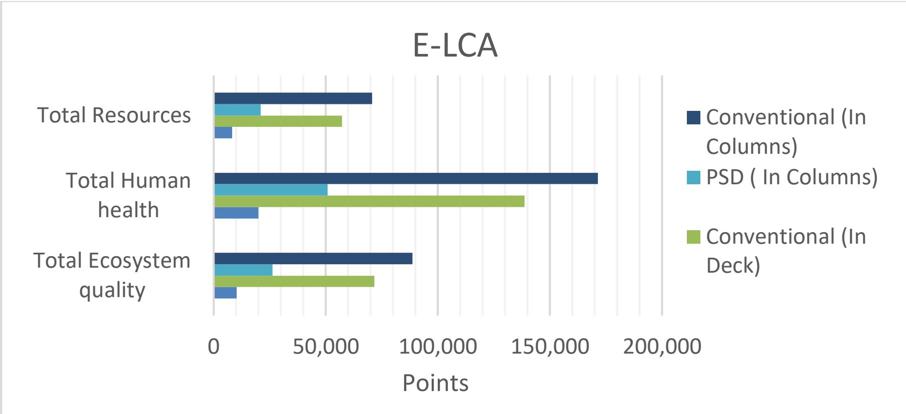

Figure 7. 11. *Total E-LCA for the deck and columns of a span of the Arosa bridge through each method.*

The research shows that using the PSD approach has made a big difference in how damaging the Arosa bridge structure is to the environment during maintenance and repair, as measured by LCA. When the PSD method for E-LCA is used instead of the usual way of maintaining and fixing bridge decks, as shown in Figure 7.10, the overall impact on the ecosystem goes down by 61,449.68 points, and the overall impact on human health goes down by 118,802.69 points. The PSD technique potentially yields savings of 49,028.9 points in bridge deck resource utilization. Additionally, in the context of coastal bridge columns, PSD has the potential to curtail environmental damage by 62,363.55, 120,608.15, and 49,774 points concerning overall ecosystem quality, human health, and resources, respectively. Compared to conventional techniques, PSD impacts ecosystem quality, human health, and resources less on the bridge deck and two columns.

Specifically, this study uses a non-destructive damage detection method called PSD to assess the social impact of fixing and maintaining a coastal concrete bridge that is prone to corrosion and could fall apart. Figure 7.11 presents the outcomes derived from the S-LCA of the Arosa Bridge, emphasizing pivotal categories such as the local community, society, value chain actors, and workers. These results are obtained by applying the PSD method, which offers insights into the social implications of maintenance and repair activities throughout the structure's lifespan.

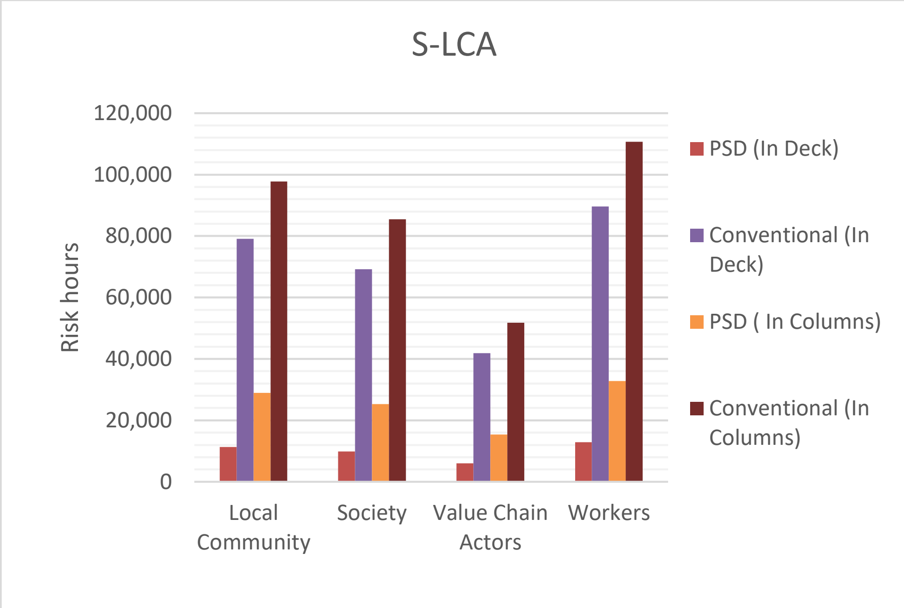

Figure 7. 12. *Total S-LCA for the deck and columns of a span of the Arosa bridge through each method.*

Figure 7.12 shows the results of the social impact survey for four groups of stakeholders. These groups are further broken down into subgroups, as seen in Figure 7.6. The PSD method was used to evaluate these subcategories for a mid-span section of the Arosa bridge with two columns and a 50-meter deck. This analysis was juxtaposed with the outcomes derived from the conventional approach for predicting corrosion damage.

Following the PSD method, the total S-LCA results for the deck and two columns of this bridge span show values of 40,283.37, 35,226.05, 21,346.03, and 45,650.65 risk hours for the local community, society, actors in the value chain, and workers. In stark contrast, the results obtained through the conventional method for the abovementioned categories are significantly higher, at 176,807.60, 154,610.55, 93,689.80, and 200,365.10, respectively.

The S-LCA results show that using the PSD approach is better than the traditional method because it has clear benefits and less of an effect on society.

7.4.3. Sustainability and MCDM Analysis Results

Eight criteria were considered for the sustainability life cycle assessment of maintenance and repair activities using the PSD method in this study. These criteria encompass total cost (C1), total ecosystem quality (C2), total human health (C3), total resources (C4), workers (C5), local community (C6), society (C7), and value chain actors (C8). The analysis was conducted employing a Multi-Criteria Decision-Making (MCDM) approach.

The AHP was utilized as a weighting method to derive scores for each LCA criterion for the sustainability assessment. The scores were then applied to the TOPSIS technique. The weights assigned to each of these diverse criteria in the bridge are outlined in Table 7.4.

Table 7. 4. *Criteria and weights pairwise comparison matrix for the bridge by AHP*

Criteria	C1	C2	C3	C4	C5	C6	C7	C8	Weights	CR
Costs (C1)	1	0.5	0.3	1	0.2	7	1	2	0.08	
Ecosystem quality – total (C2)		1	0.5	2	0.3	3	0.5	3	0.11	
Human health – total (C3)			1	4	1	8	4	7	0.27	
Resources – total (C4)				1	0.5	1	0.5	1	0.06	0.07
Workers (C5)					1	9	9	9	0.32	
Local Community (C6)						1	0.5	1	0.03	
Society (C7)							1	5	0.09	
Value Chain Actors (C8)								1	0.04	

Table 7.4 demonstrates the weights of the pairwise matrix considered for the bridge using the AHP method. Furthermore, it was verified that the number of criteria conforming to the consistency ratio (CR) is below the desired threshold. If there are more than five criteria, it should be less than 0.1. Therefore, the value for these eight criteria is 0.07, which is less than 0.1.

In order to assess the performance of the PSD method for sustainability life cycle assessment, the TOPSIS method is compared to the conventional method to predict the service life of coastal structure corrosion, as shown and outlined in Table 7.5.

Table 7. 5. *The score for each method of damage preparation is according to the TOPSIS approach.*

LCA	Criteria	Optimization direction	Alternatives		Distances				Score	
			$ŕ_{ij}$		D_i^+		D_i^-		C_i^*	
			Conv	PSD	Conv	PSD	Conv	PSD	Conv	PSD
LCCA	C1	min	0.074	0.039	0.35	0.00	0.00	0.35	0.00	1.00
E-LCA	C2	min	0.103	0.023						
	C3	min	0.265	0.043						
	C4	min	0.058	0.013						
S-LCA	C5	min	0.312	0.071						
	C6	min	0.033	0.007						
	C7	min	0.091	0.021						
	C8	min	0.035	0.008						

According to the TOPSIS process result approach for each of the criteria because of the importance of the minimum optimization direction value offered by (min) in Table 5. In addition, by obtaining alternative value results in units from the LCC (€), E-LCA (Points), and S-LCA (Risk hours) to the same units to compare the multi-criteria and sustainability of the PSD method and conventional approach calcuted. The distances to the positive ideal solution (D_i^+) and negative ideal solution (D_i^-) express that the higher the score, the better (further from the negative ideal solution). So, according to the TOPSIS approach, the optimal solution will have the highest proximity index C_i^*, and these scores for the PSD method become 1.00 and more than the conventional method by a value of 0.00.

7.5. Conclusions

In conclusion, the PSD method, employed as a non-destructive technique for detecting structural damage, has exhibited commendable efficacy in discerning chloride corrosion-induced impairments across various sites within an RC bridge, including internal rebars and concrete. The study revealed that chloride corrosion damages exerted a negligible impact on the analysis's effectiveness. The PSD technique was applied to determine the occurrence time and quantify the extent of damage in diverse sections of the coastal bridge, encompassing submerged and tide zone columns, as well as drier components such as the deck and column apexes.

By accurately predicting the location, quantity, and time of corrosion damage, implementing the PSD technique in the bridge's LCCA is projected to yield a 40% reduction in maintenance and repair expenses. Consequently, the PSD technique optimizes costs by ensuring timely infrastructure maintenance and repair. Additionally, when applied in E-LCA, the PSD method is anticipated to reduce impacts on the environment by 14.33% in the deck and 29.62% in the bridge's columns during maintenance, as compared to the conventional methods.

Furthermore, the results of the S-LCA reveal that the PSD method significantly diminishes impacts on the local community (28.27%), society (24.72%), value chain actors (14.98%), and workers (32.03%) in comparison to conventional methods during maintenance and repair activities. However, the comprehensive evaluation of total impact, encompassing E-LCA, S-LCA, and total cost in the Arosa bridge, underscores the sustainability of the PSD method. Utilizing the TOPSIS method, considering multiple criteria, the sustainability life cycle assessment affirms that the PSD method, with a score of 1, outperforms the conventional method with a score of 0, making it a highly sustainable choice for maintenance and repair activities throughout the bridge's lifespan.

Given the imperative need for social impact and sustainability assessments to evaluate the performance of non-destructive dynamic methods in damage prediction, the findings of this research offer valuable insights to researchers and experts. Beyond its application in repairing and maintaining concrete bridges in coastal environments, the PSD method proves beneficial in the design phase, as well as before and after the construction of such structures, optimizing costs at every stage of a structure's life.

Chapter 8
Discussion of the results

The present PhD thesis has posed many study inquiries about assessing damage detection technologies' efficacy in ensuring infrastructure sustainability. This study suggests a non-destructive and dynamic way of predicting damage to evaluate infrastructure sustainability from a comprehensive and integrated viewpoint.

Research question 1: *How do non-destructive damage identification methods perform in detecting different damages in materials like steel and concrete structures, considering damage factors like chloride corrosion and the structure's location and environment?*

In order to answer this inquiry, it is essential to examine the versatility and precision of non-destructive techniques in different situations. Some factors, such as material, qualities and ambient circumstances, may influence the effectiveness of vibraion base testing. This research further investigates the effectiveness of two dynamic and signal-based, non-destructive approaches, focusing on their distinctive qualities. These methods are called FRF and PSD.

As for the material type aspect, the effectiveness of non-destructive methods like PSD and FRF can differ between materials due to their varying densities and properties. In this regard, results from Chapter 2 and research by Hadizadeh-Bazaz et al. (2022), analyses on a steel truss bridge indicated that, firstly, this investigation selected eight scenarios to compare the performance of each method to detect the amount of damage compared to the actual damage that happens in some element of the bridge structure.

In this regard, in the scenario one, the PSD method, at about 5%, has a better ability to predict the real damage compared to the FRF. However, according to scenarios number two, three, four, five, and six, the FRF and PSD methods have about the same performance in terms of prediction. Nevertheless, according to scenario seven, which is more than 15%, the PSD approach can identify quantity damages in some elements close to real damages. In contrast, this is reversed in scenario eight, where the FRF performs about 20% better than PSD-based techniques.

So, according to a better answer to how and why which method has a better ability error index for each approach assessed, the PSD surpasses the FRF in average outcomes for all three error measures, with CI closer to one and MSE and RE values closer to zero. PSD had lower IQR values than FRF in all three error evaluations. So, the PSD provided more accurate damage projections than the FRF. In addition, PSD-based predictions had 8.5% fewer average CI and MSE errors than FRF-based predictions. Including RE resulted in 27% fewer mistakes in the PSD-based prediction. Regarding statistical dispersion, PSD results in IQR values that are 14% to 23% lower than FRF values.

Furthermore, the performance of FRF and PSD was also compared by Pedram et al. (2017). However, they employed a 2D one-story by one-bay steel frame numerical model and a laboratory concrete beam vibration test to expand on previous numerical results. However, they selected only two damage scenarios using the sensitivity equations and compared them with the FRF, demonstrating the ability of the PSD approach to identify and measure damages. Therefore, according to these research analyses, the PSD approach for the steel structures performs better in detecting the amount and location of damages than the FRF approach.

In the following, after demonstrating an acceptable performance in the analysis of steel structures using the PSD approach, Hadizadeh-Bazaz et al. (2023a) conducted investigations in coastal environments and for concrete structures to detect damage. Their findings in Chapter 3 indicate that the PSD method, when used as a signal base technique by various methods, has an acceptable potential in detecting corrosion-induced damages in steel rebars of an RC bridge structure, specifically those caused by chloride corrosion over time in a coastal environment. The results of using PSD for chloride corrosion show that this method also has the ability to accurately detect damages caused by chloride corrosion in an RC coastal bridge. These can be because of lower frequency ranges between the stimulation and measurement points, which has an advantage for analyses at short sensor point distances and in small structures. So, expanding the number of excitation points and measurement points may enhance the precision of damage detection in bridges and structures. Which by the following research by Hadizadeh-Bazaz et al. (2023b) considered more sensors than fewer sensors for one span of this bridge and approved this subject.

Additionally, for these purposes, a study by Pedram et al. (2018) compared a plate and a shall-shaped structure model using the FRF and PSD methods without numerical analysis. The results indicated that the PSD approach exhibited greater sensitivity than the FRF method in detecting changes in structural parameters, particularly within the natural frequency range. On the other hand, this approach requires robust and high-speed computers, which represents a notable drawback of the PSD technique when used in numerical models of bridges.

Chapter 4, Chapter 6, and Chapter 7 discuss an investigation that demonstrates the effectiveness of PSD-based approaches to damage prediction. We compare the PSD with a conventional approach to service life prediction in the context of a coastal concrete bridge. The amount and service time for repair activities at each element location were analyzed using two methods for this comparison. In this regard, according to the 100-year lifetime of the concrete coastal bridge, maintenance through a conventional approach to predict damage by corrosion to the bridge's deck should begin in the 6th year of the bridge's life.

On the other hand, the PSD approach predicts the service lifetime for each section of the bridge separately, with an average time for first repair activities ranging from 18 to 60 years, depending on the condition of each part. The beginning time for the service life of columns by the PSD method is about 16 years; this time, through the conventional method, there are about 17 years of bridge life for the first repair activities. Nevertheless, the difference between them is that the PSD method detects the exact location of the damaged palace in each element of the bridge structure. In contrast, the conventional method predicts damages generally and just according to the situation of the zone of the bridge to the seawater (under the seawater, tide zone, dry zone).

As mentioned in Chapter 5, Hadizadeh-Bazaz et al. (2023c) evaluated PSD in coastal concrete buildings. They studied how redesigns and concrete cover thickness in RC bridges can affect the performance of a non-destructive damage detection method such as PSD in a marine environment. As a result of this study, thickening the concrete layer has little effect on ultimate accuracy due to the distance between the surface and the reinforcing bars. Moreover, these design modifications enhance the service lifetime, suggesting that ions initiate damage, thereby influencing the frequency and timing of structural repairs.

In this research, firstly, the performance of two non-destructive and dynamic damage identification methods was evaluated and compared in terms of the detection, presence, location, and amount of damage in the elements of a metal truss bridge. In the next stage, the method's performance, which had the best accuracy in identifying damages, was evaluated and compared in the metal bridge was evaluated. However, this time, the analysis was done in a concrete structure. In the following, after the performance of this damage detection method was evaluated in two different types of structures, different factors and environments in creating and accelerating damage were analyzed according to the position of the structural elements.

In this regard and in response to the question raised, the results of the research on this question show that, firstly, comparing the two non-destructive dynamic identification methods, the PSD method performs better compared to the FRF method in a steel truss bridge. Also, the performance of this method in a reinforced concrete structure in conditions including exposure to the coastal environment and the corrosion of reinforcements by chloride ions was evaluated and compared with a conventional method.

The results show the proper performance of this method and a significant reduction in the costs spent during the lifetime of this concrete bridge for its repair and maintenance.

In general, how and the performance of these two damage identification methods in a concrete and metal bridge are shown in the form of steps in Figure 8.1.

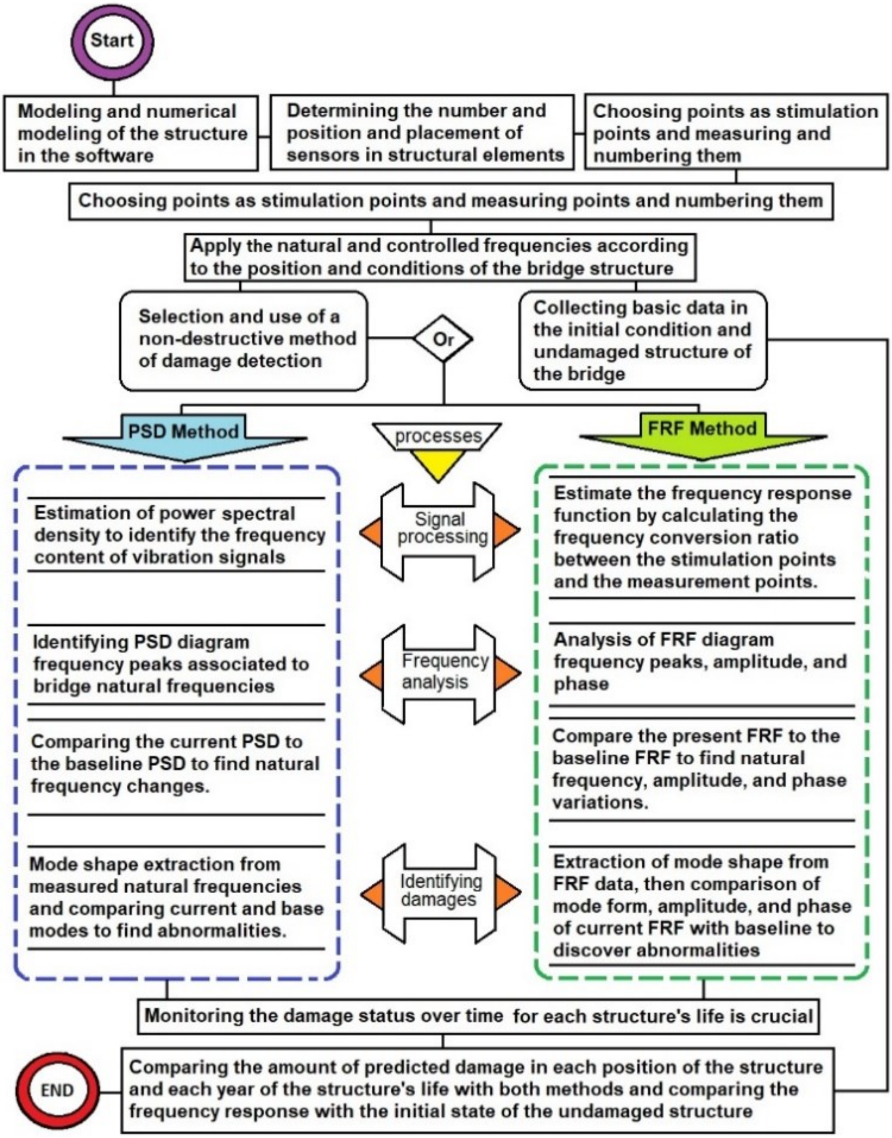

Figure 8. 1. *The process and functioning of the two damage detection methods based on FRF and PSD.*

According to Figure 8.1, structural health monitoring and damage identification use FRF and PSD methods, although with different measurement techniques, data processing, and interpretation. The difference in measurement technique is that the FRF approach evaluates the system's reaction to a known input stimulation. However, the PSD method analyzes the power distribution of the observed signals without an explicit input.

Also, different in data processing, the FRF analysis entails the calculation of transfer functions and direct comparison, while PSD analysis concentrates on extracting characteristics from the power spectrum of the observed signals. Furthermore, the FRF approach sometimes offers a valuable understanding of variations in the structure's dynamic characteristics, such as the natural frequencies through the low frequency.

In conclusion, selecting the most appropriate dynamic non-destructive method requires a nuanced understanding of the interplay between material properties, environmental factors, and the specific requirements of the structure’s location.

This research contributes to the broader field by delineating clear guidelines for choosing and applying damage detection techniques in varied contexts, supporting ongoing advancements in structural health monitoring.

Future investigations should focus on refining these methods and exploring their integration with emerging technologies, such as artificial intelligence for monitoring and predictive maintenance.

Research question 2: *How much use of the PSD method as a non-destructive damage detection method can be useful in decreasing total maintenance and repair activity costs and affecting the LCCA for the whole life of the coastal concrete bridge?*

In answer to this question, it should be said that we know that a structure like a bridge includes stages including design, construction, maintenance, repair, and demolition activities at the end of the structure's life. Costs in each of the steps can be effective for the costs of the structure. In this regard, one of the stages that can effectively reduce the costs incurred during the structure's life is the stage of repairing and maintaining the structure. Therefore, using new methods with high accuracy and reasonable costs can greatly help specialists and engineers in this field. On the other hand, it can be very popular with governments for large structures such as bridges.

In the research conducted in this thesis, the effectiveness of a non-destructive method in damage detection was investigated to reduce the costs incurred in a coastal concrete bridge. In chapter 4 of this thesis, which was done by Hadizadeh-Bazaz et al. (2023b), the ability of the PSD method in conditions where the elements of this concrete bridge are subject to damage and corrosion to detect and the amount of this type of possible damage for each year life of the structure was evaluated.

This analysis showed that the PSD method can reduce about 40% of the total repair and maintenance costs during the structure's lifetime compared to a conventional method of predicting possible damages. These results can be due to the high ability of the PSD method with a different approach in detecting the amount and location of damage in each year of the structure's life.

Additionally, Hadizadeh-Bazaz et al. (2023c) explore the cost-effectiveness of the PSD approach for bridge redesign in Chapter 5. The study takes into account several scenarios, including concrete cover thickness. The PSD approach's primary capability is to identify the exact location and extent of damage by performing a corrosion analysis and comparing it with a conventional method through different scenarios. The study evaluates the impact of chloride ions on the location and extent of degradation during the bridge's lifetime and the total costs associated with maintenance and repair operations. According to this study, applying the PSD method to maintenance and repair tasks, specifically redesigning the bridge as shown in Chapter 5's Scenario No. 3, can cut the overall LCC for repair operations by about 11.5% compared to the reference design scenario for concrete cover of the bridge. However, increasing or decreasing the concrete cover can have a less significant impact on the total cost of repair activities.

In conclusion, the PSD method can lower the high costs of inaccurate information about where and how bad damage is in structural elements. It does this differently by predicting where and how bad the damage will be over time. This approach prevents high costs in repair activities and maintenance operations and ensures timely identification of damage occurring within the structure. Additionally, due to the non-destructive nature of the method and its high performance in coastal environments, it can reduce the costs of repair and maintenance in a span or even the entire bridge by approximately 40%. This is a significant achievement for the maintenance repair activities of concrete and marine structures, as evidenced by research studies on corrosion on coastal structures.

Figure 8.2 shows the answer to this question: how much can the PSD method, compared to a conventional method for some repair activities, decrease total LCCA in each activity according to a discount rate of 5%.

According to Chapters 4 to 6, the activities mentioned in Figure 8.2 include some activities for maintenance and repair in a span of the coastal bridge during the bridge life. In this regard, Activity (A) is the demolition of the unreinforced concrete parts, and Activity (B) is the demolition of the reinforced concrete parts. Activity (C) is managing, separating, and categorizing destruction-related debris. Activity (D) is the installation and removal of formwork for the Repair of concrete activity. Activity (E) is to repair and replace damaged bar steel with corrugated bar steel with improved ductility, and Activity (F) is to prepare and pour concrete.

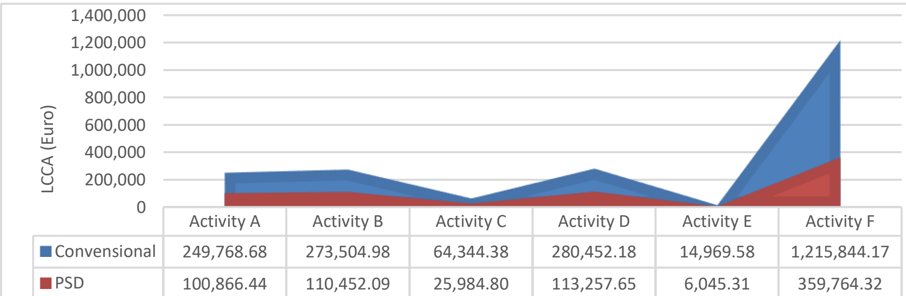

Figure 8. 2. *The total LCCA differences through the PSD method compared to a conventional method.*

So, as shown in Figure 8.2, the total LCCA for each activity by maintenance and repair through the PSD approach and compared to a conventional approach to prediction damages can decrease by about 40% cost for activities A, B . C, D, and E.

Nevertheless, this method can decrease about 29% LCCA for activity F. Total new concrete activities include preparing and pouring concrete piles, stirrups, headboards, beams, deck boards, slabs, walls, and frames.

Research question 3: *How much can a non-destructive damage detection method such as the PSD method improve the impact on the environmental and social life cycle assessment at a structure's maintenance and repair activities?*

Non-destructive damage detection methods can have essential rules for evaluating the social and environmental impacts across the whole lifespan of a structure. In this regard, the PSD method as a non-destructive damage detection method can improve impacts on the environment and society in a different stage of a structure's life, including the design, construction, maintenance, durability, repair activities, and demolition phases.

In answer to this question, some studies have been done related to LCA and environmental and social impact on maintenance and repair in a bridge structure through the PSD method in some research mentioned in Chapters 6 and 7 by Hadizadeh-Bazaz et al. (2023d) and also by Hadizadeh-Bazaz et al. (2024).

According to results from research in Chapter 6, when the PSD approach is applied for maintenance and repair activities, the result for E-LCA is expected to reduce environmental impacts by 14.33% in the deck and 29.62% in the bridge's columns.

In this regard, the PSD method can have different impact results for each category of E-LCA. These categories include: Total Ecosystem quality, Total Human health, and Total Resources, which are shown in Figure 8.3.

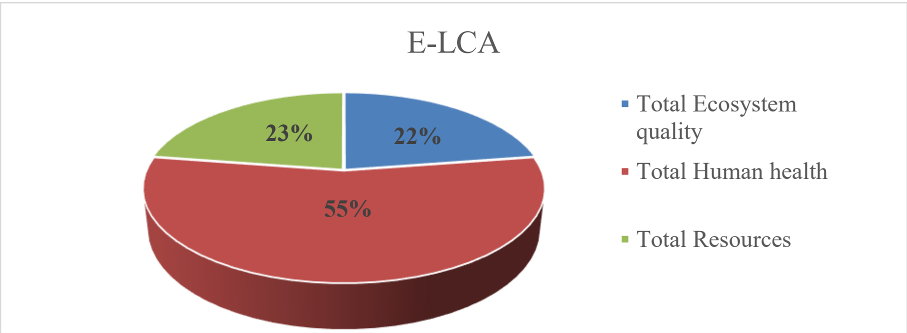

Figure 8. 3. *The percentage of the benefit of using the PSD method in each category of E-LCA.*

Figure 8.3 demonstrates that the PSD technique can reduce around 55% of the detrimental effects on overall human health. The advantages for other E-LCA categories in relation to overall ecosystem quality and total resources are 22% and 23%, respectively.

Conversely, for the S-LCA maintenance and repair through the PSD method for prediction amount, location, and time of corrosion damages in every element of a coastal concrete bridge compared to a conventional approach to service life prediction can reduce social impacts by 23% in the deck and columns of a span.

Figure 8.4 shows the percentage benefit of each category of S-LCA from the total benefit of using the PSD method on social impacts.

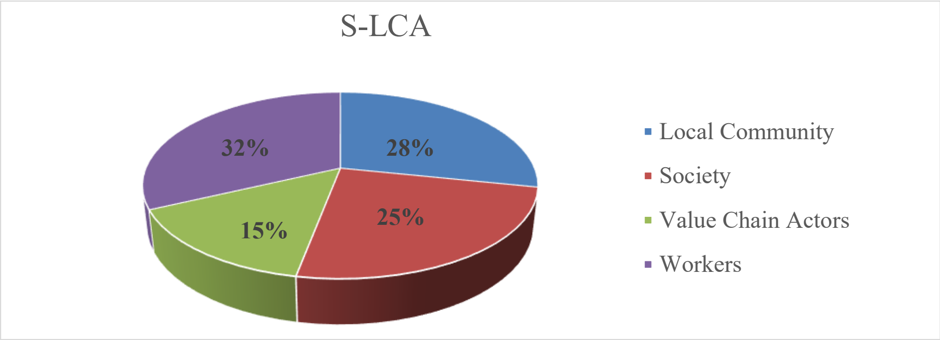

Figure 8. 4. *The percentage of the benefit of using the PSD method in each category of S-LCA.*

The data presented in Figure 8.3 illustrate that the PSD method, discussed in Chapter 7, reveals the PSD approach's diverse positive effects in different S-LCA categories. Here is a detailed analysis of the overall PSD benefit for each category. The PSD approach provides more significant benefits to the labor (32.03%), the local community (28.27%), society (24.72%), value chain actors (14.98%) and compared to conventional methods when it comes to maintenance and repair operations

In conclusion, the PSD, a non-destructive method for detecting damage, has enhanced the environmental and social effects on life cycle evaluation during maintenance and repair operations. Based on the forecasted quantity, location, and timing of corrosion-induced damage, this strategy can assist other building phases, such as design, construction, and demolition. Their less harmful impact on humans, the environment, and society makes them valuable methods, thereby reducing LCCA maintenance and repair costs.

Research question 4: *How much does LCA benefit from non-destructive damage detection methods and deal with expert subjectivity during decision-making to enhance existing multi-criteria decision-making (MCDM) techniques applied in sustainable design?*

Integrating damage detection methods with MCDM techniques in sustainable design is an innovative approach to enhance decision-making processes. However, managing expert subjectivity is crucial for the effectiveness of such integration.

MCDM methods are highly recommended for integrating the different dimensions of sustainability, as they allow for the simultaneous consideration of conflicting criteria, often related in a complex way. This approach should be employed according to the non-destructive damage detection methods to integrate the three aspects of sustainability in order to make economic, environmental, and social impact performance comparable.

ISO 14040 offers a good starting point for assessing the sustainability of infrastructure. The United Nations Environment Programme (UNEP) has already considered this when creating its Guidelines, suggesting the use of Life Cycle Assessment (LCA) as a basis for social evaluations. According to the ISO methodology, assessments need to be consistent and have clear system boundaries. However, this approach hasn't been widely used in MCDM because there isn't a standard method for evaluating the social impact of infrastructure. If a social evaluation method aligns with the LCA approach, as explained in Chapters 6 and 7, it becomes easier to integrate it into MCDM techniques like TOPSIS, as shown in Chapter 7. Solving MCDM problems in sustainability often relies on criteria chosen based on expert opinions.

According to the findings and investigations in Chapter 7, eight criteria were examined for the sustainability life cycle evaluation of maintenance and repair operations in this research, which used the PSD approach. These criteria include overall cost (C1), total ecosystem quality (C2), total human health (C3), total resources (C4), workers (C5), local community (C6), society (C7), and value chain players (C8). The analysis utilized an MCDM method, applying the Analytical Hierarchy Process (AHP) to assign weights and calculate scores for each LCA criterion, which were then integrated into the TOPSIS method for evaluation.

Table 7.4 summarizes the weights applied and the weights pairwise considered matrix for the bridge using the AHP approach for each of the bridge's varied criteria.

Furthermore, it was determined that the number of criteria that adhere to the consistency ratio (CR) is less than the necessary threshold. If there are more than five criteria, the value should be less than 0.1. Thus, the value for these eight criteria is 0.07, which is less than 0.1.

The TOPSIS process result method for each criterion states that the minimum optimization direction value provided by (min) in Table 7.5 is significant. Additionally, in order to compare the multi-criteria and sustainability of the PSD method and Conventional approach calculated, alternative value results in units from the LCCA (€), E-LCA (Points), and S-LCA (Risk hours) were obtained and converted to the same units. The greater the score, the better (far from the negative ideal solution), as indicated by the distances to the positive ideal solution (D_i^+) and negative ideal solution (D_i^-). Therefore, in accordance with the TOPSIS methodology, the best solution will have the highest C_i^* proximity index, making the PSD method's scores 1.00 and higher than the conventional method's by a value of 0.00.

By implementing these strategies, decision-makers can enhance the robustness and reliability of MCDM techniques applied in sustainable design, effectively managing expert subjectivity and improving the overall quality of decision outcomes. It should be noted that the suggested MCDM weighting model is simple to use for experts, as they simply need to complete a comparison matrix as if it were a traditional AHP procedure. They must also communicate their assurance while making conclusions. The suggested method produces crisp weights that may be employed with standard MCDM procedures.

Research question 5: *How can a system for maintenance and repair structures be created to optimize design that aligns with sustainable life cycle assessment and supports the achievement of the Sustainable Development Goals according to non-distractive damage detection methods?*

The sustainability life cycle during a structure's lifetime to the Sustainable Development Goals by choosing suitable impact indicators can be evaluated in the lifetime of a structure through a non-destructive damage detection approach to maintenance and repair. The Sustainable Development Goals, which were recently formed, consist of 17 objectives, as shown in Figure 8.1.

Figure 8. 5. *The Sustainable Development Goals United Nations, (2015).*

AS Figure 8.1, the brief titles of these seventeen SDGs are including: No poverty (SDG 1), Zero hunger (SDG 2), Good health and well-being (SDG 3), Quality education (SDG 4), Gender equality (SDG 5), Clean water and sanitation (SDG 6), Affordable and clean energy (SDG 7), Decent work and economic growth (SDG 8), Industry, innovation and infrastructure (SDG 9), Reduced inequalities (SDG 10), Sustainable cities and communities (SDG 11), Responsible consumption and production (SDG 12), Climate Action (SDG 13), Life below water (SDG 14), Life on land (SDG 15), Peace, justice, and strong institutions (SDG 16), and Partnerships for the goals (SDG 17).

In this study, assessing structural health monitoring and damage detection methods in a maintenance-related structure is consistent with SDG 3 (good health and well-being), especially with SDG 3.6, which specifically focuses on reducing the number of casualties from sudden collapse of structures due to damage and natural and unnatural erosions that directly and indirectly affect human health.

The indicator for regional economic development contributes to the achievement of SDG 8 (Decent work and economic growth) by determining how much a particular investment may contribute to a region's economic growth as measured by GDP growth. Which specifically focus on targets 8.1(Sustainable economic growth) and 8.8 (Protect labor rights and promote safe working environments).

Among these goals, SDG 9 (industry, innovation, and infrastructure) was one of the main ones considered in this study, with infrastructure design based on sustainability life cycle performance, particularly regarding SDG 9.1 (Develop sustainable, resilient, and inclusive infrastructures). Its goal is to develop resilient, high-quality, sustainable infrastructure to promote prosperity and economic development through modern structure methods.

Furthermore, these indicators offer valuable insights for achieving Sustainable Cities and Communities (SDG 11), specifically focusing on improving road safety through SDG goal 11.2. In addition, the cost indicators used in the life cycle cost analyses carried out here are consistent with SDG 12 (Responsible consumption and production) since government organizations need to exercise caution when managing financial resources to ensure they have the financial capacity to make additional investments.

In order to meet SDG 13 (Climate action), data for possible increases in global warming resulting from the predicted process activities are also measured using environmental assessment techniques. Similar to this, as the point impact categories Intermediate techniques permit, those impacts categorized under the impact category "damage to ecosystems" offer helpful information on the accomplishment of SDG 14 (life underwater) and SDG 15 (life on land) assessment of the harm done to marine, freshwater, and terrestrial species.

Develop and implement a system for doing maintenance and repair tasks that are integral to the lifespan of a building. Implementing cost-saving techniques for maintenance and repair operations benefit both the government and the public. Moreover, it safeguards the environment's well-being by mitigating detrimental ecological activities.

Using current technology across all stages of a structure's lifespan, from design to demolition, is crucial in mitigating global warming. Moreover, it is imperative for society and all individuals involved in such circumstances to give utmost importance to safeguarding human well-being in every endeavor, including those related to infrastructure. So, assessing every new and modern approach for design, construction, maintenance, and repair operations until the end life of the structure, each damage detection method, according to the performance of each of these methods, can be created to optimize design that aligns with sustainable life cycle assessment and supports the achievement of the Sustainable Development Goals. This thesis proposes a sustainable life cycle assessment that uses non-destructive damage detection methods, taking into account the various factors that cause damage to a structure. For these purposes, as mentioned in Chapter 4 of this thesis, research by Hadizadeh-Bazaz et al. (2023b) demonstrates that the LCCA using the PSD method, which supports some of the Sustainable Development Goals by reducing the total cost of maintenance and repair activities of a chloride-damaged coastal concrete bridge compared to a conventional approach to predicting damages by chloride ions. Additionally, the design was optimized to align with the sustainable life cycle assessment and support the achievement of the Sustainable Development Goals. This achievement is also constant, as the bridge's structure is re-designed to accommodate changes in specific properties, such as the concrete cover in the columns and deck (Hadizadeh-Bazaz et al., 2023c). Therefore, these researches show that using the PSD predictions resulted in approximately 40% economic savings compared to a conventional method.

In addition, the use of the PSD method as a non-destructive damage detection method for the assessment of E-LCA and S-LCA of this coastal concrete bridge in Chapters 6 and 7 by Hadizadeh-Bazaz et al. (2023a, 2024) showed that this method for maintenance and repairing can decrease between 14 to 30 percent the total impact on environment and social impacts compare to a conventional method depend on the element of the bridge.

Overall, the PSD method, according to the high performance in detecting location, amount, and time in prediction damage compared to the conventional approaches in predicting chloride damage time for LCCA, ELCA, and S-LCA, can be created to optimize design that aligns with sustainable life cycle assessment and supports the achievement of the Sustainable Development Goals.

Chapter 9

Conclusions and future work

This chapter summarizes the main general results of this study and the conclusions of the specific case related to the design, repair, and maintenance of this bridge in aggressive environments.

This thesis proposes to investigate a non-destructive dynamic method for damage detection to evaluate the sustainability of the infrastructure life cycle. The proposed model is based on the standard LCA method for the environment, which evaluates the environmental, social, and economic aspects to evaluate concrete bridge deck and column designs in a coastal area exposed to marine chlorides.

This chapter summarizes the main general results of this study as well as the conclusions of the specific case related to the design, repair, and maintenance of this bridge in aggressive environments.

9.1. General conclusions

The general conclusions drawn from this PhD thesis are:

9.1.1. Main conclusions

- According to the thesis findings, conclusions about the sustainability of an infrastructure design should not be based solely on a few selected sustainability metrics. Instead, alternatives that improve sustainability across all life cycle stages contribute more effectively to the sustainable design and maintenance of infrastructure.
- Maintenance and repair activities are essential for sustainability assessments since they substantially impact the life cycle performance of coastal structures.
- Optimizing maintenance intervals and using non-destructive damage detection methods reduce environmental, economic, and social impacts over the life cycle, with sustainability guiding the ideal maintenance period, environmental impacts being easier to optimize, and social impacts being less significant.
- The financial aspects of infrastructure development and maintenance are essential for long-term viability, with maintenance and health monitoring costs being lower for all competing designs; however, reducing maintenance expenses does not guarantee competitiveness.
- In order to accomplish the Sustainable Development Goals, the suggested sustainability life cycle assessment, using a damage identification technique, has to consider several economic, environmental, and social factors.

9.1.2. Methodological conclusions

- Different approaches for detecting and forecasting structural deterioration may be better or worse depending on the circumstances and structure. Therefore, results from comparing the performance of two non-destructive damage detection methods show that the PSD predicts and diagnoses structural element deterioration in a metal truss construction with oblique components better than the FRF, according to the numerical findings of this case study in a steel truss bridge.
- Frequency-domain approaches like the PSD involve trial and error to pinpoint measurement and excitation locations, particularly for huge and essential constructions like bridges. This sector needs expertise since inappropriate stimulation and measurement sites might impact findings.
- In the case of coastal concrete bridges, it is very challenging to discern the internal condition and damage to each component using testing on an experimental model. Finding and measuring damage throughout the life of the building was made more accessible, cheaper, and less destructive using the numerical model and PSD method.
- Sustainability assessments have a methodological gap, as there are no standards for detailed life cycle assessments that incorporate health monitoring and non-destructive damage detection methods, requiring a comprehensive and integrated ISO 14040-based approach.
- Conventional life cycle evaluations of bridge constructions have many limitations, making them unsuitable for thorough sustainability assessments. The comprehensive approach presented here addresses these gaps and effectively covers all sustainability factors.
- This research proposes a social life cycle evaluation approach compatible with ISO 14040, based on the UNEP/SETAC (2021) Guidelines, which optimizes maintenance intervals to maximize societal benefits.
- Here, AHP evaluated sustainability criterion weights by considering decision makers' subjectivity in complicated evaluations.
- This technique uses quantifiable characteristics, including experience, judgment coherency, and opinion certainty, to establish each decision-maker's significance.
- The suggested technique is user-friendly for decision-makers, requiring them to complete a comparison matrix using the AHP procedure and express their confidence level in the conclusions they provide.

9.2. Specific conclusions

The precise findings taken from the research mentioned in the context are:

- The PSD approach for detecting chloride corrosion damage is particularly effective and reliable for smaller buildings, especially in the lower frequency ranges between the stimulation and measurement points.
- Adding more stimulation and measurement points to bridges and structures improves damage detection but requires powerful and fast computers, which limits the PSD approach in bridge numerical model analysis.
- Employing the PSD approach for the LCCA of this bridge would significantly save about 40% of the overall LCCA, maintenance, and repair expenses during the bridge's lifespan due to precise forecasts of corrosion-induced damage in terms of location, extent, and timing.
- By maintaining and repairing infrastructure on schedule, PSD saves expenditures according to performance and accuracy in detected amount, location, and prediction time of damages by new approaches in a structure.
- The PSD approach has more performance for concrete structures with low concrete covers. However, raising the concrete cover thickness might lead to increased maintenance costs.
- Whether economic, social, or environmental, the impact of a structure's maintenance phase can be critical to its entire life cycle. The life cycle effects are not directly proportional to the chosen maintenance interval, as they depend on the balance between material impact and the durability of the design solution.
- By reducing economic and environmental impacts and increasing social benefits throughout the service life of the bridge deck, every prevention design considered in this study outperforms the impacts associated with the durability design of the actual bridges, regardless of the material and installation costs and impacts. Using stainless steel is the lone outlier here; it outperforms the baseline design regarding environmental performance.
- The PSD method predicts corrosion damage location, amount, and duration, saving 40% on maintenance and repair.
- Compared to conventional methods, the PSD-based damage detection method reduces the environmental impacts of bridge decks by 14.33% and columns by 29.62% per maintenance cycle.
- The S-LCA further shows that the PSD technique reduces effects on the local community (28.27%), society (24.72%), value chain actors (14.98%), and labor (32.03%) during maintenance and repair compared to traditional methods.

The overall effects, including E-LCA, S-LCA, and total cost on the Arosa bridge, suggest that PSD-based leading LCAs may be more sustainable than Conventional forecast approaches. The PSD method scored one in the sustainability life cycle evaluation utilizing the TOPSIS technique and many criteria. It outperformed the conventional method, scoring 0, making it a sustainable bridge maintenance and repair method.

9.3. Future lines of research

The concept of stability and damage detection techniques are too complex to be discussed in this thesis. More efforts should be made to develop reliable tools for evaluating sustainable infrastructure design. Suggestions for future research lines are presented based on such assumptions, considering the gaps not addressed in the current research.

In this regard, future research and studies in the following cases can greatly help specialists and engineers design, repair, and maintain structures such as bridges.

- ✓ Examining comparing the accuracy of other non-destructive methods of damage analysis in detecting different types of damage factors in different environments and for different types of structures.

- ✓ Assess the performance of different damage detection methods in reducing the costs and LCC, from the design and execution of the structure to the completion and destruction of different structures.

- ✓ Sustainability life cycle assessment includes E-LCA and S-LCA through the different damage detection methods and in various environments.

- ✓ The suggested optimization technique might incorporate structural maintenance as an objective function. The influence on each sustainability parameter for each step may be analyzed using life cycle analysis, and optimum maintenance and design of other health monitoring techniques could be developed.

Chapter 10
References

Alavinezhad, M., Hassanabad, M. G., Ketabdari, M. J., & Nekooei, M. (2022). Numerical and experimental structural damage detection in an offshore flare bridge using a proposed modal strain energy method. *Ocean Engineering, 252*, 111055. https://doi.org/10.1016/j.oceaneng.2022.111055.

Aloisio, A., Alaggio, R., & Fragiacomo, M. (2020). Time-domain identification of the elastic modulus of simply supported box girders under moving loads: Method and full-scale validation. *Engineering Structures*, *215*, 110619. https://doi.org/10.1016/j.engstruct.2020.110619.

Alonso, M. C., & Sanchez, M. (2009). Analysis of the variability of chloride threshold values in the literature. *Materials and corrosion*, *60*(8), 631-637. https://doi.org/10.1002/maco.200905296.

Altunışık, A. C., Okur, F. Y., Karaca, S., & Kahya, V. (2019). Vibration-based damage detection in beam structures with multiple cracks: modal curvature vs. modal flexibility methods. *Nondestructive Testing and Evaluation*, *34*(1), 33-53. https://doi.org/10.1080/10589759.2018.1518445.

Angst, U. M., Geiker, M. R., Alonso, M. C., Polder, R., Isgor, O. B., Elsener, B., ... & Sagüés, A. (2019). The effect of the steel–concrete interface on chloride-induced corrosion initiation in concrete: a critical review by RILEM TC 262-SCI. *Materials and Structures*, *52*, 1-25. https://doi.org/10.1617/s11527-019-1387-0.

Aquino, R. E., Barbosh, M., & Sadhu, A. (2021). Comparison of Time-Domain and Time-Frequency-Domain System Identification Methods on Tall Building Data with Noise. In *Dynamics of Civil Structures, Volume 2: Proceedings of the 38th IMAC, A Conference and Exposition on Structural Dynamics 2020* (pp. 179-184). Springer International Publishing. https://doi.org/10.1007/978-3-030-47634-2_20.

Arefi, S. L., & Gholizad, A. (2020). Damage identification of structures by reduction of dynamic matrices using the modified modal strain energy method. *Structural Monitoring and Maintenance*, *7*(2), 125-147. https://doi.org/10.12989/smm.2020.7.2.125.

Arora, V. (2011). Comparative study of finite element model updating methods. *Journal of Vibration and Control*, *17*(13), 2023-2039. https://doi.org/10.1177/1077546310395967.

Association, E. (2023). Ecoinvent Database. Ecoinvent 3.3. 2016. Available online: https://ecoinvent.org/the-ecoinvent-database.

Backes, J. G., Traverso, M., & Horvath, A. (2023). Environmental assessment of a disruptive innovation: Comparative cradle-to-gate life cycle assessments of carbon-reinforced concrete building component. *The International Journal of Life Cycle Assessment*, *28*(1), 16-37. https://doi.org/10.1007/s11367-022-02115-z.

Bagherahmadi, S. A., & Seyedpoor, S. M. (2018). Structural damage detection using a damage probability index based on frequency response function and strain energy concept. *Structural Engineering and Mechanics*, *67*(4), 327-336. https://doi.org/10.12989/sem.2018.67.4.327.

Balogun, T. B., Tomor, A., Lamond, J., Gouda, H., & Booth, C. A. (2020, March). Life-cycle assessment environmental sustainability in bridge design and maintenance. In *Proceedings of the Institution of Civil Engineers-Engineering Sustainability* (Vol. 173, No. 7, pp. 365-375). Thomas Telford Ltd. https://doi.org/10.1680/jensu.19.00042.

Barahmand, Z., & Eikeland, M. S. (2022). Life cycle assessment under uncertainty: A scoping review. *World*, *3*(3), 692-717. https://doi.org/10.3390/world3030039.

Barbosh, M., Singh, P., & Sadhu, A. (2020). Empirical mode decomposition and its variants: A review with applications in structural health monitoring. *Smart Materials and Structures*, *29*(9), 093001. https://orcid.org/0000-0001-5685-7087.

Barbhuiya, S., & Das, B. B. (2023). Life Cycle Assessment of construction materials: Methodologies, applications and future directions for sustainable decision-making. *Case Studies in Construction Materials*, e02326. https://doi.org/10.1016/j.cscm.2023.e02326.

Barman, S. K., Mishra, M., Maiti, D. K., & Maity, D. (2021). Vibration-based damage detection of structures employing Bayesian data fusion coupled with TLBO optimization algorithm. *Structural and Multidisciplinary Optimization*, *64*, 2243-2266. https://doi.org/10.1007/s00158-021-02980-6.

Bayat, M., Ahmadi, H. R., & Mahdavi, N. (2019). Application of power spectral density function for damage diagnosis of bridge piers. *Structural Engineering and Mechanics, An Int'l Journal*, *71*(1), 57-63. https://doi.org/10.12989/sem.2019.71.1.057.

Baybordi, S., & Esfandiari, A. (2023). Model updating and damage detection of jacket type platform using explicit and exact time domain sensitivity equation. *Ocean Engineering*, *269*, 113551. https://doi.org/10.1016/j.oceaneng.2022.113551.

Bendat, J. S., & Piersol, A. G. (1980). Engineering applications of correlation and spectral analysis. *New York*. https://ui.adsabs.harvard.edu/abs/1980wi...book.....B.

Benoît, C., Norris, G. A., Valdivia, S., Ciroth, A., Moberg, A., Bos, U., ... & Beck, T. (2010). The guidelines for social life cycle assessment of products: just in time!.

The international journal of life cycle assessment, *15*, 156-163. https://doi.org/10.1007/s11367-009-0147-8.

Benoît Norris, C., Traverzo, M., Neugebauer, S., Ekener, E., Schaubroeck, T., & Russo Garrido, S. (2020). Guidelines for social life cycle assessment of products and organizations 2020.

Bjørheim, F., Siriwardane, S. C., & Pavlou, D. (2022). A review of fatigue damage detection and measurement techniques. *International Journal of Fatigue*, *154*, 106556. https://doi.org/10.1016/j.ijfatigue.2021.106556.

Bru, D., González, A., Baeza, F. J., & Ivorra, S. (2018). Seismic behavior of 1960's RC buildings exposed to marine environment. *Engineering Failure Analysis*, *90*, 324-340. https://doi.org/10.1016/j.engfailanal.2018.02.011.

Brundtland, G. H., & Comum, N. F. (1987). Relatório Brundtland. *Our Common Future: United Nations*, 540-542.

Cai, Q., & Zhu, S. (2023). Optical frequency domain reflectometry sensing for damage detection in long-span bridges using influence surface. *Structural Health Monitoring*, 14759217231153678. https://doi.org/10.1177/14759217231153678.

Carbonell, A., González-Vidosa, F., & Yepes, V. (2011). Design of reinforced concrete road vaults by heuristic optimization. *Advances in Engineering Software*, *42*(4), 151-159. https://doi.org/10.1016/j.advengsoft.2011.01.002.

Caruso, M., Pinho, R., Bianchi, F., Cavalieri, F., & Lemmo, M. T. (2020). A life cycle framework for the identification of optimal building renovation strategies considering economic and environmental impacts. *Sustainability*, *12*(23), 10221. https://doi.org/10.3390/su122310221.

Celauro, C., Cardella, A., & Guerrieri, M. (2023). LCA of Different Construction Choices for a Double-Track Railway Line for Sustainability Evaluations. *Sustainability*, *15*(6), 5066. https://doi.org/10.3390/su15065066.

Chaupal, P., & Rajendran, P. (2023). A review on recent developments in vibration-based damage identification methods for laminated composite structures: 2010–2022. *Composite Structures*, *311*, 116809. https://doi.org/10.1016/j.compstruct.2023.116809.

Chen, M. J., Sivakumar, K., Banyay, G. A., Golchert, B. M., Walsh, T. F., Zavlanos, M. M., & Aquino, W. (2022). Bayesian Optimal Sensor Placement for Damage Detection in Frequency-Domain Dynamics. *Journal of Engineering Mechanics*, *148*(12), 04022078. https://doi.org/10.1061/(ASCE)EM.1943-7889.0002162.

Cheng, B., Lu, K., Li, J., Chen, H., Luo, X., & Shafique, M. (2022). Comprehensive assessment of embodied environmental impacts of buildings using normalized environmental impact factors. *Journal of Cleaner Production*, *334*, 130083. https://doi.org/10.1016/j.jclepro.2021.130083.

Chiu, C. K., Lyu, Y. C., & Jean, W. Y. (2014). Probability-based damage assessment for reinforced concrete bridge columns considering the corrosive and seismic hazards in Taiwan. *Natural hazards*, *71*, 2143-2164. https://doi.org/10.1007/s11069-013-1002-6.

Choi, J. H. (2019). Strategy for reducing carbon dioxide emissions from maintenance and rehabilitation of highway pavement. *Journal of cleaner production*, *209*, 88-100. https://doi.org/10.1016/j.jclepro.2018.10.226.

Chu, X., Cui, W., Zhao, L., & Ge, Y. (2022). Life-cycle assessment of long-span bridge's wind resistant performance considering multisource time-variant effects and uncertainties. *Journal of Structural Engineering*, *148*(8), 04022092. https://doi.org/10.1061/(ASCE)ST.1943-541X.0003388.

Ciambella, J., Pau, A., & Vestroni, F. (2019). Modal curvature-based damage localization in weakly damaged continuous beams. *Mechanical Systems and Signal Processing*, *121*, 171-182. https://doi.org/10.1016/j.ymssp.2018.11.012.

Crank, J. (2004). The Mathematics of Diffusion-Appendix A Solution of Fick's Second Law.

Cui, Y., Wang, C., Liu, X., Wu, Y., Li, Z., Li, R., & He, W. (2023). A review of subsurface damage detection methods for optical components. *AIP Advances*, *13*(6). https://doi.org/10.1063/5.0151498.

Daneshvar, M. H., Saffarian, M., Jahangir, H., & Sarmadi, H. (2023). Damage identification of structural systems by modal strain energy and an optimization-based iterative regularization method. *Engineering with Computers*, *39*(3), 2067-2087. https://doi.org/10.1007/s00366-021-01567-5.

Dessi, D., & Camerlengo, G. (2015). Damage identification techniques via modal curvature analysis: Overview and comparison. *Mechanical Systems and Signal Processing*, *52*, 181-205. https://doi.org/10.1016/j.ymssp.2014.05.031.

Dong, Y., & Frangopol, D. M. (2016). Probabilistic time-dependent multihazard life-cycle assessment and resilience of bridges considering climate change. *Journal of Performance of Constructed Facilities*, *30*(5), 04016034. https://doi.org/10.1061/(ASCE)CF.1943-5509.0000883.

Eisfeldt, F. (2017). Soca v. 1 add-on: adding social impact information to ecoinvent. *GreenDelta GmbH, Berlin*.

Ekolu, S. O. (2020). Model for natural carbonation prediction (NCP): Practical application worldwide to real life functioning concrete structures. *Engineering Structures*, *224*, 111126. https://doi.org/10.1016/j.engstruct.2020.111126.

Esfandiari, A., Bakhtiari-Nejad, F., Rahai, A., & Sanayei, M. (2009). Structural model updating using frequency response function and quasi-linear sensitivity equation. *Journal of sound and vibration*, *326*(3-5), 557-573. https://doi.org/10.1016/j.jsv.2009.07.001.

Esfandiari, A., Bakhtiari-Nejad, F., Sanayei, M., & Rahai, A. (2010). Structural finite element model updating using transfer function data. *Computers & structures*, *88*(1-2), 54-64. https://doi.org/10.1016/j.compstruc.2009.09.004.

Fallah, N., Hoseini Vaez, S. R., & Esfandiari, A. (2023). Damage identification of structures based on sensitivity equations using PCA and PSD data. *Proceedings of the Institution of Mechanical Engineers, Part C: Journal of Mechanical Engineering Science*, *237*(11), 2606-2620. https://doi.org/10.1177/09544062221138846.

Fang, Y., Xing, J., Liu, X., Liu, D., & Zhang, Y. (2023a). Damage detection of bridge structures under moving loads based on CEEMD and PSD sensitivity analysis. *Journal of Mechanical Science and Technology*, *37*(7), 3335-3346. https://doi.org/10.1007/s12206-023-0601-8.

Fang, Y., Liu, X., Xing, J., Li, Z., & Zhang, Y. (2023b). Substructure damage identification based on sensitivity of Power Spectral Density. *Journal of Sound and Vibration*, *545*, 117451. https://doi.org/10.1016/j.jsv.2022.117451.

Farshadi, M., Esfandiari, A., & Vahedi, M. (2017). Structural model updating using incomplete transfer function and modal data. *Structural Control and Health Monitoring*, *24*(7), e1932. https://doi.org/10.1002/stc.1932.

Favier, A., De Wolf, C., Scrivener, K., & Habert, G. (2018). *A sustainable future for the European Cement and Concrete Industry: Technology assessment for full decarbonisation of the industry by 2050*. ETH Zurich. https://doi.org/10.3929/ethz-b-000301843.

FIB. (2006). Model Code for Service Life Design; Federation Internationale du Beton, *fib. Bulletin*: Lausanne, Switzerland. No. 34.

Frangopol, D. M., Lin, K. Y., & Estes, A. C. (1997). Life-cycle cost design of deteriorating structures. *Journal of structural engineering*, *123*(10), 1390-1401. https://doi.org/10.1061/(ASCE)0733-9445(1997)123:10(1390).

Frangopol, D. M., Dong, Y., & Sabatino, S. (2017). Bridge life-cycle performance and cost: analysis, prediction, optimisation and decision-making. *Structure and*

Infrastructure Engineering, *13*(10), 1239-1257. https://doi.org/10.1080/15732479.2016.1267772.

Frontera, A., & Cladera, A. (2023). Long-term shear strength of RC beams based on a mechanical model that considers reinforcing steel corrosion. *Structural Concrete*, *24*(1), 25-40. https://doi.org/10.1002/suco.202200428.

Ganguli, R. (2020), *Modal Curvature Based Damage Detection. In Structural Health Monitoring*, Springer, Singapore 37–78. https://doi.org/10.1007/978-981-15-4988-5.

Gao, D. Y., Yao, W. X., Wen, W. D., & Huang, J. (2021). Equivalent spectral method to estimate the fatigue life of composite laminates under random vibration loadings. *Mechanics of Composite Materials*, *57*, 101-114. https://doi.org/10.1007/s11029-021-09937-2.

García-Segura, T., Penadés-Plà, V., & Yepes, V. (2018). Sustainable bridge design by metamodel-assisted multi-objective optimization and decision-making under uncertainty. *Journal of Cleaner Production*, *202*, 904-915. https://doi.org/10.1016/j.jclepro.2018.08.177.

Garcia-Palencia, A., Santini-Bell, E., Gul, M., & Catbas, N. (2015). A FRF-based algorithm for damage detection using experimentally collected data. *Structural monitoring and maintenance*, *2*(4), 399-418. http://dx.doi.org/10.12989/smm.2015.2.4.399.

García-Segura, T., Yepes, V., & Frangopol, D. M. (2017). Multi-objective design of post-tensioned concrete road bridges using artificial neural networks. *Structural and Multidisciplinary Optimization*, *56*, 139-150. https://doi.org/10.1007/s00158-017-1653-0.

Gil Benso, E., Vercher Sanchis, J. M., Mas Tomas, M. D. L. A., & Fenollosa Forner, E. J. (2015). Seguridad remanente a flexión en forjados con corrosión en las viguetas. *Informes de la Construcción*, *67*(537), 1-10. http://dx.doi.org/10.3989/ic.13.084.

Gillich, N., Tufisi, C., Sacarea, C., Rusu, C. V., Gillich, G. R., Praisach, Z. I., & Ardeljan, M. (2022). Beam damage assessment using natural frequency shift and machine learning. *Sensors*, *22*(3), 1118. https://doi.org/10.3390/s22031118.

Goedkoop, M., Heijungs, R., Huijbregts, M., De Schryver, A., Struijs, J., & Van Zelm, R. (2009). ReCiPe 2008. *A life cycle impact assessment method which comprises harmonised category indicators at the midpoint and the endpoint level*, *1*, 1-126.

Goh, K. C., Goh, H. H., & Chong, H. Y. (2019). Integration model of fuzzy AHP and life-cycle cost analysis for evaluating highway infrastructure investments. *Journal of Infrastructure Systems*, *25*(1), 04018045. https://doi.org/10.1061/(ASCE)IS.1943-555X.0000473.

Gomes, H. M., & Silva, N. R. S. (2008). Some comparisons for damage detection on structures using genetic algorithms and modal sensitivity method. *Applied Mathematical Modelling*, *32*(11), 2216-2232. https://doi.org/10.1016/j.apm.2007.07.002.

González, J. L., Aguilera, F. P., & García, F. R. (2013). Proyecto de rehabilitación del puente de la Isla de Arosa. *Hormigón y acero*, (270), 75-89.

Goyal, A., Pouya, H. S., Ganjian, E., & Claisse, P. (2018). A review of corrosion and protection of steel in concrete. *Arabian Journal for Science and Engineering*, *43*, 5035-5055. https://doi.org/10.1007/s13369-018-3303-2.

Gunawan, F. E. (2019). Reliability of the power spectral density method in predicting structural integrity. *International Journal of Innovative Computing, Information and Control*, *15*(5), 1717-1727. https://doi.org/10.24507/ijicic.15.05.1717.

Hadizadeh-Bazaz, M., Navarro, I. J., & Yepes, V. (2022). Performance comparison of structural damage detection methods based on Frequency Response Function and Power Spectral Density. *DYNA Ingeniería e Industria (online)*, *97*(5), 493-500. https://doi.org/10.6036/10504.

Hadizadeh-Bazaz, M., Navarro, I. J., & Yepes, V. (2023a). Power Spectral Density method performance in detecting damages by chloride attack on coastal RC bridge. *Structural Engineering and Mechanics*, *85*(2), 197-206. https://doi.org/10.12989/sem.2023.85.2.197.

Hadizadeh-Bazaz, M., Navarro, I. J., & Yepes, V. (2023b). Life-cycle cost assessment using the power spectral density function in a coastal concrete bridge. *Journal of Marine Science and Engineering*, *11(2)*, 433. https://doi.org/10.3390/jmse11020433.

Hadizadeh-Bazaz, M., Navarro, I.J. & Yepes, V. (2023c). Durability assessment and re-design of coastal concrete bridge through a non-destructive damage detection method. *AEIPRO, 10-13 de julio, Donostia/San Sebastián (Spain)*, 386-401. https://doi.org/10.61547/3371.

Hadizadeh-Bazaz, M., Navarro, I. J., & Yepes, V. (2023d). Life Cycle Assessment of a Coastal Concrete Bridge Aided by Non-Destructive Damage Detection Methods. *Journal of Marine Science and Engineering*, *11*(9), 1656. https://doi.org/10.3390/jmse11091656.

Hájková, K., Šmilauer, V., Jendele, L., & Červenka, J. (2018). Prediction of reinforcement corrosion due to chloride ingress and its effects on serviceability.

Engineering Structures, *174*, 768-777. https://doi.org/10.1016/j.engstruct.2018.08.006.

Hassani, S., Mousavi, M., & Gandomi, A. H. (2022). A mode shape sensitivity-based method for damage detection of structures with closely-spaced eigenvalues. *Measurement*, *190*, 110644. https://doi.org/10.1016/j.measurement.2021.110644.

Hassani, S., & Shadan, F. (2022). Using incomplete FRF measurements for damage detection of structures with closely-spaced eigenvalues. *Measurement*, *188*, 110388. https://doi.org/10.1016/j.measurement.2021.110388.

Hassani, S., Mousavi, M., & Dackermann, U. (2023). Johansen cointegration of frequency response functions contaminated with nonstationary colored noise for structural damage detection. *Journal of Sound and Vibration*, *552*, 117641. https://doi.org/10.1016/j.jsv.2023.117641.

He, K., & Zhu, W. D. (2011). Structural damage detection using changes in natural frequencies: theory and applications. In *Journal of Physics: Conference Series* (Vol. 305, No. 1, p. 012054). IOP Publishing. https://doi.org/10.1088/1742-6596/305/1/012054.

He, W. Y., He, J., & Ren, W. X. (2018). Damage localization of beam structures using mode shape extracted from moving vehicle response. *Measurement*, *121*, 276-285. https://doi.org/10.1016/j.measurement.2018.02.066.

Heidari, M. R., Heravi, G., & Esmaeeli, A. N. (2020). Integrating life-cycle assessment and life-cycle cost analysis to select sustainable pavement: A probabilistic model using managerial flexibilities. *Journal of Cleaner Production*, *254*, 120046. https://doi.org/10.1016/j.jclepro.2020.120046.

Hou, L., Peng, Y., Xu, R., Zhang, X., Huang, T., & Chen, D. (2021). Corrosion behavior and flexural performance of reinforced SFRC beams under sustained loading and chloride attack. *Engineering Structures*, *242*, 112553. https://doi.org/10.1016/j.engstruct.2021.112553.

Hou, R., Xia, Y., & Zhou, X. (2018). Structural damage detection based on l1 regularization using natural frequencies and mode shapes. *Structural Control and Health Monitoring*, *25*(3), e2107. https://doi.org/10.1002/stc.2107.

Huang, H., Li, Y., & Li, W. (2023). Dynamic reliability analysis of stochastic structures under non-stationary random excitations based on an explicit time-domain method. *Structural Safety*, *101*, 102313. https://doi.org/10.1016/j.strusafe.2022.102313.

Huijbregts, M. A., Steinmann, Z. J., Elshout, P. M., Stam, G., Verones, F., Vieira, M., ... & Van Zelm, R. (2017). ReCiPe2016: a harmonised life cycle impact assessment method at midpoint and endpoint level. *The International Journal of Life Cycle Assessment*, *22*, 138-147. https://doi.org/10.1007/s11367-016-1246-y.

Hwang, C. L., Yoon, K., Hwang, C. L., & Yoon, K. (1981). Methods for multiple attribute decision making. *Multiple attribute decision making: methods and applications a state-of-the-art survey*, 58-191. https://doi.org/10.1007/978-3-642-48318-9_3.

Imbabi, M., Carrigan, C., & McKenna, S. (2013). *International Journal of Sustainable Built Environment, 1*, 194-216. http://dx.doi.org/10.1016/j.ijsbe.2013.05.001.

ISO. ISO 14040. (2006). Environmental Management — Life Cycle Assessment — Principles and Framework. https://www.iso. org/standard/37456.html.

ISO. ISO 14044. (2006). Environmental Management — Life Cycle Assessment — Requirements and Guidelines. International Standards Organization. https://www.iso.org/standard/38498.html.

ISO 14040:2006/AMD 1:2020. (2020). Environmental management – Life cycle assessment – Principles and framework https://www.iso.org/standard/76121.html.

ISO 14044:2006/AMD 2:2020.(2020). Environmental management – Life cycle assessment – Requirements and guidelines. https://www.iso.org/standard/76122.html.

ISO 15686-5:2017. (2017). Buildings and constructed assets – Service-life planning – *Part 5: Life-cycle costing*. https://www.iso.org/standard/61148.html.

Jalali, M. H., & Rideout, D. G. (2022). Substructural damage detection using frequency response function based inverse dynamic substructuring. *Mechanical Systems and Signal Processing*, *163*, 108166. https://doi.org/10.1016/j.ymssp.2021.108166.

Jiang, Y., Sun, J., Lin, Q., & Xiang, J. (2023). A two-stage method to detect damages in aluminum plates using curvature modal shape subtraction indicator and particle swarm optimization. Thin-Walled Structures, 185, 110560.

Jodhani, J., Handa, A., Gautam, A., & Rana, R. (2023). Ultrasonic non-destructive evaluation of composites: A review. *Materials Today: Proceedings*, *78*, 627-632. https://doi.org/10.1016/j.matpr.2022.12.055.

Kamariotis, A., Chatzi, E., & Straub, D. (2022). Value of information from vibration-based structural health monitoring extracted via Bayesian model updating.

Mechanical Systems and Signal Processing, *166*, 108465. https://doi.org/10.1016/j.ymssp.2021.108465.

Karhade, J., Dash, S., Ghosh, S. K., Dash, D. K., & Tripathy, R. K. (2022). Time–frequency-domain deep learning framework for the automated detection of heart valve disorders using PCG signals. *ieee transactions on instrumentation and measurement*, *71*, 1-11. https://doi.org/10.1109/TIM.2022.3163156

Kazemeini, A., & Swei, O. (2023). Identifying environmentally sustainable pavement management strategies via deep reinforcement learning. *Journal of Cleaner Production*, *390*, 136124. https://doi.org/10.1016/j.jclepro.2023.136124.

Keeble, B. R. (1988). The Brundtland report:'Our common future'. *Medicine and war*, *4*(1), 17-25. https://doi.org/10.1080/07488008808408783.

Kurent, B., Brank, B., & Ao, W. K. (2023). Model updating of seven-storey cross-laminated timber building designed on frequency-response-functions-based modal testing. *Structure and Infrastructure Engineering*, *19*(2), 178-196. https://doi.org/10.1080/15732479.2021.1931893.

Khan, M. U., Ahmad, S., & Al-Gahtani, H. J. (2017). Chloride-induced corrosion of steel in concrete: an overview on chloride diffusion and prediction of corrosion initiation time. *International journal of corrosion*, *2017*. https://doi.org/10.1155/2017/5819202.

Khan, M. W., Akmal Din, N., & Ul Haq, R. (2020). Damage detection in a fixed-fixed beam using natural frequency changes. *Vibroengineering Procedia*, *30*, 38-43. https://doi.org/10.21595/vp.2019.21081.

Khanahmadi, M., Pouraminian, M., Mohammady Garfamy, H., & Dezhkam, B. (2023). Damage Detection and Identification in a Column under the Effect of Axial Load Using Modal Properties and Mode Shape-based Detection Index. *Sharif Journal of Civil Engineering*, *38*(4.2), 53-62. https://doi.org/10.24200/j30.2022.60873.3129.

Khodadadi, N., & Mirjalili, S. (2022). Truss optimization with natural frequency constraints using generalized normal distribution optimization. *Applied Intelligence*, *52*(9), 10384-10397. https://doi.org/10.1007/s10489-021-03051-5.

Khorgade, P., Rettinger, M., Burghartz, A., & Schlaich, M. (2023). A comparative cradle-to-gate life cycle assessment of carbon fiber-reinforced polymer and steel-reinforced bridges. *Structural Concrete*, *24*(2), 1737-1750. https://doi.org/10.1002/suco.202200229.

Khosravan, A., Asgarian, B., & Shokrgozar, H. R. (2021). Improved Modal Strain Energy Decomposition Method for damage detection of offshore platforms using data of sensors above the water level. *Ocean Engineering*, *219*, 108337. https://doi.org/10.1016/j.oceaneng.2020.108337.

Kim, Y. S., & Eun, H. C. (2017). Comparison of damage detection methods depending on frfs within specified frequency ranges. *Advances in Materials Science and Engineering*, *2017*. https://doi.org/10.1155/2017/5821835.

Kleingesinds, S., Lavan, O., & Venanzi, I. (2021). Life-cycle cost-based optimization of MTMDs for tall buildings under multiple hazards. *Structure and Infrastructure Engineering*, *17*(7), 921-940. https://doi.org/10.1080/15732479.2020.1778741.

Kothari, A., & Cruikshank, S. A. (2022). Artificial intelligence and journalism: An Agenda for journalism research in Africa. *African Journalism Studies*, *43*(1), 17-33. https://doi.org/10.1080/23743670.2021.1999840.

Kovačič Lukman, R., Omahne, V., & Krajnc, D. (2021). Sustainability assessment with integrated circular economy principles: A toy case study. *Sustainability*, *13*(7), 3856. https://doi.org/10.3390/su13073856.

Kurent, B., Brank, B., & Ao, W. K. (2023). Model updating of seven-storey cross-laminated timber building designed on frequency-response-functions-based modal testing. *Structure and Infrastructure Engineering*, *19*(2), 178-196. https://doi.org/10.1080/15732479.2021.1931893.

Kyriacou, A. P., Muinelo-Gallo, L., & Roca-Sagalés, O. (2019). The efficiency of transport infrastructure investment and the role of government quality: An empirical analysis. *Transport Policy*, *74*, 93-102. https://doi.org/10.1016/j.tranpol.2018.11.017.

Lan, Y., Li, Z., & Lin, W. (2023). A time-domain signal processing algorithm for data-driven drive-by inspection methods: An experimental study. *Materials*, *16*(7), 2624. https://doi.org/10.3390/ma16072624.

Le, T. C., & Ho, D. D. (2022). Structural damage identification of plates using two-stage approach combining modal strain energy method and genetic algorithm. In *Modern Mechanics and Applications: Select Proceedings of ICOMMA 2020* (pp. 1004-1017). Springer Singapore. https://doi.org/10.1007/978-981-16-3239-6_79.

Lee, K. M., Cho, H. N., & Cha, C. J. (2006). Life-cycle cost-effective optimum design of steel bridges considering environmental stressors. *Engineering Structures*, *28*(9), 1252-1265. https://doi.org/10.1016/j.engstruct.2005.12.008.

León, J., Prieto, F., Rodríguez, F., 2013. Proyecto de rehabilitaci_on del puente de la Isla de Arosa. *Hormig_on y Acero, 270*, 75e89.

Li, J. T., Zhu, X. Q., & Samali, B. (2020). Bridge operational modal identification using sparse blind source separation. In *ACMSM25: Proceedings of the 25th Australasian Conference on Mechanics of Structures and Materials* (pp. 911-920). Springer Singapore. https://doi.org/10.1007/978-981-13-7603-0_86.

Li, J., Hao, H., Xia, Y., & Zhu, H. P. (2015). Damage assessment of shear connectors with vibration measurements and power spectral density transmissibility. *Structural engineering and mechanics: An international journal*, *54*(2), 257-289. http://dx.doi.org/10.12989/sem.2015.54.2.257.

Li, Z., Lan, Y., & Lin, W. (2023). Investigation of Frequency-Domain Dimension Reduction for A2M-Based Bridge Damage Detection Using Accelerations of Moving Vehicles. *Materials*, *16*(5), 1872. https://doi.org/10.3390/ma16051872.

Liljenström, C., Björklund, A., & Toller, S. (2022). Including maintenance in life cycle assessment of road and rail infrastructure—a literature review. *The International Journal of Life Cycle Assessment*, *27*(2), 316-341. https://doi.org/10.1007/s11367-021-02012-x.

Liu, K., Yan, R. J., & Soares, C. G. (2018). Damage identification in offshore jacket structures based on modal flexibility. *Ocean Engineering*, *170*, 171-185. https://doi.org/10.1016/j.oceaneng.2018.10.014.

Liu, N., Schumacher, T., Li, Y., Xu, L., & Wang, B. (2023). Damage Detection in Reinforced Concrete Member Using Local Time-Frequency Transform Applied to Vibration Measurements. *Buildings*, *13(1)*, 148. https://doi.org/10.3390/buildings13010148.

Longarini, N., Crespi, P. G., Zucca, M., Giordano, N., & Silvestro, G. (2014). The advantages of fly ash use in concrete structures. *Inżynieria Mineralna*, *15*(2), 141-145. https://hdl.handle.net/11584/328913.

Loya, J. A., Aranda-Ruiz, J., & Zaera, R. (2022). Natural frequencies of vibration in cracked Timoshenko beams within an elastic medium. *Theoretical and Applied Fracture Mechanics, 118*, 103257. https://doi.org/10.1016/j.tafmec.2022.103257.

Malekghaini, N., Ghahari, F., Ebrahimian, H., Bowers, M., Azari, H., & Taciroglu, E. (2023). Time-Domain Finite Element Model Updating for Operational Monitoring and Damage Identification of Bridges. *Structural Control and Health Monitoring*, *2023*. https://doi.org/10.1155/2023/4170149.

Marques, D. E., Vandepitte, D., & Tita, V. (2021). Damage detection and fatigue life estimation under random loads: A new structural health monitoring methodology in the frequency domain. *Fatigue & Fracture of Engineering Materials & Structures*, *44*(6), 1622-1636.

Martínez-Muñoz, D., Martí, J. V., & Yepes, V. (2022). Social impact assessment comparison of composite and concrete bridge alternatives. *Sustainability*, *14*(9), 5186. https://doi.org/10.3390/su14095186.

Micheli, L., Alipour, A., Laflamme, S., & Sarkar, P. (2019). Performance-based design with life-cycle cost assessment for damping systems integrated in wind excited tall buildings. *Engineering Structures*, *195*, 438-451. https://doi.org/10.1016/j.engstruct.2019.04.009.

Mirzaeefard, H., Mirtaheri, M., & Hariri-Ardebili, M. A. (2023). Life-cycle cost analysis of pile-supported wharves under multi-hazard condition: aging and shaking. *Structure and Infrastructure Engineering*, *19(2)*, 269-289. https://doi.org/10.1080/15732479.2021.1940216.

Mitseas, I. P., Kougioumtzoglou, I. A., & Beer, M. (2015). Nonlinear stochastic dynamic analysis for performance based multi-objective optimum design considering life cycle seismic loss estimation. http://hdl.handle.net/2429/53286.

MITMA (2022). Reference Price Base of the General Directorate of Highways; Ministry of Transport, Mobility and Urban Agenda: Madrid, Spain, 2022.

Molina-Moreno, F., García-Segura, T., Martí, J. V., & Yepes, V. (2017). Optimization of buttressed earth-retaining walls using hybrid harmony search algorithms. *Engineering Structures*, *134*, 205-216. https://doi.org/10.1016/j.engstruct.2016.12.042.

Momeni, H., & Ebrahimkhanlou, A. (2022). High-dimensional data analytics in structural health monitoring and non-destructive evaluation: A review paper. *Smart Materials and Structures*, *31*(4), 043001. https://doi.org/10.1088/1361-665X/ac50f4.

Muñiz-Calvente, M., Álvarez-Vázquez, A., Pelayo, F., Aenlle, M., García-Fernández, N., & Lamela-Rey, M. J. (2022). A comparative review of time-and frequency-domain methods for fatigue damage assessment. *International journal of fatigue*, *163*, 107069. https://doi.org/10.1016/j.ijfatigue.2022.107069.

Najafabadi, A. A., Daneshjoo, F., & Bayat, M. (2017). A novel index for damage detection of deck and dynamic behavior of horizontally curved bridges under moving load. *Journal of Vibroengineering*, *19*(7), 5421-5433. https://doi.org/10.21595/jve.2017.19370.

United Nations, (2015). Indicators for sustainable development goals.

Navarro, I. J., Yepes, V., & Martí, J. V. (2018a). Life cycle cost assessment of preventive strategies applied to prestressed concrete bridges exposed to chlorides. *Sustainability*, *10*(3), 845. https://doi.org/10.3390/su10030845.

Navarro, I. J., Yepes, V., & Martí, J. V. (2018b). Social life cycle assessment of concrete bridge decks exposed to aggressive environments. *Environmental Impact Assessment Review*, *72*, 50-63. https://doi.org/10.1016/j.eiar.2018.05.003.

Navarro, I. J., Yepes, V., Martí, J. V., & González-Vidosa, F. (2018c). Life cycle impact assessment of corrosion preventive designs applied to prestressed concrete bridge decks. *Journal of Cleaner Production*, *196*, 698-713. https://doi.org/10.1016/j.jclepro.2018.06.110.

Navarro, I. J., Martí, J. V., & Yepes, V. (2019a). Reliability-based maintenance optimization of corrosion preventive designs under a life cycle perspective. *Environmental Impact Assessment Review*, *74*, 23-34. https://doi.org/10.1016/j.eiar.2018.10.001.

Navarro, I. J., Yepes, V., & Marti, J. V. (2019b). A review of multicriteria assessment techniques applied to sustainable infrastructure design. *Advances in civil engineering*, *2019*, 1-16. https://doi.org/10.1155/2019/6134803.

Navarro, I. J., Penadés-Plà, V., Martínez-Muñoz, D., Rempling, R., & Yepes, V. (2020). Life cycle sustainability assessment for multi-criteria decision making in bridge design: a review. *Journal of Civil Engineering and Management*, *26*(7), 690-704. https://doi.org/10.3846/jcem.2020.13599.

Navarro, I. J., Martí, J. V., & Yepes, V. (2022). Analytic network process-based sustainability life cycle assessment of concrete bridges in coastal regions. *Sustainability*, *14*(17), 10688. https://doi.org/10.3390/su141710688.

Navarro, I.J., Martí, J.V. and Yepes, V. (2023). Enhancing sustainability assessment of bridges in aggressive environments through multi-criteria group decision-making. *DYNA-Ingeniería e Industria, 98*. https://doi.org/10.6036/10816.

NBN EN 1504-9 (2008). Products and Systems for the Protection and Repair of Concrete Structures - Definitions, Requirements, Quality Control and Evaluation of Conformity - *Part 9: General Principles for the Use of Products and Systems*, NBN Belgian Standardization, p. 29.

Nguyen, D. H., Nguyen, Q. B., Bui-Tien, T., De Roeck, G., & Wahab, M. A. (2020). Damage detection in girder bridges using modal curvatures gapped smoothing method and Convolutional Neural Network: Application to Bo Nghi bridge. *Theoretical and Applied Fracture Mechanics, 109*, 102728. https://doi.org/10.1016/j.tafmec.2020.102728.

Nguyen, Q. T., & Livaoğlu, R. (2022). Modal strain energy-based updating procedure for damage detection: a numerical investigation. *Journal of Mechanical Science and Technology, 36(4)*, 1709-1718. https://doi.org/10.1007/s12206-022-0307-3.

Nguyen, D. H., & Wahab, M. A. (2023). Damage detection in slab structures based on two-dimensional curvature mode shape method and Faster R-CNN. *Advances in Engineering Software*, *176*, 103371. https://doi.org/10.1016/j.advengsoft.2022.103371.

Nguyen, Q. T., & Livaoğlu, R. (2023). Modal strain energy based enhanced approaches for damage detection and severity estimation. *Engineering Failure Analysis*, 146, 107142. https://doi.org/10.1016/j.engfailanal.2023.107142.

Nilsson, A. and Liu, B. (2015), "Frequency domain", *Vibro-Acoust.*, 1, 31-66. https://doi.org/10.1007/978-3-662-47934-6.

Niu, Y., & Fink, G. (2019). Life Cycle Assessment on modern timber bridges. *Wood Material Science and Engineering*, *14*(4), 212-225. https://doi.org/10.1080/17480272.2018.1501421.

Niu, Z. (2020). Frequency response-based structural damage detection using Gibbs sampler. *Journal of Sound and Vibration*, *470*, 115160. https://doi.org/10.1016/j.jsv.2019.115160.

Omidi Soroor, A., Asgari, M., & Haddadpour, H. (2023). On the dynamic behavior interpretation of sandwich beams with axially graded face sheets and magnetorheological core using modal strain energy approach. *Acta Mechanica*, *234*(7), 2985-3008. https://doi.org/10.1007/s00707-023-03534-1.

Orozco, C. R., Babel, S., Tangtermsirikul, S., & Sugiyama, T. (2023). Understanding the environmental, economic, and social impact of fly ash utilization on early-age high-strength mass concrete using life cycle analysis. *Materials Today: Proceedings*. https://doi.org/10.1016/j.matpr.2023.03.141.

Padil, K. H., Bakhary, N., Abdulkareem, M., Li, J., & Hao, H. (2020). Non-probabilistic method to consider uncertainties in frequency response function for vibration-based damage detection using Artificial Neural Network. *Journal of Sound and vibration*, *467*, 115069. https://doi.org/10.1016/j.jsv.2019.115069.

Pau, A., & Eroglu, U. (2023). The minimum variance distortionless response beamformer for damage identification using modal curvatures. *Theoretical and Applied Mechanics: AIMETA 2022*, *26*, 455. https://doi.org/10.21741/9781644902431-74.

Paya-Zaforteza, I., Yepes, V., González-Vidosa, F., & Hospitaler, A. (2010). On the Weibull cost estimation of building frames designed by simulated annealing. *Meccanica*, *45*, 693-704. https://doi.org/10.1007/s11012-010-9285-0.

Pedram, M., Esfandiari, A., & Khedmati, M. R. (2016). Finite element model updating using strain-based power spectral density for damage detection. *Structural Control and Health Monitoring*, *23*(11), 1314-1333. https://doi.org/10.1002/stc.1833.

Pedram, M., Esfandiari, A., & Khedmati, M. R. (2017). Damage detection by a FE model updating method using power spectral density: Numerical and experimental investigation. *Journal of Sound and Vibration*, *397*, 51-76. https://doi.org/10.1016/j.jsv.2017.02.052.

Pedram, M., Esfandiari, A., & Khedmati, M. R. (2018). Frequency domain damage detection of plate and shell structures by finite element model updating. *Inverse Problems in science and engineering*, *26*(1), 100-132. https://doi.org/10.1080/17415977.2017.1309398.

Pedram, M., & Esfandiari, A. (2019). Mitigating the effect of incomplete measurement in sensitivity-based FE model updating by enhanced transfer function. *Iranian Journal of Science and Technology, Transactions of Civil Engineering*, *43*, 467-486. https://doi.org/10.1007/s40996-018-0180-6.

Pehlivan, H. (2018). Frequency analysis of GPS data for structural health monitoring observations. *Structural Engineering and Mechanics*, *66*(2), 185-193. https://doi.org/10.12989/sem.2018.66.2.185.

Penadés-Plà, V., Martí, J. V., García-Segura, T., & Yepes, V. (2017). Life-cycle assessment: A comparison between two optimal post-tensioned concrete box-girder road bridges. *Sustainability*, *9*(10), 1864. https://doi.org/10.3390/su9101864.

Penadés-Plà, V., García-Segura, T., Martí, J. V., & Yepes, V. (2018). An optimization-LCA of a prestressed concrete precast bridge. *Sustainability*, *10*(3), 685. https://doi.org/10.3390/su10030685.

Penadés-Plà, V., García-Segura, T., & Yepes, V. (2019). Accelerated optimization method for low-embodied energy concrete box-girder bridge design. *Engineering Structures*, *179*, 556-565. https://doi.org/10.1016/j.engstruct.2018.11.015.

Penades-Pla, V., Martinez-Munoz, D., García-Segura, T., Navarro, I. J., & Yepes, V. (2020). Environmental and social impact assessment of optimized post-tensioned concrete road bridges. *Sustainability*, *12*(10), 4265. https://doi.org/10.3390/su12104265.

Peng, J., Yang, Y., Bian, H., Zhang, J., & Wang, L. (2022). Optimisation of maintenance strategy of deteriorating bridges considering sustainability criteria. *Structure and Infrastructure Engineering*, *18*(3), 395-411. https://doi.org/10.1080/15732479.2020.1855215.

Pérez, M. A., Font-Moré, J., & Fernández-Esmerats, J. (2021). Structural damage assessment in lattice towers based on a novel frequency domain-based correlation approach. *Engineering Structures*, *226*, 111329. https://doi.org/10.1016/j.engstruct.2020.111329.

Pérez-Fadón Martínez, S. (1985). Puente a la Isla de Arosa. *Hormigón y Acero*, *36*(157). http://www.hormigonyacero.com/index.php/ache/article/view/966.

Pérez-Fadón Martínez, S. (1986). Puente sobre la Ría de Arosa. *Rev. Obras Publicas*, *3243*, 1-16.

Pons, J. J., Penadés-Plà, V., Yepes, V., & Martí, J. V. (2018). Life cycle assessment of earth-retaining walls: An environmental comparison. *Journal of Cleaner Production*, *192*, 411-420. https://doi.org/10.1016/j.jclepro.2018.04.268.

Pons, J. J., Sanchis, I. V., Franco, R. I., & Yepes, V. (2020). Life cycle assessment of a railway tracks substructures: Comparison of ballast and ballastless rail tracks. *Environmental Impact Assessment Review*, *85*, 106444. https://doi.org/10.1016/j.eiar.2020.106444.

Pooya, S. M. H., & Massumi, A. (2021). A novel and efficient method for damage detection in beam-like structures solely based on damaged structure data and using mode shape curvature estimation. *Applied mathematical modelling*, *91*, 670-694. https://doi.org/10.1016/j.apm.2020.09.012.

Rahmatalla, S., Eun, H. C., & Lee, E. T. (2012). Damage detection from the variation of parameter matrices estimated by incomplete FRF data. *Smart Structures and Systems*, *9*(1), 55-70. https://doi.org/10.12989/sss.2012.9.1.055.

Rathod, H., & Gupta, R. (2019). Sub-surface simulated damage detection using Non-Destructive Testing Techniques in reinforced-concrete slabs. *Construction and Building Materials*, *215*, 754-764. https://doi.org/10.1016/j.conbuildmat.2019.04.223.

Renne, N., Kara De Maeijer, P., Craeye, B., Buyle, M., & Audenaert, A. (2022). Sustainable assessment of concrete repairs through life cycle assessment (LCA) and life cycle cost analysis (LCCA). *Infrastructures*, *7*(10), 128. https://doi.org/10.3390/infrastructures7100128.

Rezvani, K., NMM, M., & Sabour, M. H. (2018). A comparison of some methods for structural damage detection. *Scientia Iranica*, *25*(3), 1312-1322. https://doi.org/10.24200/sci.2017.4494.

Rizvi, S. H. M., & Abbas, M. (2023). From data to insight, enhancing structural health monitoring using physics-informed machine learning and advanced data collection methods. *Engineering Research Express*, *5*(3), 032003. https://orcid.org/0000-0002-4039-6121.

Ronchei, C., Vantadori, S., Carpinteri, A., Iturrioz, I., Rodrigues, R. I., Scorza, D., & Zanichelli, A. (2021). A frequency-domain approach for damage detection in welded structures. *Fatigue & Fracture of Engineering Materials & Structures*, *44*(4), 1134-1148. https://doi.org/10.1111/ffe.13419.

Sajedi, S., & Huang, Q. (2019). Reliability-based life-cycle-cost comparison of different corrosion management strategies. *Engineering Structures*, *186*, 52-63. https://doi.org/10.1016/j.engstruct.2019.02.018.

Sánchez-Garrido, A. J., Navarro, I. J., & Yepes, V. (2022). Multi-criteria decision-making applied to the sustainability of building structures based on Modern Methods of Construction. *Journal of Cleaner Production*, *330*, 129724. https://doi.org/10.1016/j.jclepro.2021.129724.

Seyedpoor, S. M., Ahmadi, A., & Pahnabi, N. (2019). Structural damage detection using time domain responses and an optimization method. *Inverse Problems in Science and Engineering*, *27*(5), 669-688. https://doi.org/10.1080/17415977.2018.1505884.

Sha, G., Radzieński, M., Cao, M., & Ostachowicz, W. (2019). A novel method for single and multiple damage detection in beams using relative natural frequency changes. *Mechanical Systems and Signal Processing*, *132*, 335-352. https://doi.org/10.1016/j.ymssp.2019.06.027.

Shadan, F., Khoshnoudian, F., & Esfandiari, A. (2016). A frequency response-based structural damage identification using model updating method. *Structural Control and Health Monitoring*, *23*(2), 286-302. https://doi.org/10.1002/stc.1768.

Shekhar, S., Ghosh, J., & Padgett, J. E. (2018). Seismic life-cycle cost analysis of ageing highway bridges under chloride exposure conditions: Modelling and recommendations. *Structure and Infrastructure Engineering*, *14*(7), 941-966. https://doi.org/10.1080/15732479.2018.1437639.

Shetty, D., & Prabhu, N. (2023). Power spectral density based identification of low frequency oscillations in multimachine power system. *Journal of Operation and Automation in Power Engineering*, *11*(3), 173-181. https://doi.org/10.22098/joape.2023.10072.1710.

Shirazi, M. I., Khatir, S., Benaissa, B., Mirjalili, S., & Wahab, M. A. (2023). Damage assessment in laminated composite plates using modal Strain Energy and YUKI-ANN algorithm. *Composite Structures, 303*, 116272. https://doi.org/10.1016/j.compstruct.2022.116272.

Sierra, L. A., Pellicer, E., & Yepes, V. (2017). Method for estimating the social sustainability of infrastructure projects. *Environmental Impact Assessment Review*, 65, 41-53. https://doi.org/10.1016/j.eiar.2017.02.004.

Silik, A., Noori, M., Altabey, W. A., Ghiasi, R., & Wu, Z. (2021). Analytic wavelet selection for time–frequency analysis of big data form civil structure monitoring. In *Civil Structural Health Monitoring: Proceedings of CSHM-8 Workshop 8* (pp. 431-455). Springer International Publishing. https://doi.org/10.1007/978-3-030-74258-4_29.

Skowronek, K., Barszcz, T., Antoni, J., Zimroz, R., & Wyłomańska, A. (2023). Assessment of background noise properties in time and time–frequency domains in the context of vibration-based local damage detection in real environment. *Mechanical Systems and Signal Processing*, *199*, 110465. https://doi.org/10.1016/j.ymssp.2023.110465.

Sobhani, J. and Ramezanianpour, A.A. (2007), “Chloride-induced corrosion of RC structures”, *Asian Journal of Civil Engineering*, 8(5), 531-547.

Sousa, M., Almeida, M. F., & Calili, R. (2021). Multiple criteria decision making for the achievement of the UN sustainable development goals: A systematic literature review and a research agenda. *Sustainability*, *13*(8), 4129. https://doi.org/10.3390/su13084129.

Soust-Verdaguer, B., Galeana, I. B., Llatas, C., Montes, M. V., Hoxha, E., & Passer, A. (2022). How to conduct consistent environmental, economic, and social assessment during the building design process. A BIM-based Life Cycle Sustainability Assessment method. *Journal of Building Engineering*, *45*, 103516. https://doi.org/10.1016/j.jobe.2021.103516.

Spanish Ministry of Public Works (2008), *EHE-08 Instrucción del Hormigón Estructural*.

Su, Y., Dong, L., & Pei, Z. (2022). Non-Destructive Testing for Cavity Damages in Automated Machines Based on Acoustic Emission Tomography. *Sensors, 22(6)*, 2201. https://doi.org/10.3390/s22062201.

Sun, B., Xiao, R. C., Ruan, W. D., & Wang, P. B. (2020). Corrosion-induced cracking fragility of RC bridge with improved concrete carbonation and steel reinforcement corrosion models. *Engineering Structures*, *208*, 110313. https://doi.org/10.1016/j.engstruct.2020.110313.

Sulaiman, M. S. A., Yunus, M. A., Bahari, A. R., & Rani, M. A. (2017). Identification of damage based on frequency response function (FRF) data. In *MATEC Web of*

Conferences (Vol. 90, p. 01025). EDP Sciences. https://doi.org/10.1051/matecconf/20179001025.

Tang, F., Chen, G., & Brow, R. K. (2016). Chloride-induced corrosion mechanism and rate of enamel-and epoxy-coated deformed steel bars embedded in mortar. *Cement and Concrete Research*, *82*, 58-73. https://doi.org/10.1016/j.cemconres.2015.12.015.

Tang, Q., Xin, J., Jiang, Y., Zhou, J., Li, S., & Chen, Z. (2022). Novel identification technique of moving loads using the random response power spectral density and deep transfer learning. *Measurement*, *195*, 111120. https://doi.org/10.1016/j.measurement.2022.111120.

Teixeira, B., Vieira, H., Martins, S., & Mendes, R. (2023). Development of a Rapid and Non-Destructive Method for the Detection of Water Addition in Octopus Species (Octopus vulgaris and Eledone cirrhosa) Using Time Domain Reflectometry (TDR). *Foods*, *12*(7), 1461. https://doi.org/10.3390/foods12071461.

Teng, S., Chen, G., Liu, G., Lv, J., & Cui, F. (2019). Modal strain energy-based structural damage detection using convolutional neural networks. *Applied Sciences*, *9*(16), 3376. https://doi.org/10.3390/app9163376.

Tran, K. T., Nguyen, T. D., Hiltunen, D. R., Stokoe, K., & Menq, F. (2020). 3D full-waveform inversion in time-frequency domain: Field data application. *Journal of Applied Geophysics*, *178*, 104078. https://doi.org/10.1016/j.jappgeo.2020.104078.

Tuutti, K. (1982). Corrosion of steel in concrete. Cement-och betonginst, Swedish Cement and Concrete Research Institute, Stockholm, Sweden. Report No 4-82.

Benoît Norris, C., Traverzo, M., Neugebauer, S., Ekener, E., Schaubroeck, T., & Russo

UNEP/SETAC (2009). Guidelines for Social Life Cycle Assessment of Products, *United Nations Environment Program. In: Paris SETAC Life Cycle Initiative United Nations Environment Programme*.

UNEP, (2020). Guidelines for Social Life Cycle Assessment of Products and Organization 2020.

UNEP, (2021). Methodological Sheets for Subcategories in Social Life Cycle Assessment (S-LCA) 2021.

Vahedi, M., & Khoshnoudian, F. (2018). Sensitivity-based damage identification method for structures exposed to ground excitation. *Inverse Problems in Science and Engineering*, *26*(10), 1404-1431. https://doi.org/10.1080/17415977.2017.1406487.

Vasishta, T., Mehany, M. S. H. M., & Killingsworth, J. (2023). Comparative life cycle assessment (LCA) and life cycle cost analysis (LCCA) of precast and cast–IN–

place buildings in United States. *Journal of Building Engineering*, 105921. https://doi.org/10.1016/j.jobe.2023.105921.

Wang, Y., Ni, Z., Hu, M., Li, J., Wang, Y., Lu, Z., ... & Xia, B. (2020). Environmental performances and energy efficiencies of various urban green infrastructures: A life-cycle assessment. *Journal of Cleaner Production*, 248, 119244. https://doi.org/10.1016/j.jclepro.2019.119244.

Wang, Y. (2021). Adaptive finite element algorithm for damage detection of non-uniform Euler-Bernoulli beams with multiple cracks based on natural frequencies, *Adaptive Analysis of Damage and Fracture in Rock with Multiphysical Fields Coupling* Springer, Singapore.

Wittocx, L., Buyle, M., Audenaert, A., Seuntjens, O., Renne, N., & Craeye, B. (2022). Revamping corrosion damaged reinforced concrete balconies: Life cycle assessment and life cycle cost of life-extending repair methods. *Journal of Building Engineering*, *52*, 104436. https://doi.org/10.1016/j.jobe.2022.104436.

Wickramasinghe, W. R., Thambiratnam, D. P., & Chan, T. H. (2020). Damage detection in a suspension bridge using modal flexibility method. *Engineering failure analysis*, *107*, 104194. https://doi.org/10.1016/j.engfailanal.2019.104194.

Wu, Z., Zhang, Z., Wu, J., Liang, J., Ge, J., Liu, X., & Fang, G. (2022). A new time-frequency domain simulation method for damage accumulation and life prediction of composite thin-wall structures under random cyclic loadings. *Composite Structures*, *281*, 114999. https://doi.org/10.1016/j.compstruct.2021.114999.

Xu, W., Zhu, W., Cao, M., Wu, H., & Zhu, R. (2020). A novel damage index for damage detection and localization of plate-type structures using twist derivatives of laser-measured mode shapes. *Journal of Sound and Vibration*, *481*, 115448. https://doi.org/10.1016/j.jsv.2020.115448.

Yang, D., Kang, C., Hu, Z., Ye, B., & Xiang, P. (2019). On the study of element modal strain energy sensitivity for damage detection of functionally graded beams. *Composite Structures*, *224*, 110989. https://doi.org/10.1016/j.compstruct.2019.110989.

Yang, G., Yang, Z. B., Zhu, M. F., Tian, S. H., & Chen, X. F. (2022). Directional wavelet modal curvature method for damage detection in plates. *In Journal of Physics: Conference Series* (Vol. 2184, No. 1, p. 012027). IOP Publishing.

Yang, X., & Kersemans, M. (2023). Ultrasonic imaging of damage in plates in spectral ripple frequency domain. *Mechanical Systems and Signal Processing*, *195*, 110312. https://doi.org/10.1016/j.ymssp.2023.110312.

Yang, Y., Zhang, Y., & Tan, X. (2021). Review on vibration-based structural health monitoring techniques and technical codes. *Symmetry*, *13*(11), 1998. https://doi.org/10.3390/sym13111998.

Yang, Y. B., Li, Z., Wang, Z. L., Liu, Z., Mo, X. Q., & Qiu, F. Q. (2023). Closely spaced modes of bridges estimated by a hybrid time–frequency method using a multi-sensor scanning vehicle: Theory and practice. *Mechanical Systems and Signal Processing*, *192*, 110236. https://doi.org/10.1016/j.ymssp.2023.110236.

Yao, J., Zeng, B., Zhou, Z., & Zhang, Q. (2023). Damage identification analysis of Cable-stayed arch-truss based on multi-node time-domain data fusion. *Latin American Journal of Solids and Structures*, *20*. https://doi.org/10.1590/1679-78257207.

Yeo, G. L. (2005). *Stochastic characterization and decision bases under time-dependent aftershock risk in performance-based earthquake engineering*. Stanford University.

Yu, H., Wang, B., Xia, C., Gao, Z., & Li, Y. (2021). Efficient non-stationary random vibration analysis of vehicle-bridge system based on an improved explicit time-domain method. *Engineering Structures*, *231*, 111786. https://doi.org/10.1016/j.engstruct.2020.111786.

Zara, A., Belaidi, I., Khatir, S., Brahim, A. O., Boutchicha, D., & Wahab, M. A. (2023). Damage detection in GFRP composite structures by improved artificial neural network using new optimization techniques. Composite Structures, 305, 116475. https://doi.org/10.1016/j.compstruct.2022.116475.

Zavadskas, E. K., Antuchevičienė, J., & Kapliński, O. (2015). Multi-criteria decision making in civil engineering. Part II–applications. *Engineering Structures and Technologies*, *7*(4), 151-167. https://doi.org/10.3846/2029882X.2016.1139664.

Zhang, C. L., Chen, W. K., Mu, S., Šavija, B., & Liu, Q. F. (2021). Numerical investigation of external sulfate attack and its effect on chloride binding and diffusion in concrete. *Construction and Building Materials*, *285*, 122806. https://doi.org/10.1016/j.conbuildmat.2021.122806.

Zhang, D., Zeng, Y., Fang, M., & Jin, W. (2019). Service life prediction of precast concrete structures exposed to chloride environment. *Advances in Civil Engineering*, *2019*. https://doi.org/10.1155/2019/3216328.

Zhang, J., Yi, T. H., Qu, C. X., & Li, H. N. (2022). Detecting hinge joint damage in hollow slab bridges using mode shapes extracted from vehicle response. *Journal of Performance of Constructed Facilities*, *36(1)*, 04021109. https://doi.org/10.1061/(ASCE)CF.1943-5509.0001694.

Zhang, Q., Hou, J., An, X., Jankowski, Ł., Duan, Z., & Hu, X. (2023). Vehicle parameter identification based on vehicle frequency response function. *Journal of Sound and Vibration, 542*, 117375. https://doi.org/10.1016/j.jsv.2022.117375.

Zhao, J., & Li, S. (2022). Life cycle cost assessment and multi-criteria decision analysis of environment-friendly building insulation materials-A review. *Energy and Buildings*, *254*, 111582. https://doi.org/10.1016/j.enbuild.2021.111582.

Zheng, X. W., Li, H. N., & Gardoni, P. (2021). Life-cycle probabilistic seismic risk assessment of high-rise buildings considering carbonation induced deterioration. *Engineering Structures*, *231*, 111752. https://doi.org/10.1016/j.engstruct.2020.111752.

Zheng, Z. D., Lu, Z. R., Chen, W. H., & Liu, J. K. (2015). Structural damage identification based on power spectral density sensitivity analysis of dynamic responses. *Computers & Structures*, *146*, 176-184. https://doi.org/10.1016/j.compstruc.2014.10.011.

Zhu, Y. P., Lang, Z. Q., Mao, H. L., & Laalej, H. (2022). Nonlinear output frequency response functions: A new evaluation approach and applications to railway and manufacturing systems' condition monitoring. *Mechanical Systems and Signal Processing*, *163*, 108179. https://doi.org/10.1016/j.ymssp.2021.108179.

Zuo, H., & Guo, H. (2023). Structural Nonlinear Damage Identification Method Based on the Kullback–Leibler Distance of Time Domain Model Residuals. *Remote Sensing*, *15*(4), 1135. https://doi.org/10.3390/rs15041135.